

https://dspace.org/

Curing and the durabilty of concrete

Ballim, Yunus

2016-06-08
http://hdl.handle.net/10539/20449

Downloaded from a DSpace repository. https://dspace.org/

C U R I N G A N D T H E D U R A B I L I T Y O F C O N C R E T E

Yunus Ballim

A thesis submitted to the Faculty of Engineering, University of the Witwatersrand, Johannesburg, in fulfilment of the requirements for the degree of Doctor of Philosophy.

Johannesburg, 1994.

DECLARATION

I declare that this thesis is my own, unaided work. It is being submitted for the degree of Doctor of Philosophy in the University of the Witwatersrand, Johannesburg. It has not been submitted before for any degree or examination in any other university.

Yunus Ballim

14th day of April 1994

STATEMENT OF ACHIEVEMENT

I believe that the work reported in this thesis has made the following contributions to the field of durability research:

- the development of low-cost equipment of simple operation, which could be used on construction projects for specifying and controlling concrete durability;
- an understanding of the influence of strength, water/binder ratio and cement extender type on the fluid transport properties of the cover concrete;
- development of the form of an empirical model for predicting durability index values based on controllable parameters at the early stages of construction.

The following technical papers have derived from this investigation:

1. Ballim, Y. A low cost, falling head permeameter for measuring concrete gas permeability. *Concrete Beton*. Magazine of the Concrete Society of S.A. No. 61, Nov. 1991. pp. 13-18.
2. Ballim, Y. Curing and the durability of OPC, fly ash and blast-furnace slag concretes. *Materials and Structures*. Vol. 26, 1993. pp. 238-244.
3. Ballim, Y. Towards an early-age index for the durability of concrete. To be presented at the Int. Conf: *CONCRETE 2000 - Economic and durable construction through excellence*. Dundee, Scotland. Sept. 1993. 10 pgs.

ABSTRACT

This thesis presents the details and results of an investigation into the effects of early age curing on the durability of concrete. The two main objectives of the investigation were:

- to develop simple test methods, applied at relatively early ages, for measuring the effects of early-age moist curing on the advance of hydration in the cover zone of concrete;
- to quantify the effect of early age curing on the durability performance of concretes of various strength grades and made with different binder types.

Apparatus and methods were developed for measuring the oxygen permeability and water sorptivity of concrete slices taken from the surface of larger samples. These parameters were used as early-age indicators of the potential durability of concrete.

In the investigation into the effects of curing on the different concrete types, the following variables were used:

- binder type
  * plain OPC
  * 70%/30% blend of OPC and fly ash
  * 50%/50% blend of OPC and ground granulated blastfurnace slag.
- nominal compressive strength of concrete
  * 35 MPa
  * 45 MPa
  * 55 MPa
- duration of early-age moist curing
  * 1 day
  * 3 days

* 7 days
* 28 days

Permeability and sorptivity tests were carried out at 28 days and 10 months after casting. Carbonation of concretes exposed to a controlled laboratory environment was measured at 10 and 20 months after casting. Mathematical models are also developed for predicting the permeability and sorptivity of surface concrete based on controllable parameters such as w/c ratio, binder type and duration of curing.

The main conclusions of the project are:

- The oxygen permeability and water sorptivity test methods are sufficiently sensitive to detect the effects of variations in moist curing on the pore structure of surface concrete.
- Increasing the duration of curing has a significant effect in reducing the oxygen permeability and water sorptivity index values of the surface zone of concrete made with each of the three binder types used.
- For a given curing condition and b/w ratio, OPC concretes generally give lower permeability and sorptivity values than the OPC/FA and OPC/GGBS concretes.
- For equal surface permeability or sorptivity, OPC concretes carbonate slower than OPC/FA and OPC/GGBS concretes.

For
Faeeza and Imraan

Behold! In the creation
of the heavens and the earth;
in the alternation of the
night and the day;
in the sailing of the ships
through the ocean
for the profit of mankind;
in the rain which God
sends down from the skies,
and the life which He
gives therewith to an
earth that is dead;
in the beasts of all kinds;
that He scatters
through the earth;
In the change of the winds
and the clouds which they
trail like their slaves
between the sky and the earth; -
here indeed are signs
for the people that are wise

- Quraan: S. ii. 164.

ACKNOWLEDGEMENTS

There are many people and organisations to whom I am indebted for their contributions to this project and it would be difficult to mention all of them here. However, some individuals and groups require special mention:

* my supervisors, Prof. G.E. Blight and Prof. M.G. Alexander, for their friendship, guidance and patience over the duration of this project;

* members of staff in the Dept. of Civil Engineering, University of the Witwatersrand, for their material and spiritual support;

* the Portland Cement Institute for their financial support through the Fellowship as well as for the kindness of all their staff members in allowing me access to their facilities;

* Anglo Alpha Limited, Ash Resources (Pty) Ltd., Slagment (Pty) Ltd. and Samancor's Delmas Silica Mine for donating the raw materials for the project.

Finally, I wish to express my gratitude to my family (again, too numerous to mention), friends and, in particular, my wife Naseera, for all their support and tolerance over these past years.

TABLE OF CONTENTS

CHAPTER 1
GENERAL INTRODUCTION - THE NEED FOR RESEARCH ON CURING
1.1 Cement Hydration and the Effect of Curing 1-1
1.2 The Need for Research on the Influence of Curing 1-4
1.2.1 Changing conceptions of the role of curing 1-4
1.2.2 Developments in concrete materials, design and construction technology 1-8
1.2.3 The need for local information on the subject 1-10
1.2.4 Development of specifications . . 1-10
1.3 The Southern African Climate and the Need for Curing 1-12
1.3.1 Rainfall 1-13
1.3.2 Duration of bright sunshine . . . 1-15
1.3.3 Temperature 1-15
1.3.4 Relative humidity 1-18
1.3.5 General comment 1-18
1.4 Definition of Terms 1-20
1.4.1 Durability index 1-20
1.4.2 Durability performance 1-20
1.4.3 Potential durability 1-21
1.5 Project Scope and Layout of this Dissertation 1-21
1.6 Apologia. 1-23
List of References 1-23

CHAPTER 2
CONCRETE DETERIORATION IN RELATION TO ITS PROPERTIES: A LITERATURE SURVEY
2.1 Introduction 2-1

2.2 Dominant Agencies and Mechanisms of Deterioration 2-2
2.2.1 Chemical deterioration 2-2
2.2.2 Physical deterioration 2-13
2.3 Permeability and Other Fluid Transport Properties of Concrete 2-14
2.3.1 The pore structure of concrete . 2-14
2.3.2 Movement of fluids through the pore structure 2-16
2.4 Intrinsic Material Factors Affecting the Durability of Concrete 2-20
2.4.1 Water/cement ratio 2-21
2.4.2 Maximum aggregate size 2-22
2.4.3 Water content 2-23
2.4.4 Cement content 2-24
2.4.5 The degree of hydration 2-24
2.4.6 Influence of binder type 2-25
2.5 Effect of Curing on Durability 2-32
2.5.1 Curing and the transport properties of concrete 2-33
2.5.2 Curing requirements of different binder types 2-34
2.6 Approaches to Specifying for Concrete Durability 2-35
2.7 General Discussion 2-36
List of References 2-37

CHAPTER 3
DEVELOPMENT OF TEST METHODS FOR CHARACTERISING POTENTIAL DURABILITY
3.1 Introduction 3-1
3.2 Types of Characterisation Test Methods . 3-2
3.2.1 Absorption tests 3-3
3.2.2 Water penetration tests 3-3
3.2.3 Permeability tests. 3-4

3.2.4 Mechanical tests 3-5

3.3 Selection of Durability Characterisation Test Methods 3-6
3.3.1 Test parameters 3-6
3.3.2 Test method and apparatus 3-9
3.3.3 Concrete sample thickness 3-10
3.4 Selection of Air Permeability Test Apparatus 3-11
3.4.1 Selected survey of proposed air permeability test methods 3-12
3.5 Development of the Air Permeability Test Apparatus 3-18
3.5.1 Detailed description of the Blight apparatus 3-18
3.5.2 Modifications made to the Blight permeameter 3-19
3.5.3 Description of the Falling Head Permeameter Developed 3-20
3.5.4 Testing the air-tightness of the sealing methods 3-30
3.5.5 Operation of the permeameter . . 3-32
3.5.6 Development of the equation governing the falling head permeameter 3-33
3.6 Selection of the Water Absorption Test Method 3-40
3.6.1 Selected survey of various water absorption test methods 3-42
3.6.2 Development of the water sorptivity test method 3-46
3.6.3 Theoretical considerations . . . 3-50
3.6.4 Experimental verification of the sorptivity theory 3-52
3.7 General Discussion and conclusions . . 3-56
List of References 3-57

CHAPTER 4

CHARACTERISING THE INFLUENCE OF THE VARIABLES ASSOCIATED WITH THE PROPOSED TEST METHODS

4.1 Introduction 4-1

4.2 Influence of Sample Variables on the Test Results 4-2

4.2.1 Sample thickness 4-2

4.2.2 Moisture content of the sample . . 4-7

4.2.3 Drying history of the sample . . 4-12

4.3 Laboratory Investigation 4-17

4.3.1 Duration of drying at 50 °C required to achieve stable moisture conditions 4-19

4.3.2 The influence of sample thickness in relation to aggregate size . . . 4-23

4.3.3 The influence of sample thickness for samples cut from larger specimens 4-30

4.3.4 The influence of sample drying method on measured permeability . . 4-45

4.3.5 The influence of drying method on water sorptivity measurements . . . 4-59

4.4 Conclusions 4-63

List of References 4-64

CHAPTER 5

LABORATORY INVESTIGATION AND RESULTS

5.1 Introduction 5-1

5.2 Variables of the Test Programme 5-2

5.2.1 Binder type 5-2

5.2.2 Strength grade 5-3

5.2.3 Early age moist curing 5-3

5.2.4 Depth from the concrete surface . . 5-3

5.2.5 Age at testing 5-3

5.3 Properties of the Materials Used 5-4

5.3.1 Cement 5-4

5.3.2 Ground granulated blastfurnace slag 5-6
5.3.3 Fly ash 5-6
5.3.4 Aggregates 5-7
5.4 Laboratory procedure 5-12
5.4.1 Mixes 5-12
5.4.2 Cube sample manufacture and storage 5-13
5.5 Test Methods 5-17
5.5.1 Compressive strength tests . . . 5-17
5.5.2 Durability index tests 5-18
5.5.3 Depth of carbonation 5-21
5.6 Results and Discussion 5-23
5.6.1 Compressive strength 5-23
5.6.2 Oxygen permeability at 28 days after casting 5-27
5.6.3 Oxygen permeability at 10 months after casting 5-35
5.6.4 Water sorptivity at 28 days after casting 5-40
5.6.5 Water sorptivity at 10 months after casting 5-46
5.6.6 Depth of carbonation 5-51
5.7 General Discussion of the Results . . . 5-59
5.8 Conclusions 5-61
List of References 5-64

CHAPTER 6
DEVELOPMENT OF A GENERALISED APPROACH TO THE EFFECT OF CURING ON DURABILITY
6.1 Introduction 6-1
6.2 Effect of Binder/Water Ratio on Durability Index Values 6-2
6.2.1 Permeability 6-2
6.2.2 Sorptivity 6-7

6.3 Effect of Compressive Strength on Durability Index Values 6-11
6.3.1 Permeability 6-11
6.3.2 Sorptivity 6-15
6.4 Effect of Initial Curing Time on Durability Index Value 6-19
6.4.1 Durability index of the surface segment 6-19
6.4.2 Using the models to determine surface index values 6-29
6.4.3 Variation of durability index wich depth from drying surface 6-33
6.5 Relating the Depth of Carbonation to Durability Index Values 6-36
6.6 Relationship Between the Coefficient of Permeability and Water Sorptivity . . . 6-42
6.7 General Discussion 6-45
6.8 Conclusions 6-47

CHAPTER 7
CASE STUDIES
7.1 Introduction 7-1
7.2 CASE 1: Cast-in-situ concrete culverts in Namibia: Effectiveness of curing compound 7-2
7.2.1 Concrete details 7-2
7.2.2 Laboratory procedure 7-3
7.2.3 Results and discussion 7-4
7.2.4 Summary of findings 7-8
7.3 CASE 2: Mzimkulu River Incrementally Launched Bridge on the Natal N2 7-9
7.3.1 Description of the samples . . . 7-11
7.3.2 Sample Preparation 7-13
7.3.3 Test methods and procedure . . . 7-13
7.3.4 Results and Discussion 7-14

7.3.5 Recommendations 7-17
7.4 CASE 3: Slip formed concrete: Effect of very early exposure of concrete to drying environments 7-19
7.4.1 Introduction 7-19
7.4.2 Mixes and materials 7-20
7.4.3 Laboratory procedure 7-20
7.4.4 Results and discussion 7-23
7.4.5 Conclusions 7-27
7.5 CASE 4: Ready mixed concretes: Durability effects of a proposed alternative mixing procedure. 7-28
7.5.1 Introduction 7-28
7.5.2 Mixes and Sample Preparation . . 7-29
7.5.3 Results and Discussion 7-31
7.5.4 General discussion 7-35
7.5.5 Conclusions 7-36
List of References 7-38

CHAPTER 8
GENERAL CONCLUSIONS
8.1 Introduction 8-1
8.2 Test Method 8-1
8.3 The Performance of Concretes Tested . . . 8-2
8.4 Future Research Directions 8-4

LIST OF FIGURES

CHAPTER 1

1.1 Schematic section through a reinforced concrete member 1-6
1.2 Mean annual Precipitation for South Africa (from Ref. 8) 1-13
1.3 Seasonal rainfall Distribution (after Shultze[10]) 1-14
1.4 Average annual duration of bright sunshine as a % of possible (after Shultze[10] 1-15
1.5 Average summer temperature distribution (°C) - January (after Shultze[10]) 1-16
1.6 Average winter temperature distribution (°C) - July (after Shultze[10]) 1-16
1.7 Absolute maximum temperature distribution (°C) (after Shultze[10]) 1-17
1.8 Absolute minimum temperature distribution (°C) (after Shultze[10]) 1-17
1.9 Mean RH distributions for selected months of the year (after Shultze[10]) 1-19

CHAPTER 2

2.1 Summary of some of the chemical reactions responsible for concrete deterioration (after Lauer[12]) 2-8
2.2 Two periods in the deterioration of concrete caused by reinforcement corrosion (after Schiessl[13]) 2-9
2.3 The carbonation "front" 2-11
2.4 Range of pore sizes obtained in concrete (after Gowripalan et al[21]) 2-15
2.5 Idealised model of three forms of water movement through a pore in concrete[25] . . . 2-18
2.6 Relationship between the coefficient of permeability and w/c ratio for concretes and

mortars[16] 2-21
2.7 Influence of w/c ratio on the water vapour transmission of concrete (after Henry and Kurtz[29]) 2-22
2.8 Schematic diagram showing the influence of w/c ratio and degree of hydration on the reduction of capillary pore volume[30]. . . . 2-25
2.9 Effect of FA in reducing the volume of pores > 10 nm (after Cabrera[36]) 2-27
2.10 Effect of GGBS in reducing chloride penetration into concrete (after Blundell[44]) 2-30
2.11 Effect of GGBS in reducing expansion due to alkali silica reaction (after Higgins and Uren[45]) 2-31
2.12 Effect of duration of curing on the oxygen permeability of mortars (after Gowripalan et al[21]) 2-34

CHAPTER 3
3.1 Schematic arrangement of the permeability test apparatus developed by Dhir et al[17] using (a) air and (b) water 3-14

3.2 Section through the Leeds University permeameter showing the rubber collar seal[19] 3-15

3.3 Schematic arrangement of the rising pressure head permeameter developed by Schonlin and Hilsdorf[15] 3-16

3.4 Schematic arrangement of the falling head permeameter developed by Blight[20] 3-17

3.5 Schematic arrangement of the falling head permeameter 3-21

3.6 A completed permeameter unit with the cover plate removed 3-21

3.7 Schematic arrangement of the test sample fixed into a PVC ring with epoxy. 3-23

3.8 Detail of the rubber O-ring on the top plate 3-23

3.9 Some of the steps involved in the preparation of the sample for epoxy fixing. 3-25

3.10 Schematic arrangement of a sample ready for epoxy casting 3-26

3.11 Examples of the PVC rings together with a concrete sample epoxy-cast into a PVC ring . 3-26

3.12 Movement of the timber spacer when the perforated cover plate is tied down. 3-28

3.13 Schematic arrangement of the silicone rubber seal assembly 3-29

3.14 Cross section through the mild steel rubber collar mould. 3-30

3.15 Various components of the rubber llar seal arrangement 3-30

3.16 Schematic arrangement of the blank sample used for ensuring the air-tightness of the epoxy/PVC ring sealing method 3-31

3.17 Blank sample used to check the air-tightness of the silicone rubber collar seal 3-32

3.18 Experimental verification of the ratio of pressure heads vs. time relationship 3-39

3.19 Schematic arrangement of Kelham's[30] sorptivity test apparatus 3-45

3.20 Schematic arrangement of the water sorptivity test method for (a) the epoxy/PVC ring sealed samples and (b) for the rubber collar sealed samples 3-47

3.21 A completed epoxy/PVC ring sealed sample ready to be tested for water sorptivity. . . 3-48

3.22 A completed rubber collar sealed sample ready to be tested for water sorptivity 3-48

3.23 Typical plot of the results from a sorptivity test 3-51

3.24 Experimental verification of the sorptivity equation 3-53

3.25 Water absorption of samples tested at three suggested time intervals 3-55

CHAPTER 4

4.1 Effect of sample thickness in relation to aggregate size. 4-3

4.2 Schematic representation of a sample with varying porosity 4-5

4.3 Generalised form of results obtained in a

sorptivity test on the sample shown in Figure 4.2 4-5

4.4 Variation in the covercrete absorption test results with changes in moisture content of the sample (after Lampacher[10]) 4-10

4.5 Variation in moisture profile with time in a concrete sample exposed to air drying (after Ujike and Nagataki[6]) 4-11

4.6 Hypothetical relationship between durability index value and durability performance of concrete. 4-16

4.7 Variation in the rate of mass loss for samples dried at 50 °C 4-22

4.8 Timber tray with plastic sheet for casting concrete slabs. 4-23

4.9 Samples of the stone sizes used in the sample thickness/aggregate size ratio tests. . . . 4-24

4.10 Location of the cores drilled from each concrete slab. 4-27

4.11 Variation in coefficient of permeability with sample thickness to aggregate size ratio 4-28

4.12 Method of cutting, coring and obtaining disc samples from cast beam sections 4-33

4.13 Relationship between average coefficients of variability of permeability measurements and

sample thickness 4-40

4.14(a) Variation in coefficient of permeability with cut sample thickness for mixes with water content of 200 l/m^3 4-43

4.14(b) Variation in coefficient of permeability with cut sample thickness for mixes with water content of 210 l/m^3 4-44

4.15 Method of coring and slicing cubes to obtain samples for testing the influence of drying method on permeability 4-47

4.16 Various components and container sealing method used for the samples dried over silica gel. 4-49

4.17(a) Permeability of samples after various drying methods relative to permeability after 100 °C drying of the OPC samples 4-56

4.17(b) Permeability of samples after various drying methods relative to permeability after 100 °C drying of the OPC/FA samples 4-56

4.17(c) Permeability of samples after various drying methods relative to permeability after 100 °C drying of the OPC/GGBS samples 4-57

4.18(a) Relative sorptivities after various drying phases for samples initially dried over silica gel 4-61

4.18(b) Relative sorptivities after various drying phases for samples initially vacuum dried 4-63

CHAPTER 5

5.1 Grading curve of the modified silica sand in relation to Fulton's preferred grading limits 5-11

5.2 Photograph of sand and stone used, showing particle shape and grading 11

5.3 Arrangement of cube samples on shelves in the drying room 5-17

5.4 Method of cutting and coring cube samples . 5-19

5.5 Concrete cube used for depth of carbonation determination at 10 and 20 months 5-22

5.6 Method of breaking cube segment for depth of carbonation determination 5-23

5.7 Compressive strength of the concretes at 1 and 10 months after casting 5-25

5.8 28 day and 10 month strength vs. w/b ratio curves for the different binders tested . . 5-26

5.9 Permeability vs. extent of moist curing for the P1 concretes 5-31

5.10 The data shown in Figure 5.10 with permeability plotted on a log scale 5-31

5.11 Permeability vs. extent of moist curing for the P2 concretes 5-32

5.12 Permeability vs. extent of moist curing for the P3 concretes 5-32

5.13 Combined results of 28-day oxygen permeability for the OPC concretes 5-33

5.14 Combined results of 28-day oxygen permeability for the FA concretes 5-33

5.15 Combined results of 28-day oxygen permeability for the GGBS concretes 5-34

5.16 Combined results of the 10-month oxygen permeability for the OPC concretes 5-39

5.17 Combined results of the 10-month oxygen permeability for the FA concretes 5-39

5.18 Combined results of 10-month oxygen permeability for the GGBS concretes 5-40

5.19 Combined results of 28-day water sorptivity for the OPC concretes 5-44

5.20 Combined results of 28-day water sorptivity for the FA concretes 5-44

5.21 Combined results of 28-day water sorptivity for the GGBS concretes 5-45

5.22 Combined results of 10-month water sorptivity for the OPC concretes 5-50

5.23 Combined results of 10-month water sorptivity for the FA concretes 5-50

5.24 Combined results of 10-month water sorptivity for the GGBS concretes 5-51

5.25 Carbonation depths of the OPC concretes at different degrees of moist curing 5-55

5.26 Carbonation depths of the FA concretes at different degrees of moist curing 5-55

5.27 Carbonation depths of the GGBS concretes at different degrees of moist curing 5-56

5.28 Samples of the P2 concrete sprayed with phenolphthalein to determine the depth of carbonation 5-56

5.29 Relationship between D_{10} and D_{20} for the FA and GGBS concretes 5-58

CHAPTER 6

6.1 28-day oxygen permeability vs. b/w ratio for the 0-15 mm slices of the three binder type concretes 6-4

6.2 28-day oxygen permeability vs. b/w ratio for the 15-30 mm slices of the three binder type concretes 6-5

6.3 28-day oxygen permeability vs. b/w ratio for the 30-45 mm slices of the three binder type concretes 6-6

6.4 28-day water sorptivity vs. b/w ratio for the 0-15 mm slices of the three binder type concretes 6-8

6.5 28-day water sorptivity vs. b/w ratio for the 15-30 mm slices of the three binder type concretes 6-9

6.6 28-day water sorptivity vs. b/w ratio for the 30-45 mm slices of the three binder type concretes 6-10

6.7 28-day oxygen permeability vs. compressive strength for the 0-15 mm slices of the three binder type concretes 6-12

6.8 28-day oxygen permeability vs. compressive strength for the 15-30 mm slices of the three binder type concretes 6-13

6.9 28-day oxygen permeability vs. compressive strength for the 30-45 mm slices of the three binder type concretes 6-14

6.10 28-day water sorptivity vs. compressive strength for the 0-15 mm slices of the three binder type concretes 6-16

6.11 28-day water sorptivity vs. compressive strength for the 15-30 mm slices of the three binder type concretes 6-17

6.12 28-day water sorptivity vs. compressive strength for the 30-45 mm slices of the three binder type concretes 6-18

6.13(a) Trends of permeability responses of the concretes to changes in the duration of moist curing 6-20

6.13(b) Trends of sorptivity responses of the concretes to changes in the duration of moist curing 6-20

6.14(a) Relationship between the ln(A) coeff. for the permeability results, and the b/w ratio of the concrete 6-23

6.14(b) Relationship between the B coeff. for the permeability results, and the b/w ratio of the concrete 6-24

6.15(a) Relationship between the ln(A) coeff. for the sorptivity results, and the b/w ratio of the concrete 6-24

6.15(b) Relationship between the B coeff. for the sorptivity results, and the b/w ratio of the concrete 6-25

6.16 Permeability predicted using Equations 6.3 to 6.5 compared with the measured permeability values 6-27

6.17 Sorptivity predicted using Equations 6.6 to 6.8 compared with the measured sorptivity values 6-29

6.18 Modelled relationship between permeability and b/w ratio for the various concretes . . 6-31

6.19 Modelled relationship between sorptivity and b/w ratio for the various concretes 6-32

6.20 Variation of sorptivity with depth from a drying surface - OPC concretes 6-34

6.21 Variation of sorptivity with depth from a drying surface - FA concretes 6-34

6.22 Variation of sorptivity with depth from a drying surface - GGBS concretes 6-35

6.23 28-day surface permeability vs. 10-month carbonation for the three binder types . . . 6-37

6.24 28-day surface sorptivity vs. 10-month carbonation for the three binder types . . . 6-38

6.25 28-day surface permeability vs. 20-month carbonation for the three binder types . . . 6-38

6.26 28-day surface sorptivity vs. 20-month carbonation for the three binder types . . . 6-39

6.27 Relationship between permeability and sorptivity for the surface slices 6-43

6.28 Relationship between permeability and sorptivity for all the samples tested . . . 6-44

CHAPTER 7

7.1 Method of estimating the equivalent water curing duration of the curing compound coated samples (after Ballim et al[3]) 7-6

7.2 Early stages of the bridge deck launch . . . 7-10

7.3 View of the piers looking Northwards across the river 7-10

7.4 Average mass loss of the curing compound

coated samples 7-23

7.5 Average mass loss of the uncoated samples . 7-24

7.6 Oxygen permeability of the various concretes for the three exposure conditions 7-25

7.7 Water sorptivity of the various concretes for the three exposure conditions 7-26

7.8 Relative values of permeability and sorptivity for the surface slices 7-32

LIST OF TABLES

CHAPTER 2

2.1 Classification of pore sizes in hydrated cement pastes (after Mindess and Young[22]) . 2-16

2.2 Relationship between permeability, w/c ratio and nominal maximum aggregate size[19] 2-23

2.3 Relationship between heat of hydration and % GGBS in the Binder (after Reeves[46]) 2-32

2.4 Required duration of moist curing for capillary discontinuity (after Powers[53]) . . 2-33

CHAPTER 3

3.1 Results of tests conducted to verify the falling head permeameter equation 3-38

3.2(a) Results of the water sorptivity verification tests - Sample 1 3-52

3.2(b) Results of the water sorptivity verification tests - Sample 2 3-53

3.2(c) Results of the water sorptivity verification tests - Sample 3 3-53

3.3 Results of water sorptivity tests using three suggested time intervals 3-55

CHAPTER 4

4.1 Values of R calculated from data presented by Ujike and Nagataki[6] 4-8

4.2 Time rate of moisture loss of samples drying in the 50 °C oven 4-21

4.3 Combinations of stone size and sample thickness tested 4-25

4.4 Material proportions (kg/m^3) of the various mixes tested 4-26

4.5 Results of the coefficient of permeability (x 10^{-10} m/s) tests conducted on the samples cored from the slabs 4-29

4.6 Mix proportions (kg/m^3) of concretes used to test the influence of cut sample thickness on oxygen permeability measurements 4-31

4.7 Compressive strength results of concretes used to measure the influence of cut sample thickness on permeability 4-34

4.8(a) Coefficients of permeability for the various sample thicknesses of the concretes with water content of 200 l/m^3. 4-36

4.8(b) Coefficients of permeability for the various sample thicknesses of the concretes with water content of 210 l/m^3 4-37

4.9(a) Analysis of the coefficients of variation of oxygen permeability results on the basis of mix characteristics . . 4-38

4.9(b) Analysis of coefficients of variation (%) of oxygen permeability results on the basis of sample thickness 4-39

4.10 Average coefficients of permeability for the various mixes and sample thicknesses after the rejection of outlier results 4-43

4.11 Mix proportions (kg/m^3) of the mixes used for monitoring the influence of drying history on measured oxygen permeability 4-46

4.12(a) Measured oxygen permeability at the end of the various drying phases, for the OPC concretes 4-51

4.12(b) Measured oxygen permeability at the end of the various drying phases, OPC/FA concretes 4-52

4.13 Results of water sorptivity tests conducted after various drying methods 4-62

CHAPTER 5

5.1 Chemical and physical analyses of Dudfield OPC used in the concretes 5-5

5.2 Physical and chemical properties of the GGBS used in the concretes 5-6

5.3 Typical analysis of the fly ash used in the concretes 5-7

5.4 Grading analysis of the -10 mm material as received from the Delmas Silica Mine 5-9

5.5 Grading analysis of the reconstituted silica sand used in the concretes 5-10

5.6 Mix proportions (kg/m^3) of the various

concretes used 5-13

5.7 Measured slump values of the various mixes . 5-14

5.8 Number of cube samples used for the various tests 5-16

5.9 Average compressive strengths of the various concretes at 28 days and 10 months 5-24

5.10 28-day oxygen permeability (x 10^{-10} m/s) of the OPC concretes 5-28

5.11 28-day oxygen permeability (x 10^{-10} m/s) of the OPC/FA concretes 5-29

5.12 28-day oxygen permeability (x 10^{-10} m/s) of the OPC/GGBS Concretes 5-30

5.13 10-month oxygen permeability (x 10^{-10} m/s) of the OPC concretes 5-36

5.14 10-month oxygen permeability (x 10^{-10} m/s) of the OPC/FA concretes 5-37

5.15 10-month oxygen permeability (x 10^{-10} m/s) of the OPC/GGBS Concretes 5-38

5.16 28-day water sorptivity (mm/$hr^{½}$) of the OPC concretes 5-41

5.17 28-day water sorptivity (mm/$hr^{½}$) of the FA concretes 5-42

5.18 28-day water sorptivity (mm/$hr^{½}$) of the GGBS concretes 5-43

5.19 10-month water sorptivity (mm/hr^{½}) of the OPC concretes 5-47

5.20 10-month water sorptivity (mm/hr^{½}) of the FA concretes 5-48

5.21 10-month water sorptivity (mm/hr^{½}) of the GGBS concretes 5-49

5.22 10-month carbonation depths (mm) and carbonation coefficient (mm/month^{½}) of the OPC concretes 5-52

CHAPTER 6

6.1 Equation 6.2 coefficients for the permeability results of the 0-15 mm slices 6-22

6.2 Equation 6.2 coefficients for the sorptivity results of the 0-15 mm slices 6-22

6.3 Values of the λ_1 to λ_4 factors for use in Equations 6.4 and 6.5 6-26

6.4 Values of the λ_5 to λ_8 factors for use in Equations 6.7 and 6.8 6-28

6.5 Values of coefficients λ_9 to λ_{12} for use with Equations 6.9 and 6.10 6-40

CHAPTER 7

7.1 Results of Oxygen permeability and water sorptivity tests 7-5

7.2 Equivalent water curing period of the curing compound treated samples 7-6

7.3 Estimated rate of carbonation for the curing compound treated concretes and an equivalent OPC/fly ash concrete 7-8

7.4 Physical Condition of the Cores as Received 7-12

7.5 Average Results of Sample density and Compressive Strength Tests 7-15

7.6 Average Results of Oxygen Permeability Coefficient, Water Sorptivity and Carbonation Depth Tests 7-16

7.7 Mix proportions (kg/m^3) and slump measurements of the concretes tested 7-20

7.8 Results of compressive strength tests . . . 7-27

7.9 Mix proportions (kg/m^3) for the various mixes tested 7-30

7.10 7- and 28-day compressive strength results 7-30

7.11 Permeability and sorptivity results for all the concretes tested 7-32

7.9 Relative values of permeability and sorptivity for the internal slices 7-34

7.10 Relationship between strength and oxygen permeability for the concretes tested . . . 7-35

CHAPTER 1

GENERAL INTRODUCTION - THE NEED FOR RESEARCH ON CURING

1.1 Cement Hydration and the Effect of Curing

The hydration of cement is a process in which the compounds in cement are transformed by chemically reacting with water. This transformation results in the individual cement particles being mechanically bound together, producing a material mass with excellent strength and durability characteristics. There are four important compounds in cement which act as the binding agents when water is added. These are[1]:

- tricalcium silicate (C_3S)
- dicalcium silicate (C_2S)
- tricalcium aluminate (C_3A)
- tetracalcium aluminoferrite (C_4AF).

When water is added to cement, the C_3S starts hydrating first and is mainly responsible for the early strength of the cement paste. Most of the C_3S is hydrated after approximately one month of exposure to water. The other compounds hydrate more slowly and contribute to later strength. For example, C_2S requires approximately one year of constant exposure to water to be substantially hydrated. The point to be noted here is that the hydration process requires a considerable time and constant access to water to be advanced.

The continued hydration of cement also improves the impermeability of the cement paste. At a micro level, the products of hydration are deposited in the pores and the permeability is reduced by decreasing the pore size and the degree of interconnection between pores. At a macro level, continued hydration decreases the

extent of shrinkage cracking of the concrete. This is of fundamental importance to the durability of the material, since the permeability of concrete determines the ease with which aggressive elements may enter the concrete and advance deterioration[2]. Clearly, the promotion of hydration in concrete has beneficial implications for both strength and durability.

It is very difficult to achieve full hydration in concrete[3]. As hydration proceeds, the deposition of the hardening products of hydration, calcium silicate hydrate or C-S-H gel, makes the access of water to unhydrated zones increasingly more difficult. Even under the most favourable conditions, a small proportion of the cement remains unhydrated for long periods of time. Also, it is thought that with w/c ratios less than approximately 0.42, the hydration reaction requires more water than is readily available in the pores and this may cause self desiccation in localised areas. In this case, a considerable amount of cement remains unhydrated despite adequate curing conditions being provided on the surface of the concrete member.

Hence, rather than full hydration, it is more appropriate to refer to the "required extent" of hydration which is based on the requirements of service to which the concrete is to be exposed. If correctly designed, there will be sufficient water in the original mix to ensure that the required extent of hydration takes place. In practice, however, much of this water can be lost by evaporation from the concrete surface and must be replaced or prevented from evaporating if hydration is to continue. An important part of the process of curing is therefore to prevent the loss of water from the microstructure of the

hydrating cement phase.

The need for continuous curing is most critical during the first few days after the concrete has been cast. When curing is interrupted in this period and the cement paste is allowed to dry out, hydration of the cement ceases. More importantly, it becomes difficult to get water back into the pore structure upon subsequent wetting in order to re-activate the hydration process. This is caused by the following developments which take place when the concrete dries out[4]:

- the pore water is saturated with calcium hydroxide ($Ca(OH)_2$) and when the water evaporates, this $Ca(OH)_2$ is deposited in the pore structure near the surface of the concrete;
- the $Ca(OH)_2$ reacts with atmospheric carbon dioxide to form poorly soluble calcium carbonate ($CaCO_3$) which occupies a larger volume than the original $Ca(OH)_2$;
- this volume increase, together with the fact that $CaCO_3$ is considerably less soluble than $Ca(OH)_2$, reduces the access of water back into the pore structure.

In this way, when concrete is allowed to dry, pockets of unhydrated cement are created which are surrounded by hydrated material and pores blocked with $CaCO_3$. Because of their inaccessibility to water, these pockets of cement will not be hydrated when the concrete is re-wet and they serve only as expensive fine aggregate particles. Hence the quality of concrete exposed to intermittent cycles of wetting and drying during the early stages of hydration, will be inferior to that of continuously moist cured concrete.

1.2 The Need for Research on the Influence of Curing

1.2.1 Changing conceptions of the role of curing

The Highway Research Board[5] defines concrete curing as:

> *"The process of maintaining a satisfactory moisture content and a favourable temperature in concrete during the period immediately following placement so that hydration may continue until the desired properties are developed to a sufficient degree to meet the requirements of service"*

In this definition, curing is seen as an active process, involving the maintenance of adequate moisture and temperature conditions to encourage cement hydration. As discussed above, this process is mainly necessary during the period immediately after casting.

It should be noted that the definition calls for concrete to be cured until the properties of the material have developed sufficiently to meet the requirements of service. The onus is therefore placed on designers of concrete structures to understand the "requirements of service" and specify the duration of curing accordingly. This approach assumes that the designer understands the relationship between the duration of curing and the development of concrete properties.

For the designers of concrete structures, "development of concrete properties" has, for a long time, been measured as the development of the compressive strength. Hence, curing was seen as a process which

develops the load carrying capacity of a concrete structure, with properties such as durability being catered for "by default".

A review of the Highway Research Board's concrete curing bibliography[6] shows that, of the research items annotated for the period 1925 to 1960 under the heading "Significance of Curing", only 17% mention the influence of curing on the durability performance of concrete. The remaining items are concerned mainly with the development of strength and other bulk engineering properties of the material. This view of the role of curing ignores the equally important influence that curing has on the durability of concrete.

In this context, durability can be defined[7] as:

> *"..the capability of maintaining the serviceability of a product, component, assembly or construction over a specified time."*

while serviceability is defined as:

> *"..the capability of a building product, component, assembly or construction to perform the functions for which it was designed or constructed."*

When applied to concrete, the concept of durability, as a recognisable property of the material, should be considered in relation to the nature of the environment of exposure. This derives from the varied nature of the agencies and mechanisms by which concrete is deteriorated. However, in the context of this discussion, the term is used to refer to the ability for the material to resist deterioration in a general sense, given the types of environments to which concrete would normally be exposed.

The importance of curing in developing the durability

of concrete can be shown by considering the schematic in Figure 1. This figure shows a cross section through a reinforced concrete member divided into two zones termed "covercrete" and "heartcrete".

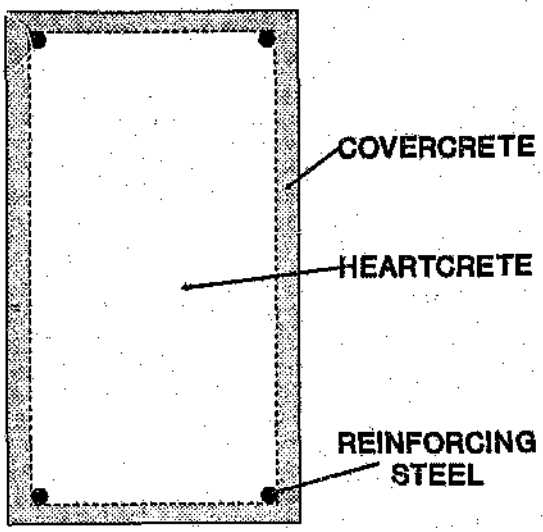

Figure 1.1 Schematic section through a reinforced concrete member

Covercrete, or zone of cover concrete, is the concrete between an external surface of the member and the reinforcing steel closest to that surface. The main function of the covercrete is to act as a barrier between the external environment and the underlying heartcrete and reinforcing steel. Since most forms of concrete deterioration are associated with the movement of aggressive ions from the external environment into the concrete, the covercrete primarily serves a durability function.

On the other hand, the function of the heartcrete is to provide mechanical strength and dimensional stability to the member. If the member is exposed to drying conditions, the detrimental effects of moisture loss on

cement hydration are first experienced by the covercrete. Hence, loss of moisture from concrete first manifests itself as a decrease in the durability of the material. The relative effects of drying on the heartcrete and covercrete, and therefore on strength and durability, depend on the surface area to volume ratio of the member. In a thin concrete section, both strength and durability can be considerably impaired by the effects of drying.

However, with most structural concrete members, the heartcrete will always retain some moisture. The drying gradient in this zone is generally not large enough to force all the water to migrate from the inside of the member to the surface. Strength development in the heartcrete can therefore continue despite evaporation from the surface. In these instances, it is clear that a lack of curing has a greater effect on durability than on strength. This fact is borne out by the relatively large number of durability failures experienced by the building and construction industry in comparison with failures resulting from inadequate strength. Carrier[8] summarises this by noting that:

> *"...even with no curing in a severe exposure only the upper 1.5 inch (38 mm) of concrete dries below the 80% (RH) value....This is why compressive test cylinders can be cured in very unfavourable conditions and still not show much strength loss. Only the near-surface concrete is weakened by poor curing."*

Under present practice, the strength of concrete, determined in the laboratory using cores retrieved from the in-situ structure or specially manufactured cubes,

is generally considered an adequate measure of the structural integrity and, by implication, the durability of the concrete. Design requirements are often based on strength considerations with the understanding that durability requirements would automatically be catered for. The distinction drawn above between covercrete and heartcrete shows the inadequacy of this approach. The current methods of testing for strength give no indication of the potential durability of the concrete because the curing of the in-situ concrete, and hence the condition of the covercrete, is not accounted for.

The discussion presented above shows that curing should be considered primarily for its influence on durability rather than the development of bulk engineering properties. Hence, considering the Highway Research Board's definition of curing[5] presented above, designers are expected to understand the influence of curing on the development of the covercrete zone of concrete in order to specify the duration and method of curing. A need has therefore been recognised for research to be focused towards developing an understanding of the relationship between curing and durability of concrete. Recent research on the subject has recognised this need and a considerable amount of work has already been done (see Chapter 2).

1.2.2 Developments in concrete materials, design and construction technology

The past few decades have seen major advances in the effectiveness with which concrete is used as a construction material. Improved design procedures, better and more consistent quality of cement and a

greater understanding of the engineering performance of the material has led to increased strength-to-weight ratios of structural elements. Added to this, construction techniques are developing to allow concrete structures to be completed in increasingly shorter time periods. Waste materials, such as fly ash (FA), ground granulated blastfurnace slag (GGBS) and silica fume have become commonplace in concrete applications. The general use of "workability-enhancing" admixtures have also caused reductions in the cement content required to achieve target strengths.

These developments are all to be encouraged as they are aimed at optimising the use of resources which are now recognised as not being inexhaustible. Current developments in this area of concrete technology means that we will increase the effectiveness with which we use the material in future.

However, these developments also mean that concrete structures are now more sensitive to bad curing practice than in the past. Given the discussion presented above, this also means that concrete structures are now more durability-sensitive. The main factors accounting for this problem are:

- Reduced OPC contents caused by the use of plasticisers and blends of cement extenders, means that there is less active material to resist the advance of certain deterioration mechanisms;
- The use of thin structural members means that a greater proportion of the member is affected by early drying, which causes the hydration process to be interrupted.
- Reduced cement contents required to achieve target strengths mean that there is less "spare capacity"

to ensure an acceptable quality of surface concrete despite the hydration process being interrupted.

- The slower rate of hydration of FA and GGBS blended with OPC, makes these materials more sensitive to abuse, especially during the early stages after casting.

These developments therefore present new durability challenges which must be met with a clear understanding of the influence of procedures like early-age curing in ensuring long-term durability.

1.2.3 The need for local information on the subject

Most of the research on the influence of curing on durability has been conducted in the developed countries of the Northern hemisphere. The problem with importing these research conclusions to Southern Africa is that the materials, concretes and applications of concrete technology are different for the two regions. Also, as Bentur[9] notes, much of this research is conducted in environments which would be considered as "mild" environments in Southern Africa.

There is therefore a need for research on the influence of curing on concretes made with local materials under local exposure conditions. Also, in developing a relationship between curing and durability, emphasis needs to be placed on the dominant mechanisms of deterioration encountered locally.

1.2.4 Development of specifications

Because of an incomplete understanding of the influence of curing on the properties of concrete, specifications

for concrete construction have been forced to resort to "method specification" in dealing with curing aspects. With this approach, the contractor is instructed as to the method and duration of curing to be employed on the project. The method of curing is usually selected on the basis of practicality and, where appropriate, the duration of curing is related to the environmental temperature during the early stages after casting.

The main problem with this approach is that there is no means of verifying that the specified method has been sufficiently effective or that it has adequately been adhered to by the contractor. Also, specifications for curing are generally written without consideration for the degree of aggressiveness of the environment to which the structure is to be exposed. For example, the same curing requirements are usually set for structural elements exposed outdoors or indoors. This uncertainty regarding its usefulness encourages a negligent attitude towards curing in practice.

A good example of the extent of this uncertainty is provided by the recently published SABS Code of Practice[10] on the use of structural concrete. In Section 10.8.1.2, of Part II, the contractor is given the option of curing the concrete using any one of a list of methods, which include water ponding or spraying, curing compounds, steam curing or plastic wrapping. In so doing, a statement is made regarding the equivalent curing effectiveness of each of these methods, assuming the correct procedure is followed in each case. Preliminary evidence presented by Ballim et al[11] shows that this is an unrealistic assumption.

The same Code of Practice goes further to specify a minimum duration of curing. This approach is confusing

since, if the contractor opts to use a curing compound, a concept of minimum duration of curing is superfluous. It is also unrealistic to expect that steam curing be maintained for the same duration as water curing.

There is clearly a need for the relative effectiveness of these different curing methods to be established through testing. This will allow for more effective specification and control of curing procedures for concrete construction.

However, the problem discussed above arises as a result of our inability to quantify the durability effect of different curing procedures on concrete. This problem was recognised as long ago as 1938 by Crum[12] who noted:

> *"We should be able to analyse a sample of concrete, say at seven days, ... and tell whether or not it had been subjected to favourable influences during that period. But before this can be done, means must be found to recognise the evidence of favourable conditions."*

1.3 The Southern African Climate and the Need for Curing

As was mentioned earlier, the climate in the Southern African region is considered to be harsh from the point of view of concrete curing. Climatic conditions range from humid, subtropical areas in the Eastern coastal and near-coastal areas, to arid and semi arid areas which make up the largest part of the country[13,14]. The Dept. of Water Affairs' report on the water resources of South Africa[13] states:

> *"There are only a few isolated areas in South Africa where the average annual potential*

evaporation is less than the average annual rainfall."

This statement gives an indication of the need to protect concrete from early drying in this region.

In order to characterise the effect of climate in the region on early drying of concrete, appropriate climatic factors are discussed in more detail below. The intention is to present a general view of the severity of the climate rather than to give specific detail on the drying effects on concrete.

1.3.1 Rainfall

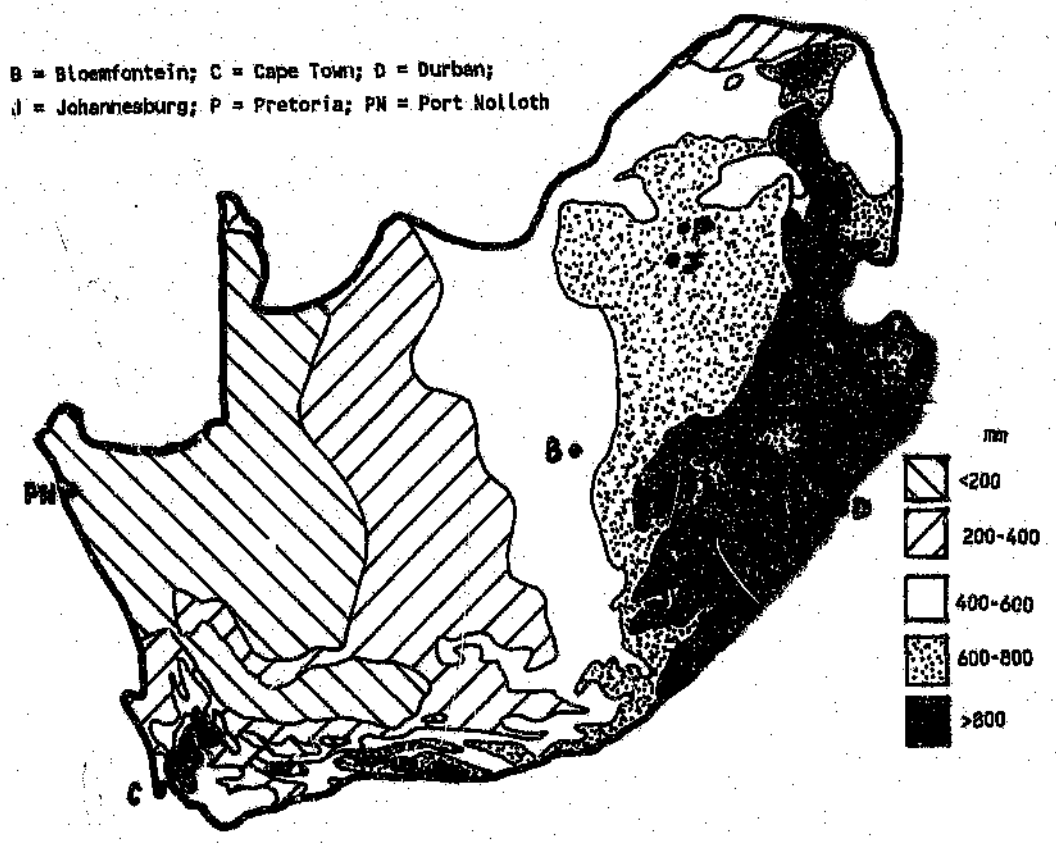

Figure 1.2 Mean annual Precipitation for South Africa (from Ref. 13)

Figure 1.2 shows the distribution of mean annual precipitation over South Africa[13]. It can be seen that mean rainfall ranges from <200 mm/yr in the Western parts (eg. 58 mm/yr at Port Nolloth), to >800 mm/yr in the Eastern parts (eg. 3000 mm/yr in some parts of Northern Natal).

An important feature of the rainfall in this region is that it follows an annual cycle and is almost entirely a summer phenomenon[14,15]. This is shown in Figure 1.2, which presents the distribution of summer (October to March) rainfall as a percentage of the average annual rainfall. It is only the South-Western Cape region which experiences most of its rain during the winter months.

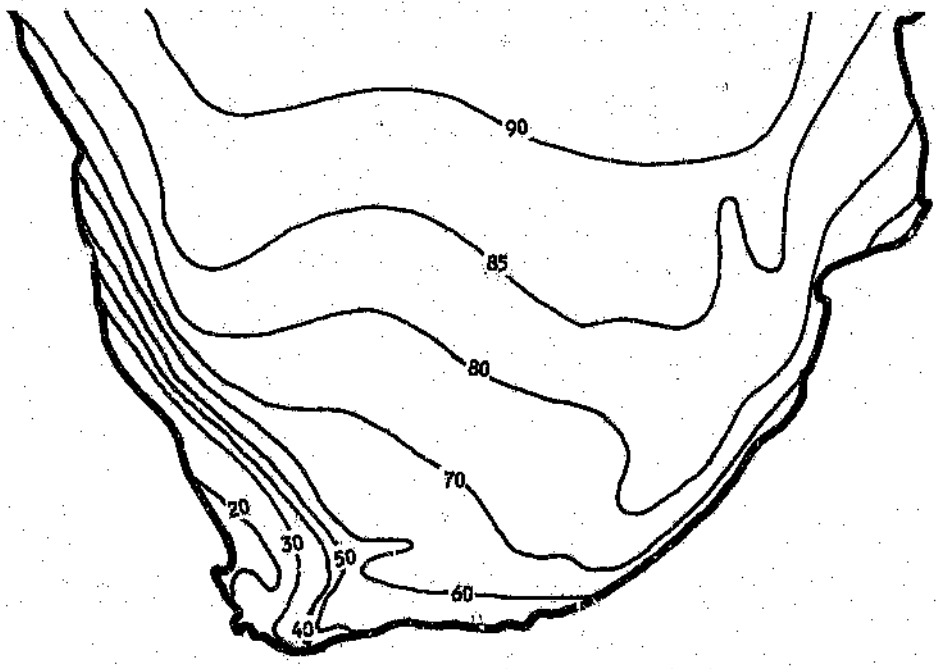

Figure 1.3 Seasonal rainfall Distribution (after Shultze[15])

1.3.2 Duration of bright sunshine

Figure 1.4 shows the annual duration of bright sunshine over the region, expressed as a percentage of the possible sunshine duration. It can be seen that, except at the coastal areas, this value rarely drops below 60%. The low values along the West coast, particularly in Namibia, can be ascribed to persistent fog and low cloud which do not penetrate far inland. This figure shows that, for most of the region, there is a high probability that concrete cast during the day will be exposed to bright sunshine conditions.

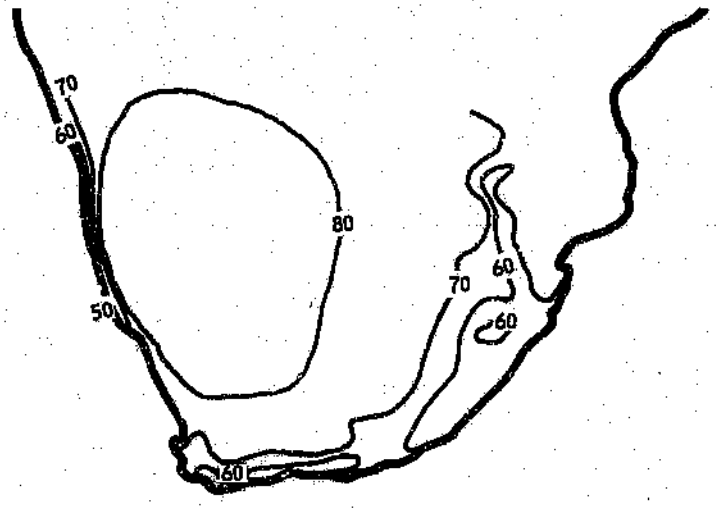

Figure 1.4 Average annual duration of bright sunshine as a % of possible (after Shultze[15])

1.3.3 Temperature

The early-age curing requirements of concrete are significantly affected by ambient temperature. High temperatures indicate the need to prevent drying, while low temperatures mean that the concrete may require a longer curing period or protection against freezing.

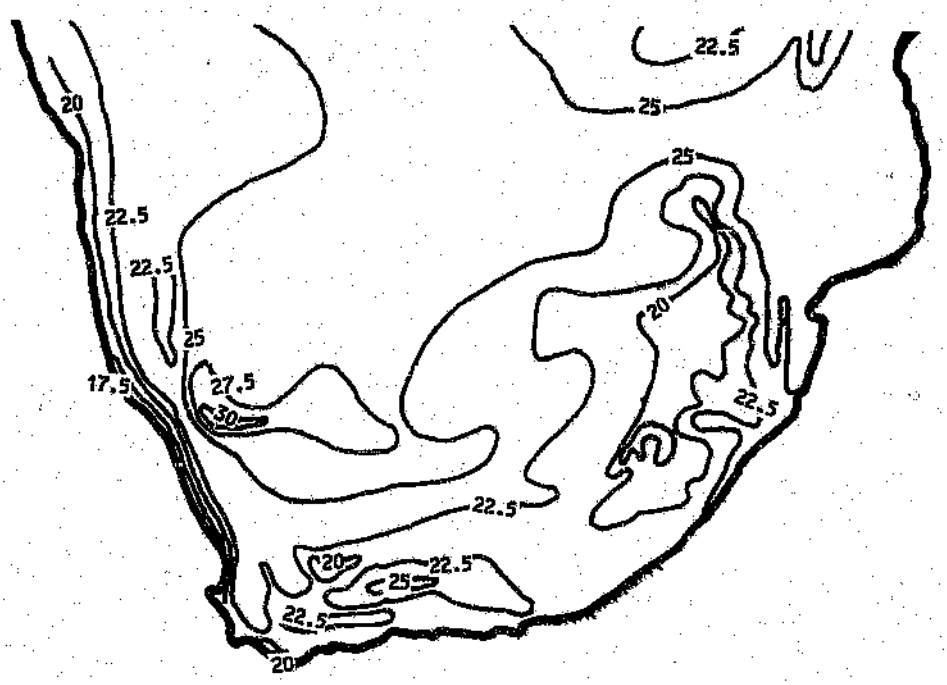

Figure 1.5 Average summer temperature distribution (°C) - January (after Shultze[15])

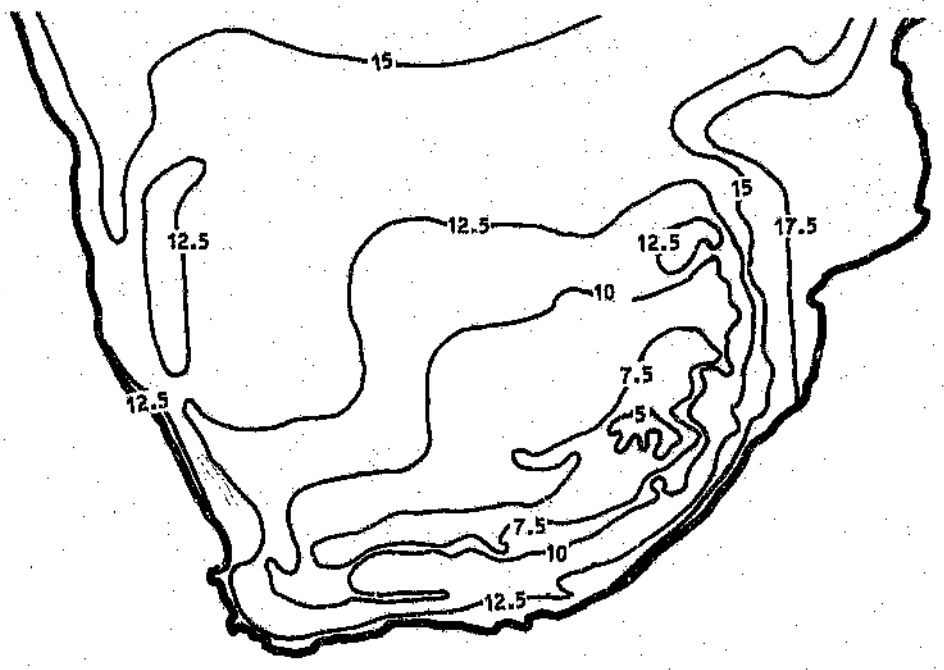

Figure 1.6 Average winter temperature distribution (°C) - July (after Shultze[15])

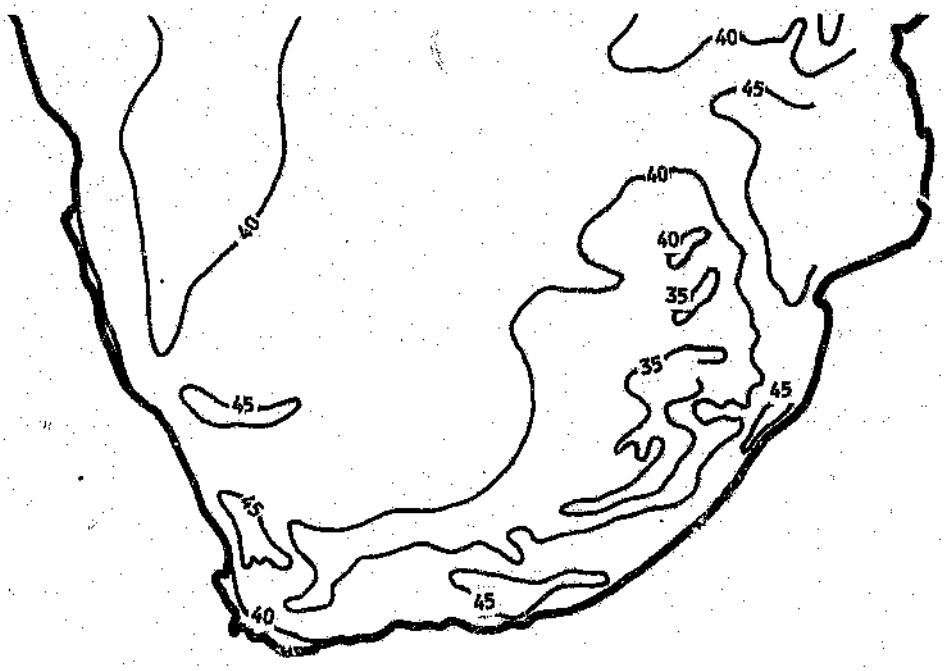

Figure 1.7 Absolute maximum temperature distribution (°C) (after Shultze[15])

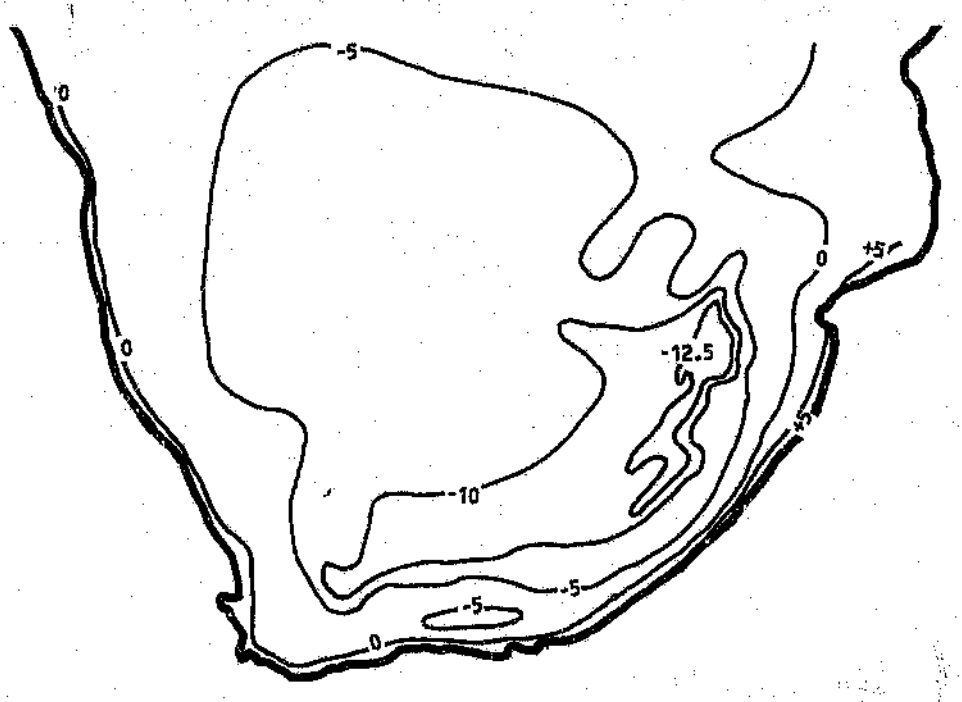

Figure 1.8 Absolute minimum temperature distribution (°C) (after Shultze[15])

Figures 1.5 and 1.6 give an indication of the average summer (January) and winter (July) temperature distributions respectively. It can be seen that the summer temperatures are generally above 20 °C, while the winter temperatures are generally below 15 °C.

Figures 1.7 and 1.8 show the distribution of absolute maximum (hottest day) and minimum (coldest night) temperatures respectively. It can be seen that most of the country experiences temperatures greater than 40 °C as a maximum and lower than -5 °C as an absolute minimum temperature.

1.3.4 Relative humidity

Figures 1.9 (a) to (f) show the distribution of monthly average relative humidity (RH) measured at 14h00 for alternate months over the year. These show that the coastal regions rarely experience RH values below 60%. On the other hand, the western and central interior of the region regularly experience RH values of 30% and lower, especially during the winter months.

1.3.5 General comment

The discussion on the nature of the weather and climate in Southern Africa shows that large parts of the region are characterised by hot, dry conditions with a high frequency of bright sunshine periods. For the most part, rain periods are almost entirely a summer phenomenon.

The risk of premature drying of concrete in these conditions is high and indicates the need for careful attention to be paid to moist curing during the early period after casting.

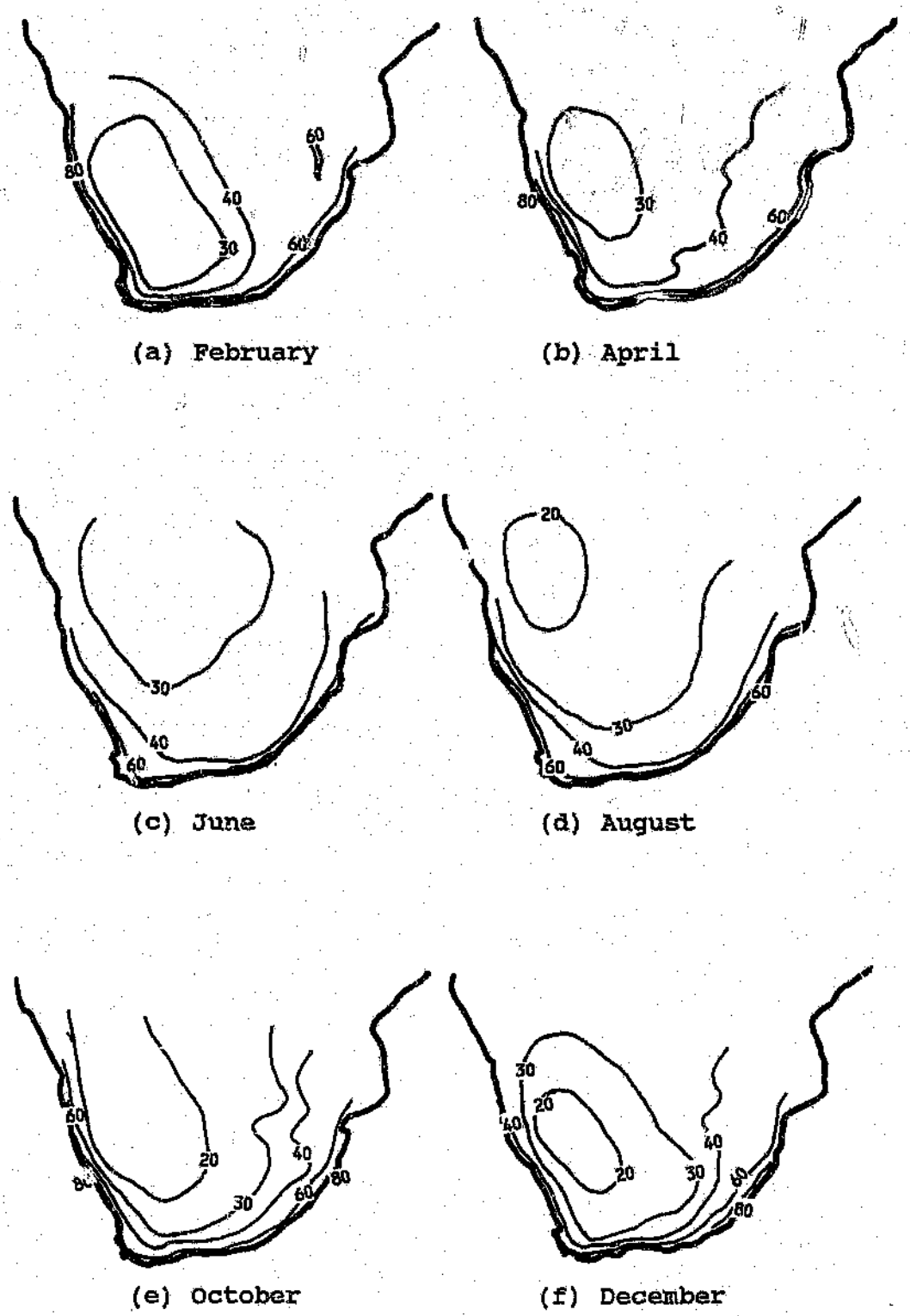

Figure 1.9 Mean RH distributions for selected months of the year (after Shultze[15])

An understanding of the significance of this need and its implications for long-term durability of concrete structures, must therefore be developed through further research. It is also important that this research be conducted using local materials and conditions.

1.4 Definition of Terms

Broad definitions of durability and curing have been presented above. However, in order to provide clarity, some further terms used in this dissertation require definition at this stage. These are presented below.

1.4.1 Durability index

The durability index of a particular concrete is the result of a test intended to measure the development of the quality of concrete in the covercrete zone. The test usually measures some fluid transport property of this zone of the structure on the basis that this is related to deterioration mechanisms associated with concrete.

1.4.2 Durability performance

Durability performance refers to the extent to which a concrete resists deterioration when exposed to an actual aggressive environment. This performance could be under natural or accelerated aggressive conditions. The means of characterising the durability performance varies with the nature of the aggressive agent and the mechanism of deterioration.

1.4.3 Potential durability

This indicates the durability performance to be expected of a particular concrete on the basis of tests conducted at a relatively early age (usually 28 days). The tests referred to are those which quantify the development of concrete quality in the covercrete zone and are therefore, not direct durability tests.

The concept of potential durability is also considered separately from the aggressive nature of the environment. Hence, potential durability must ultimately be related to actual durability performance in situ, for the concept to be useful in durability studies.

1.5 Project Scope and Layout of this Dissertation

The investigation reported in this dissertation mainly involves the development of a means for characterising the influence of curing on the potential durability and durability performance of concrete. In particular, test methods were developed for measuring the fluid transport properties of the covercrete zone, so that these properties could be used as the means for characterisation.

These test methods were then used to monitor the influence of different curing methods on the potential durability of various concretes. The following binder types were used in preparing these concretes:

- plain OPC;
- 70%/30% blend of OPC and fly ash;
- 50%/50% blend of OPC and ground granulated blastfurnace slag.

The tests included a range of three concrete strength grades using each of the binder types. The durability performance of these concretes was based on measurements of the depth of carbonation of samples exposed in the laboratory.

Chapter 2 of this dissertation presents a discussion of the mechanisms of some of the dominant agencies by which concrete is deteriorated. A survey of the literature on deterioration, durability and curing is also presented in Chapter 2.

The development of the characterisation test methods is discussed in Chapter 3, while an assessment of the variables influencing these test methods is presented in Chapter 4. Details of the laboratory investigation using the test methods to characterise the influence of curing on potential durability, are presented in Chapter 5. This chapter also presents the results analyses of this investigation.

In Chapter 6, the results generated in the laboratory investigation are used to develop a generalised approach to the influence of curing. An attempt is made to mathematically model the response of different concretes to changes in the curing regime.

Chapter 7 presents a series of case studies in which the test apparatus or the concepts developed in this investigation were used to solve actual concrete problems. Four case studies are presented here and they are aimed at underlining the usefulness and limitations of these test methods and approaches.

Where appropriate, specific conclusions and a list of references are provided at the end of each chapter.

Finally, Chapter 8 provides a list of the important general conclusions associated with the complete project.

1.6 Apologia

As with many other aspects of South African life, a transition is presently taking place in the field of concrete technology in South Africa. People involved in the concrete industry are being asked to move away from the cement/water (c/w) ratio form of expression to the internationally more acceptable water/cement (w/c) ratio form.

In some way, this thesis reflects this transition in that both forms are used. When the ratio is used to identify a "characteristic" of a particular concrete mix, the w/c ratio form is employed. However, in Chapter 6, where the ratio is used as a controllable variable of the mix, against which other parameters can be measured, the c/w ratio form is employed. This was done because the graphical and mathematical relationships were easier to conceptualise and manipulate when the c/w ratio form was used.

List of References

1. Lea, F.M. *The chemistry of cement and concrete*. 3rd Edition. Edward Arnold, London. 1970.

2. Addis, B.J. (Ed.) *Fulton's concrete technology*. 6th Edition. Portland Cement Institute. Midrand, South Africa. 1986. Chapter 8.

3. R.H. Mills. Ultimate hydration of water cured

cement pastes. *The Civil Engineer in South Africa*, Nov. 1965. pp. 253-264.

4. Concrete Society of Southern Africa. *Concrete curing: Description, method and control*. CSSA, Midrand. South Africa. 1991.

5. Highway research Board. *Curing concrete pavements*. Current Road Problems No. 1-R (Revised Ed.). Washington, 1952.
6. F. Slate. *Curing of concrete: 1925-1960*. Highway Research Board Annotated Bibliography No. 32. Washington, 1963.
7. American Society for Testing and Materials. *Annual book of standards*. Part 18, ASTM E632-78. Philadelphia, 1978.
8. Carrier, R.E. Concrete curing tests. *Concrete International*. April, 1983. pp. 23-26.
9. Bentur, A. *Curing and the need for durability testing*. Proceedings of Workshop on: Aspects of Testing Concrete for Durability. Ballim, Y and Alexander, M.G. (Eds.) University of the Witwatersrand, Johannesburg. Oct. 1991. pp. 1-4.
10. South African Bureau of Standards. Code of Practice: *The structural use of concrete*. SABS 0100: Part 2: Materials and execution of work. Pretoria, 1992.
11. Ballim, Y, Taylor, P.C. and Macdonald, H.K. *A preliminary assessment of the effectiveness of liquid membrane-forming curing compounds*. Concrete Beton, No. 66, Jan. 1993. pp. 25-26.
12. Crum, R.W. *Current problem - Curing of concrete*. Highway Research Abstracts, No. 51, June 1938. pg. 10.
13. Department of Water Affairs. *Management of the water resources of the Republic of South Africa*.

Pretoria, 1986.

14. Tyson, P.D. *Climatic change and variability in South Africa*. Oxford University Press. Oxford, UK. 1986.

15. Shultze, B.R. *Climate of South Africa: Part 8: General Survey*. South African Weather Bureau Report WB28. 5th Edition, 1984.

CHAPTER 2

CONCRETE DETERIORATION IN RELATION TO ITS PROPERTIES: A LITERATURE SURVEY

2.1 Introduction

A large volume of literature exists on the subjects of concrete curing and durability and a selected survey of this literature, as appropriate to the present study, is presented in this chapter. The literature reviewed was organised into the following categories and is presented in this order:

a) A general discussion of the dominant agencies and mechanisms responsible for concrete deterioration.

b) The properties of concrete responsible for limiting deterioration, thus enhancing durability. A discussion of the intrinsic factors affecting the development of these properties is also included here.

c) The curing process and its effect on the development of surface microstructure and the durability performance of concrete.

d) Current approaches in specifications for concrete durability.

Where available, preference was given to "state-of-the-art" reports which draw on past literature and present the information in a more accessible form. Also, a number of the publications reviewed straddle two or more of the subject categories listed above. Where this has occurred, an attempt has been made to adequately cross-reference the publication between the appropriate categories.

2.2 Dominant Agencies and Mechanisms of Deterioration

Far from being an indestructible material, concrete can be deteriorated by a number of agencies and mechanisms, many of which are well documented and the processes of deterioration fairly well understood. This section presents a general overview of the different forms of deterioration and an attempt is made to group the various aggressive agencies according to the mechanism of deterioration.

The two broad categories of concrete deterioration are:

- Chemical deterioration: constituents of the concrete undergo chemical reactions which lead either directly to the destruction of the material or set up expansive forces, causing deterioration through extensive cracking.
- Physical deterioration: here the concrete is deteriorated by the direct application of forces on the surface of the structural element. This category includes external forces causing surface erosion as well as "intra-pore" forces caused by the freezing of water or the crystallisation of salts.

2.2.1 Chemical deterioration

The role of calcium hydroxide ($Ca(OH)_2$), formed during the hydration of cement, is important to an understanding of the chemical deterioration of concrete. Using idealised cement hydration reactions[1] and typical cement compositions, it can be shown that, on complete hydration, 100 kg of OPC produces approximately 25 kg of $Ca(OH)_2$. While having no binding

capacity, this $Ca(OH)_2$ contributes significantly to the high pH of the concrete pore water, typically at 12,5. This high pH of the pore water ensures passivation of any embedded reinforcing steel against corrosion and stabilises the calcium silicate hydrates[1,2] (C-S-H), the main binding agents of cement. As will be discussed below, the maintenance of this pH level in the pore fluid of the concrete is important to the long-term durability of the material.

There is a wide range of chemicals[3] which are aggressive to concrete and the mechanisms of deterioration are equally varied. A general categorisation of the chemical deterioration agents and mechanisms is presented below. The following points should be noted with regard to the categories presented:

- there are often "grey areas" in which a particular deterioration form cannot be placed in one of the categories with certainty. For example, the oxidation of pyrites in the aggregates in concrete is a problem of incompatibility which results in sulphate attack;
- there is often more than one category of deterioration operating at the same time. For example, concrete in contact with soft water containing dissolved carbon dioxide, is deteriorated simultaneously by leaching and acid attack.

Dissolution of the products of cement hydration

The products of cement hydration are dissolved and leached out of the concrete causing the destruction of calcium silicate hydrate (C-S-H) gel with a concomitant loss of concrete strength. Dissolution of ($Ca(OH)_2$) from concrete by pure or soft water is typical of this

form of deterioration.

Eglinton[4] and Ballim[5] have prepared state-of-the-art reports on this form of deterioration. The dissolution and removal of $Ca(OH)_2$ from the surface of the concrete leads to instability and decomposition of the C-S-H gel. The attacked surface of the concrete loses its strength capacity and is easily removed to expose fresh surfaces for attack.

A new mechanism of this form of "leaching" attack has been noted by Leroy[6]. In studying the rapid deterioration of a buried asbestos-cement pipe, it was noted that, despite the quality of the water being the same on the inside and outside of the pipe, only the outside was severely deteriorated. It was concluded that the deterioration was caused by the adsorption of calcium ions in the cement by clay minerals in the soil surrounding the pipeline. It was found that the potential for leaching calcium from the cement was influenced by:

- the type of clay mineral;
- temperature;
- concentration gradient between the water solutions of the cement paste and the surrounding soil;
- the pH of the soil.

Exchange reactions between acids and components of hardened cement paste.

Because of its generally alkaline nature, the products of hydration as well as unhydrated cement react with acids causing corrosion of the concrete matrix. This form of deterioration starts from the surface and continues into the concrete until all the acid or the cement paste has been consumed.

The degree of aggressiveness of the acid to concrete is determined by both the pH of the acid solution and the nature of the anion associated with the H^+ ion. For example[7], concrete deterioration in phosphoric acid is slow because the calcium compound formed in the reaction with the acid is poorly soluble in water and is therefore not readily removed from the concrete surface. On the other hand, concrete is rapidly deteriorated in sulphuric acid because the anion also participates in sulphate attack reactions (discussed below), which accelerate the ingress of the acid into the concrete.

Conversion of the products of hydration by external agents with associated expansive forces causing deterioration.

External aggressive agents enter the pore structure of the concrete and through crystallisation or reaction with the products of hydration, set up expansive forces which cause cracking and mechanical destruction of the concrete. The effect of sulphates on concrete is an example of this form of deterioration.

The deterioration effect of sulphates on concrete occurs through a fairly complex mechanism which involves a number of secondary processes. The major cause of deterioration is sulphoaluminate corrosion which occurs as follows[8,4]:

$$\underset{\text{Monosulphoaluminate}}{C_4A\bar{S}H_{12}} + \underset{\text{Gypsum}}{2C\bar{S}H_2} + \underset{\text{Water}}{16H} \rightarrow \underset{\text{Ettringite}}{C_6A\bar{S}_3H_{32}}$$

where: C = CaO, A = Al_2O_3, $\bar{S}$ = SO_3 and H = H_2O.

This reaction is accompanied by a large increase in solid volume, causing internal stresses which lead to cracking. The cation accompanying the sulphate ion can

affect the aggressiveness of the sulphate. Ammonium and magnesium sulphate are particularly aggressive because these cations also participate in deleterious reactions with $Ca(OH)_2$ in the hardened cement paste (hcp)[9].

Internal processes of deterioration.
Incompatibilities between the constituents of the concrete or effects of the methods of concrete production, produce secondary products internally which cause the concrete to deteriorate. This deterioration process usually requires only water to be supplied to the reaction site. This water is mainly supplied from the outside of the concrete but there can sometimes be sufficient internal moisture to significantly advance the deterioration. Alkali aggregate reaction is typical of this form of deterioration.

Three types of alkali aggregate reaction have been identified[10]:

- *Alkali-silica reaction:* this is a reaction between the alkalies in the cement and the microcrystalline phases of silica found in many aggregate types. This is the most commonly encountered form of the reaction.
- *Alkali-carbonate reaction:* carbonate aggregates like dolomite and limestone usually produce good quality concrete with premium strength characteristics. However, some forms of dolomitic limestone have been found to produce expansion in concrete resulting in surface map cracking. This reaction is different from alkali-silica reaction because of the absence of reaction products and is therefore not detected visually or with an optical microscope.

  The reaction involves a de-dolomitization of the

aggregate which is chemically expressed as:

$$CaMg(CO_3)_2 + 2MOH \rightarrow Mg(OH)_2 + CaCO_3 + M_2CO_3$$

where M = K or Na.

The mechanism of expansion due to alkali-carbonate reaction is not clearly understood but it appears to be an interaction of texture, calcite/dolomite ratio and the presence of clay minerals in the aggregate. This lack of understanding means that it is difficult to predict the potential expansion of particular aggregates.

- *Alkali-silicate reaction:* this form of the reaction has been identified fairly recently and has not yet obtained general acceptance as a separate category of alkali aggregate reaction. It manifests itself differently from alkali-silica reaction in that no correlation exists between the magnitude of expansion and the amount of gel formed, has a very slow rate of expansion and occurs in the absence of some of the minerals known to promote alkali silica reaction.

A further mechanism of deterioration caused by an internal process is the expansion resulting from delayed ettringite formation[11,12]. In this case, concrete products made with high early-strength cements and steam cured at temperatures greater than 75 °C, may subsequently exhibit abnormal expansions. The expansion is associated with the delayed formation of ettringite (see above) in the hcp and may take many years to manifest itself in cracking of the concrete.

The deterioration mechanisms discussed above are summarised in Figure 2.1, which was developed by Lauer[13]. This diagram shows the interaction of the

different mechanisms of deterioration and the methods by which durability is affected.

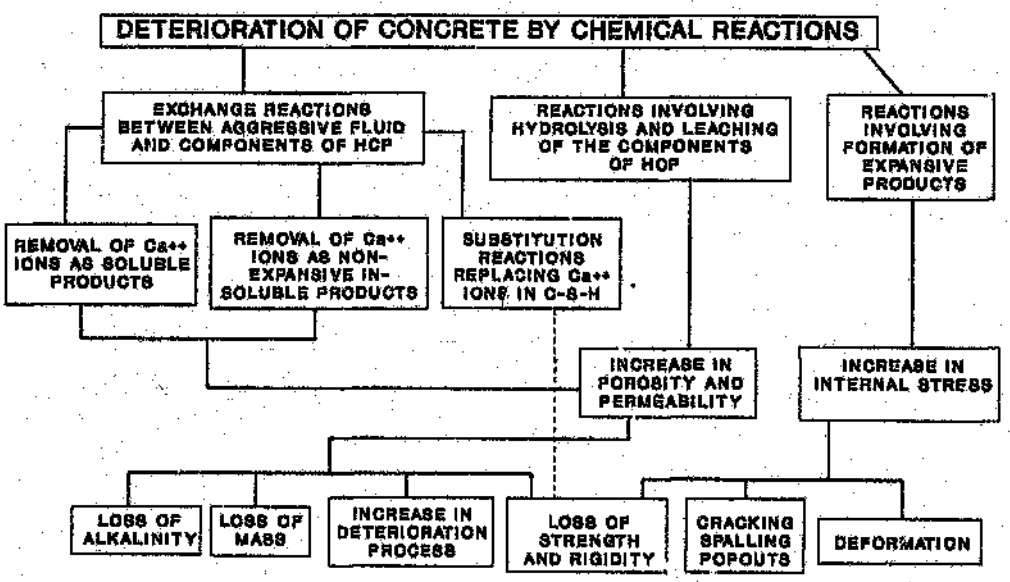

Figure 2.1 Summary of some of the chemical reactions responsible for concrete deterioration (after Lauer[13])

Steel corrosion in reinforced concrete caused by de-passivation of the steel.

In this category are listed chemical processes and actions which, in themselves, are not aggressive to concrete but cause the destruction of the gamma-ferric oxide layer on the reinforcement. This de-passivates the steel, exposing it to corrosion if the correct quantities of oxygen and moisture are present. The serviceability of the structure is then impaired because:

- the products of corrosion deposit on the surface of the structure causing staining which reduces the aesthetic value of the structure;
- the expansive forces set up by the corroding steel

cause surface cracking and spalling, leading to further corrosion;

- the loss of steel cross-sectional area reduces the load carrying capacity of the structure.

In the deterioration of concrete caused by reinforcement corrosion, two distinct periods are identified[14] as shown in Figure 2.2:

a) the initiation period during which the reinforcing steel is de-passivated and no physical deterioration takes place;

b) the corrosion period during which physical deterioration of the concrete manifests itself, leading to serviceability failure of the structure.

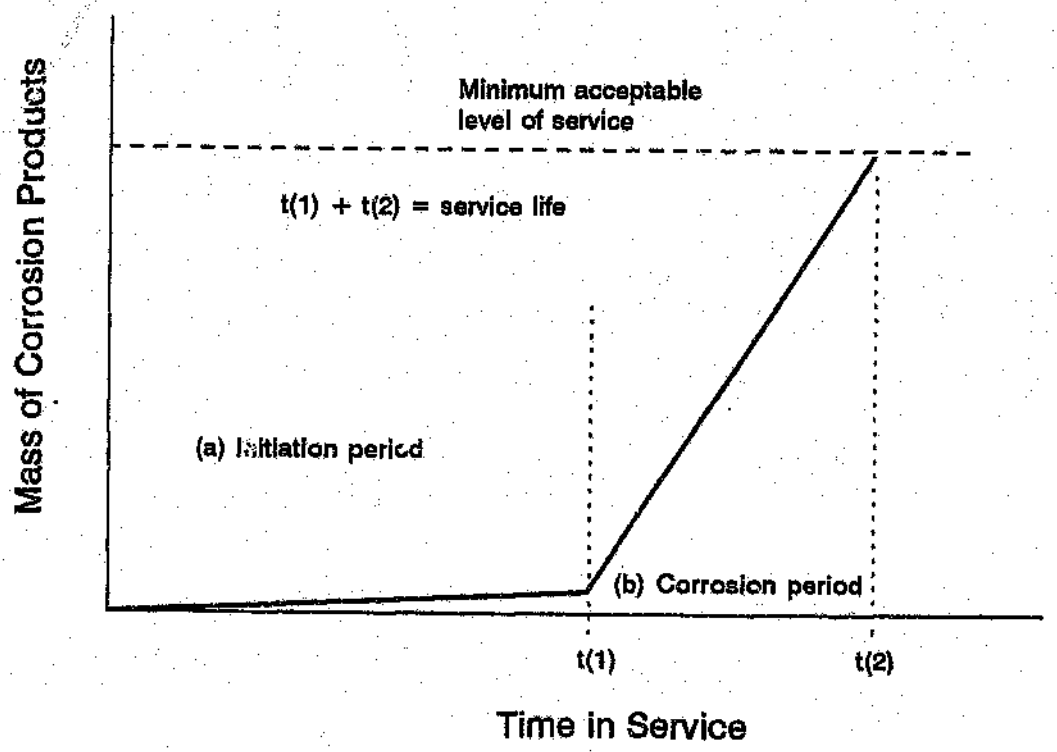

Figure 2.2 Two periods in the deterioration of concrete caused by reinforcement corrosion (after Tutti[14])

The most important physical processes operating in the initiation period are carbonation and chloride ion diffusion. Carbonation is discussed here in some detail since this was the durability process used to characterise the concretes tested in the main investigation of this project.

Carbonation: This is the process whereby atmospheric carbon dioxide (CO_2) enters the pore structure of the hcp and reacts with $Ca(OH)_2$ to form calcium carbonate ($CaCO_3$). This involves the following chemical reaction, which requires the presence of some moisture in the pore structure of the hcp:

$$CO_2 + Ca(OH)_2 \rightarrow CaCO_3 + H_2O$$

In this process, the pH of the pore water is reduced from ±12.5 to ±8.5 upon complete carbonation. When the carbonation front reaches the reinforcing steel, the low pH causes the gamma-ferric oxide layer to become unstable and the steel is de-passivated. If sufficient oxygen and moisture is available, the steel will start corroding with subsequent loss in the load-bearing capacity of the structure.

Carbonation moves as a "front"[15] into the concrete as shown in Figure 2.3. This front does not advance beyond a particular point until all the $Ca(OH)_2$ at that point has been converted to $CaCO_3$. Hence, the amount of $Ca(OH)_2$ in the pore structure of the concrete also has an influence on the rate of carbonation.

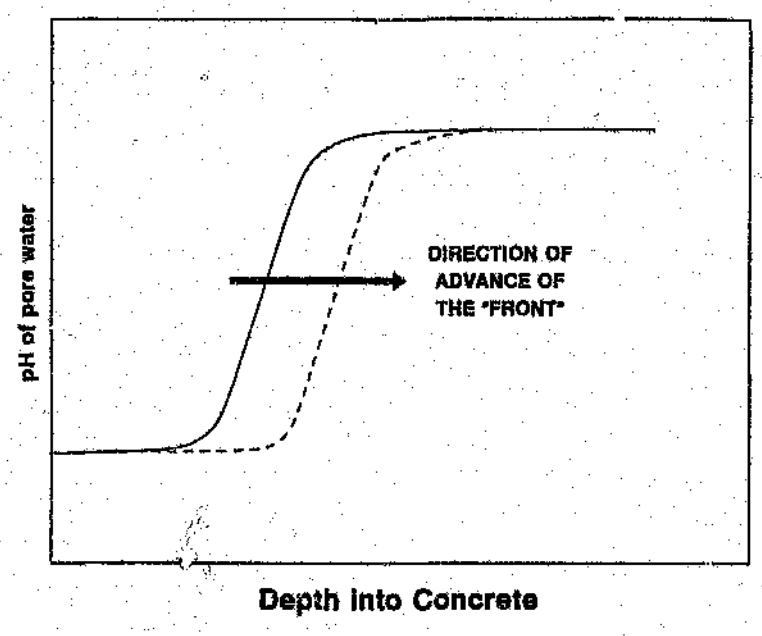

Figure 2.3 The carbonation "front"

The position of the carbonation front at any time t, can be expressed as:

$$x = x_o + D\sqrt{t} \qquad 2.1$$

where:

x = depth of carbonation
x_o = initial depth of carbonation
D = carbonation coefficient

Although Equation 2.1 is the commonly accepted form of the carbonation rate equation, Bentur and Jaegerman[16] have proposed the following alternative equation, claiming that this form gives better correlation with measured results:

$$x = x_o + D.t^{(0.4)} \qquad 2.2$$

where the terms are as described above.

The rate of carbonation is strongly affected by the

moisture content or relative humidity of the concrete pore structure. No carbonation takes place when the pores are completely dry or when they are fully saturated. The maximum rate of carbonation is considered to occur at relative humidity values between 45% and 65%[17] and is increased with increasing temperature.

Periods of dryness promote carbonation whereas periods of wetness promote corrosion if de-passivation of the steel has already occurred. The risk of corrosion therefore increases with increasing time of dry periods with relative humidity greater than 60%[18]. Hence, a better quality of concrete cover is required in climates with long dry periods and short wet periods.

Chloride ion diffusion: A problem which presents itself at coastal environments is the ingress of chloride ions into the concrete. Chlorides may also be introduced into the concrete at the mixing stage, either as contamination of the mix constituents or as a component of an admixture. The presence of free chlorides at the level of the reinforcing steel causes de-passivation despite the pH being maintained at a high level[15]. The reinforcing steel is then exposed to possible corrosion.

Some of the chloride which enters the concrete is bound by the cement and it is only when a critical concentration of free chlorides is reached that de-passivation takes place[15]. The ability for the cement to bind chlorides varies considerably with the cement type. The addition of GGBS in the binder has been found to be beneficial in this respect because of its high chloride binding ability.

The diffusion of chloride ions into concrete only takes place when there is moisture in the pore structure of the concrete. The higher the moisture content of the concrete, the higher is the rate of diffusion. Alternate wetting and drying cycles create the added problem of salt crystallisation with the associated expansive cracking of the concrete.

Synergy between carbonation and chloride penetration
When carbonation takes place in concrete into which chlorides have already penetrated, the two processes interact to accelerate the de-passivation of the reinforcement[15]. The pH-lowering effect of carbonation causes some of the chloride bound to the cement to be released. This increases the amount of free chloride ions available for de-passivating the reinforcement.

2.2.2 Physical deterioration

Deterioration of concrete due to physical effects is initiated at the surface and is the result of erosion or intra-pore expansion forces. These actions are discussed further below.

Surface erosion: The erosion of a concrete surface is caused by cavitation and abrasion forces. Cavitation can occur when water flows over concrete at velocities greater than approximately 12 m/s[19] and as low as 7.5 m/s in a closed conduit[20]. The collapse of water vapour bubbles in turbulent flow regions is associated with fairly large localised forces, causing pitting of the concrete surface. This problem is most severe at bends and changes in cross-section of the conduit.

Abrasion of the surface of concrete is also caused by

wind or water borne particles impacting on the surface as well as foot or wheel traffic travelling over the surface. Addis[18] states that:

> *"These mechanisms result in a probing action which concentrates wear on weaker micro areas and plucks out aggregate particles when sufficient of the surrounding matrix has been removed."*

Intra-pore expansion: This form of deterioration is caused by changes in external atmospheric conditions causing physical changes of the pore solution under the surface of the concrete. The two actions commonly resulting in this form of attack are expansion of water upon freezing[21] and expansion of salts upon crystallisation[22]. The expansive forces initiate microcracking and cumulative damage is caused by the cyclical nature of these actions.

2.3 Permeability and Other Fluid Transport Properties of Concrete

2.3.1 The pore structure of concrete

Pores in concrete are generally classified as gel pores, capillary pores, entrained air voids and entrapped air bubbles. Gowripalan et al[23] have prepared the schematic diagram shown in Figure 2.4 giving the range of pore sizes for the different pore types. It is seen here that the common ions and gas molecules which are aggressive to concrete, are smaller than the size of typical gel pores.

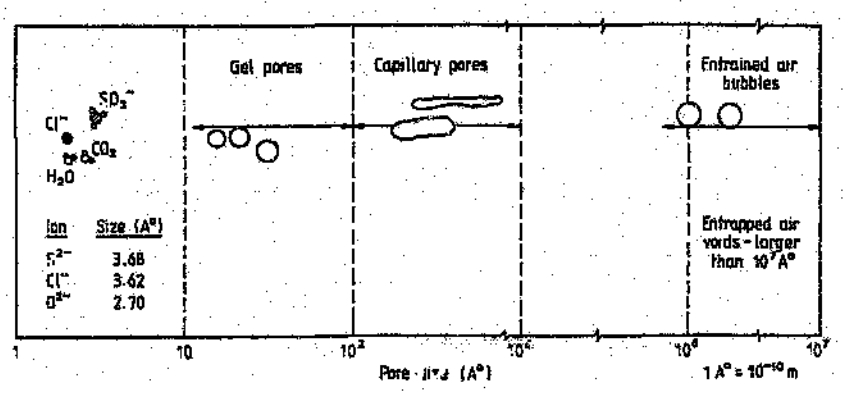

Figure 2.4 Range of pore sizes obtained in concrete (after Gowripalan et al[23])

Mindess and Young[24] have developed a classification of the capillary and gel pores in terms of size, indicating the effect of each size grouping on the properties of cement paste. This classification is shown in Table 2.1. It should be noted that, although more detailed in its categorisation of the pore sizes, the Mindess and Young classification agrees well with the Gowripalan classification in their distinction between capillary and gel pores. However, on the large end of the scale, Mindess and Young include pore sizes up to 10^5 Å in their classification of capillary pores.

A zone of particularly high porosity in concrete occurs at the interface between hcp and aggregate particles. Mindess[25] states:

> *"... the interfacial regions are, in general, profoundly different from the "bulk" cement paste, in terms of morphology, composition and density. At least in part because of... bleeding..., the interfacial regions (except for those within the hcp itself) are more porous than the bulk paste, leading to lower densities."*

Table 2.1 Classification of pore sizes in hydrated cement pastes (after Mindess and Young[24])

Pore type	Diameter (Å)	Description	Paste properties affected
Capillary	100 000 - 500	large capillaries	strength; permeability
	500 - 100	medium capillaries	strength; permeability; shrinkage at high RH.
Gel	100 - 25	small (gel) capillaries	shrinkage to 50% RH.
	25 ~ 5	micropores	shrinkage; creep.
	< ~ 5	micropores "interlayer"	shrinkage; creep.

2.3.2 Movement of fluids through the pore structure

Almost all the deterioration mechanisms discussed above involve the movement of gases or liquids into or out of the pore structure of concrete. The fluid transport properties of a concrete are therefore an important determinant of its ability to resist deterioration. Mehta[26]:

> "*.... firmly believes that the permeability of concrete is indeed the key to overall durability.*"

In this statement, Mehta uses the term "permeability" to refer to a measurable property of concrete, which is an indication of the general fluid transport properties

of the material. In this sense, both the volume of pores as well as the degree of interconnection of these pores are important in determining the ease with which aggressive agents may enter the concrete.

There are a number of mechanisms by which fluids move through the pore structure of concrete and the laws governing these movements are equally varied. Definitions of some of the terms related to fluid transport in concrete are presented below[27,28]:

Adsorption: This is the process in which molecules of the fluid adhere to the surfaces of the pores and are held there by Van der Waal's forces or through chemical bonding.
Absorption: This is the process whereby a liquid is drawn into the concrete tending to fill the permeable pore spaces. It is generally quantified by monitoring the increase in mass as the liquid penetrates the pore structure.
Diffusion: This is the process in which a fluid or ion passes through the pore structure of concrete under the action of a concentration gradient. The capacity for a porous material to transfer fluids or ions by means of diffusion is referred to as the diffusivity of that material.
Permeation: This describes the process of movement of fluids through the pore structure, generally under an externally applied pressure head, when the pores are saturated with the particular fluid. Permeability is therefore a measure of the capacity for concrete to transfer fluids by permeation.

Figure 2.5 shows three forms of water transport, relevant to durability, through an idealised pore in concrete.

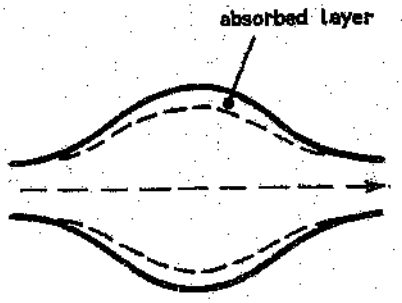

(a) Vapour diffusion

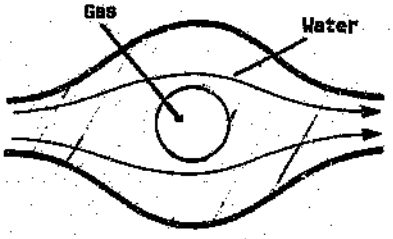

(b) Partially saturated liquid flow

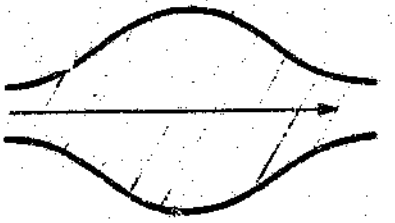

(c) Saturated liquid flow

Figure 2.5 Idealised model of three forms of water movement through a pore in concrete[27]

At stage (a), an adsorbed layer has been established and vapour is able to diffuse through the pore. The mass vapour transport rate (J) is described by Fick's first law:

$$J = -D.\frac{\partial c}{\partial x} \qquad 2.3$$

where $\partial c/\partial x$ is the concentration gradient and D is the diffusion coefficient.

At stage (b), partially saturated liquid flow occurs

due to an external source of liquid initiating capillary suction. The rate of liquid flow is described by the Washburn equation:

$$v = \cos\theta . \frac{r\gamma}{4d\mu} \qquad 2.4$$

where:

v = rate of flow
θ = contact angle
r = capillary radius
γ = surface tension
d = depth of penetration
μ = fluid viscosity

This equation is not easily applied to concrete and, in the context of durability testing, researchers have preferred to use a measure of sorptivity (S) to describe partially saturated flow. Sorptivity is described by the equation[29]:

$$i = S\sqrt{t} \qquad 2.5$$

where i is the depth of infiltration after time t. This parameter is discussed in more detail in Chapter 3.

At stage (c) in Figure 2.4, the pore is fully saturated and fluid flow may take place if a sufficiently high differential pressure head exists. Under these conditions the mass flow rate (Q) is described by the Darcy equation:

$$Q = k.A.\frac{\partial P}{\partial x} \qquad 2.6$$

Where k is the coefficient of permeability, in units of velocity, A is the cross sectional area of flow and $\partial P/\partial x$ is the pressure gradient.

In Equation 2.6, k is dependent on the porous medium and the type of permeating fluid. This equation has been generalised to apply to any fluid flowing through the material by using an intrinsic permeability factor (K), with units of area. The two factors are related to each other as shown in Equation 2.7.

$$K = \frac{k\mu}{\rho g} \qquad 2.7$$

where μ is the viscosity of the fluid, ρ is the fluid density and g is the acceleration due to gravity.

In practice, however, it is found that intrinsic permeabilities determined using gases are greater than those determined using liquids as the permeating fluid[30]. This is ascribed to a phenomenon known as "gas slippage"[31] and empirical correction factors have to be applied in order to equate the values obtained. The use of the intrinsic permeability measurement has therefore not been successful in unifying the different types of test fluids used for determining concrete permeability.

2.4 Intrinsic Material Factors Affecting the Durability of Concrete

The durability performance of a concrete exposed to a given aggressive environment is influenced by two intrinsic factors:

- the fluid transport properties of the hardened concrete as discussed above and particularly those at the outside surface of the concrete;
- any chemical interaction between the constituents of the hcp and the aggressive agent.

To clarify this distinction by way of example, it was noted above that only free chlorides are responsible

for de-passivation of reinforcing steel. Hence, the rate of advance of free chlorides into the concrete is determined by both the ease of access for chlorides (fluid transport properties) as well as the ability of the hcp to bind chlorides (chemical interaction), thereby making them unavailable for de-passivating the steel. The discussion below focuses on both these aspects in considering the influence of the intrinsic material properties on concrete durability.

2.4.1 Water/cement ratio

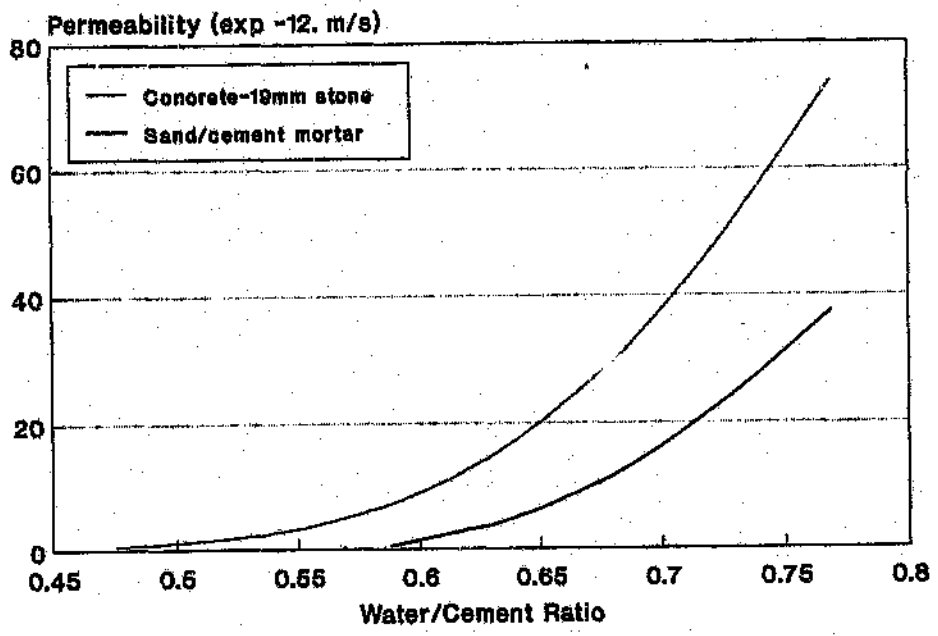

Figure 2.6 Relationship between the coefficient of permeability and w/c ratio for concretes and mortars[19]

Figure 2.6 shows the effect of w/c ratio on the coefficient of permeability of well cured mortars and concretes with 19 mm stone[19]. Permeability increases considerably with increasing w/c ratio because of the increasing volume and degree of interconnection of

capillary pores.

Figure 2.7 shows results obtained by Henry and Kurtz[32] where a similar trend of increasing fluid transport ability with increasing w/c ratio can be seen. In this case, they used water vapour transmission as an indicator of the fluid transport characteristics of the concrete. The approximately linear relationship shown in Figure 2.7 compared with the curvilinear relationships shown in Figure 2.6, is an indication of the influence of different mechanisms of fluid movement through the pore structure of concrete.

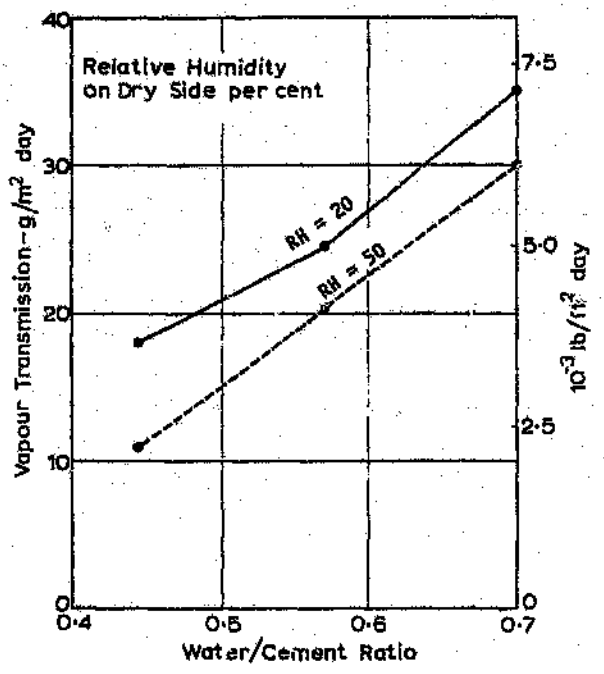

Figure 2.7 Influence of w/c ratio on the water vapour transmission of concrete (after Henry and Kurtz[32])

2.4.3 Maximum aggregate size

It has been found that, the larger the maximum aggregate size, the higher is the permeability of the concrete. This is thought to be the result of the

interfacial effects discussed above.

By analysing data from reference (32), Fulton[18] gives an indication of the relationship between permeability and maximum aggregate size. This relationship, together with the influence of the w/c ratio, is shown in Table 2.2 below.

Table 2.2 Relationship between permeability, w/c ratio and nominal maximum aggregate size[18]

w/c ratio	0.476	0.526	0.588	0.667
Max. Aggregate Size	Relative Permeability			
9.5 mm	1	1.3	7	30
13.2 mm	1	2	8	32
19.0 mm	1*	3	12	48
37.5 mm	2	6	20	66

* used as the datum for comparisons

It may appear from Table 2.2 that for improved impermeability, concretes should be made with smaller aggregates. However, the increased cost and time-dependent movement properties of such concretes militates against too large a decrease in maximum aggregate size.

2.4.3 Water content

Fulton[18] argues that:

> *"...provided the c/w ratio is high enough (>~1.5 or w/c <~0.667), a low permeability concrete will be produced irrespective of the total water in the mix."* - parentheses are mine.

This statement is true for well proportioned mixes in

which bleeding is kept to a minimum. However, if the water content is increased while maintaining the w/c ratio, the bleed voids which would tend to form around aggregate particles would have a considerable effect in increasing the fluid transport properties of the concrete.

2.4.4 Cement content

While cement content is not a basic parameter in determining the permeability of concrete[18], it does have an influence on the durability of concrete. In deterioration mechanisms involving, for example, carbonation or soft water attack of concrete, the rate of attack is influenced by the amount of hydration products available for reaction. Hence, for the same permeability, a concrete with more cement will show a slower rate of deterioration.

2.4.5 The degree of hydration

As hydration proceeds, the initially water-filled, fully interconnected pores within the cement paste, are filled with hydration products and become discontinuous. Figure 2.8, taken from work done by Graf and Grube[33], shows this process schematically.

Using a cement paste with w/c ratio 0.7, Powers et al[34] show that the water permeability reduces from 2×10^{-6} m/s in the fresh state, to 1×10^{-12} m/s after 24 days of hydration. They also show that the "ultimate" permeability of this cement paste to be 0.6×10^{-12}, only a 40% reduction on the 24-day value.

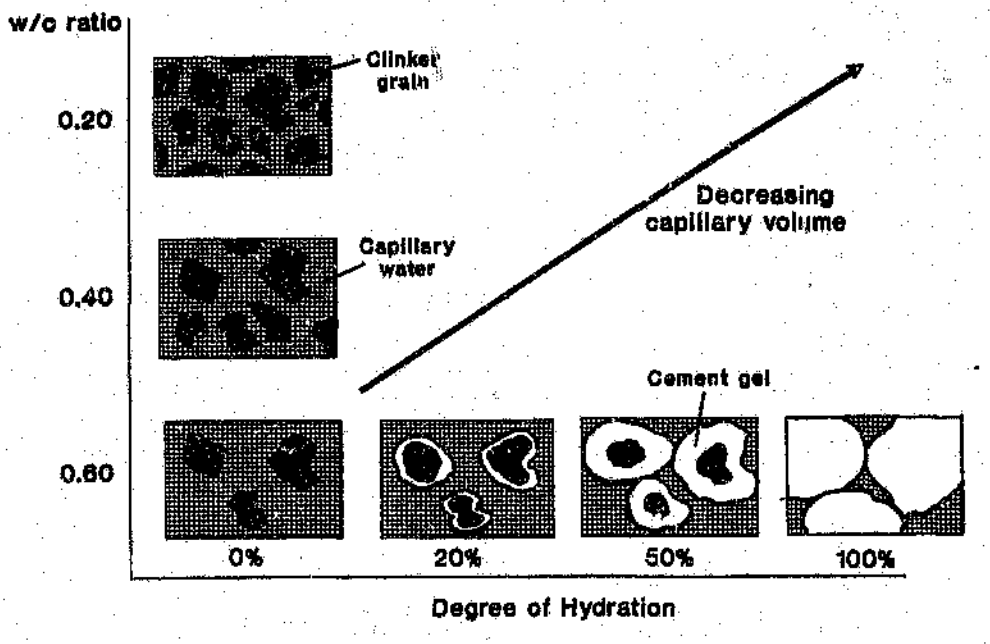

Figure 2.8 Schematic diagram showing the influence of w/c ratio and degree of hydration on the reduction of capillary pore volume[33].

It is clear that continued hydration, especially during the early period after casting, has a significant effect on reducing the fluid transport characteristics of concrete. It is in this context that curing is important, but this subject will be dealt with later, as an extrinsic factor influencing durability.

2.4.6 Influence of binder type

Portland cement

Portland cements are often "tailored" to suit particular aggressive environments. An example of this is the use of cements with low tricalcium aluminate contents to reduce sulphate attack[9]. Furthermore, Powers[34] showed that finely ground OPC, equivalent to South African rapid hardening portland cement (RHPC), decreases the permeability of cement pastes, provided the porosity benefits of the RHPC are realised.

However, this has not always been confirmed when RHPC is used in concrete. It is suggested that the fineness benefit of RHPC is counteracted by its tendency for lower creep and higher drying shrinkage[18].

Fly ash as cement extender

The pozzolanic action of fly ash (FA) in concrete is well documented in the literature and a useful review of this aspect is presented by Helmuth[35]. Manmohan and Mehta[36] have shown that a significant effect of the addition of FA to portland cement was that it effected a refinement of the pore structure upon hydration, by transforming large pores into fine pores. As a result of this effect, Mehta[37] reports decreases in cement paste permeability from 11-13 x 10^{-11} m/s to 1 x 10^{-11} m/s after the addition of FA.

Figure 2.9, taken from Cabrera's work[38], shows the effect of FA in reducing the volume of pores > 10 nm. Reference to Table 2.1 shows that these pore sizes mainly influence the strength and permeability of concretes and mortars. No indication is given as to the basis on which the mortars in Figure 2.9 are being compared.

Berry and Malhotra[39] show that well cured concrete pipes with FA replacements of 30% and 50%, were approximately 5 times less permeable than corresponding pipes made with OPC only. They cite a large amount of research work which confirms the general conclusion that FA decreases the fluid transport properties of concrete.

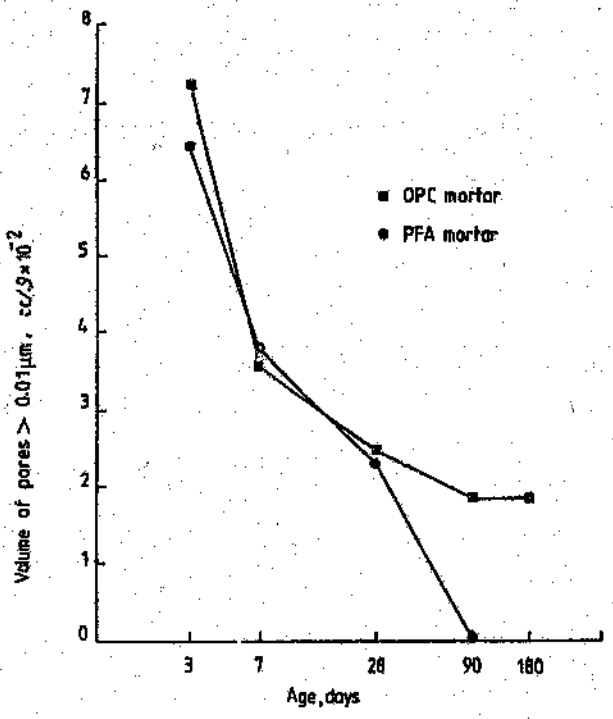

Figure 2.9 Effect of FA in reducing the volume of pores > 10 nm (after Cabrera[38])

Regarding the durability performance of FA concrete, opinions have differed and conflicting research results have sometimes been presented. Part of the reason for this is that the pozzolanic reaction consumes $Ca(OH)_2$, leaving less active material to resist deterioration actions such as carbonation and soft water attack. This has led Alexander[40] to conclude:

> *"Fly ash concretes may or may not carbonate faster than comparable plain OPC concretes under similar conditions, depending on such interlinked factors as permeability and $Ca(OH)_2$ content."*

In a survey of the literature on the effects of FA on concrete, the NBRI[41] reports that the rate and extent of carbonation is largely unaffected by FA. It is argued that the strength grade is the determining

factor of carbonation and it is here that part of the disagreement on the performance of FA may be located. If the concretes are compared on the basis of equal 28-day strength, a FA concrete must have a lower water/binder ratio (w/b) than an OPC concrete and it can be expected that the FA concrete would have a lower permeability. However, if the concretes are compared on the basis of equal w/b ratio, the FA concrete may have a similar permeability, but would carbonate faster because of the lower $Ca(OH)_2$ content.

Thomas et al[42] report on durability investigations carried out on 5 FA concrete structures ranging in age from 2 to 33 years. For each structure, a comparable OPC structure was available for similar investigation. They conclude that:

- all the FA concretes had greater strength and reduced permeability;
- for equal strength grades, depths of carbonation were similar for the FA and OPC concretes;
- FA concretes give improved resistance to chloride penetration.

The effect of improved resistance of FA concrete to chloride penetration is also noted by Lees and Berke[41].

Cabrera[38] notes that:

> *"...(FA) improves the performance of concrete exposed to chloride and sulphate environments. It also reduces the damage due to the silica-alkali reactions."*

He also concludes that, at higher strength levels and together with air entraining agents, FA improves the resistance of concrete to abrasion and freeze-thaw deterioration. On the other hand, Alonso et al[44], in testing a number of cement extenders including slag and FA, note that:

- blended cements are not as effective as plain OPC in passivating reinforcing steel and therefore, increase the probability of corrosion;
- in the presence of chlorides, the corrosion rate of reinforcing steel is higher when blended cements are used.

A further contribution of FA to the long-term durability of concrete is its ability to reduce the heat generated by concrete during the early stages of hydration[45]. This is an important consideration for the construction of large concrete elements, where the cracking due to thermal strains can present serious strength and durability problems.

Slag as a cement extender

Unlike FA, ground granulated blastfurnace slag (GGBS) is a cementing material which, when mixed with water, will form CSH compounds similar to those of OPC. However, the reactions are very slow because the amount of $Ca(OH)_2$ released in the reaction is too low to allow a rapid dissolution of the glass phases of the material. GGBS is therefore more commonly used together with portland cement which, when hydrating, releases sufficient quantities of $Ca(OH)_2$ to encourage the hydration of the GGBS.

Research[46,47] appears to indicate that GGBS/OPC pastes cured for 28 days, have similar total porosity values as plain OPC pastes at the same w/c ratio. However, the GGBS pastes have more gel pores and fewer capillary pores than the corresponding OPC pastes. However, this does not appear to have a significant effect on the fluid transport properties of the material in concrete. Reeves[48] shows that the water permeability of a 70/30

GGBS/OPC concrete is slightly higher than that of a plain concrete. The concretes compared had the same total binder content and b/w ratio.

From a durability performance point of view, an important benefit of the use of GGBS in concrete is its ability to bind chlorides, thereby reducing the rate of reinforcement corrosion[49]. The mechanism by which chlorides are bound is not clearly understood but is thought to be a combination of chemical and physical actions. Figure 2.10, which was presented by Blundell[50], shows this effect of GGBS.

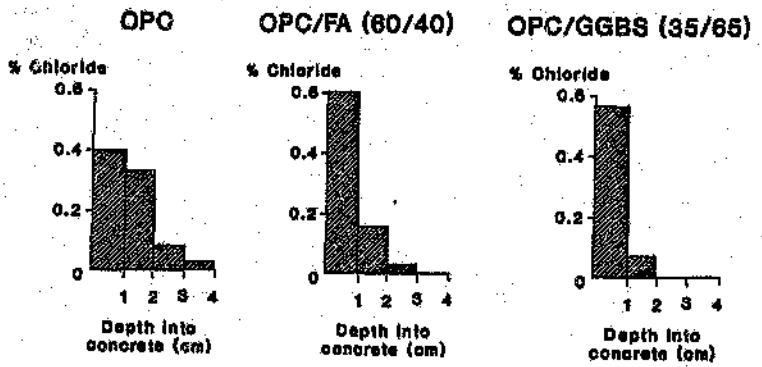

	OPC	OPC/FA (60/40)	OPC/GGBS (35/65)
Pore volume > 66 nm (%)	3.5	3.4	2.1
Water permeability (exp -11 m/s)	2.3	3.3	1.7
Diffusion coefficient (exp -8 cm^2/s)	12	7	3

Figure 2.10 Effect of GGBS in reducing chloride penetration into concrete (after Blundell[50])

Although the three concretes tested have similar volumes of pores >65 nm and similar permeability values, the chloride diffusion coefficient of the GGBS concrete is less than 50% that of the FA concrete and

only 25% that of the plain OPC concrete.

GGBS has also been found to be effective in reducing the deterioration of concrete due to sulphate attack. Higgins and Uren[51] report that:

> *"When the GGBS content is 65% or greater, most combinations of GGBS and OPC provide equivalent of better sulphate resistance than sulphate resisting portland cement"*

Hooton et al[52] have shown that a 50% replacement of OPC with a Canadian GGBS gives equivalent sulphate resistance as a sulphate resisting portland cement.

It is commonly accepted that GGBS has a significant effect in reducing the expansion of concrete due to alkali silica reaction. This is shown in Figure 2.11, where it is seen that a 50% replacement of GGBS reduced the 12-month expansion from approximately 0.5% to 0%. This observation is confirmed by tests conducted by Hogan and Meusel[53].

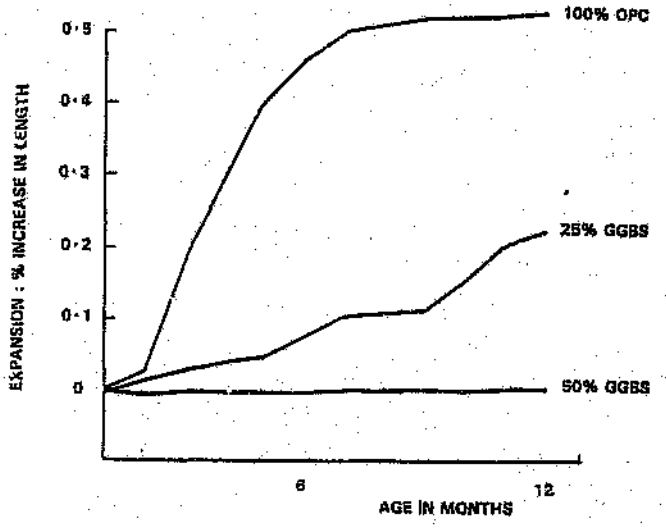

Figure 2.11 Effect of GGBS in reducing expansion due to alkali silica reaction (after Higgins and Uren[51])

Research conducted by Osborne[54] shows that the replacement of OPC with GGBS increases the rate of carbonation of concrete. The extent of increase in the carbonation rate is deceased as the total binder content of the concrete increases. He also notes that the permeability of the concretes increased with increasing GGBS replacements.

As with FA, GGBS is also effective in reducing the heat generated during the early hydration of cement. Used in this application, GGBS has a longer history than FA. Table 2.3 shows the effectiveness of various levels of GGBS replacement in reducing the heat generation of cement.

Table 2.3 Relationship between heat of hydration and % GGBS in the Binder (after Reeves[48])

% GGBS	Cumulative heat generated (kJ/kg) after:	
	7 days	28 days
0	360	400
30	325	395
40	305	360
50	255	325
70	200	260
90	125	185

2.5 Effect of Curing on Durability

In Chapter 1, curing was defined as a process aimed at encouraging the hydration of cement during the early period after casting. In promoting the hydration of cement, curing ensures that engineering properties of

concrete develop to their required potential. The relationship between curing and durability is discussed in more detail below.

2.5.1 Curing and the transport properties of concrete

Continued hydration of concrete decreases both the size and continuity of the pores in hcp. Powers[55] has estimated the duration of moist curing required to achieve capillary discontinuity for pastes with varying w/c ratios. These times are shown in Table 2.4 below.

Table 2.4 Required duration of moist curing for capillary discontinuity (after Powers[55])

w/c Ratio	Duration moist curing for capillary discontinuity (days)
0.40	3
0.45	7
0.50	14
0.60	180
0.70	365
>0.70	Impossible

Since moist curing has a primary influence on the covercrete zone, its effect is to decrease the fluid transport properties of this zone. Gowripalan et al[23] show the effect of duration of curing on oxygen permeability of mortars. Figure 2.12 shows some of the results of their work. This figure shows that curing is most effective during the first three days after casting. Thereafter, the marginal improvements in concrete quality decreases with increasing duration of curing. The curves also show that early-age curing has

a larger effect on the lower strength mortar.

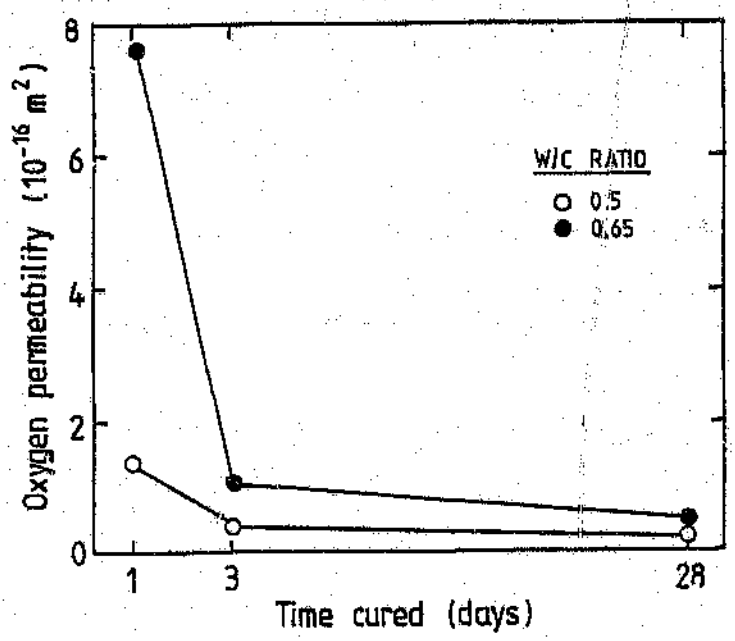

Figure 2.12 Effect of duration of curing on the oxygen permeability of mortars (after Gowripalan et al[23])

These observations are confirmed by Montgomery et al[56] and Ho[57]. Using water sorptivity as an indicator test, Ho notes that:

> *"... low strength concretes are extremely sensitive to lack of curing. However, the effectiveness of practical curing is reduced as the strength (or cement content) of the concrete increases."*

2.5.2 Curing requirements of different binder types

It is commonly accepted (amongst researchers at least) that when part of the cement is replaced by extenders like FA and GGBS, the duration of early-age curing has to be extended to achieve the same quality of surface

concrete. Haque[58] concludes that:

> *"...fog curing for at least 7 days is more important when concrete containing fly ash will be exposed to drying ambient conditions."*

This observation of the greater sensitivity of FA concrete to early age curing is also noted by Cabrera[38], Norton[59] and Bijen and van Selst[60]. However Amtsbuchler[39] shows that the compressive strength of a nominal 25 MPa concrete is no more adversely affected by cold or dry curing than an equivalent OPC concrete. He also found that the water permeability of a nominal 30 MPa FA concrete was slightly less affected by dry curing than an equivalent OPC concrete. Amtsbuchler largely ascribes this disagreement with past results to improvements in the quality of FA in South Africa.

With regard to the curing response of GGBS concrete, it has been shown[62,63] that, with an appropriate selection of w/b ratio and continuous water curing, concrete with a 50/50 blend of GGBS/OPC will develop the same 28-day strength as a plain OPC concrete. However, it is also generally accepted that, because of its slower rate of hydration, GGBS concretes are considerably more sensitive to inadequate curing at early ages than OPC concretes[64,65].

2.6 Approaches to Specifying for Concrete Durability

SABS 0100[66], BS 8110[67] and the new Eurocode No. 2: EC2[68] address durability by specifying aspects such as:

- maximum w/c ratio;
- minimum cement content;
- method and degree of curing;

and, for specific aggressive environments:

- maximum chloride content;
- alkali content of the cement;
- tricalcium aluminate content of the cement.

All these aspects are not easily determined after the concrete has hardened and are therefore almost never used for routine quality control testing.

The Australian code: AS 3600[69] takes the unusual approach of specifying concrete quality only in terms of compressive strength. The justification for this is apparently that strength is the only easily measured property of concrete, ie. a parameter which is not easily measured as a site control test [illegible]t be specified. The discussion in Chapter 1 [illegible] the relative effects of curing on durabili[illegible]nd strength indicates the potential problems which could be encountered with this Australian approach.

2.7 General Discussion

An important feature of the literature reviewed in this chapter is that most of the research on concrete durability has been carried out overseas. This is particularly applicable to aspects such as the effect of binder type and curing on durability performance. As a result, concrete technology in Southern Africa has relied heavily on foreign research and local specifications are often duplicates of overseas practice.

The problem with this approach being applied to durability, is that the materials used overseas are very different to those used locally. The important effect of differences in the nature and quality of local cements, FA and GGBS are not accounted for in

such an approach.

The second important difference is the nature of the environments to which concretes are exposed. Not only does this have implications for the deterioration processes affecting concrete but it also limits the applicability of research into the effects of curing on concrete durability. Bentur[70] argues:

> *"Israel, like many parts of South Africa, experiences extremely hot and dry conditions which have a detrimental effect on the surface properties of the concrete. What is considered as a harsh environment in Europe and the USA, is a mild environment in Israel (and South Africa).*
>
> [parentheses are the author's]

It is therefore important that this research be conducted in South Africa in order to develop a local strategy for concrete durability.

It is evident that specifications for the durability of concrete should ideally be expressed in terms of measurable parameters of the hardened concrete. However, the development of such specifications is hampered by the absence of test methods which are easily conducted and which can be used for routine quality control on site, in the same manner as the concrete cube test.

List of References

1. Czernin, W. *Cement chemistry and physics for civil engineers*. 2nd edition. Georg Godwin Ltd. London. 1980.

2. Moskvin, V. (Ed.) *Concrete and reinforced concrete deterioration and protection*. Mir Publishers, Moscow. 1983.

3. Portland Cement Association. *Effects of substances on concrete and guide to protective treatments*. PCA. Skokie, Illinois. 1986.

4. Eglinton, M.S. *Review of concrete behaviour in acidic soils and ground waters*. Report N0. 69. CIRIA. London. 1975.

5. Ballim, Y. Soft water attack of concrete: A review and limited laboratory study. To be published in *The Civil Eng. in SA*. 1993.

6. Leroy, P. Interaction between argillaceous soils and cement materials (in French). *Jnl. of Water Supply, Research and Technology - Aqua*. Vol. 41, No. 3. 1992. pp. 151-157.

7. American Concrete Institute. Proposed revision of: Guide to durable concrete. Reported by ACI Committee 201. *ACI Materials Jnl*. Sept-Oct. 1991. pp. 544-582.

8. Mindess, S. and Young, J.F. *Concrete*. Prentice Hall, New Jersey. 1981. Chapter 20.

9. Lawrence, C.D. Sulphate attack on concrete. *Mag. of Concr. Research*. Vol. 42, No. 153. Dec. 1990.

pp. 249-264.

10. Hobbs, D.W. *Alkali-silica reaction in concrete.* Thomas Telford Ltd. London. 1988.

11. Heinz, D and Ludwig, U. Mechanism of secondary ettringite formation in mortars and concrete subjected to heat treatment. Proc. of Int. Conf. on ..... ACI SP-100. pp. 2059-2071.

12. Lawrence, C.D, Dalziel, J.A. and Hobbs, D.W. *Sulphate attack arising from delayed ettringite formation.* British Cement Association Interim Technical Note 12. BCA, Slough. May 1990.

13. Lauer, K.R. Classification of concrete damage caused by chemical attack. *Materials and Structures.* Vol 23, 1990. pp. 223-229.

14. Tutti, K. Service life of structures with regard to corrosion of embedded steel. ACI SP-65: *Performance of concrete in marine environment.* ACI, Detroit. 1980. pp. 223-236.

15. Schiessl, P. (Ed.). *Corrosion of steel in concrete.* RILEM TC 60-CSC report. Chapman Hall, London. 1988.

16. Bentur, A and Jaegermann, C. Effect of curing on the properties of the outer skin of concrete. *ASCE Jnl of Materials in Civil Engineering.* Vol. 3, No. 4. Nov. 1991. pp. 252-262.

17. Comite Euro-International du Beton. *Durable concrete structures - Design guide.* Thomas Telford, London. 1992.

18. Addis, B.J. (Ed.) *Fulton's concrete technology*. 6th Edition. Portland Cement Institute. Midrand, South Africa. 1986. Chapter 8.

19. US Bureau of Reclamation. *Concrete manual*. 8th Ed. Denver. 1975.

20. American Concrete Institute. Committee 210. Erosion resistance of concrete in hydraulic structures. *Proc. of ACI*. Vol. 52. Nov. 1955. pp. 259-271.

21. Addis, B.J. *Physical deterioration of concrete*. Lecture notes for CEE course: Concrete Durability. University of the Witwatersrand. Nov. 1992.

22. Lea, F.M. *The chemistry of cement and concrete*. 3rd Edition. Edward Arnold, London. 1970. pg. 671.

23. Gowripalan, N, Cabrera, J.G, Cusens, A.R. and Wainwright, P.J. Effect of curing on durability. *Concrete International*. Vol. 12, No.2. February 1990. pp. 47-54.

24. Mindess, S. and Young, J.F. Ibid. Chapter 4.

25. Mindess, S. Interfaces in concrete. In: *Materials Science of Concrete I*. Skalny, J.P. (Editor). American Ceramic Society. 1989. pp. 163-180.

26. Mehta, P.K. Durability of concrete exposed to marine environment - A fresh look. *Concrete in Marine Environment*. American Concrete Institute. ACI SP109. pp. 1-29.

27. Concrete Society. *Permeability testing of site*

concrete - A review of methods and experience. Technical Report No. 31. The Concrete Society, London. 1987.

ACI C116 .....

29. Hanks, R.J. and Ashcroft, G.L. *Applied soil physics*. Springer-Verlag, New York. 1980.

30. Bamforth, P.B. The relationship between permeability coefficients for concrete obtained using liquid and gas. *Mag. of Concr. Res*. Vol. 39, No. 138. March 1987. pp. 3-11.

31. Klinkenberg, L.J. The permeability of Porous media to liquids and gases. *Drilling and Production Practice*. American Petroleum Institute. 1941. pp. 200-214.

32. Henry, R.L. and Kurtz, G.K. *Water vapour transmission of concrete and of aggregates*. United States Naval Civil Engineering Laboratory. California. June, 1963.

33. Graf, H and Grube, H. Einfluß der zusammensetzung und der nachbehandlung des betons auf seine gasdurchassigkeit. *Beton*. Vol. 36. 1986.

34. Powers, T.C; COpeland, L.E; Hayes, J.C and Mann, H.M. Permeability of portland cement paste. *Proc. of ACI*. Vol. 51. Nov. 1954. pp. 285-298.

35. Helmuth, R. *Fly ash in cement and concrete*. Portland Cement Association. Skokie, Illinois. 1987.

36. Manmohan, D and Mehta, P.K. Influence of pozzolanic, slag and chemical admixtures on pore size distribution and permeability of hardened cement paste. *Cement, Concrete and Aggregates*. Vol. 3 No. 1. Summer 1981. pp. 63-67.

37. Mehta, P.K. Pozzolanic and cementitious by-products as mineral admixtures for concrete - A critical review. *ACI SP-79: Fly ash, silica fume, slag and other mineral by-products in concrete*. Vol. 1. Malhotra, V.M. (Ed.). ACI, Detroit, 1983. pp. 1-46.

38. Cabrera, J.G. The use of pulverised fuel ash to produce durable concrete. *Proc. of ICE Seminar: Improvement of Concrete Durability*. Thomas Telford, London. May 1985. pp. 29-46.

39. Berry, E.E. and Malhotra, V.M. Fly ash in concrete. Chapter 2, *CANMET Publication SP 86-8E: Supplementary cementing materials for concrete*. Malhotra, V.M. (Ed.). 1987. pp. 37-163.

40. Alexander, M.G. Fly ash concrete and carbonation. *Proc. Concrete Society of S.A. Symposium: Achievement and Evaluation of Quality Concrete*. CSSA, Midrand. April, 1989.

41. National Building Research Institute. *Report on fly ash for use in concrete*. NBRI, CSIR. Pretoria. January 1985.

42. Thomas, M.D.A, Mathews, J.D. and Cripwell, J.B. *The durability of PFA concrete - A survey of existing structures*. Building Research Establishment Report PD 87/90. BRE, Watford. May,

1990.

43. Lees, T.P. and Berke, N.S. Influence of surpeplasticisers on the durability of concretes containing fly ash, silica fume and calcium nitrite. In: *Blended Cements in Construction*. Swamy, R.N. (Ed.) Elsevier Applied Science, London. 1991. pp. 389-400.

44. Alonso, M.C, Andrade, C, Moragues, A. and Goni, S. Influence of the use of blended cements on the corrosion behaviour of reinforcements. *Proc. of 2nd Int. Conf. on Engineering Materials*. June 1990. Bologna, Italy. Vol. 1, Part 3. pp. 837-844.

45. Mehta, P.K. Pozzolanic and cementitious by-products in concrete - Another look. *Proc. of 3rd Int. ACI-CANMET Conference: Fly ash, silica fume, slag and natural pozzolans in concrete*. Trondheim, Norway. ACI SP114. 1989. pp. 1-43.

46. Pigeon, M and Regourd, M. Freezing and thawing durability of three cements with various granulated blastfurnace slag contents. *Proc. CANMET/ACI Conf. ACI Publication SP-79. Vol. 2.* 1983. pp. 979-998.

47. Smolczyk, H.G. Slag structure and identification of slag. *Proc. of 7th Int. Congress on Chemistry of Cements. Vol. 1, III.* Paris, 1980. pp. 1-17.

48. Reeves, C.M. The use of ground granulated blast furnace slag to produce durable concrete. *Proc. of ICE Seminar: Improvement of Concrete Durability.* Thomas Telford, London. May 1985. pp. 59-76.

49. Rose, T. The effect of cementitious blast furnace slag on chloride permeability of concrete. *ACI SP-102: Corrosion, Concrete and Chlorides. Steel corrosion in concrete - causes and restraints.* Gibson, F.W. (Ed.). ACI, Michigan. 1987. pp. 107-125.

50. Blundell, R. Discussion of Reference 47, in the same publication.

51. Higgins, D. and Uren, M. The effect of GGBS on the durability of concrete. *Concrete*. Sept./Oct. 1991. pp. 17-19.

52. Hooton, R.D, Emery, J.J. and Low, C.A. Sulphate resistance of slag cements. *Int. Conference on Slags and blended cements*. Mons, Belgium. Sept. 1981.

53. Hogan, F.J. and Meusel, J.W. Evaluation for durability and strength development of a ground granulated blast furnace slag. *Cement, Concrete and Aggregates*. Vol. 3, No. 1. 1981. pp. 40-52.

54. Osborne, G.J. Carbonation and permeability of blast furnace slag cement concretes from field structures. *Proc. of 3rd Int. ACI-CANMET Conference: Fly ash, silica fume, slag and natural pozzolans in concrete*. Trondheim, Norway. ACI SP114. 1989. pp. 1209-37.

55. Powers, T.C. *Capillary continuity and discontinuity in cement pastes*. Portland Cement Association, Skokie. Research Dept. Bulletin 110. 1959.

56. Montgomery, F.R, Basheer, P.A.M. and Long, A.E. Influence of curing conditions on the durability related properties of near surface concrete and cement mortars. *G.M. Idorn Int. Symposium: Durability of Concrete*. ACI SP-131. ACI, Detroit. 1992. pp. 127-138.

57. Ho, D.W.S. *The effectiveness of curing techniques on the quality of concrete*. CSIRO, Australia. Technical Report TR92/3. 1992.

58. Haque, M.N. Some concretes need 7 days initial curing. *Concrete International*. Vol. 12, No.2. February 1990. pp. 42-46.

59. Norton, S.W. *Carbonation of concrete containing pfa*. Portland Cement Institute TIP No. 162. PCI, Midrand. 1988.

60. Bijen, J. and van Selst, R. Effects of fly ash on carbonation of concrete with portland blast-furnace slag cement. *ACI Publication SP-126: Concrete Durability*. pp. 1001-1030.

61. Amesbuchler, R. Effects of different curing regimes on fly ash concrete. *Int. Symposium on: Ash - A Valuable Resource*. CSIR, Pretoria. Feb. 1987.

62. Stutterheim, N. Properties and uses of high-magnesia portland slag cement concretes. *J. American Concr. Inst.* Vol. 31, No. 10. April, 1960. pp. 1027-1045.

63. Fulton, F.S. and Davis, D.E. *Normal portland vs. portland blast furnace cement*. Portland Cement

Institute Report DF-1. PCI, Aug. 1961.

64. van der Meulen, G.J.R. *Effect of duration of curing on slag-portland cement concrete*. NBRI, CSIR Reference No. R/BOU 158. Jan. 1965.

65. Concrete Society of Southern Africa. *Concrete curing - Description, method and control*. CSSA, Midrand. Nov. 1991.

66. South African Bureau of Standards. *The structural use of concrete. Part 2: Materials and execution of work*. SABS 0100 - Part 2: 1992.

67. British Standards Institution. Structural use of concrete. Part 1: Code of practice for design and construction. BSI, London. BS 8110: Part 1. 1985.

68. Eurocode No. 2. *Design of concrete structures. Part 1: General rules and rules for buildings*. EC2 Part 19xx, Final Draft 1990.

69. Australian Standard. *Concrete Structures*. AS 3600: 1988.

70. Bentur, A. Curing and the need for durability testing. *Proc. of a Workshop on: Aspects of testing concrete for durability*. Ballim, Y.and Alexander, M.G. (Eds.) University of the Witwatersrand, Dept. of Civil Engineering. Johannesburg. OCT. 1991. pp. 1-4.

CHAPTER 3

DEVELOPMENT OF TEST METHODS FOR CHARACTERISING POTENTIAL DURABILITY

3.1 Introduction

It will be noted in the discussion presented in Chapter 2, that various researchers characterise potential durability of concrete using different parameters, often measured in different ways. However, the common assumption underlying all these characterisation methods is that, at a particular time, the more refined and "closed" the pore structure is, the more durable the concrete is likely to be. This refinement of the pore structure may result from advance states of hydration, low b/w ratios, the use of cement extenders of a combination of these. Added to this is the understanding that, to be relevant to durability assessment, the degree of pore structure refinement should be monitored by measuring one of the transport characteristics of the concrete such as water penetration or permeability.

This approach is intuitively sound, since most of the deterioration processes associated with concrete involve the movement of aggressive agents or dissolved substances into or out of the concrete. Hence, if potential durability, as a physical property of the material, is to be quantified, this would have to involve a measure of the mass fluid transport ability of concrete. These measurements provide engineers and researchers with the ability to compare the potential durability of a particular concrete relative to a pre-defined notion of the required extent of pore structure

refinement. They also provide a single parameter by which the potential durabilities of different types of concrete can be compared, accounting for all the physical and chemical factors influencing the relevant physical properties of such concrete.

However, these characterisation test results ultimately have to be related to actual concrete deterioration processes. They will have to be correlated with long-term in situ measurements of concrete deterioration by the various aggressive agents and mechanisms. For example, the rate of chloride diffusion into concrete is considerably lower in GGBS concretes because the aluminate of the GGBS increases its ability to chemically bind chlorides[1]. This means that, for the same numerical value of the durability characterisation parameter (say, permeability), GGBS concrete can be expected to be more durable in a chloride environment than, say, fly ash concrete.

Hence, of themselves, the durability characterisation tests do not necessarily indicate the relative resistance of a concrete to a particular deterioration process. The intention is rather to indicate the relative ease with which liquids or gases may move through the concrete on the basis of a measure of the nature of the pores and the degree of inter-connection of the pore structure. This provides a global indicator, obtained at a relatively early age of the concrete, which is then correlated with the long-term performance of the concrete in a given aggressive environment.

3.2 Types of Characterisation Test Methods

A large and varied number of characterisation test

methods have been developed by researchers working in the field of concrete durability. These vary not only in the physical parameter being measured but also in the degree of sophistication and ease of use of the test equipment. Some tests have been developed for laboratory use only while others are intended for in situ use as well. All these tests can, however, broadly be categorised in terms of the physical property of concrete being measured. These categories are discussed below.

3.2.1 Absorption tests

These tests generally measure the volume or time rate of water absorbed when a concrete surface is brought into contact with the liquid. The absorption takes place under a low to negligible pressure head so that water uptake is mainly due to capillary action and the hydrophillic nature of the hardened cement paste.

Because of the nature of these tests, it is important that the samples being tested be brought to some standard of dryness before they are placed in contact with water for absorption to take place. As no standard has yet been established on the method of drying and immersion of the samples, widely varying results have been obtained for the water absorption of concrete from tests done using different test procedures[2].

3.2.2 Water penetration tests

In these tests, water is forced into the concrete under a high pressure head and, after a fixed time, either the depth or amount of water penetration is measured. A well known example of this form of test is the DIN

1048[3] test in which water is forced into an approximately 100 mm thick concrete sample over a period of 96 hours. The sample is then split at right angles to the penetration face to obtain a measure of the depth of penetration.

A problem with this test and the similarly conducted ISO/DIS 7031[4] test, is that doubt has been expressed as to the accuracy with which the depth of water penetration can be measured visually[5]. These tests have also been criticised because the test fluid (water) reacts with the unhydrated cement in the concrete and therefore alters the pore structure of the test sample during the test. The significance of this criticism increases as the contact time between test water and the sample increases.

3.2.3 Permeability tests.

In this category of tests, an attempt is made to measure the D'Arcy coefficient of permeability of the concrete. A fluid is forced to flow through the concrete under an applied pressure gradient and, by monitoring the pressure gradient and/or the amount of fluid passing through the concrete, a value of permeability is calculated. This value is expressed either as a coefficient of permeability, k, in units of velocity (m/s) or as an intrinsic permeability, K, in units of area (m^2). The difference in these two measures of permeability is that k is a function of the type of permeating fluid while K is (theoretically) independent of the fluid used in the test. Intrinsic permeability is therefore the parameter preferred by researchers. Tests to determine the permeability of concrete generally use water, nitrogen or oxygen as the permeating fluids.

Permeability tests can further be placed into the two categories discussed below. Note that, because of the many varieties of permeability test methods available, this review is limited to the most prominent examples in each category of test method.

Constant pressure head tests:
In this type of test, a fluid under constant pressure head is applied to one side of a concrete specimen and the change in pressure or amount of fluid emerging on the downstream side of the specimen is measured. An important consideration in this type of test is that steady state flow conditions (inflow = outflow) have to be established for the results to be applicable to the D'Arcy equation. The low flow rate of water through concrete means that a long time is required to establish steady state conditions[6,7]. Most researchers have therefore resorted to air permeability measurements. This, however, introduces the difficulty of measuring relatively small amounts of a compressible fluid on the downstream side of the sample.

Varying pressure head tests:
In these tests, a positive or negative air pressure (relative to atmospheric) is applied to one side of a concrete specimen and the rate of decay of the pressure or vacuum is monitored. Compared to the constant pressure test, the main advantage of this approach to permeability measurement is the elimination of the complex and expensive equipment required to maintain the pressure on the upstream side and measure the amount of fluid emerging on the downstream side. The apparatus is therefore less costly, easier to operate and yields results in a relatively shorter period of time.

3.2.4 Mechanical tests

Attempts have been made to characterise the quality of the covercrete region of concrete by measuring one of its physical properties such as strength. One of the advantages of this approach is that it would provide a parameter which engineers are familiar with and would find easy to apply. However, the limited thickness of the covercrete region makes it difficult to test directly and a number of indirect tests have been proposed[8,9,10] which are aimed at measuring the strength of the covercrete and thereby providing an indicator of its durability characteristics.

The main criticism of instruments such as the Schmidt Rebound Hammer as a means of measuring compressive strength has been that the results are influenced by the condition of the concrete surface. However, this may be a positive consideration when these instruments are used to indicate the quality of the covercrete. Such instruments are therefore being considered by some researchers for providing indirect measures of the effectiveness of curing[11].

3.3 Selection of Durability Characterisation Test Methods

A number of guidelines were identified in selecting the test methods to be used for characterising the potential durability of concretes under this project. These are discussed below.

3.3.1 Test parameters

It was decided that mechanical test methods (as

discussed in 3.4.2 above) would not be used for characterising the durability properties of covercrete. This decision was taken on the basis of the limited success and acceptability which these tests appear to be enjoying. Also, in considering methods for testing the effectiveness of various curing procedures, Dransfield[12] argues that the effect of carbonation is to increase the surface hardness of the concrete and:

> *"Since poor curing is likely to increase the amount of carbonation which occurs in the surface layer, this test method (the Rebound Hammer) cannot be considered as a reliable method of testing the curing of concrete"*

It was rather decided that tests had to be adopted or developed to measure the air and water transport properties of the concretes. Testing both the air and water transport properties was necessary for two reasons:

- As mentioned before, most of the concrete deterioration processes involve the movement of gases or ions dissolved in water. While the characterisation test method is not expected to replicate the movement of aggressive agents through concrete, it is important to simulate the real situation as closely as possible. It was therefore felt that the measurement of an air and a water transport property of concrete would be necessary to maximise the possibility of correlating the potential durability test with a wide range of actual deterioration processes.

- The debate on the usefulness of potential durability characterisation testing has not yet been resolved. This is evidenced by the large

variety of test methods that have been proposed, some of which were discussed above, coupled with the relatively small number of tests that have been accepted in specifications. The tests which have been adopted as standard specifications (for example, the British Standards initial surface absorption test (ISAT)[13] and the DIN water penetration[3] tests) have been criticised[14,5] for not being sufficiently accurate or applicable to all types of concrete.

Hence, the development of a test method for measuring potential concrete durability is located at a stage where the general direction has been established, but the specific parameter to be tested and the method of testing has not been isolated. It was felt that measurements of air and water transport properties would be sufficient to ensure compatibility with international research directions on concrete durability testing. This would allow the results to be compared with those of other researchers and possibly assist in the development of an acceptable test method.

An important disadvantage with the water penetration tests is that the fluid being used in these tests is reactive with cement. Hence, further reaction with unhydrated cement takes place during the test and this influences the parameter being measured. It was felt that this criticism was significant enough to avoid the pressurised water penetration method of testing. In addition, this test is not applicable to poor quality concretes where water passes through the sample before the end of the required test time and the depth of penetration cannot be measured.

3.3.2 Test method and apparatus

In order to exercise maximum control over the quality of the concretes being tested, it was decided that the test was to be laboratory-based rather than an in situ test. This decision was based on the problems associated with in situ tests related to an inability to control the moisture content of the concrete. Whilst it would have been an additional advantage if the test was designed to be used on in situ concrete as well, this was not to be an important design requirement. However, it was considered essential that the apparatus allow for laboratory testing of samples which have been retrieved from in-service structures. This requirement precluded test methods which use "custom-made" samples, cast specially to suit the test apparatus such as that proposed by Schonlin and Hilsdorf[15] (discussed later).

It was also considered important that the test apparatus developed be of simple design and be easy to construct. The test itself was to be such that it provided results within as short a time as possible. Since the main objective of these tests would be to ensure better on-site control of concrete quality, a simple design and short test time would encourage the test apparatus to be used in a construction site laboratory. Also, given the relatively low level of technical sophistication of a large proportion of construction personnel in Southern Africa, the test method was to be simple to perform.

An attempt was made to keep the cost of the apparatus as low as possible. However, as with most test apparatus, the cost of the facility can vary considerably depending on the sophistication of the measuring, recording and control systems. For example,

the cost of manually recording measurements can be very different from electronically capturing measurement data into a processing facility for analysis. Hence, in the design of the apparatus, it was considered advantageous to provided users with an option as to the level of sophistication of apparatus they are willing to develop, depending on the rate of usage of the apparatus and their perception of relative costs.

3.3.3 Concrete sample thickness

One of the objectives of this research project was to attempt to provide guidance on the relationship between depth of cover and durability. There are punitive economic implications to providing both too much or too little concrete cover over the reinforcing steel. Hence, information was required on the gradation of concrete properties in the covercrete zone from the outer skin to the level of reinforcing steel.

Given that the average depth of concrete cover is approximately 40 mm, this consideration meant that the test apparatus and method adopted had to be able to test relatively thin sections of concrete. The test was also to be sensitive enough to detect changes in the durability properties at various depths in the covercrete.

With these considerations and concerns in mind, it was decided that, as a starting point, the test methods should include measurements of air permeability and water absorption of the covercrete for the purpose of characterising potential durability of concrete. The selection and detailed development of these tests are further discussed below.

3.4 Selection of Air Permeability Test Apparatus

It must be emphasised that, when testing concrete for permeability in the context of its durability, an attempt is not being made to measure permeability as a fundamental property of the material. The objective is rather to obtain an indication of the ability for fluids to pass into or out of the concrete by testing samples of that concrete which have been subjected to a controlled or uniform pre-treatment procedure. To determine permeability as a fundamental property requires expensive equipment and time consuming procedures which do not alter the "natural" pore structure of the concrete during the test.

Hence, in the selection of a durability test, it is accepted that some alteration of the pore structure will occur during the sample pre-treatment and testing procedure. However, as Dhir argues[16], it is also accepted that the same relative degree of pore structure alteration occurs with different concrete types. This means that, while a distorted value of permeability is obtained from the test, the results still allow the relative durability performance of different concretes to be compared (see further discussion on this aspect in Section 4.2.3, Chapter 4).

This approach can well be compared with the cube compressive strength test. The numerical value of strength obtained when a set of cubes are crushed bears little resemblance to the strength of the in situ concrete to which these results are meant to refer. This difference derives mainly from the following reasons:

- the concrete in the cube has been compacted and

cured in a very different way from that of the in situ concrete;

- the stress states in the cube during testing are different from those experienced by the in situ concrete; and
- the test cube is not subject to the spatial variation in engineering properties which is characteristic of in situ concrete.

Despite these unknown components of the cube strength test, it does provide an indication of the quality of the in situ concrete and experience with the test gives engineers enough confidence to use it in specifications for the quality of concrete.

3.4.1 Selected survey of proposed air permeability test methods

A number of air permeability test apparatus have been proposed by various researchers. A selection of the more promising of these apparatus is discussed below.

Dundee University permeameter

Dhir et al[17] have developed a sophisticated apparatus which measures the permeability of concrete to gas and water under a constant applied pressure head. The apparatus allows steady state flow to be achieved in a relatively short time, ensures accurate measurement of the downstream conditions through the provision of sensitive measuring equipment and appears to provide reliable measures of intrinsic permeability. Figure 3.1 is a schematic arrangement of this apparatus, giving an indication of the complexity concomitant with its degree of sophistication. The apparatus is expensive, does not appear to be easy to use and is not conducive

to general, on-site laboratory use.

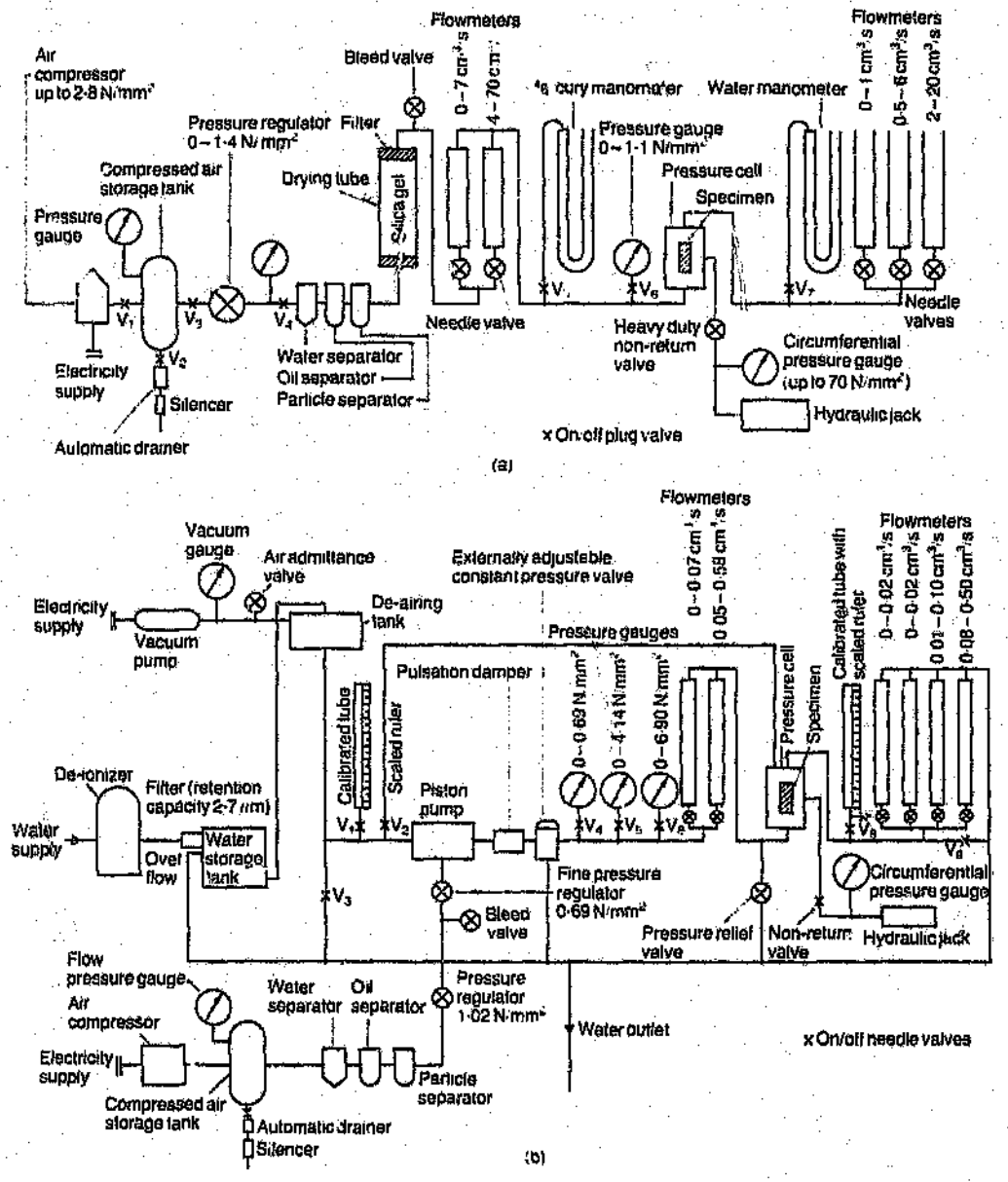

Figure 3.1 Schematic arrangement of the permeability test apparatus developed by Dhir et al[17] using (a) air and (b) water

Division of Building Technology permeameter

The Division of Building Technology at the South African CSIR has developed a basic permeability test apparatus[18] which forces air, under a constant pressure of approximately 200 kPa, through a 50 mm thick concrete slice. The amount of air emerging on the downstream side is collected and measured after a fixed time has elapsed. This measurement is then used to calculate a permeability value for the concrete. The test apparatus is also suitable for use with water as the permeating fluid, with the constant pressure then being increased to approximately 1 MPa.

The test method requires that the concrete sample be epoxy cast into a mould and the seal in the permeameter is then established against the epoxy surface. The steel mould has a well machined and highly polished inner surface to allow easy removal of the sample after casting and to ensure a close tolerance on the dimensions of the epoxy seal.

Leeds University permeameter

Cabrera and Lynsdale[19] have proposed a constant head air permeameter which uses a novel sample sealing method. The concrete test sample is placed in a silicone rubber collar which is then axially compressed in the permeameter. The rubber collar expands transversely because of the Poisson ratio effect. Outward expansion is restrained by a steel sleeve and the expansion is concentrated onto the edge of the sample, creating an air-tight seal. This arrangement is shown in Figure 3.2 below.

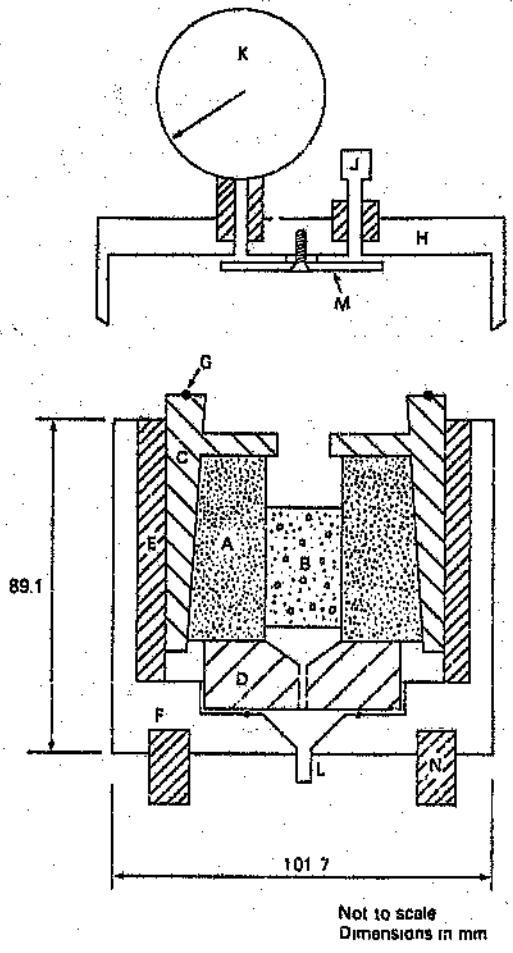

A inner silicone rubber cylinder
B sample
C inner stainless steel cylinder
D bottom stainless steel seating
E PVC collar
F outer stainless steel body
G Rubber O-ring
H stainless steel cap
J gas inlet
K pressure gauge
L gas outlet
M plastic circular baffle
N sitting guides

Figure 3.2 Section through the Leads University permeameter showing the rubber collar seal[19]

Vacuum pressure permeameter

Schonlin and Hilsdorf[15] have developed a rising pressure head apparatus which applies a vacuum pressure of 1 kPa below atmospheric on one surface of the concrete sample and monitors the time required for the pressure to increase to 50 kPa. Although this apparatus

uses "custom -made" samples for testing, it is mentioned here because the vacuum pressure is used to seal the sample (in its holder) into the permeameter. This is an interesting principle when considering the cost and complexity of ensuring air-tight sealing in a permeameter. Figure 3.3 shows a schematic arrangement of this apparatus. A possible weakness with this apparatus is that air in the environment is used as the permeating fluid. In the absence of any control over the quality of the air, it may be difficult to compare results obtained using the apparatus in different environments and laboratories.

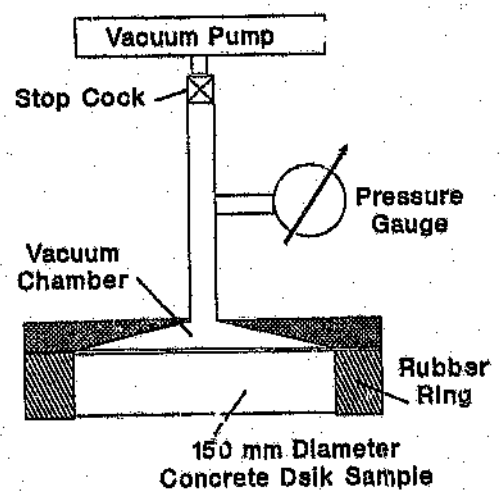

Figure 3.3 Schematic arrangement of the rising pressure head permeameter developed by Schonlin and Hilsdorf[15]

Falling head permeameter

Blight[20] has developed a falling head permeameter for measuring the permeability of compacted asphalt mixes. In this case, a positive pressure is applied to one side of the specimen and the time rate of pressure

decay is monitored to derive a D'Arcy coefficient of permeability. The apparatus is inexpensive, uses a mercury filled manometer to monitor upstream pressure and is relatively simple to operate. As with the vacuum pressure permeameter discussed above, this apparatus also uses air as the permeating fluid. A schematic arrangement of this apparatus is shown in Figure 3.4.

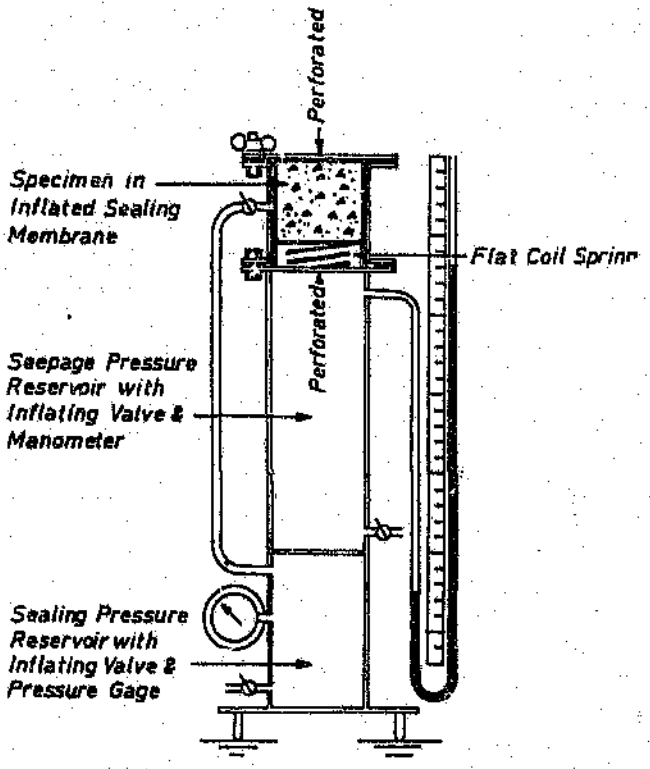

Figure 3.4 Schematic arrangement of the falling head permeameter developed by Blight[20]

In view of the requirements of the permeability test apparatus discussed in Section 3.3 above, it was decided to develop a permeameter based on this model of the falling pressure head permeability cell for the following reasons:

- simplicity of operation;
- low cost;
- design flexibility to accommodate different

sample sizes; and

- ease of manufacture.

3.5 Development of the Air Permeability Test Apparatus

3.5.1 Detailed description of the Blight apparatus

As shown in Figure 3.4, the Blight apparatus consists mainly of a cylindrical pressure chamber with a volume of approximately 5ℓ. The sample, in this case a 100 mm high x 100 mm diameter asphalt briquette, is placed in the top section of the permeameter, covered by the perforated plate. To prevent leakage of air along the sides of the sample, the curved surface of the briquette is coated with a soft wax and the coated sample is placed in a custom-made, latex rubber sleeve. This rubber sleeve, with a skin thickness of approximately 2 mm, is made so as to have flanges on the top and bottom which assist in sealing the sample into the apparatus. The sample in the rubber sleeve is then placed into the steel sample holder which is assembled onto the top of the permeameter together with the perforated cover plate.

The annulus formed between the steel sample holder and the rubber sleeve is pressurised through an independent pressure chamber, located at the bottom of the permeameter. A pressure of approximately 70 kPa is required to seal the sides of the sample.

When the sample is located and fixed into the permeameter, the sealing pressure is applied and held constant by isolating the lower pressure chamber. The

pressure in the main chamber is increased to the required test pressure and the time is recorded when this chamber is isolated. The time rate of pressure decay is then monitored by noting the height of the mercury in the manometer at various times.

3.5.2 Modifications made to the Blight permeameter

In developing the permeameter for testing concrete rather than bitumen samples, modifications were made to the Blight permeameter. These modifications are discussed below.

Pressure monitoring

The mercury-filled manometer was replaced by a 0 to 160 kPa air pressure gauge. It was felt that this would allow for a more convenient measure over a wider range of test pressures.

Test gas

A problem with the use of compressed air as the permeating fluid, is that it is difficult to determine or control the composition of the air. Added to this, the presence of moisture and carbon dioxide in the air is undesirable as these are both reactive with cement. It was therefore decided to use oxygen as the permeating fluid as this would allow for greater control over the test gas and hence, greater repeatability of the test method.

Sample sealing

The latex rubber sleeve method used by Blight was

thought to be inappropriate for concrete testing because:

- the rubber sleeve system requires a fixed sample height and it was expected that concrete samples of varying height would be tested;
- the permeameter should be flexible enough to accommodate irregularly shaped samples as well as cylindrical samples of varying diameter.

Two sample sealing methods were developed for use with the permeameter. These are discussed in more detail below.

3.5.3 Description of the Falling Head Permeameter Developed.

Figure 3.5 shows a schematic arrangement of the permeameter while Figure 3.6 shows a completed unit with the perforated cover plate removed. The main pressure cylinder is made from a length of 106 mm internal diameter, mild steel water piping with a wall thickness of approximately 4 mm.

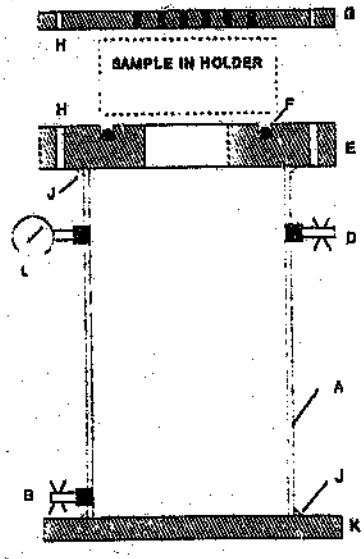

A	106 mm ID mild steel tube
B	Gas inlet valve
C	Pressure gauge
D	Gas outlet valve
E	Top plate
F	Rubber O-ring in 5 x 5 mm groove
G	Perforated cover plate
H	3 holes per plate for 8 mm bolts
J	Fillet weld
K	base plate

Figure 3.5 Schematic arrangement of the falling head permeameter

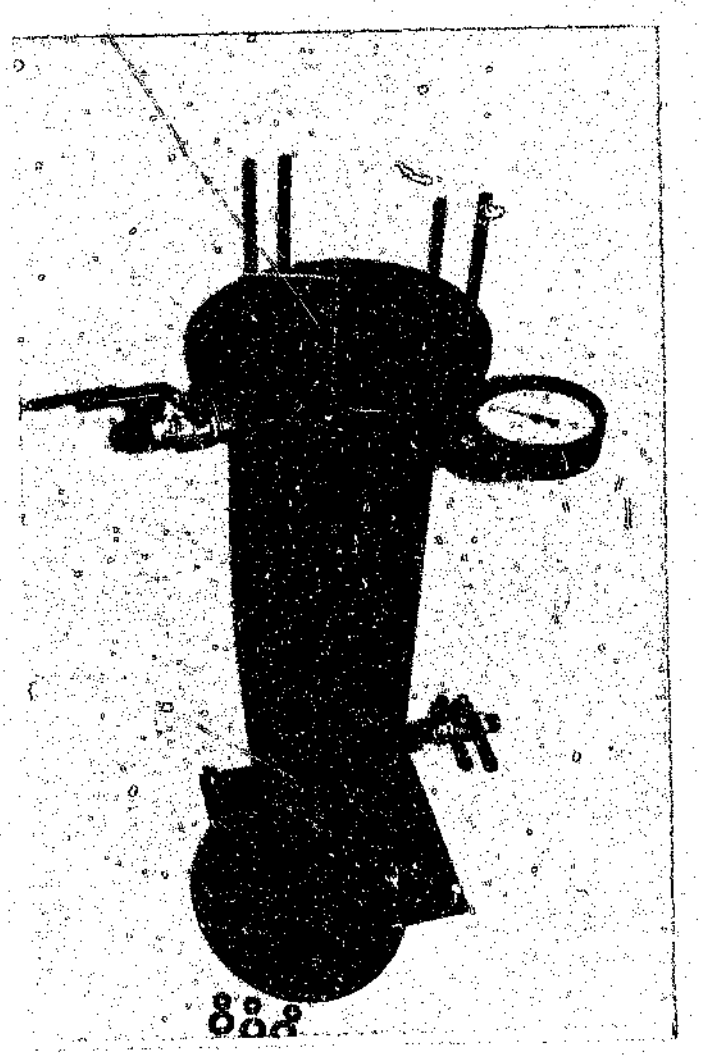

Figure 3.6 A completed permeameter unit with the cover plate removed

A square base plate was used and four screws were located in the corners to allow the unit to be stabilised and levelled in its final position. The only essential machining required is the 90 mm diameter opening and the 5 mm groove in the top plate. It is not important that the top plate and the perforated cover plate be circular as shown. It may be easier, from a cutting point of view, if these plates were square.

Ordinary fillet welds are used throughout the unit for connecting sections together. These welds were tested by sealing the top plate and applying a pressure of 130 kPa. It was expected that the maximum test pressure would be approximately 100 kPa. Leaks were identified using soapy water and sections were re-welded until the unit was air-tight.

Sealing the sample in the permeameter

As was mentioned earlier, two methods of sample sealing were developed. The first method, which involves epoxy bonding of the sample into a PVC ring, was used during the initial part of the work. The second method, which uses a rubber collar to seal the sample, was developed later and, while being easier to use, is not as flexible as the first method in the size and shape of the sample which can be accommodated.

Method 1: PVC ring and epoxy seal. This method involves fixing the sample to be tested into a PVC ring using epoxy as shown schematically in Figure 3.7. The ring is cut from standard 102 mm diameter PVC tubing with a wall thickness of ±3 mm. The lower rim of the PVC ring seats on a rubber O-ring placed in the groove on the top plate of the permeameter. Figure 3.8 shows a detail of the O-ring on the top plate. When the perforated cover plate is tied down, the PVC ring is pressed onto the rubber O-ring, providing an air tight seal.

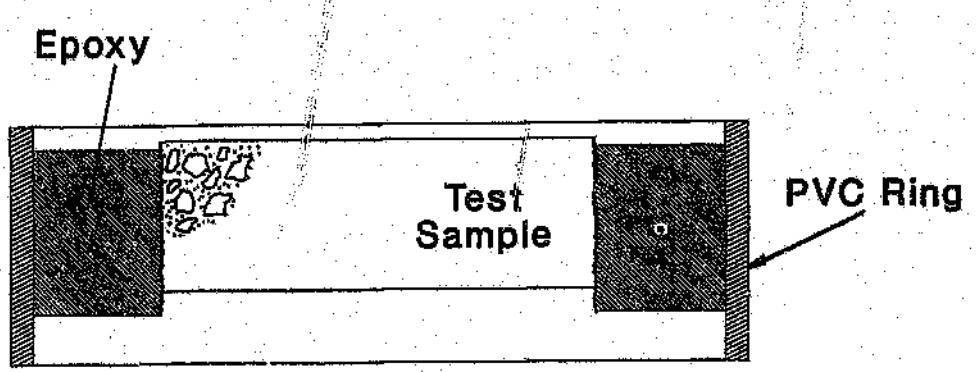

Figure 3.7 Schematic arrangement of the test sample fixed into a PVC ring with epoxy.

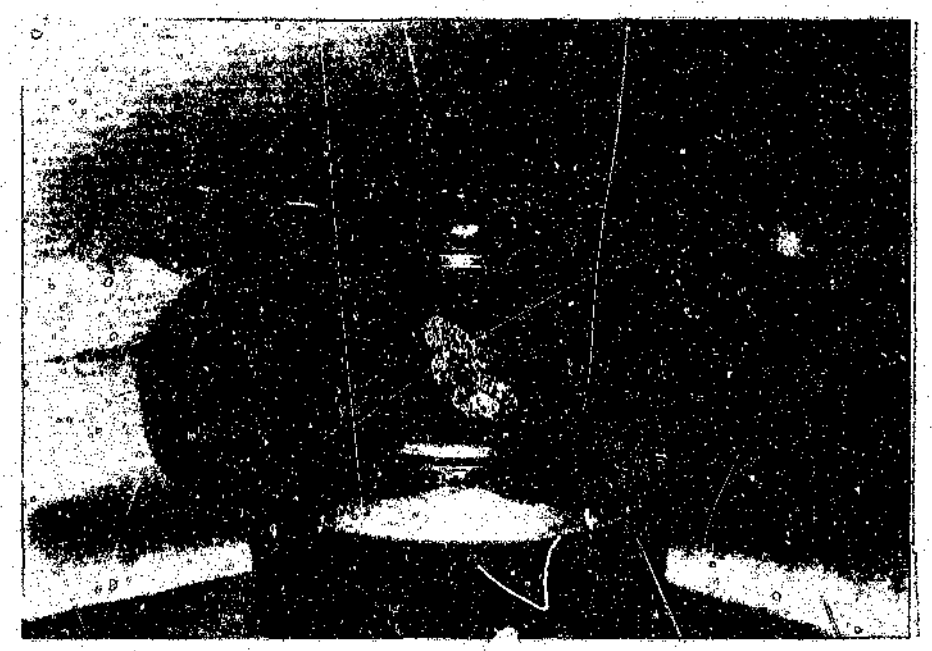

Figure 3.8 Detail of the rubber O-ring on the top plate

The O-ring is manufactured from 5.6 mm diameter neoprene rubber cord with a Shore hardness[21] of approximately 70 degrees. The cord is formed into a ring by bonding the ends with a commercially available cyanoacrylate glue. A 6% stretch is allowed in the cord to ensure that it seats well in the groove. This means that the cord is cut 6% shorter than the average circumferential length of the groove.

The procedure used for fixing the sample into the PVC

ring is described below. Figure 3.9 shows some of the steps involved in this procedure.

a. A PVC ring of height approximately 10 mm greater than the sample height is cut from the tube sections. One end of the ring (to be the lower end) is made perfectly flat by uniformly rubbing this end on a sheet of sand paper placed on a flat surface.

b. The inside of the ring is roughened by rubbing with a wire brush and this surface was carefully cleaned with a de-greasing agent and water.

c. The ring is placed over a mounted masonite disc (step A in Figure 3.9) and the annulus between the ring and the masonite disc was filled with plasticine.

d. A disc of thin plastic sheet is placed onto the masonite and edge of the plastic was sealed with plasticine (Steps B and C in Figure 3.9). It was later found that a thin coating of petroleum jelly on the masonite was sufficient to ensure de-bonding of the epoxy and the plastic sheet was therefore discarded.

e. The outer edges of the underside of the concrete sample is covered with masking tape (step D in Figure 3.9). A bead of plasticine is placed on the masking tape along the lower perimeter of the sample and this is lightly pressed onto the plastic sheet (or petroleum jelly) in the PVC ring (step E in Figure 3.9).

f. Epoxy is then poured into the space between the

sample and the PVC ring to a level just below the top of the sample.

Figure 3.10 schematically shows the sample and PVC ring fixed in position before epoxy casting. Figure 3.11 shows samples of the PVC rings together with a completed sample ready for permeability testing.

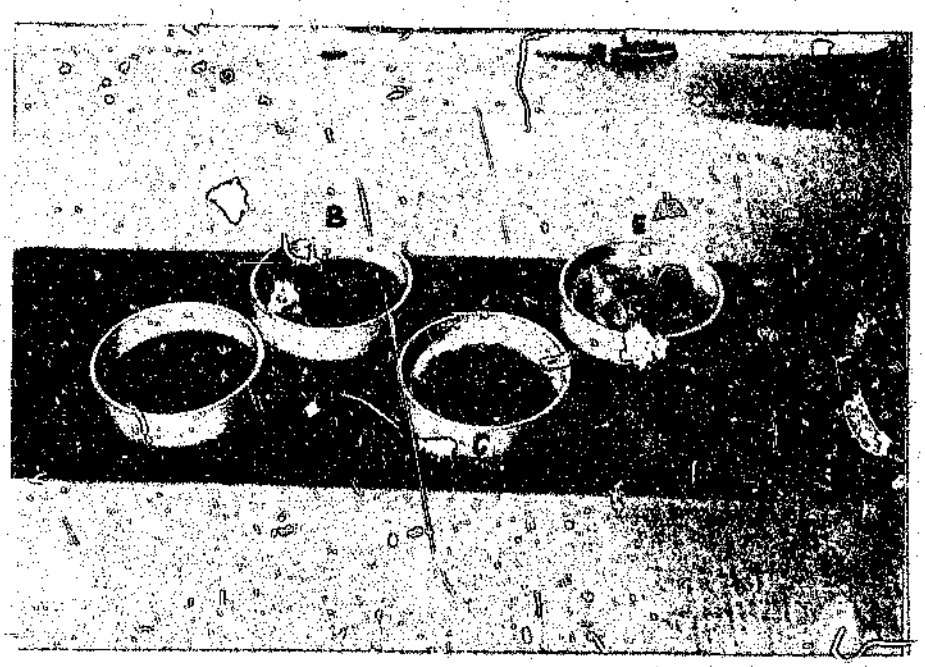

Figure 3.9 Some of the steps involved in the preparation of the sample for epoxy fixing.

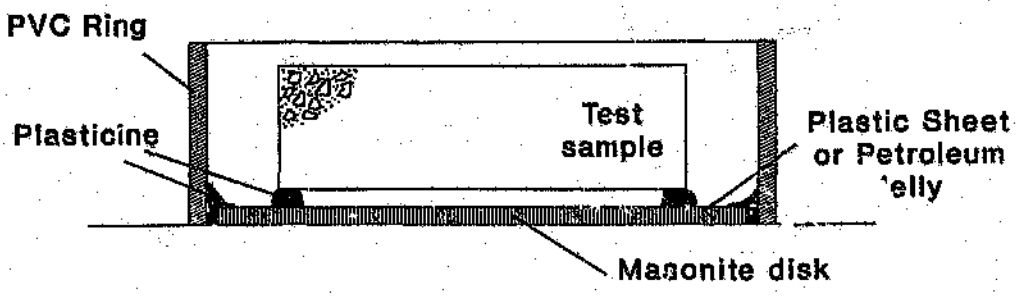

Figure 3.10 Schematic arrangement of a sample ready for epoxy casting



Figure 3.11 Examples of the PVC rings together with a concrete sample epoxy-cast into a PVC ring

An important requirement of the epoxy used in this application is that it should not creep under the applied test pressure. Creep in the epoxy would cause an increase in the volume of the cylinder and would be reflected as a decrease in pressure in the cylinder thereby causing a distortion in the test result. In this project, Epidermix 365 epoxy, manufactured by African Bitumen Emulsions (Pty) Ltd. was used. This epoxy requires a curing time of 24 hours after the resin is mixed with the activator. A flowable mortar was prepared using the epoxy and a clean silica sand, with the sand making up approximately 74% of the mass of the mixture. The addition of sand reduced the cost of sample preparation and minimised any creep potential in the epoxy.

Method 2: Silicone rubber collar seal. This method of sample sealing, based on that proposed by Cabrera and Lynsdale[17], was developed for routine testing of concretes from which 68 mm diameter sample slices can be obtained. The sample disc, cut to the appropriate thickness, is placed in a rubber collar which is axially compressed when the arrangement is tied in the permeameter unit. As described before, the sample is sealed circumferentially by the transverse expansion of the rubber. Outward expansion of the collar is restrained by placing the collar in a PVC sleeve which is cut from the same tube as the rings used in the epoxy sealing method. The inside diameter of the PVC sleeve is 0.5 to 1.0 mm larger than the outer diameter of the rubber collar. When this method of sample sealing is used, the rubber ring on the top plate is removed and the lower edge of the PVC sleeve is located in the 5 mm groove so as to centralise the sample on the top plate.

As with the epoxy seal, it is important that the rubber used for the collar does not creep under load. If this happens, the seal between the sample and the collar will be broken, causing air leakage during the test.

The amount of axial compression of the rubber collar is controlled by the thickness of the timber spacer. The perforated cover plate is tied down until it reaches the top of the PVC sleeve. Figures 3.12 (a) and (b) show the position of the perforated cover plate before and after it is tied down to compress the rubber collar.

During tests for air-tightness, it was found that, for a 15 mm thick sample, a 12 mm thick timber spacer provided a sufficient seal on the sample. Thicker

samples would require smaller timber spacers to provide the same amount of sealing pressure because of the larger contact area between the sample and the rubber collar. Figure 3.13 shows a schematic arrangement of the rubber collar assembly with the sample in place.

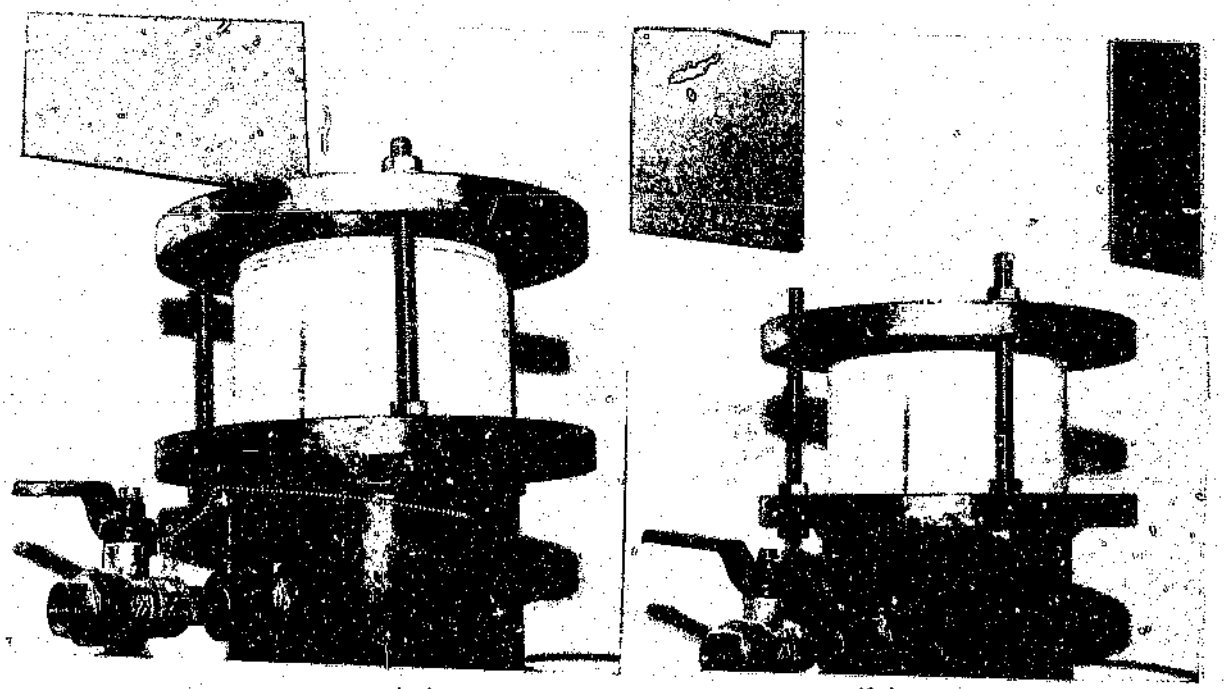

(a) (b)

Figure 3.12 Movement of the timber spacer when the perforated cover plate is tied down.

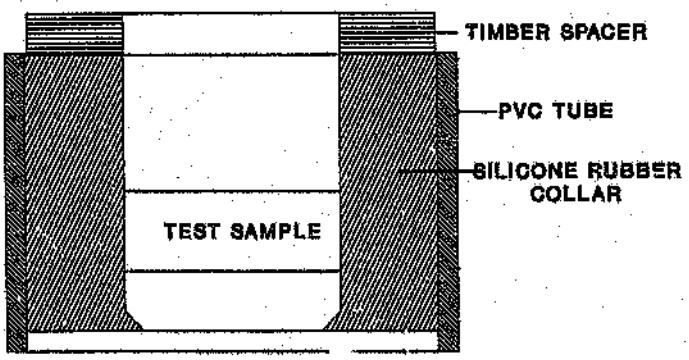

Figure 3.13 Schematic arrangement of the silicone rubber seal assembly

The rubber collar was designed so as to accommodate a maximum sample thickness of approximately 45 mm. Also, the lower end of the collar was tapered on the inside to prevent the sample from falling through. However, it was later found that this was a superfluous feature since the samples always fitted snugly in the collars.

The rubber collars were moulded in the laboratory using Silastic 9161 RTV silicone rubber with 2% 9162 catalyst (both manufactured by Dow Corning). Figure 3.14 shows a cross section through the mould used to make the rubber collars. The recess cut on the lower edge of the outer ring former simply located onto the base plate of the inner former. It was found that, with a film of petroleum jelly applied to the surfaces of the recess, the weight of the outer ring former was sufficient to prevent any leakage of the rubber while in its liquid state. Figure 3.15 shows the various components of the rubber collar seal arrangement together with the two components of the mild steel mould.

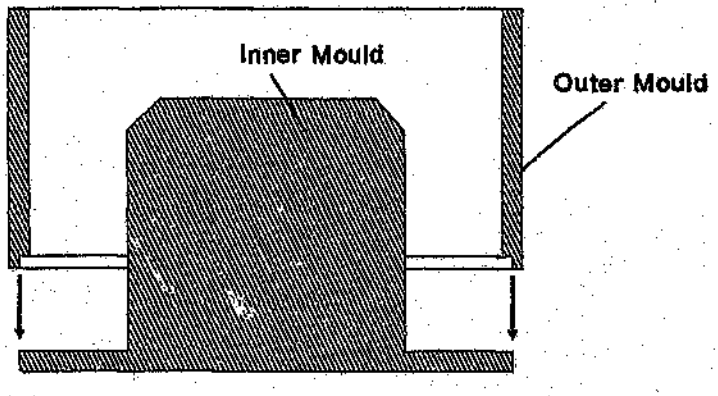

Figure 3.14 Cross section through the mild steel rubber collar mould.

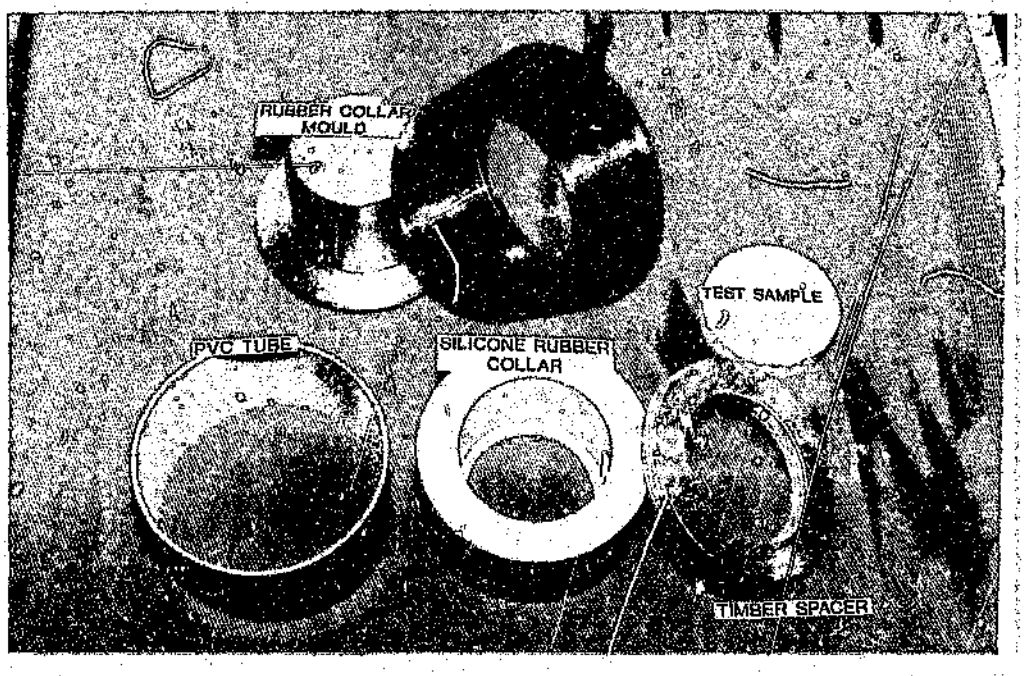

Figure 3.15 Various components of the rubber collar seal arrangement.

3.5.4 Testing the air-tightness of the sealing methods

Epoxy/PVC ring sample seal

A blank sample was prepared in which the PVC ring was prepared and mounted as discussed before but was filled with the epoxy/sand mixture only. This arrangement is shown schematically in Figure 3.16.

When hardened, the blank sample was tied into the permeameter with the lower edge seated on the rubber ring in the groove. The cylinder pressure was increased to 130 kPa when the valves were shut and the cylinder isolated. The contact between the edge of the PVC ring and the rubber ring was coated with soapy water to check for leaks. The pressure in the cylinder was then monitored for 24 hours.



Figure 3.16 Schematic arrangement of the blank sample used for ensuring the air-tightness of the epoxy/PVC ring sealing method

This test was carried out on all the permeameter cells manufactured for this project. In each case, no measurable drop in air pressure was observed after 24 hours. On the basis that the permeameter itself was air tight and that the epoxy mixture was impervious to oxygen, this test indicated the air-tightness of the PVC ring-to-rubber ring seal as well as the epoxy-to-PVC ring seal. The test also showed that no creep deflection occurred in the epoxy disk for the duration of the test pressure. The epoxy-sand mixture was therefore acceptable for use in the permeameter.

Silicone rubber collar seal

A similar test as described above, was carried out to check the air-tightness of this sample sealing method. In this case, the blank sample was made using a concrete disk specimen which had its top and bottom surfaces coated with plain epoxy. The epoxy coating was approximately 2 mm thick and this was sufficient to ensure the required imperviousness to oxygen. This blank sample is shown in Figure 3.17.

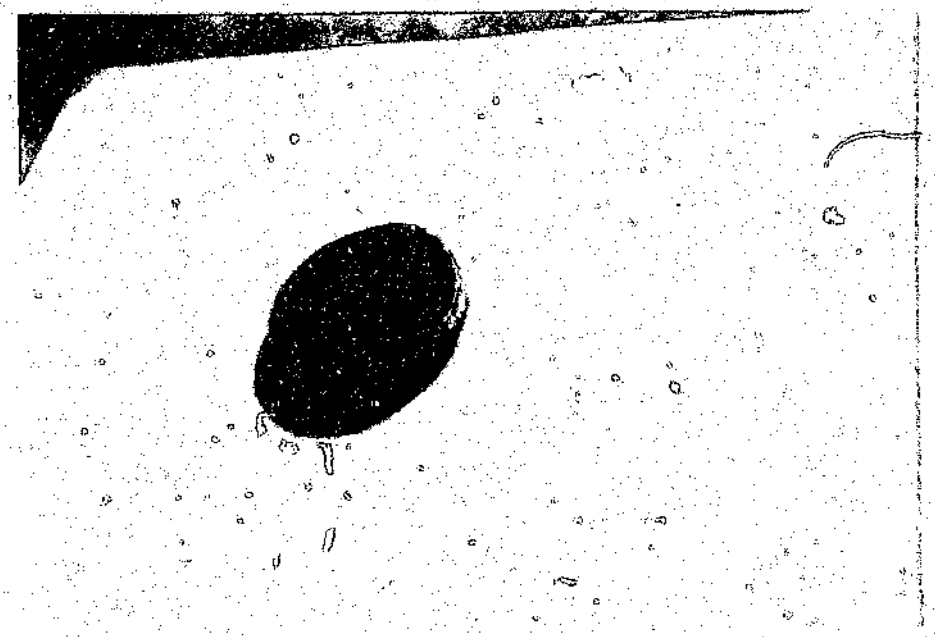

Figure 3.17 Blank sample used to check the air-tightness of the silicone rubber collar seal

The circumferential edges of the epoxy layers were chamfered back to the concrete level to ensure that the rubber collar seated against the circumferential edge of the concrete only. The sample in the rubber collar was mounted in the permeameter and the pressure was increased to 110 kPa. No pressure drop was noted after the pressure was maintained for 24 hours. It was therefore accepted that the rubber-to-top plate and the rubber-to-concrete seals were adequate.

3.5.5 Operation of the permeameter

The sample, either in the epoxy cast PVC ring or in the silicone rubber collar, is positioned on the top plate of the permeameter cell and compressed against the perforated cover plate using the 8 mm bolts and nuts. With the sample in the epoxy cast PVC ring, care must be taken not to over-tighten the nuts as this could cause debonding between the epoxy and the PVC ring.

With the sample in the silicone rubber collar, the collar is compressed by tying the cover plate down to the top of the PVC collar. It is found that, with this method of sample sealing, the 8 mm bolts are quickly damaged with repeated use and these had to be replaced with 10 mm bolts and nuts.

The inlet and outlet valves (refer to Figure 3.6) are then opened and the pressure cylinder is purged by allowing oxygen to flow through the cylinder for a few minutes. The oxygen is supplied from commercially available, pressurised cylinders with a fitted outlet pressure regulator. Since the molecular mass of oxygen is greater than that of air, the lower valve was used as the inlet valve. When purging is complete, the outlet valve is shut and the pressure allowed to increase to approximately 100 kPa. By adjusting the regulator on the pressure cylinder, the pressure in the permeameter chamber is stabilised and the inlet valve is shut. The time and pressure is recorded at this point and the pressure decay is then monitored with time. Readings are taken in decrements of approximately 10 kPa down to 50 kPa. It was found that the time required for testing varied between approximately 12 minutes for a 15 mm thick sample of a low strength, poorly cured concrete, to approximately 20 hours for a well cured, high strength concrete sample of the same thickness.

3.5.6 Development of the equation governing the falling head permeameter

The rate of pressure decay in the falling head permeameter is governed by the D'Arcy equation for the flow of fluids through porous media. The D'Arcy equation can be expressed as[20]:

$$\frac{\partial m}{\partial t} = -\frac{k}{g} \cdot \frac{\partial P}{\partial z} \qquad 3.1$$

Where:

$\frac{\partial m}{\partial t}$ is the rate of mass flow per unit cross sectional area, and

$-\frac{\partial P}{\partial z}$ is the pressure gradient in the direction of flow (- sign because the pressure decreases as the distance along the flow path increases). k is the coefficient of permeability (in units of velocity) and g is the acceleration due to gravity.

Equation 3.1 is Fick's Law which applies to the flow of compressible fluids such as air. For air, mass is related to volume V and pressure P by the equation:

$$m = \frac{\omega V P}{R\theta} \qquad 3.2$$

in which ω is the molecular mass of the permeating air, θ is the absolute temperature and R is the universal gas constant.

The change in the total mass of stored air ($\partial m'$) in time ∂t is

$$\frac{\partial m'}{\partial t} = \frac{\omega V}{R\theta} \cdot \frac{\partial P}{\partial t}$$

For a test specimen of cross sectional area A measured normal to the direction of flow and thickness d,

Equation 3.1 can be rewritten

$$\frac{\partial m'}{\partial t} = -\frac{k}{g} \cdot \frac{PA}{d}$$

Hence

$$\frac{\omega V}{R\theta} \cdot \frac{\partial p}{\partial t} = -\frac{k}{g} \cdot \frac{PA}{d}$$

Rearranging

$$-\frac{\omega Vgd}{R\theta kA} \cdot \frac{\partial P}{P} = \partial t$$

Integrating

$$-\frac{\omega Vgd}{R\theta kA} \cdot \ln(P) = t + constant \qquad 3.4$$

At $t = 0$, $P = P_o$. Therefore

$$constant = -\frac{\omega Vgd}{R\theta kA} \cdot \ln(P_o)$$

Substituting into Equation 3.3

$$t = \frac{\omega V g d}{R \theta k A} \cdot \ln \frac{P_o}{P} \qquad 3.4$$

Rearranging

$$k = \frac{\omega V g}{R A} \cdot \frac{d}{\theta t} \cdot \ln \frac{P_o}{P} \qquad 3.5$$

A description of the terms used in Equation 3.5 in its application to the falling head permeameter is given below. The units used for each of these terms in this project are also presented here.

k = coefficient of permeability (m/s)
ω = molecular mass of permeating air (kg/mol)
V = the volume of the pressure cylinder (m^3)
g = acceleration due to gravity (m/s^2)
R = universal gas constant = 8313 (Nm/K mol)
A = superficial cross sectional area of the sample (m^2)
d = sample thickness (m)
θ = absolute temperature (K)
t = time (s) for pressure to decrease from P_o to P
P_o = pressure at beginning of test (kPa)
P = pressure at end of test (kPa)

Hence, Equation 3.5 allows the coefficient of permeability of a test sample to be calculated on the basis of time and pressure measurements using the falling head permeameter.

Verification of Equation 3.5

Equation 3.4 can be re-written as :

$$t = \Pi \cdot \ln \frac{P_o}{P}$$

in which

$$\Pi = \frac{\omega V g d}{R \theta k A}$$

The factor Π is constant for a particular design of permeameter, environmental conditions and test sample. Hence, during the same test, the natural logarithm of the ratio of pressure heads should be directly proportional to the time required for the pressure to decrease. The apparatus was tested to check the applicability of this theory to the flow of gas through concrete. Three samples of OPC concrete with varying cement/water ratios were tested using the epoxy/PVC ring sealing method. The results of these measurements are shown in Table 3.1 and plots of the ratio of heads versus time relationship are shown in Figure 3.18. The samples used here were approximately 15 mm thick.

Table 3.1 Results of tests conducted to verify the falling head permeameter equation

SAMPLE 1 w/c = 0.67			SAMPLE 2 w/c = 0.56			SAMPLE 3 w/c = 0.47		
TIME (sec)	PRESSURE (kPa)	$\ln(P_o/P)$	TIME (sec)	PRESSURE (kPa)	$\ln(P_o/P)$	TIME (sec)	PRESSURE (kPa)	$\ln(P_o/P)$
0	102.5	0.00	0	102.5	0.00	0	102.0	0.00
600	90.0	0.13	540	96.5	0.06	1620	90.0	0.13
1080	80.5	0.24	1140	90.0	0.13	3120	80.5	0.24
1560	72.0	0.35	3660	68.5	0.40	4380	72.5	0.34
2460	59.5	0.54	6060	52.5	0.67	6660	61.0	0.51
4230	40.5	0.92	9180	38.0	0.99	8760	52.5	0.66
R^2 =	0.999226			0.999750			0.999630	

Note: R^2 = Linear regression coefficient of correlation

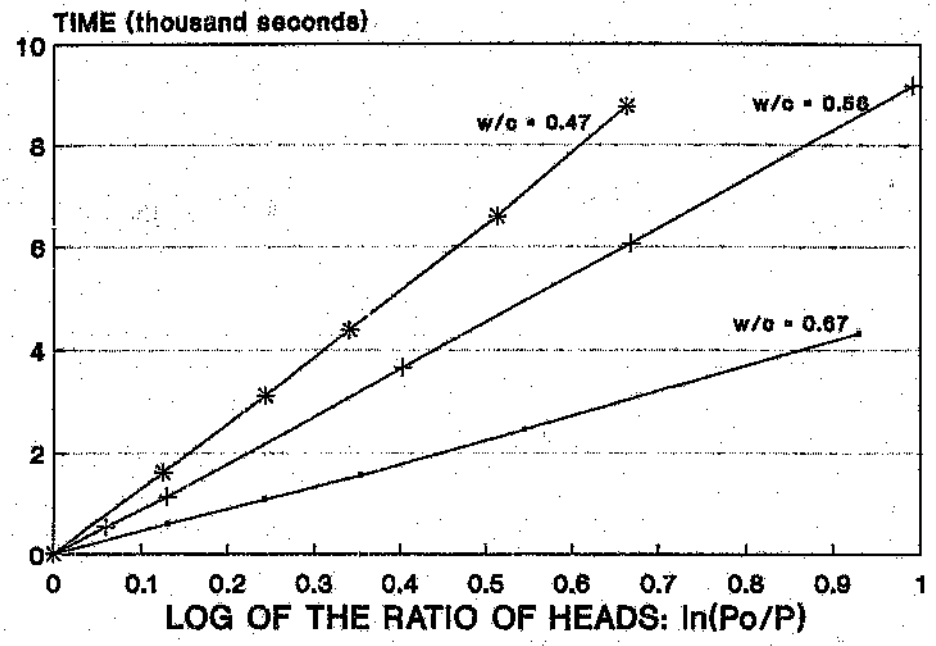

Figure 3.18 Experimental verification of the ratio of pressure heads vs. time relationship

The curves in Figure 3.18 all show a slight upward curvature indicating a very small decrease in permeability with time. It is thought that this could be due to two possible reasons:

- an imperfect applicability of the assumptions inherent in the derivation of Equation 1
- a slight increase in the moisture content of the sample during the test resulting from absorbed atmospheric moisture. This would manifest itself as a decrease in oxygen permeability as the water acts as a solid to the permeating air.

Notwithstanding this observed deviation, as shown in Table 3.1, linear regression analyses of the data shown in Figure 3.18 gave correlation coefficients which were better than 0.999. This was considered more than

adequate for the accuracy required in the determination of the permeability of concrete.

It should be noted that a value of the coefficient of 8permeability, k, is determined directly from the slope of the straight line obtained in a graph as shown in Figure 3.18. in this case:

$$k = \frac{\omega V g d}{\Pi P \theta A}$$

where the terms are as described before.

Lastly, a further advantage of the falling head permeameter can be noted from Equation 3.5. The sensitivity of the apparatus, and hence the time required for testing, can be adjusted by varying the volume of the pressure cylinder (V). A permeameter with a smaller pressure cylinder could be used to reduce the required testing time of low permeability concretes. This will be accompanied by a decrease in the sensitivity of the apparatus.

3.6 Selection of the Water Absorption Test Method

The decision to use a water absorption test as one of the methods of characterising the durability of concrete, was based largely on the logical relationship between such a test and a number of concrete deterioration processes. However, as was noted before, water is a reactive fluid in concrete and acts to advance the hydration of any unhydrated cement in the pore structure. Thus, if the objective is to obtain an indication of the pore structure of the concrete, using

water as the test fluid introduces the problem of having the test method alter the parameter being measured.

As with the permeability test, it is accepted that some alteration of the pore structure during testing has to be tolerated in the interest of practicality and convenience. It was , however, considered important that the method chosen for measuring the water absorption of concrete should not involve excessive contact time between the sample and the test water. While a notion of "excessive contact" is difficult to define, it was felt that if this period could be restricted to 24 Hours or less, the amount of additional hydration which takes place during this time would not significantly affect the results.

An important further consideration was that, if possible, the water absorption test was to use the same sample as used in the oxygen permeability test. Aside from its convenience value, this requirement would allow a direct comparison of the two test methods as durability index tests. Absorption tests such as the initial surface absorption test[13], the Figg apparatus[22] and the covercrete absorption test developed by Dhir et al[14] were excluded by this consideration. These tests, designed for in situ use but adaptable to laboratory testing, require holes to be drilled into the concrete to depths greater than the individual sample thickness which was to be tested in this project.

3.6.1 Selected survey of various water absorption test methods

In this category of tests, the samples are dried to some pre-defined standard and then brought into contact with water. The amount of water absorbed into the pore structure of the concrete is monitored by weighing the sample after a given time. Some of the more promising methods which have been developed in this test category are discussed below.

The BS absorption test

A number of concrete water absorption tests have been accepted as BS specifications[23,24,25]. However, the BS 1881: Part 122[26] test described here is aimed at general structural concrete. In this test, a 75 mm diameter core of length up to 150 mm, is retrieved from a structure or a larger laboratory specimen and dried at 105 °C for 72 hours. After cooling, the sample is placed in a water bath at 20 °C with its long axis horizontal and such that there is a 25 mm depth of water over the top of the sample. The sample is immersed for 30 minutes, then surface dried and weighed to determine the amount of water absorbed. Absorption therefore takes place only in the outer surface regions of the sample.

While this basic test describes the principles involved in water absorption testing, an important weakness is that it does not account for differences in the concrete properties of the different areas of the sample in which absorption takes place. If the hydration process had been interrupted in situ by lack of curing, the (then) exposed surfaces would be of poorer quality than the internal concrete. This

absorption test may not detect such effects since the higher absorption rates of the end surfaces would be masked by the lower absorption of the curved surfaces of the test core. Hence, the test is probably of little value as a durability test method.

Absorption by capillary rise

Jornet and Torrent[27] as well as Parrott[28] propose the use of water absorption through capillary rise as a measure of the quality of cover concrete. This involves bringing one surface of a concrete sample into contact with a water surface allowing only approximately 2 mm of immersion. The time rate of water uptake through capillary suction is then monitored by weighing the sample at regular intervals.

In this test, water is absorbed through the pore structure of the concrete mainly by the capillary tension of the water meniscus. It is argued[27] that the larger the capillary pores, the lower the resistance to the passage of water and hence, the faster the volume rate of absorption. This underlines the appeal which these tests have as durability indicator tests.

Senbetta and Scholer[29] have proposed a similar test to monitor the efficiency of curing. In this test, a 25 mm core is retrieved from a larger sample and this core is cut into 10 mm thick discs, starting at the exposed surface. The downstream surface of each disc (with respect to the direction of drying) is then brought into contact with a free water surface and the water absorbed after one minute of exposure is determined by weighing the discs. This value is used to calculate a coefficient of absorptivity which is a measure of the

extent of hydration and, hence, the effectiveness of curing of the samples.

The Kelham sorptivity test

Kelham[30] has proposed a test based on a measurement of the water sorptivity of concrete. The concept of sorptivity is more commonly used as a soil physics parameter in the study of water infiltration into soil but is applicable to the infiltration of water into any porous material. When one surface of a body of porous material is brought into contact with water, the depth of infiltration, i, after time t is described by the equation[31]:

$$i = S\, t^{\frac{1}{2}} \qquad 3.6$$

Where S is the sorptivity, a measure of the water transmissibility and, hence, pore structure properties of the material. This equation shows that there is a linear relationship between the depth of water infiltration and the square root of the time required for the infiltration to take place.

The advantage of using sorptivity as a durability characterisation method is that it involves unsaturated flow conditions in concrete. Unlike water permeability which measures fully saturated flow properties, sorptivity more closely resembles the form of water penetration into real structures[32]. Concrete is only rarely exposed to saturated flow conditions and the more common circumstance is where water infiltrates the surface of the concrete under a small gravity pressure

head.

Kelham's apparatus, shown in Figure 3.19, continuously monitors the weight change of a concrete sample into which water is allowed to infiltrate under a small pressure head acting against gravity. The slope of the sample weight versus square root of time curve is then used to determine the sorptivity of the concrete.

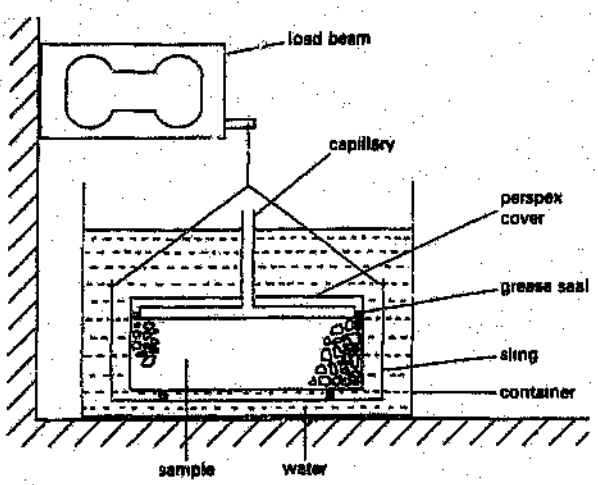

Figure 3.19 Schematic arrangement of Kelham's[30] sorptivity test apparatus

In this test, the sample is a 150 mm diameter by 50 mm thick cylinder, of which the curved surface has been sealed with epoxy. A perspex cover is placed onto the top surface of the sample and sealed along the circumference using grease. The perspex disc has a capillary tube sealed into its centre such that, when the sample arrangement is suspended in a water bath, the capillary tube protrudes above the water surface. The sling supporting the sample is attached to a weighing apparatus and, as water is absorbed through the underside of the sample, air is expelled through the capillary tube and the change in weight is

recorded. The sample is kept submerged until saturation occurs and the change in weight becomes negligible.

It was felt that, in view of its similarity with the movement of water in real concrete, the principle of sorptivity should be used in a test to characterise the potential durability of concrete. Kelham's test suffers the weakness that only one sample can be tested in the apparatus and that this sample could occupy the apparatus for up to 45 hours. In addition, the 50 mm thick samples used would negate the intention of studying the gradation of properties in the cover concrete zone. Hence, a test was developed based on the Kelham approach to sorptivity testing but modified to suit the requirements of this project.

3.6.2 Development of the water sorptivity test method

As mentioned above, it was desirable that the water sorptivity test be carried out on the same samples used in the oxygen permeability test. The test was therefore developed around a 68 mm diameter disc of concrete as the test sample.

It has been shown[30,32] that, given the small capillary sizes in concrete and the consequently high capillary forces, the direction of water absorption with respect to the action of gravity, has little effect on the sorptivity measurement. It was therefore decided that it would be more convenient to allow absorption to take place in a vertically downward direction by placing a layer of water on the top surface of the sample.

In the case of the samples which had been sealed using the epoxy/PVC ring method, the sample in the ring is

merely turned over and the recess formed by the plasticine on the underside of the sample (see Figure 3.10) is used as a water reservoir. This is shown schematically in Figure 3.20 (a). Figure 3.21 shows a completed sample ready for water sorptivity testing.

In the case of the rubber collar sealed samples, a reservoir to hold this water is formed by coating the curved surface of the disc with epoxy and immediately placing a strip of plastic tape around the full circumference of the sample. The plastic tape is placed so that it protrudes approximately 5 mm above the surface of the sample and the epoxy coating is allowed 24 hours to set. This arrangement is shown schematically in Figure 3.20 (b). A completed sample ready to be tested for water sorptivity is shown in Figure 3.22.

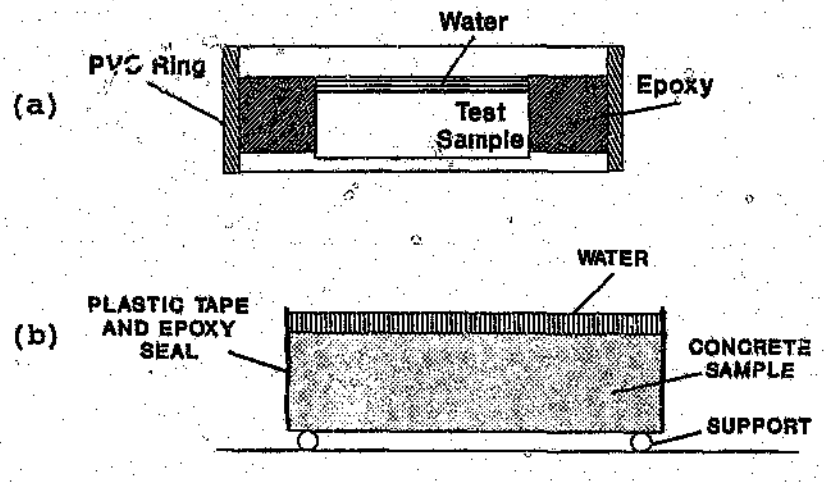

Figure 3.20 Schematic arrangement of the water sorptivity test method for (a) the epoxy/PVC ring sealed samples and (b) for the rubber collar sealed samples.



Figure 3.21 A completed epoxy/PVC ring sealed sample ready to be tested for water sorptivity.



Figure 3.22 A completed rubber collar sealed sample ready to be tested for water sorptivity.

After the sample is prepared as described above, the following procedure is used for testing:

a. The sample is weighed to an accuracy of 0.01 g to determine its dry weight and, in the case of the

rubber collar sealed samples, supported on a metal or plastic grid placed on a flat surface.

b. Using a ±20 ml syringe, a layer of water is gently placed onto the concrete surface, the water layer being approximately 3 mm deep. A clock, measuring to an accuracy of one second, is set to zero when the water first comes into contact with the concrete.

c. At pre-determined time intervals, the water is poured off the sample and the top of the sample is surface dried using slightly damp, absorbent paper. The sample is then weighed and the water layer is replaced. This procedure requires approximately 30 seconds to complete and the clock is not stopped during this period.

d. After the last measurement is recorded, the sample is submerged in a beaker of water. The beaker is placed in an evacuation chamber and a vacuum pressure of 75 kPa is applied for approximately 24 hours.

e. The sample is then weighed to determine the (apparent) saturated weight.

After some experience with the test method, it was found that weighing the sample at 1, 6 and 12 minutes was sufficient to determine the sorptivity of the ±15 mm samples used in this project. These time intervals also allowed three samples to be tested with two minute spacings in starting times.

The need to raise the rubber collar sealed sample off the surface using a support grid is only important for poor quality concretes where the water may percolate through the sample before the twelve-minute weight is determined. If this happens while the sample is on a flat surface, water will be absorbed from the underside

of the sample and a distorted result is obtained.

3.6.3 Theoretical considerations

Using Equation 3.6 above, the change in mass of the sample with time after the water infiltration has started, can be described by the following equation[30]:

$$\Delta M_t = An\rho_w S t^{\frac{1}{2}} \qquad 3.7$$

where:

ΔM_t = the change in mass of the sample with respect to the dry mass, after time t;

A = cross sectional area of the sample at right angles to the direction of absorption;

n = the effective porosity of the sample;

ρ_w = density of the water;

S = sorptivity

The porosity is determined from the difference between the dry and the saturated weights of the sample as follows:

$$n = \frac{(M_{sat} - M_o)}{Ad\rho_w}$$

where M_{sat} and M_o are the saturated and dry weights of the sample respectively and d is the thickness of the sample. Substituting into Equation 3.7 above yields:

$$\Delta M_t = \frac{(M_{(sat)} - M_o)}{d} \cdot St^{(\frac{1}{2})} \qquad 3.8$$

Figure 3.23 shows a typical plot of the mass change versus square root of time curve for the sorptivity test. The slope of the line in Region I of this graph represents the coefficient of $t^{1/2}$ in Equation 3.8. Hence:

$$Slope = \frac{(M_{sat} - M_o)}{d} \cdot S \qquad 3.9$$

A value of sorptivity can therefore be calculated from Equation 3.9

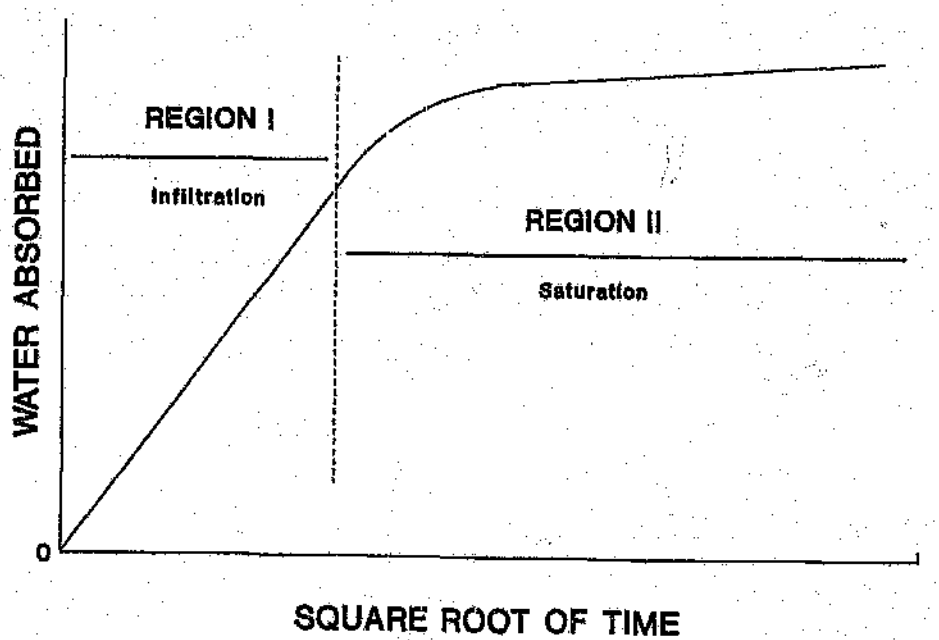

Figure 3.23 Typical plot of the results from a sorptivity test

3.6.4 Experimental verification of the sorptivity theory

Three samples of OPC concrete with varying c/w ratios were selected for water sorptivity testing to verify the linear relationship reflected in Equation 3.8 above. These samples had been tested in the oxygen permeameter using the epoxy/PVC sealing method. The results obtained from these tests are shown in Tables 3.2(a) to 3.2(c).

Table 3.2(a) Results of the water sorptivity verification tests - Sample 1

w/c = 0.67		
Time (min)	Time^{½} (sec^{½})	Water Abrorbed (g)
0	0.00	0.00
1	7.75	0.70
10	24.49	2.26
30	42.43	3.93
60	60.00	5.23
180	103.92	5.99
R^2 = Linear regression correlation coeff.= 0.999		

Table 3.2(b) Results of the water sorptivity verification tests - Sample 2

w/c = 0.56		
Time (min)	Time$^{1/2}$ (sec$^{1/2}$)	Water Absorbed (g)
0	0.00	0.00
1	7.75	0.75
12	26.83	2.32
60	60.00	4.71
240	120.00	6.28
R^2 = 0.997		

Table 3.2(c) Results of the water sorptivity verification tests - Sample 3

w/c = 0.47		
Time (min)	Time$^{1/2}$ (sec$^{1/2}$)	Water Absorbed (g)
0	0.00	0.00
1	7.75	0.46
12	26.83	1.60
46	52.54	3.35
163	98.89	6.05
R^2 = 0.999		

Figure 3.24 shows a plot of the sorptivity test results presented in Tables 3.2(a) to 3.2(c) . The correlation coefficient was calculated on the basis of the first four data points, including the zero point. Note that the slope of the Region I part of the curves, and hence the sorptivities, increases as the w/c ratio increases.

Figure 3.24 also shows the positions of the 1, 6 and 12 minute measurement times in the Region I part of the curves. The results show that good correlation coefficients were obtained using this test, indicating strong agreement between theoretical prediction and experimental results.

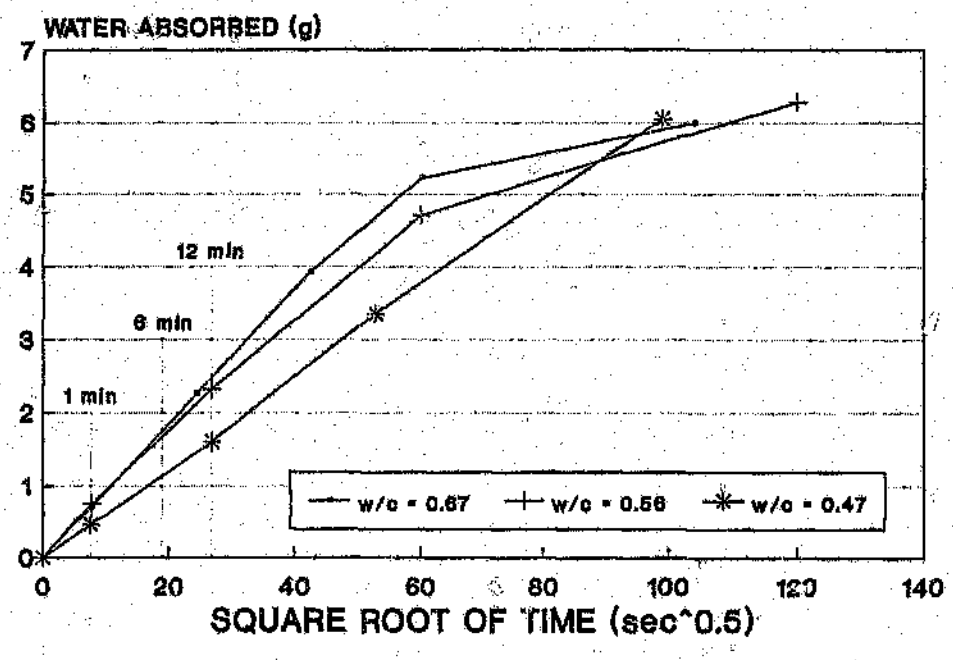

Figure 3.24 Experimental verification of the sorptivity equation

Table 3.3 shows the water absorption results of a set of samples from similar concretes as those tested above but which had been subjected to poor initial moist curing. In this case, the three test times suggested earlier (1, 6 and 12 minutes) were used. These results are plotted in Figure 3.25 below.

Table 3.3 Results of water absorption tests using three suggested time intervals

Time		Water absorbed (g) by samples with w/c ratio:		
Min.	Sec.$^{1/2}$	0.67	0.56	0.47
0	0	0	0	0
1	7.75	1.59	1.15	1.04
6	18.97	3.66	2.57	2.27
12	26.83	4.88	3.56	3.23
	R^2 =	0.996	0.998	0.997

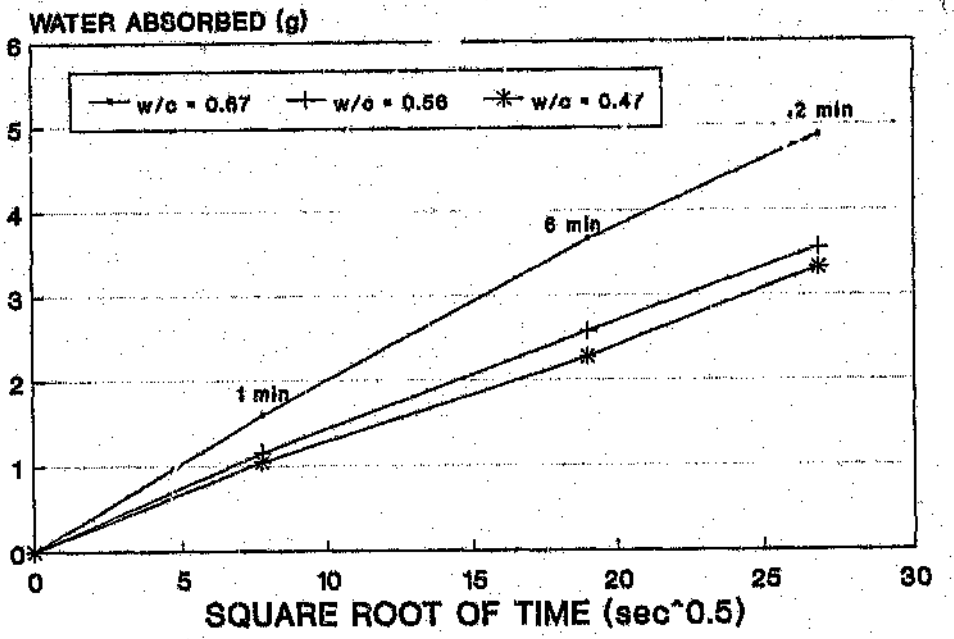

Figure 3.25 Water absorption of samples tested at three suggested time intervals

The results presented in Figures 3.24 and 3.25 show that the three suggested time intervals of measurement are sufficient for determining the sorptivity of the samples.

3.7 General Discussion and conclusion

Part of the intention of this Chapter was to expose the range of methods used by researchers to measure fluid transport properties of concrete, with the intention of characterising the potential durability of the material. A second objective was to develop the rationale for selecting the particular test methods to be used in this study. Finally, the development of the specific apparatus chosen was discussed in detail. The following general conclusions can therefore be drawn at this stage:

- There is a wide variation in both the nature and complexity of test methods used for measuring the fluid transport properties of concrete.
- A variation of the falling head permeability test apparatus, developed by Blight[20], is considered to be the most appropriate apparatus for measuring permeability. The advantages are: low cost, simple construction, easy to use.
- A variation of the Kelham[30] water absorption test is considered to be the most appropriate method for measuring the water transport properties of concrete. Using the method developed, it is sufficient to measure water absorbed by the sample at 1, 6 and 12 minutes after the start of the test. An important advantage is that this test has been developed to use the same sample as that used for the permeability test.
- Theoretical equations have been developed for both the oxygen permeability and water sorptivity test methods. Good correlations has also been demonstrated between the actual results of these tests and those predicted by the theoretical equations.

List of References

1. Schiessl, P. ed, *Corrosion of Steel in Concrete*, Report of the RILEM Technical Committee 60-CSC. Chapman and Hall, London. 1988.

2. Lea, F.M. *The Chemistry of Cement and Concrete*, Edward Arnold, London. 1970

3. Deutshe Institut für Normung. *Methods for concrete: Impermeability to water. Part 2.* DIN 1048. Germany.

4. International Standards org. *Concrete hardened - determination of the depth of penetration of water under pressure*, ISO/DIS 7031. Geneva 1983.

5. Concrete Society. *Permeability testing of site concrete - A review of methods and experience*, Technical report No. 31. London. 1989.

6. Powers, T.C. et al. Permeability of Portland cement paste, *Proc. ACI*. Vol. 51. Nov. 1954. pp. 285-98.

7. Dhir, R.K. et al. PFA in structural precast concrete: measurement of permeability. *CONCRETE* vol. 20 No. 12. Dec. 1986. pp. 4-8.

8. Andrews, A.J. Curing membrane efficiency, *ACT project*, 1982.

9. Amtsbuchler, R. Significant aspects of temperature matched curing and in situ testing. *Proc. of a CSSA Symposium on achievement and evaluation of quality concrete*. Concrete Society

of Southern Africa. Halfway House. Apr. 1989. 14 pgs.

10. Bungey, J.H. *Testing of concrete in structures*. 2nd Ed. Chapman Hall, USA. 1989.

11. Ballim, Y, Nemeth, T.M and Perrie, B. Concrete curing for water retaining structrures. Paper No. 8. *Proc. of a CSSA Symposium on concrete water retaining structures*. Concrete Society of Southern Africa. Halfway House. Nov. 1990. 15 pgs.

12. Dransfield, J.M. Developments in concrete testing for durability. Proc. of a Concrete Society symp. on *DEVELOPMENTS IN TESTING CONCRETE FOR DURABILITY*. London, Sept. 1984.

13. British Standards Instutute. *Methods for testing concrete for other than strength*. BS 1881: Part 5. 1971.

14. Dhir, R.K. et al. Near surface characteristics of concrete: Assessment and development of in situ test methods. *Mag. of Concrete Research*. Vol. 39, No. 141. Dec. 1987. pp. 183-195.

15. Schonlin, K. and Hilsdorf, H.K. Permeability as a measure of potential durability of concrete - Development of a suitable test apparatus. In ACI SP-108: *Permeability of Concrete*. American Concrete Institute. Detroit. 1988.

16. Dhir, R.K. Private communication. Dundee. Jun. 1991.

17. Dhir, R.K. et al. Near surface characteristics of concrete: Intrinsic permeability. *Mag. of Concrete Research*. Vol. 41. No. 147. June 1989. pp. 87-97.

18. van der Meulen, G.J.R. and van Dijk, J. A permeability-testing apparatus for concrete. *Mag. of Concrete Research*. Vol. 21. No. 67. June 1969. pp. 121-123.

19. Cabrera, J.G. and Lynsdale, C.J. A new gas permeameter for measuring the permeability of mortar and concrete. *Mag. of Concrete Research*. Vol. 40. No. 144. Sept. 1988. pp. 177-182.

20. Blight, G.E. A falling head permeameter for testing asphalt. *Trans. of the S.A. Inst. of Civil Engineers*. June, 1977. pp. 123-126.

21. American Society for Testing and Materials. Method D2240: *Standard test method for rubber. Property: Durometer hardness*. ASTM annual book of standards, Sectn. 09.01, 1993.

22. Figg, J.W. Methods if measuring the air and water permeability of concrete. *Mag. of Concrete Research*. Vol. 25. No. 85. Dec. 1973. pp 213-219.

23. British Standards Institution. *Precast concrete pipes and fittings for drainage and sewerage. Part 1: Spec for concrete cylindrical pipes, bends, junctions and manholes, unreinforced or reinforced with steel cages and hoops*. London. BS 5911: Part 1: 1981.

precast concrete kerbs, channels, edgings and quadrants. London. BS 340: 1979.

26. British Standards Institution. *Methods of testing concrete. Part 122: Method for determination of water absorption*. London. BS 1881: Part 122: 1983.

27. Jornet, A. and Torrent, R. Special methods to assess the durability of concrete, From: *31st HOLDERBANK Technical Meeting*. Baden, Switzerland. June, 1990.

28. Parrott, L. Water absorption in cover concrete, To be published in *RILEM: Materials and Structures*.

29. Senbetta and Scholer. A new approach to testing concrete curing efficiency. *Jnl. of ACI*. Jan/Feb 1984.

30. Kelham, S. A water absorption test for concrete, *Mag. of Concrete Research*. Vol. 40, No. 143. June, 1988. pp. 106-110.

31. Hanks, R.J. and Ashcroft, G.L. *Applied Soil Physics* Springer-Verlag Berlin Heidelberg New York. 1980.

32. Hall, C. Water sorptivity of mortars and concretes: a review. *Mag. of Concrete Research*. Vol. 41, No. 147. June, 1989. pp. 51-61.

CHAPTER 4

CHARACTERISING THE INFLUENCE OF THE VARIABLES ASSOCIATED WITH THE PROPOSED TEST METHODS

4.1 Introduction

In Chapter 3, the test methods to be used to measure the potential durability of concrete, were selected, developed and shown to be useful in testing the fluid transport characteristics of concrete. In this chapter, the intention is to calibrate the condition-of-test variables associated with a single concrete sample, which affect the results of the tests. These variables relate to:

- the thickness of the sample, measured in the direction of test fluid movement, in relation to the maximum size of the aggregate;
- the moisture content of the sample at the time of test; and
- the drying history of the sample.

In addition, an attempt is made to understand the effect, if any, of these variables on different quality concretes as affected by mix design parameters such as binder type and strength grade.

This chapter presents a review of the literature dealing with the effects of these variables. Where it was felt that further clarity was required on certain aspects, a test programme was developed in order to characterise the falling head permeameter and water sorptivity tests. The results of these tests provided guidance for the development of sample preparation and pre-treatment aspects of the test methods to be used in the main test programme.

4.2 Influence of Sample Variables on the Test Results

4.2.1 Sample thickness

Sample thickness and oxygen permeability

Equation 3.5 in Chapter 3 shows that, ceteris paribus, a linear relationship exists between the thickness of the sample (d) and the time required for the pressure to fall from P_o to P. This means that, for the same material under test, the same value of coefficient of permeability should be obtained regardless of the thickness of the sample. However, when considering the two-phase, internally flawed nature of concrete, there is a limit to the validity of this relationship. As the sample thickness decreases, the possibility of flaws (such as micro-cracks and bleed voids) short-circuiting the air flow through the sample increases and the apparent permeability of the material increases.

This effect is particularly important when the thickness of a sample, cut from a larger specimen, is less than the maximum size of the aggregate. It is known[1] that the interface between aggregate and hardened cement paste is more porous than the bulk of the material. Also, if local bleeding is likely, a bleed void could form on the lower surface of the aggregate with respect to the direction of water movement[2]. Hence, if the sample thickness is less than the maximum aggregate size, a surface of the same aggregate particle could appear on both sides of the sample. Flaws on the perimeter of such an aggregate particle would be a direct short circuit for air flow through the sample. This effect is shown in Figure 4.1 below.

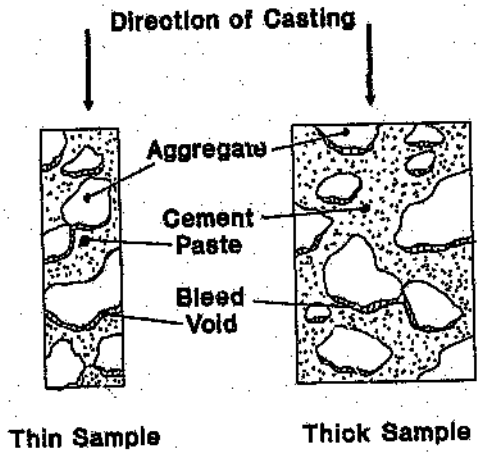

Figure 4.1 Effect of sample thickness in relation to aggregate size.

Because of this effect, Grube[3] has suggested that the sample thickness be at least three times that of the maximum aggregate size. However, the issue appears to be far from being resolved since Hooton[4] found that, using concrete with a 25 mm maximum aggregate size, the permeabilities of samples 23 mm and 45 mm thick were almost identical. He does suggest that more tests are required before final conclusions can be reached.

As stated in Section 3.3.3 of Chapter 3, a requirement of this project was to obtain a measure of the gradation of properties in the cover concrete region. This zone is commonly 25 mm to 40 mm thick and the maximum aggregate size in South African concretes is usually 25 mm. The requirement could clearly not be satisfied if the suggested minimum sample thickness of three times the maximum aggregate size was adhered to. It was therefore necessary to understand the influence of sample thickness on measured permeability under conditions where the sample thickness is close to, or smaller than, the maximum aggregate size.

Sample thickness and water absorption

In the development of the sorptivity equation in Chapter 3, it was shown that the effective porosity (n) of the sample is determined from the equation:

$$n = \frac{(M_{sat} - M_o)}{Ad\rho_w} \qquad 4.1$$

where:

n = effective porosity of the sample;
M_{sat} = water saturated mass of the sample;
M_o = sample mass at the start of the test;
A = cross sectional area of the sample;
d = sample thickness; and
ρ_w = density of water.

An assumption inherent in this analysis is that the porosity determined from Equation 4.1 is uniformly distributed throughout the test sample. If the porosity is indeed uniform through the sample, the thickness of the sample is of little consequence to the value of sorptivity obtained in the test. However, if the porosity varies with depth into the sample, the straight line relationship between water absorbed and the square root of time is no longer valid. This situation occurs in the case of concrete which has been exposed to inadequate curing: the porosity of the surface concrete can be expected to be greater than that of the internal concrete. Such a sample is shown schematically in Figure 4.2 and the general, imagined form of results from a water sorptivity test on this sample is shown in Figure 4.3.

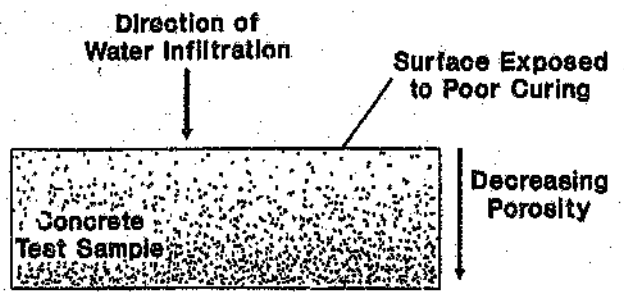

Figure 4.2 Schematic representation of a sample with varying porosity

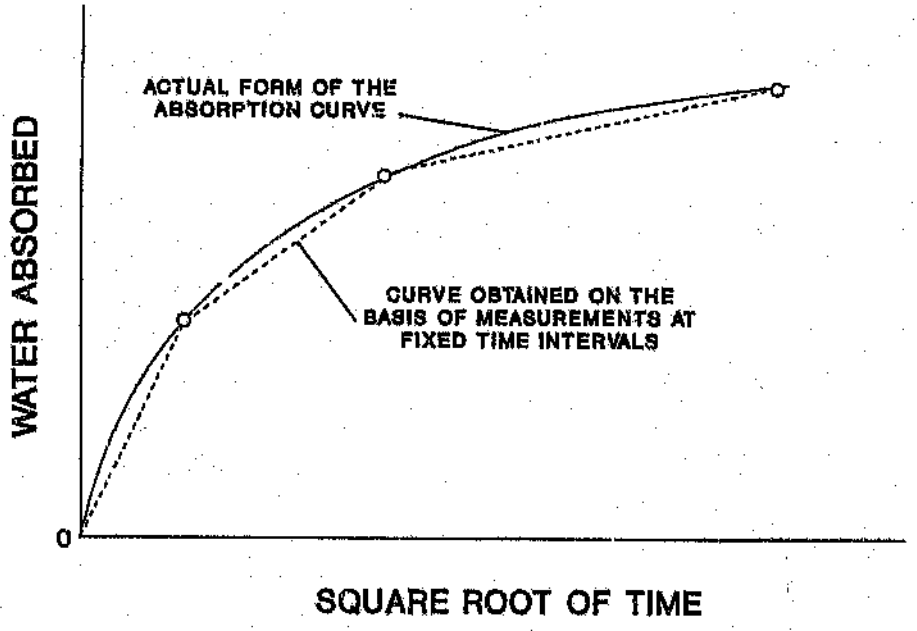

Figure 4.3 Generalised form of results obtained in a sorptivity test on the sample shown in Figure 4.2

Figure 4.3 shows that the decreasing porosity with depth into the sample is reflected by a non-linear relationship developed in the water absorbed versus square root of time plot. For the orientation of the

sample as shown in Figure 4.2, the curve shows decreasing slope indicating decreasing sorptivity with depth into the sample. Figure 4.3 also shows the form of the results obtained on the basis of mass measurements at regular intervals, as would be the case in the sorptivity test method proposed in Chapter 3.

The problem with results as shown in Figure 4.3, is that there is no clear portion of the curve to be used to determine a sorptivity value. This derives from the fact that, at any time during the test, there is no measure of the depth of water penetration into the sample. Parrott[5] argues that:

> *"... calculations of the depth of water penetration from the weight or volume of water imbibed involve the assumption that porosity does not vary with depth and that water penetrates as a sharp liquid front. These assumptions are only approximations of reality in a material like concrete."*

It is therefore not possible to divide the curve into small, discrete sections, the slope of which could be used to determine a sorptivity value. Such a value could not be ascribed to a particular depth of the sample and would therefore be of little use. One may then be forced to adopt an "average" straight line value to determine the sorptivity and incur the error of masking the poor quality of the surface concrete.

A way of minimising this error would be to use samples with as small a thickness as possible. The variation of sorptivity with depth could then be determined, as the curve in Figure 4.3 would be divided into sections of known depth.

Since the concretes in the main research programme were to be subjected to a range of curing regimes, it was expected that surface samples would show variations in porosity with depth and that test results of the form in Figure 4.3 would be obtained. It could be expected that a similar problem would arise when samples with macro-flaws, such as cracks and bleed voids, are tested. At the beginning of infiltration, these large voids are filled first, giving a high value of sorptivity in the first minute of the test and lower values as the test proceeds. An analysis of this problem is presented when the results of the main research programme are discussed.

4.2.2 Moisture content of the sample

Moisture content and oxygen permeability

Because of the low diffusivity of oxygen through water, a water filled capillary in concrete acts as a solid barrier in the oxygen permeability test. This means that a fully saturated concrete would exhibit extremely low oxygen permeability values, almost independent of the size of pores and the degree of interconnection of these pores. As the sample is dried and the pore structure is "opened" to the passage of oxygen, the measured value of permeability increases.

This effect was well illustrated by Ujike and Nagataki[6] who exposed concrete samples to various relative humidity conditions for air drying and monitored the change in air permeability with time. The temperature in the drying environments was held constant at 20 ± 1 °C. Their results showed that an

approximately linear relationship exists between "open porosity" and the measured coefficient of permeability regardless of the relative humidity of the drying environment. Open porosity is defined as the ratio of the volume of evaporated water to the volume of the sample.

A linear regression analysis of the data presented in reference 6 showed that, over an open porosity range of 2% to 11%, the coefficient of air permeability, k (in cm/s) is related to the open porosity, n (%), as follows:

$$log\ (k) = R.n - 13$$

where R is a constant dependent on the mix parameters of the concrete. Table 4.1 shows values of R calculated for the concretes tested by Ujike and Nagataki.

Table 4.1 Values of R calculated from data presented by Ujike and Nagataki[6]

w/c ratio of concrete	R
0.4	0.597
0.5	0.500
0.6	0.455

Parrott and Hong[7] present results of the variation of air permeability with sample moisture loss due to drying which agree well with those presented in reference 6. They also show an approximately linear relationship between the sample weight loss after 10 days of drying and the air permeability measured after 80 days. This, they argue, emphasizes the utility of early-age weight-loss data, implying that such data

could possibly be used as a durability characterisation parameter.

The discussion above has underlined the important influence of moisture content on the gas permeability of concrete. This indicates the importance of concrete samples being tested at a similar moisture condition if gas permeability is to be used as a durability index parameter. Unless this is achieved, it will be difficult to compare the relative performance of different types of concretes.

Moisture content and sorptivity

It is easily reasoned that the rate of water absorption into a porous material such as concrete will depend on the amount of water in the pore structure at the start of infiltration. As with air permeability, this dependence of water absorption on moisture content has plagued the development of a useful in situ absorption test method. The inability to determine the moisture content of the in situ concrete make results from tests such as the ISAT method[8] difficult to interpret and implement as a specification test. For example, the time lapse between a rain period and the actual performance of the test could have a significant effect on the results obtained. The specification attempts to overcome this problem by prescribing the minimum number of rain-free days which have to elapse before the test can be conducted. However, this is only a partial solution since the moisture content of the concrete will be affected by the temperature, relative humidity and duration of the rain-free days.

The sensitivity of the ISAT test to moisture content of

the sample was demonstrated by Dhir et al[9]. In characterising the covercrete absorption test developed by Dhir et al[9], Lampacher[10] showed the sensitivity of this test to moisture content by testing concrete samples subjected to varying degrees of uniaxial drying at 50 °C. His results are presented in Figure 4.4 where it can be seen that stability in the test results is only achieved after approximately 30 days of drying.

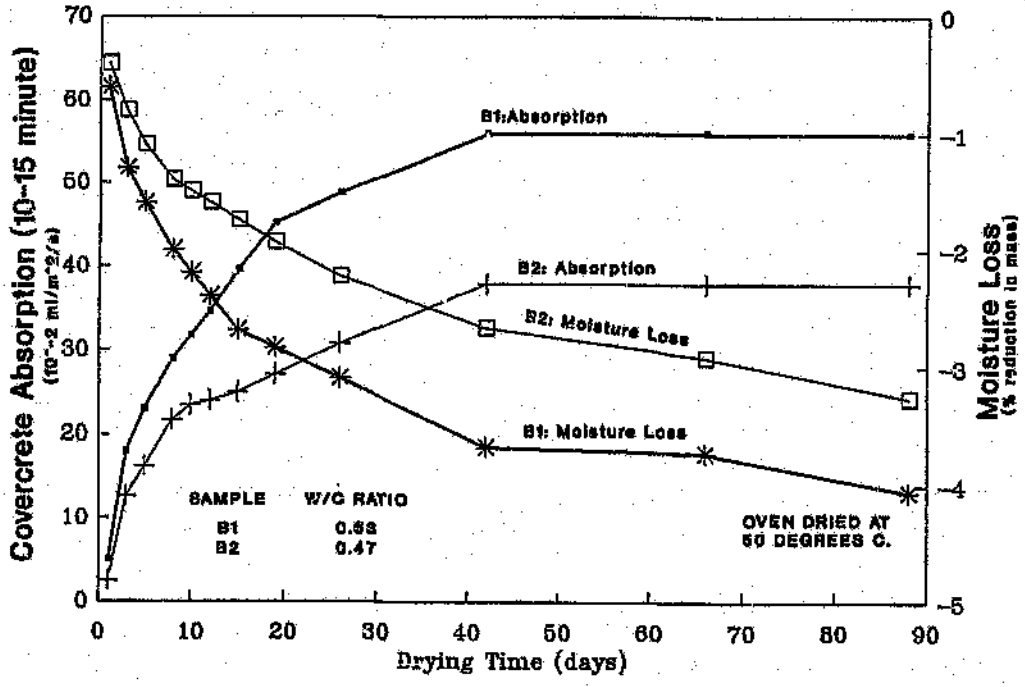

Figure 4.4 Variation in the covercrete absorption test results with changes in moisture content of the sample (after Lampacher[10])

Another factor which could affect the outcome of the test results is the distribution of moisture in the pore structure, despite a uniform distribution of porosity through the sample. If the sample has been dried such that a gradient of moisture content exists from the surface to the interior of the sample, the rate of water absorption will change with depth into

the sample. As with the non-uniform distribution of porosity, this will have the effect of distorting the straight-line relationship between the water absorbed and the square root of time. Figure 4.5 shows the results obtained by Ujike and Nagataki[6] on the drying profile of a 60 mm thick concrete sample exposed to drying from two opposite surfaces only. The sample was exposed to a relative humidity of 60% and temperature of 20 °C for drying. Under these drying conditions, uniform moisture distribution was only achieved after 104 days, the earliest time at which the sorptivity test could be conducted.

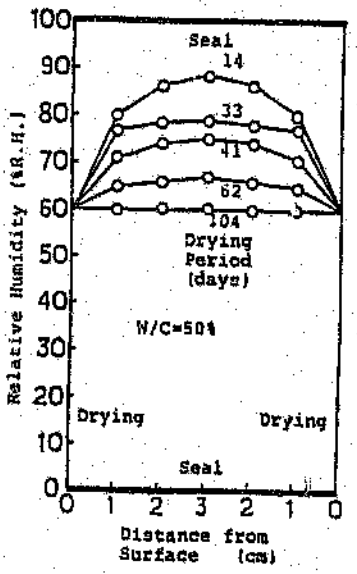

Figure 4.5 Variation in moisture profile with time in a concrete sample exposed to air drying (after Ujike and Nagataki[6])

4.2.3 Drying history of the sample

Drying history and air permeability

The way in which the sample is brought to a stable and uniform moisture condition before testing is the basis of a considerable and, as yet unresolved debate amongst researchers. The debate relates to the amount of damage or alteration caused to the pore structure of the sample during pre-treatment procedures. A question is therefore raised regarding the extent to which the test results can be considered to be representative of the parent concrete.

A range of techniques has been used by various researchers for drying their samples and, on the basis of the extent of microstructural damage caused, these techniques can be placed in the broad categories listed below.

Gentle drying: In this category, samples are dried without exposure to high temperatures or moisture gradients. Methods such as air drying[11], solvent replacement or freeze drying[12] are used in order to minimise the damage caused to the concrete microstructure. In support of these drying methods, Hooton[4] states that:

> *"(F)or air or gas permeabilities, extreme drying such as at 110 °C should be avoided due to the potential for both collapse of the microstructure and cracking."*

The problem with air drying of samples is the long time required to achieve uniform moisture conditions as shown in Figure 4.5 above. This is an important

consideration if the test is to be used for early-age characterisation of concrete quality.

Mild heating: The air permeability test method used by The Division of Building Technology at the CSIR involves drying the 50 mm thick samples in a ventilated oven at 50 °C for 14 days before testing. It is argued[13] that this is a compromise between short sample preparation times and microstructural damage due to excessive heating. Parrott[14] also argues for the merits of drying at 50 °C but adds that the sample should not be exposed to this temperature suddenly. He suggests that the temperature of the sample should be increased from ambient to 50 °C at a rate of 0,5 °C per minute.

Drying at ±105 °C: With this method, the sample is placed in a ventilated oven operating at between 100 °C and 110 °C for between 24 and 48 hours before testing. Cabrera and Lynsdale[15] report that their samples required between 24 and 36 hours of drying at 105 °C to reach constant weight. Dhir et al[16] also exposed their samples to 105 °C and continued drying until a weight change of less than 0.1% over a 24 hour period was obtained. This required drying times of between 2 and 4 days. They argue that the advantages of drying at 105 °C are:

> *"... a short conditioning period for the test specimen, a simplified test procedure (since both gas and specimen could easily be brought to a minimum relative humidity quickly), a high flow rate with dry specimens and, particularly, an improved reproducibility of test results."*

Drying history and water absorption

Lea[17] presents data on the water absorption of concrete dried in different ways. He shows that the water absorption of samples dried at 105 °C is higher than that of samples dried in vacuum at 20 °C for 30 days. However, with these results, it is difficult to distinguish between the effects of higher drying temperature and the increased dryness of the sample, in itself causing an increase in water absorption.

In the development of their test methods, both Kelham[18] and Dhir et al[9] dried their samples at 105 °C before testing and this appears to have been done in the interest of a reduced sample pre-treatment time.

Consideration of the issues associated with drying history.

In Section 3.4 of Chapter 3, it was argued that, when measuring a particular parameter of concrete to be used as a durability indicator, we need not measure such a parameter as a fundamental property of the material. It is understood that some alteration of the microstructure may occur as a result of the pre-treatment method and this is accepted in the interest of practicality. Inherent in this acceptance is the understanding that the method of sample pre-treatment causes a similar relative amount of alteration to the microstructure of different concrete types. Hence, the ability to compare the durability performance of different concretes on the basis of the measured parameter remains intact, since their performances in the test correctly reflects their relative performances in situ.

Since each of the drying methods discussed above will result in microstructural alteration, although to different extents, the focus of the debate should rather be aimed at assessment of the relative degree of alteration caused by the drying methods. To illustrate this argument, consider that a hypothetical relationship has been developed which describes the long-term durability performance of concrete (say, in a particular sulphate environment) on the basis of a short-term durability index value (say, air permeability), determined with the minimum alteration of the microstructure caused during the test. Experience with the relationship has also shown that it is generally applicable to all types of concrete. The relationship would be of the form:

$$D = f(I) \qquad 4.2$$

Where: D = a durability performance measure, and
I = a durability index test measure.

Assume that this function plots as Curve I in Figure 4.6. If a different drying procedure is used and this causes the relationship to be represented by, say, Curve II, the procedure is acceptable since Equation 4.2 is still applicable, although with altered values. However, if the new drying procedure causes the relationship for some concretes (say, OPC/fly ash) to be represented by Curve II and other concretes (say, OPC or OPC/GGBS) to be represented by Curve III, then the drying procedure has had different relative effects in altering the microstructure of the different concretes.

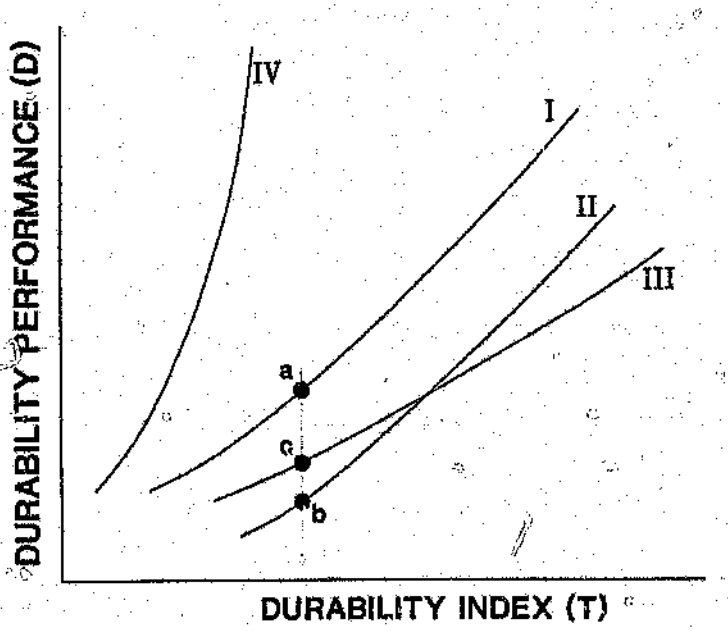

Figure 4.6 Hypothetical relationship between durability index value and durability performance of concrete.

Hence, two concretes which were assessed to have the same durability performance on the basis of the "correct" index test procedure (point a on Curve I), are now assessed to have different durability performances (points b and c on Curves II and III) because of the distortion introduced by the drying procedure. The effect has been simplified here to illustrate the point. In reality it can be expected that T will also change in moving from Curve I to Curves II and III. The extent of this change will have an influence on the final result and conclusion.

In this situation, Equation 4.2 has to be adjusted to account for the effect of concrete type on the test result and will then take the form:

$$D = f(T,c) \qquad 4.3$$

where c is a variable accounting for the concrete type. The problem introduced into Equation 4.3 is that, for the durability index to be useful as a design and quality control tool, the variable c has to be quantified through testing.

Another problem which could be introduced by the drying procedure is where the extent of microstructural alteration is such that the relationship between durability index and durability performance is transformed to that represented by curve IV. Here the sensitivity of the index has been affected and small changes in the measured index reflect large changes in durability performance. The effect of experimental error and inter-laboratory differences become magnified and the usefulness of the test is blunted.

The discussion presented above is not intended to imply that a single relationship, such as Curve I, exists or is indeed achievable. It is likely that the relationships are more complex than indicated in Equations 4.2 and 4.3.

4.3 Laboratory Investigation

Where insufficient guidance was provided by reported research, a series of tests was developed to characterise the influence of some of the parameters discussed above on the test methods developed in Chapter 3. This was necessary to finally select the sample parameters and pre-treatment procedures to be used for testing concretes in the main programme.

The following tests were conducted in this part of the investigation:

a) the influence of sample thickness (as cast) to aggregate size ratio on measured oxygen permeability;
b) the influence of sample thickness, cut from a larger specimen, on measured oxygen permeability;
c) The influence of drying history on permeability and sorptivity measurements.

The tests were conducted in this sequence so that the measurement of the influence of drying history could be determined on samples of the same thickness to be used in the larger test programme. This thickness would be determined by the results of tests conducted under a) and b) above.

This meant that a drying method had to be selected in order to conduct the tests for a) and b). In this selection, guidance was provided by the work done by Nagataki and Ujike[19] who show that the relationship between the open porosity (resulting from increased moisture loss) of a sample and its permeability remains uniform if the samples are dried in air or at 50 °C. On the other hand, when the samples were dried at 100 °C, the relationship between open porosity and permeability was no longer compatible with that of the "more gently" dried samples. The authors do not discuss the implications of this observation for permeability as a durability indicator test. However this research prompted the decision to dry samples at 50 °C on the basis that this was the fastest way of achieving uniform moisture condition in the samples without causing any significant alteration to the microstructure.

It was therefore necessary to address the question of the required time of drying at 50 °C to achieve stable

moisture condition. The first set of tests conducted was therefore aimed at a determination of the required drying time.

4.3.1 Duration of drying at 50 °C required to achieve stable moisture conditions

The samples for the initial characterisation programme were to be of varying thicknesses within the range of normal concrete cover. These samples were to be dried in an air ventilated oven having a thermostatic control between ambient temperature and 120 °C. The thermostat was set so that the temperature in the oven could be maintained at 49 ± 1 °C.

It was decided that, for the tests on the required drying time to be sufficiently representative, a good quality, well cured concrete should be used. Two concrete cubes which had been in a standard curing tank for approximately 12 months were used for this part of the investigation. The cubes were manufactured using plain OPC and crushed granite as aggregate and it was known that the 28-day compressive strength of this concrete was approximately 45 MPa.

Each cube was cut so that a central prism measuring 70 x 70 x 80 mm was obtained. The cutting was arranged so that the long axis of the prism was at right angles to the direction of casting. Each prism was then cut into three slices of thickness 10 mm, 0 mm and 45 mm using a 2 mm thick, continuous diamond grit blade. Immediately after cutting, the slices were rinsed with water, surface dried and weighed to an accuracy of 0.01 g on an electronic scale. The slices were then placed in the oven and weighed at regular intervals for the

next 10 days.

Results and discussion

Table 4.2 shows the results of change in mass with time in the oven for the various samples tested. Dhir et al[10] have shown that a 0.1% mass change over 24 hours is an acceptable criterion for determining stable moisture condition for the permeability test. The results are therefore presented in terms of the percentage mass loss over a 24 hour period. The table also shows the time required to achieve a rate of mass loss of 0.1%. This value was determined by linear interpolation between the relevant points. Finally, the table shows the average drying time required for the varying sample thicknesses. As an illustration, Figure 4.7 shows the variation in the rate of mass loss with time for the three sample thicknesses of the PC/1 samples. A log scale is used on the vertical axis of this figure to show the trends more clearly. The slopes of these curves are sufficiently uniform at the point of crossing the 0.1% line to justify the linear interpolation used in determining the required drying time.

Table 4.2 Time rate of moisture loss of samples drying in the 50 °C oven

Sample	Thickness (mm)	Saturated Weight (g)	Rate of Mass Loss (%/24 hrs) After Drying for (days): 0.75	1.81	2.79	3.78	4.75	6.75	9.75	Time to 0.1% M_r (days)
PC/1	10.00	110.39	3.61	0.63	0.35	0.23	0.13	0.06	-0.02	5.50
	20.00	237.69	2.51	0.57	0.40	0.28	0.22	0.15	0.05	8.20
	45.00	549.67	1.74	0.49	0.34	0.26	0.21	0.16	0.07	8.90
PC/2	10.00	116.73	3.14	0.45	0.26	0.09	0.08	0.02	-0.03	3.70
	20.00	228.83	2.51	0.56	0.38	0.25	0.21	0.13	0.04	7.70
	45.00	532.02	1.64	0.44	0.30	0.23	0.19	0.14	0.07	8.40
							Sample Thickness (mm)	10	20	45
							Average Time to 0.1% M_r (days)	4.60	7.95	8.65

Note: M_r = Rate of mass loss (g/24 hrs)

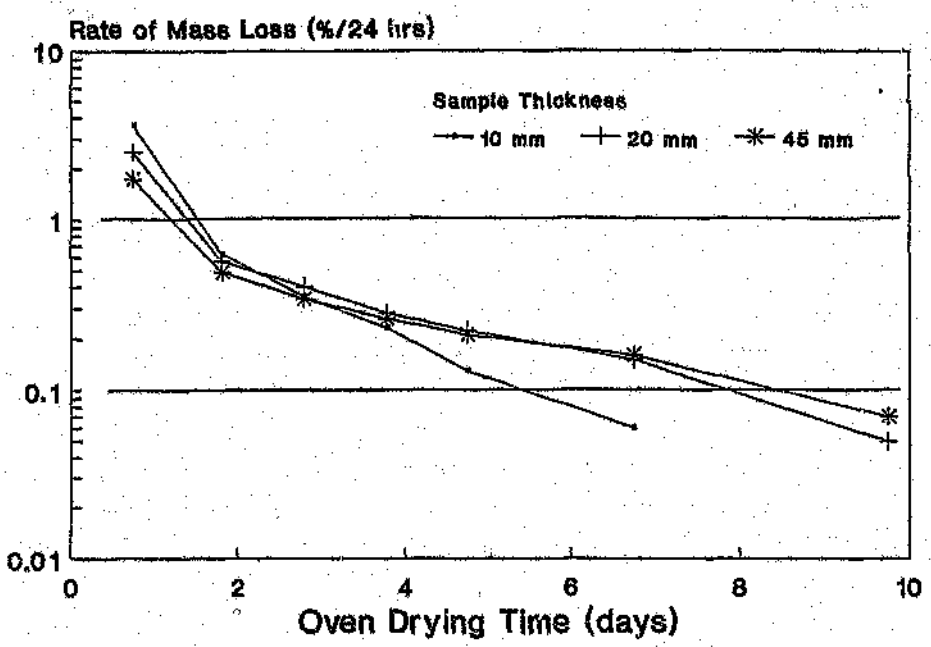

Figure 4.7 Variation in the rate of mass loss for samples dried at 50 °C

Both the 10 mm thick samples showed a negative rate of mass loss after 9.75 days in the oven. It is thought that this was caused by the samples showing a slight mass gain at this age resulting from an increase in the ambient relative humidity. This would cause an increased relative humidity in the oven which would be reflected by a mass increase of the samples.

On the basis of the results above, it was decided that, when necessary, the following minimum drying times would be used:

Sample thickness	Drying time in 50 °C oven
≤17 mm	7 days
>17 mm, <50 mm	14 days

4.3.2 The influence of sample thickness in relation to aggregate size

In this part of the investigation, the intention was to determine the influence of the sample thickness, in relation to the maximum aggregate size, on the measured permeability of similar concretes. Samples were cast to the required thickness to avoid the need for cutting which may have had a distorting influence on the results.

Concrete slabs measuring 100 mm x 300 mm and of varying thickness were cast in timber trays, manufactured as shown in Figure 4.8. The thicknesses of the slabs were controlled by altering the height of the side walls of the timber trays. A plastic sheet was placed on the bottom of the tray to avoid loss of water from the fresh concrete to the timber base.

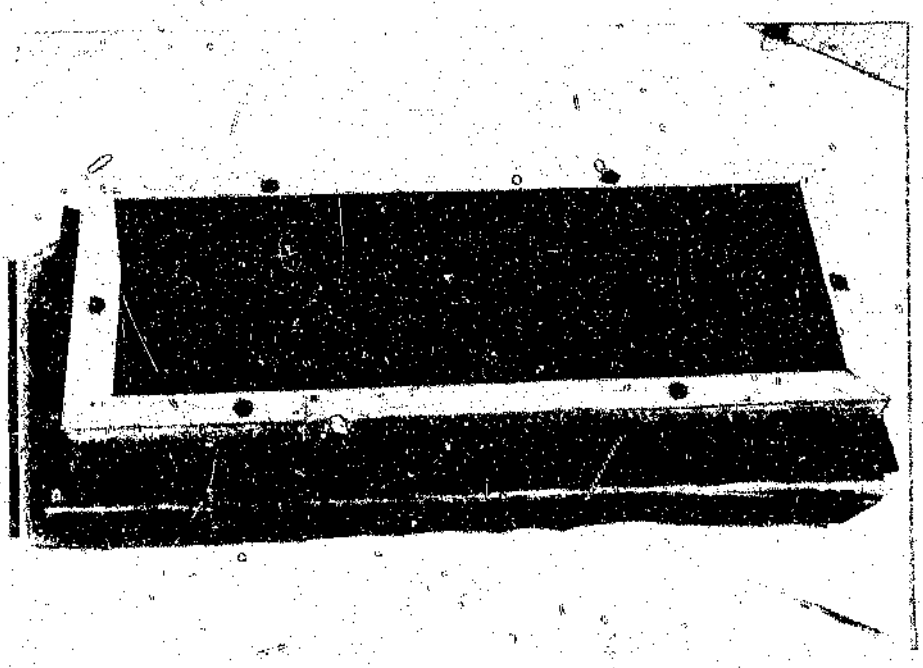

Figure 4.8 Timber tray with plastic sheet for casting concrete slabs.

It was decided to prepare concretes using two w/c ratios and two maximum aggregate sizes. The large aggregates were obtained by passing a nominal 13.5 mm dolomite aggregate through a jaw crusher and manually sieving the crushed material to separate the -9.5 +6.7 mm and the -6.7 +4.75 mm fractions. These sizes were used to increase the range of sample thickness to aggregate size ratios which could be tested in the falling head permeameter. Figure 4.9 shows samples of the aggregates used.

Table 4.3 shows the combination of sample thickness and stone size tested. A combination of the small stone with a 45 mm thick sample was not tested as the ratio of stone size to sample thickness was thought to be unrealistic at this level.



Figure 4.9 Samples of the stone sizes used in the sample thickness/aggregate size ratio tests.

Table 4.3 Combinations of stone size and sample thickness tested

Sample Thickness	Stone Size (mm)	
	-9.5 to +6.7	-6.7 to +4.75
10	Y	Y
20	Y	Y
30	Y	Y
45	Y	

Y indicates tested combination

It was also felt that 10 mm was the minimum physical sample size which could be cored and tested in the permeameter.

Table 4.4 shows the mix proportions used to prepare the samples. w/c ratios of 0.67 and 0.56 were used for both aggregate types. The mixes were designed to be fairly dry because of the thinness of the slabs being cast and the fact that high-speed, mechanical vibration was used for compaction.

A crushed granite sand, with a fineness modulus of 3.1, was used for these mixes. The mixes were prepared in a small, 10 litre capacity mixer. Mixing was continued for 2.5 minutes with the water being added over the first 30 seconds.

Before casting, the various components of the timber trays were coated with mould release oil and then assembled using 15 mm wood screws. The trays were individually clamped onto a high-speed vibrating table and filled with concrete with the vibrator activated.

Table 4.4 Material proportions (kg/m^3) of the various mixes tested.

Material	Mix Identification			
	9/15	9/18	6/15	6/18
Water	205	205	210	210
OPC	307.5	369	315	378
Stone:				
-9.5 +6.7	740	740		
-6.7 +4.75			500	500
Sand	1161	1130	1360	1315
w/c Ratio	0.67	0.56	0.67	0.56

When sufficient compaction was achieved, the tray was removed from the vibrating table and the top surface of the concrete was finished by rolling with a 10 mm diameter glass rod. This ensured that the top of the concrete was even with the top of the tray sides. The slab was then covered with plastic sheet until demoulding.

Approximately 24 hours after casting, the sides of the trays were removed and the concrete slabs, on their timber bases, were placed in a standard curing tank for a further 13 days. After this curing period, the slabs were removed from the water and the tray sides were replaced. Three 68 mm diameter cores were then obtained from each slab in the positions shown in Figure 4.10. The tray sides ensured that the slab was firmly held during the coring operation.

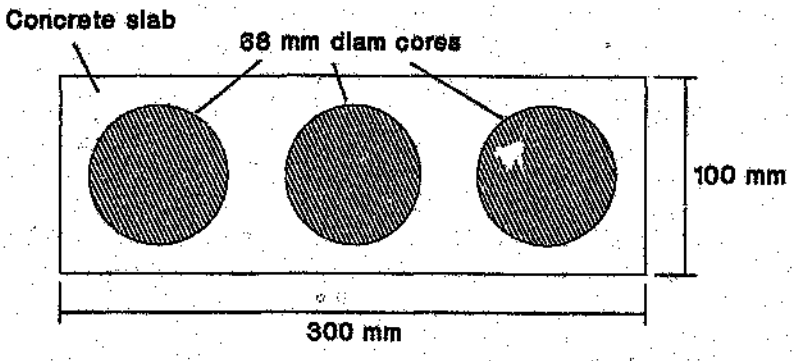

Figure 4.10 Location of the cores drilled from each concrete slab.

Each core was identified by being marked on its circumferential edge. All the cores were placed in a ventilated oven held at 49 ±1 °C for 14 days before being tested for oxygen permeability in the falling head permeameter.

Results and discussion

Table 4.5 shows the permeability results obtained for this series of tests. These results are presented graphically in Figure 4.11 where the permeability values are plotted against the sample thickness to aggregate size ratio. The aggregate size was taken to be 9 mm for the -9.5 +6.7 stone and 6 mm for the -6.7 +4.75 stone.

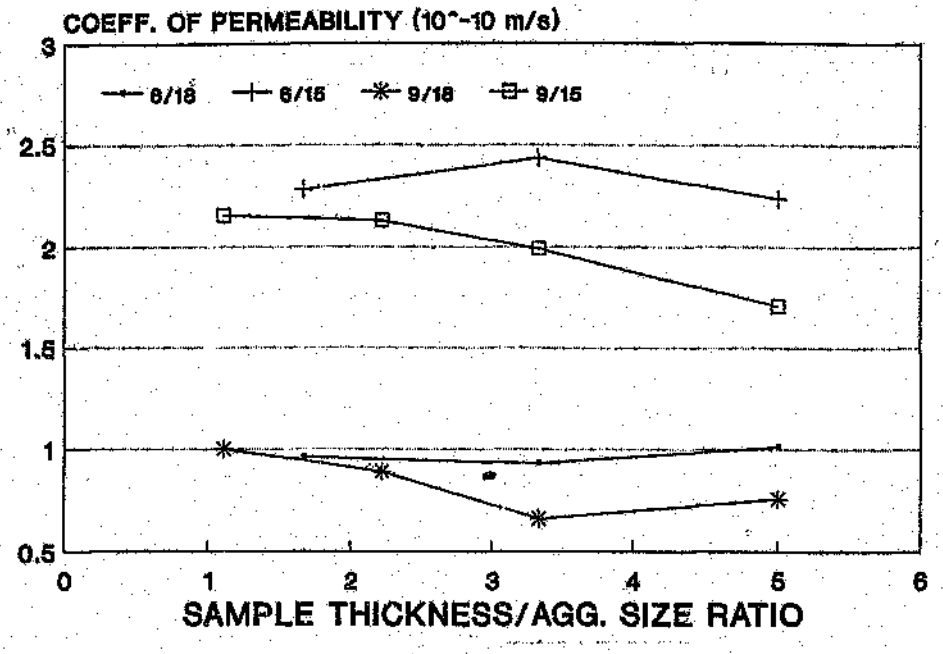

Figure 4.11 Variation in coefficient of permeability with sample thickness to aggregate size ratio

From the results shown in Table 4.5 and Figure 4.11, it can be seen that:

- the 0.56 w/c ratio concr' es gave lower oxygen permeability results than the 0.67 w/c concretes;
- for equal w/c ratios and t/a ratios, the concretes with the larger stone size gave lower permeability results;
- concretes with the larger stone size showed greater variation in permeability with varying t/a ratio than the concretes with the smaller stone size;

Table 4.5 Results of the coefficient of permeability (x 10^{-10} m/s) tests conducted on the samples cored from the slabs.

Sample Thkness (mm)	Coeff. of Permeability, k ($x10^{-10}$ m/s) of Sample No:			Average k	t/a# Ratio
	1	2	3		
Mix I.D: 9/15					
10	2.09	1.65	2.73	2.16	1.11
20	2.42	2.08	1.89	2.13	2.22
30	1.44	2.46	2.08	1.99	3.33
45	1.67	1.68	1.77	1.71	5.00
Mix I.D: 9/18					
10	1.24	0.81	0.95	1.00	1.11
20	0.76	0.90	1.01	0.89	2.22
30	0.63	0.76	0.60	0.66	3.33
45	0.69	0.82	0.77	0.76	5.00
Mix I.D: 6/15					
10	2.03	2.54	*	2.29	1.67
20	2.53	2.07	2.71	2.44	3.33
30	1.78	3.14	1.80	2.24	5.00
Mix I.D. 6/18					
10	1.06	0.86	*	0.96	1.67
20	0.78	0.96	1.06	0.93	3.33
30	1.08	0.94	1.02	1.01	5.00

* = Sample broken during coring.

#t/a = sample thickness/aggregate size

- within the range of sample thickness to aggregate size ratios tested, the largest variation in permeability was observed with the larger stone concrete. Maximum percentage differences were 21% and 34% for the 0.67 and 0.56 w/c ratio concretes respectively.

Hooton[4] has shown that the permeability of a high quality concrete could differ from that of a poor quality concrete by a factor of 1000 times. In view of this observation, the differences observed in the results shown in Figure 4.11 could be considered to be marginal. It could therefore be argued that, for the as-cast samples used in this study, measured gas permeability is not significantly affected by the maximum aggregate size in relation to the sample thickness.

4.3.3 The influence of sample thickness for samples cut from larger specimens.

In this part of the characterisation testing, the objective was to obtain a measure of the influence of sample thickness on permeability measurements, when the samples are cut from larger specimens. This is a more common application of the permeability test since test samples derived from in situ structures would be obtained in this manner.

The following aspects were considered important in the development of the mixes for this investigation:

- all concretes should contain the same large aggregate size;
- a single binder type should be used throughout

the test samples;

- a range of strengths and workabilities should be tested.

The mix proportions shown in Table 4.6, developed in consideration of these criteria, were used in this part of the investigation. A nominal 19 mm crushed granite stone and a crushed granite sand were used as aggregates.

Table 4.6 Mix proportions (kg/m^3) of concretes used to test the influence of cut sample thickness on oxygen permeability measurements.

Material	Mix Identification					
	200A	200B	200C	210A	210B	210C
Water	200	200	200	210	210	210
OPC	300	350	400	315	368	420
19mm Stone	1030	1000	1000	1030	1000	1000
Sand	837	824	782	798	784	739
w/c Ratio	0.67	0.57	0.5	0.67	0.57	0.5
Slump (mm)	15	25	30	45	60	45

Sufficient material of each mix was prepared to fill one standard 700 x 101.6 x 101.6 mm beam mould. This material was mixed in a 40 litre capacity pan mixer for 3 minutes, with the water being added over the first minute.

The beam moulds were clamped onto a high-speed vibrating table and were filled with the vibrator activated. After casting, the moulds were covered with plastic sheeting and stored in the laboratory. On the

following day, the moulds were stripped and the concrete beams placed in standard water curing tanks fitted with submerged circulation pumps. The water temperature was maintained at 22 ±1 °C with the aid of thermostatically controlled immersion heaters.

At 14 days after casting, the beams were removed from the curing tanks and cut into segments as shown in Figure 4.12 (a). The two end segments were discarded so as to ensure that the properties of the segments tested were as uniform as possible. The two 100 mm segments were used to determine the 14-day strength as a means of characterising the particular concrete and monitoring the influence of the different water contents. Compressive strengths were determined in the standard manner using an Amsler compression testing machine with a capacity of 2000 kN. The load was applied at right angles to the direction of casting, onto the two opposite moulded faces.

A central, 68 mm diameter core was drilled longitudinally from each of the three 140 mm segments as shown in Figure 4.12 (b). From each core, disks measuring 10, 15, 20, 30 and 45 mm thick were cut using a high-speed, continuous fine cut blade, with the remaining segment being discarded as shown in Figure 4.12 (c). The order in which the various disk thicknesses were cut from the core was not necessarily as shown in Figure 4.12 (c). In this way, three samples were obtained for each concrete type and sample thickness combination, with each sample taken from a different segment of the beam.

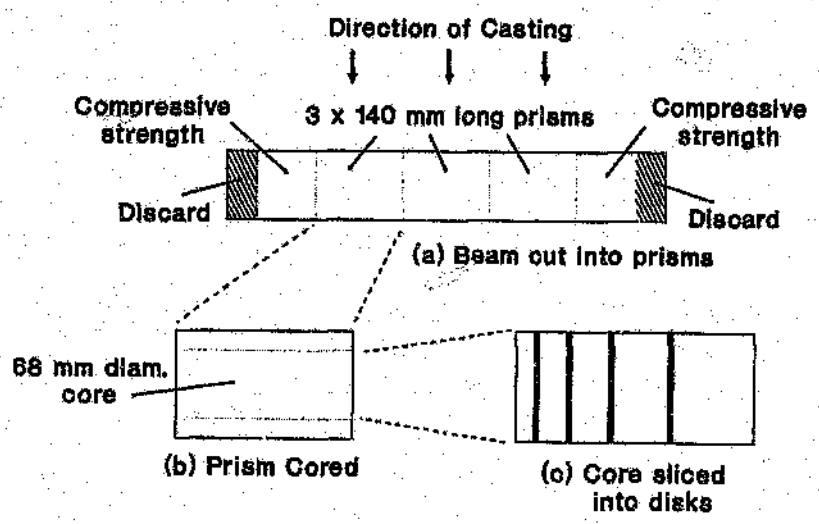

Figure 4.12 Method of cutting, coring and obtaining disc samples from cast beam sections.

The discs were then marked and placed in the 50 °C oven for 14 days. The samples were then tested for oxygen permeability in the falling head permeameter using the rubber collar method of sample sealing.

Results and discussion

Table 4.7 presents the results of the compressive strength determinations on the end segments of the beams. The strength and density values presented in this table have been corrected for the actual measured distance between the two cut faces of the segments. This dimension varied between 101 mm and 106 mm after cutting.

Table 4.7 Compressive strength results of concretes used to measure the influence of cut sample thickness on permeability.

Sample I.D.	Sample No.	Sample Density (kg/m^3)	Compress. Strength (MPa)	Average Strength (MPa)
200A	1	2426.7	23.9	24.4
	2	2407.8	24.9	
200B	1	2403.2	30.7	32.3
	2	2389.0	33.8	
200C	1	2417.0	44.6	42.2
	2	2422.1	39.8	
210A	1	2402.9	24.3	24.0
	2	2378.9	23.7	
210B	1	2441.0	31.0	30.0
	2	2408.7	29.1	
210C	1	2379.9	37.2	38.8
	2	2375.2	40.5	

Tables 4.8 (a) and (b) show the oxygen permeability results for the various slices. The tables also show the standard deviation and coefficient of variation for each group of results. These parameters are calculated as follows:

$$S_D = \sqrt{\frac{\Sigma(x_i - x')^2}{n - 1}}$$

$$V' = \frac{S_D}{x'}$$

where:

S_D = sample standard deviation
x_i = one of a group of three results
x' = the average of three results
n = the number of results (three)
V' = coefficient of variation

Variability of the results: The results presented in Tables 4.8(a) and 4.8(b) reflect the considerable variability in oxygen permeability results obtained on nominally similar samples. Hooton[4] mentions this as a major drawback of gas permeability testing and notes the importance of interpreting the results in the light of the variability of the test procedure. Tables 4.9(a) and 4.9(b) show analyses of the coefficients of variation calculated in Tables 4.8.

Table 4.8(a) Coefficients of permeability for the various sample thicknesses of the concretes with water content of 200 l/m^3.

Sample Thknes (mm)	Mix Identification											
	200A				200B				200C			
	k	k_{ave}	S_D	V′	k	k_{ave}	S_D	V′	k	k_{ave}	S_D	V′
10	2.00 2.30 4.40*	2.90	1.31	45.1	0.70 2.21* 0.95	1.28	0.81	63.0	0.65 0.39 0.50	0.51	0.13	26.1
15	1.66 1.60 2.08	1.78	0.26	14.7	0.97 0.86 0.79	0.87	0.09	9.9	0.42 0.29 0.30	0.34	0.07	21.6
20	2.41 1.57 2.21	2.06	0.44	21.3	0.94 0.85 0.99	0.93	0.07	7.7	0.38 0.33 0.37	0.36	0.03	7.1
30	2.96 2.06 3.17	2.73	0.59	21.6	0.92 0.80 0.71	0.81	0.11	13.1	0.35 0.28 0.39	0.34	0.06	16.3
45	2.28 2.29 2.08	2.22	0.12	5.3	0.91 0.88 0.90	0.89	0.02	1.8	0.39 0.23 0.26	0.30	0.08	27.6

Legend: k = coefficient of oxygen permeability ($x10^{-16}$ m/s);
k_{ave} = average coefficient for the three samples; S_D = standard deviation
V′ = coefficient of variation (%); * see later discussion.

Table 4.8(b) Coefficients of permeability for the various sample thicknesses of the concretes with water content of 210 l/m^3.

Sample Thknes (mm)	Mix Identification											
	210A				210B				210C			
	k	k_{ave}	S_D	V′	k	k_{ave}	S_D	V′	k	k_{ave}	S_D	V′
10	14.1 5.88* 10.8	10.3	4.14	40.3	1.28 3.30 6.57*	3.72	2.67	71.8	2.91 2.91 2.53	2.78	0.22	7.90
15	5.61 2.13 11.1*	6.28	4.52	72.0	1.10* 3.04 2.67	2.27	1.03	45.4	1.80 1.45 2.04	1.76	0.30	16.8
20	8.09* 2.29 2.70	4.36	3.24	74.2	2.26 2.57 9.72*	4.85	4.22	87.0	1.32* 1.89 1.82	1.68	0.31	18.5
30	2.73 2.37 1.82	2.31	0.49	19.9	1.68 3.02* 1.72	2.14	0.76	35.6	1.18* 0.82 0.88	0.96	0.19	19.9
45	1.75 2.19 2.14	2.03	0.24	11.9	0.83 0.74 7.82*	3.13	4.06	130	0.92 0.96 0.79	0.89	0.09	10.4

Legend: k = coefficient of oxygen permeability (x10^{-10} m/s);
k_{ave} = average coefficient for the three samples; S_D = standard deviation
V′ = coefficient of variation (%); * see later discussion.

Table 4.9(a) Analysis of the coefficients of variation of oxygen permeability results on the basis of mix characteristics

Mix I.D.	w/c Ratio	Max. V′ (%)	Min. V′ (%)	Ave. V′ (%)
200A	0.67	45.1	5.3	21.6
200B	0.57	63.0	1.8	19.1
200C	0.5	27.6	7.1	19.7
Average		45.2	4.7	20.1
210A	0.67	74.2	11.9	43.7
210B	0.57	130	35.6	73.8
210C	0.5	19.9	7.9	14.7
Average		74.7	18.5	44.1

From Table 4.9(a) it can be seen that the concretes with the lower water content generally gave the lower coefficients of variation. However, the lowest average value was obtained for Mix 210C, indicating that there may not be a clear relationship between water content and variability of results. The high value obtained for Mix 210B is caused by the single anomalous result obtained for the 45 mm thick sample of this mix.

Table 4.9(b) Analysis of coefficients of variation (%) of oxygen permeability results on the basis of sample thickness.

t	Water = 200 l/m³			Water = 210 l/m³		
	Max V′	Min V′	Ave V′	Max V′	Min V′	Ave V′
10	63.0	26.1	44.7	71.8	7.9	40.0
15	21.6	9.9	15.4	72.0	16.8	44.7
20	21.3	7.1	12.0	87.0	18.5	59.9
30	21.6	13.1	17.0	35.0	19.9	24.9
45	27.6	1.8	11.6	130.0	10.4	50.8
Ave	31.0	11.6	20.1	79.2	14.7	44.1

Note: t = sample thickness

The analysis presented in Table 4.9(b) is also shown graphically in Figure 4.13. From this figure, it can be seen that, for the lower water content mixes, the coefficient of variability reduces from an average of 44.7% for the 10 mm thick sample to an almost uniform value of ±15% for sample thicknesses of 15 mm and greater. On the other hand, reflecting the trend shown in Table 4.9(a), the results for the higher water content mixes are erratic and no trend can be discerned. However, it is again clear from this diagram that the variability of the 210 l/m³ mixes is generally greater than that of the 200 l/m³ mixes for the range of sample thicknesses tested.

The above analysis indicates that the variability in the measurements of permeability on nominally similar concretes is dependent on the workability of the concrete. This is perhaps a reflection of the influence of bleeding on the interconnection of capillary pores,

especially at aggregate interfaces. The variability would then derive from local differences in the aggregate distribution through the cut sample thickness.

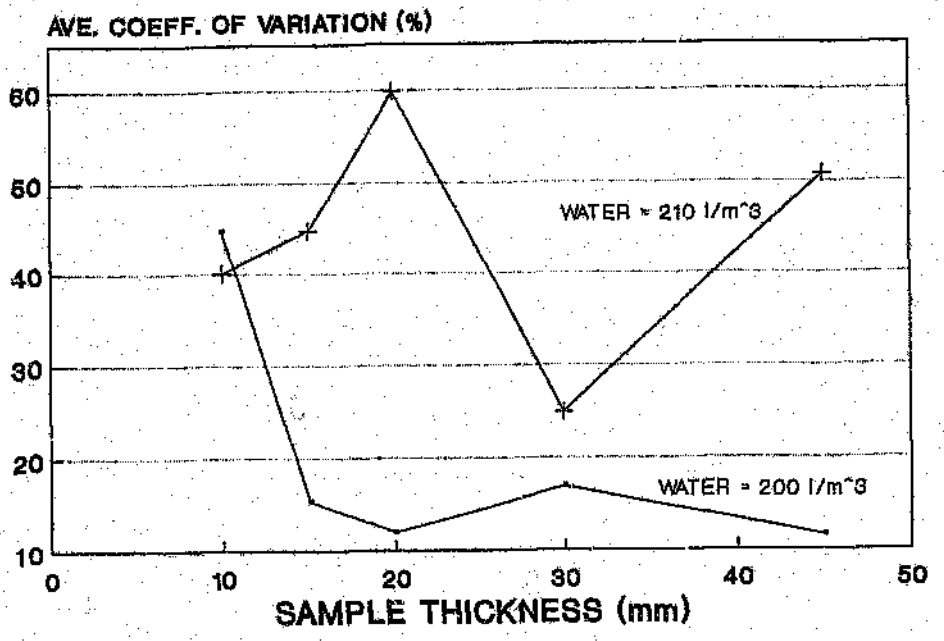

Figure 4.13 Relationship between average coefficients of variability of permeability measurements and sample thickness

Rejection of individual results. In order to understand the influence of sample thickness on the measured permeability of a particular concrete, it is necessary to first address the variability issue discussed above. It is clear from the data presented in Tables 4.8(a) and (b), that much of the variability in a group of three results can be ascribed to a single "anomalous" result in the group. For example, the coefficient of variation of 130% obtained for the 45 mm thick samples of the 210B concrete (see Table 4.8(b)), is the result

of the single, high value obtained on the third sample. This result (7.82×10^{-10} m/s) is almost ten times larger than the average of the other two results. Intuitively, it appears that there is justification for rejecting this result and using the average of the remaining two results as the value representing the performance of the particular combination of parameters.

The rejection of data is often a controversial exercise and in this case, where the decision is being made on the basis of only three measurements, it would be difficult to justify data rejection statistically. However, it appears that these individual "outlier" results are masking the trends and should be excluded to allow meaningful conclusions to be drawn.

The statistical approach to rejection of data is based on an assessment of the probability of the suspect result occurring in a range of measurements. This probability is related to the difference between the particular result and the mean of the group of results. The probability that a result will fall within an interval $T.S_D$ (T = a constant) of the mean value is given by:

$$P(T) = \frac{1}{\sqrt{2\pi}} \int_{-T}^{T} e^{\left(-\frac{t^2}{2}\right)} dt \qquad 4.6$$

and

$$t = \frac{x - m}{S_D} \qquad 4.7$$

where:

x = an individual result

m = the mean of the group of results

S_D = the standard deviation of the group of results.

Standard tables are available for evaluating this integral[20] and from these it is calculated that:

P(1) = 0.683;

P(2) = 0.954;

P(3) = 0.997; etc.

This means that there is a 68.3% probability that a result will fall within one standard deviation of the mean. On the other hand, there is only a 0.3% chance that a result will fall further than three standard deviations from the mean.

Using this approach, it was decided to exclude one of a group of three results if such a result was more than one standard deviation away from the mean. Hence, referring to Tables 4.8 (a) and (b), a result was rejected if:

$$k_{ave} + S_D < k_i < k_{ave} - S_D$$

where k_i is the individual, suspect result. Borderline results were retained rather than discarded. The results rejected on this basis are marked with an asterisk (*) in Tables 4.8 (a) and (b). The average coefficients of permeability resulting from this "smoothing" of the data, is shown in Table 4.10.

The results in Table 4.10 are also shown graphically in Figure 4.14(a) and Figure 4.14(b) where, for reasons of clarity, the scale on the vertical axes had to be changed to show the trends.

Table 4.10 Average coefficients of permeability for the various mixes and sample thicknesses after the rejection of outlier results.

Sample Thkness (mm)	Ave. Coeff. of Permeability ($x10^{-10}$ m/s) for Mix I.D:					
	200A	200B	200C	210A	210B	210C
10	2.15	0.83	0.51	12.45	2.29	2.78
15	1.78	0.87	0.34	3.87	2.86	1.76
20	2.06	0.83	0.36	2.50	2.42	1.68
30	2.73	0.81	0.34	2.31	1.70	0.85
45	2.22	0.89	0.30	2.03	0.79	0.89

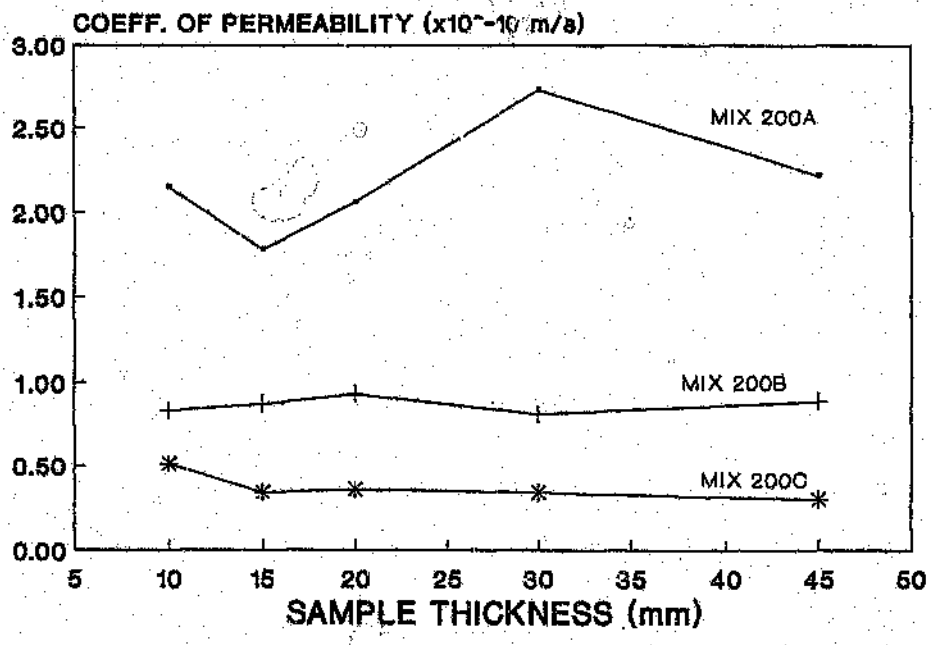

Figure 4.14(a) Variation in coefficient of permeability with cut sample thickness for mixes with water content of 200 l/m^3

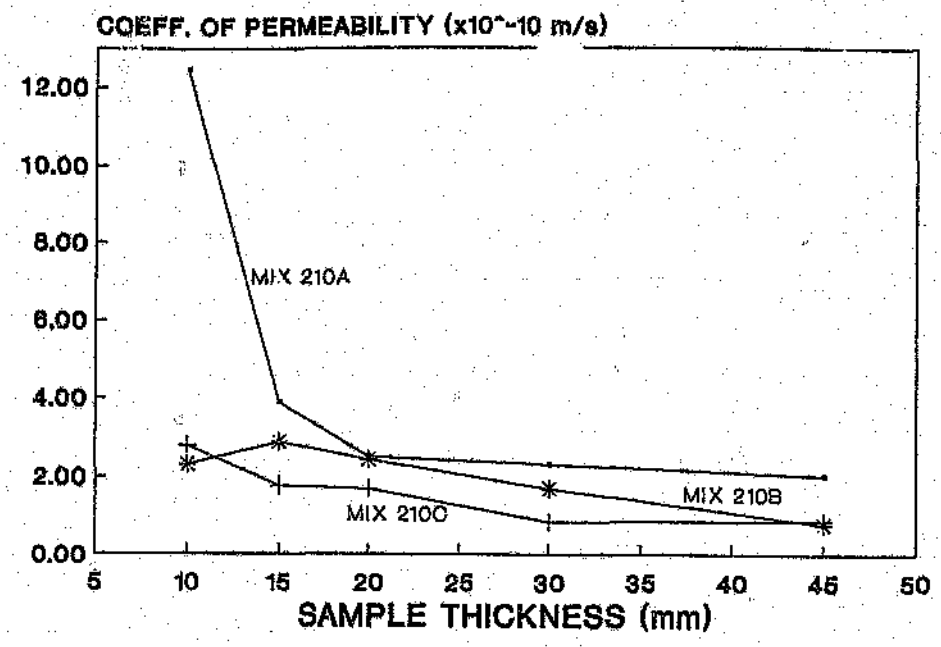

Figure 4.14(b) Variation in coefficient of permeability with cut sample thickness for mixes with water content of 210 l/m^3

The following observations are drawn from these figures:

- The medium and high strength mixes (w/c = 0.57 and 0.5) showed small variations in the measured coefficient of permeability while the low strength concretes (w/c = 0.67) showed considerably greater variations.
- The low water content mixes appear to be less sensitive to changes in sample thickness than the higher water content mixes.
- The high variation observed with mix 210A is due to the high result obtained with the 10 mm thick sample. This variation reduces considerably for samples of thickness 15 mm and greater.
- The results obtained for Mix 200A are erratic and shows no clear trend between permeability and

sample thickness. However the results only vary between permeability values of 2.73×10^{-10} and 1.78×10^{-10} m/s which is smaller than the variation obtained for Mix 210C of between 2.78×10^{-10} and 0.89×10^{-10} m/s.

- For samples of thickness 15 mm and greater, mixes with a water content of 210 l/m^3 show reducing permeabilities with increasing sample thickness. However, the variations are in a relatively narrow band of permeability values.

It was stated in Chapter 3 that one of the objectives of this research was to obtain a measure of the gradation of properties in the zone of cover concrete. To achieve this, it is necessary to use the thinnest possible sample which will maximise the number of sample points within the cover concrete. The results obtained above indicate that, to obtain a measure of permeability which reasonably reflects the performance of concrete made with 19 mm stone, the sample should not be less than approximately 15 mm thick.

4.3.4 The influence of sample drying method on measured permeability

It was indicated in Section 4.2.3 that considerable differences existed between researchers regarding the method of sample drying in preparation for gas permeability testing. In this part of the characterisation test programme, the intention was to address some of the issues raised here and to provide guidance on the sample drying procedure to be used for the main test programme.

Concretes were prepared using three binder types with two binder/water ratios for each binder type. Crushed granite sand and 19 mm stone were used as aggregate and the slump was controlled between 40 and 60 mm by adjusting the water contents of the mixes with different binder types. For each binder type, the water content was held constant for the two binder/water ratios. Table 4.11 shows the mix identifications and proportions used for this part of the investigation. This table also shows the average 28-day compressive strength of these concretes determined on three 101,6 mm cubes for each mix.

Table 4.11 Mix proportions (kg/m^3) of the mixes used for monitoring the influence of drying history on measured oxygen permeability

Material	Mix Identification					
	PC1	PC2	FC1	FC2	SC1	SC2
Water	200	200	185	185	195	195
OPC	320	380	207	246	156	185
FA	-	-	89	106	-	-
GGBS	-	-	-	-	156	185
19 mm Stone	1000	1000	1000	1000	1000	1000
Sand	850	800	882	831	866	816
w/b Ratio	0.63	0.53	0.63	0.53	0.63	0.51
$f_{c,28}$	38.8	52.8	28.8	39.1	32.1	44.3

Note: w/b = water/binder ratio

$f_{c,28}$ = Average 28-day compressive strength (MPa)

One 101.6 mm cube of each of these mixes was prepared and, after 28 days of water curing, a 68 mm diameter core was drilled from each cube perpendicular to the direction of casting. Three 15 mm thick slices were then cut from the central portion of each core as shown in Figure 4.15. A 2 mm thick, high speed, continuous diamond grit blade was used to cut the slices from the cores.

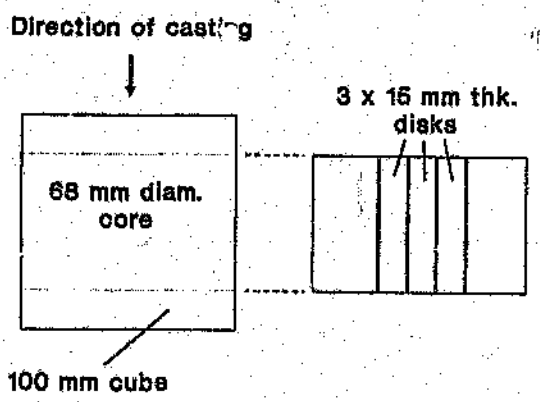

Figure 4.15 Method of coring and slicing cubes to obtain samples for testing the influence of drying method on permeability

After slicing, the samples were placed in a water filled container inside a vacuum chamber. The chamber was then evacuated to pressure of ±7. kPa below atmospheric pressure. This pressure was maintained for 24 hours, after which the samples were surface dried and weighed to obtain the water saturated weight of each sample. The samples were then exposed to the following sequence of drying methods:

a) over silica gel or in a vacuum chamber for 3 months;

b) over phosphorus pentoxide (P_2O_5) for 7 days;

c) in a 50 °C oven for 7 days;

d) in a 100 °C oven for 24 hours.

At each stage in the drying process, the samples were kept in the particular environment until weight equilibrium was achieved. This was determined from experience with the drying method or by regular monitoring of the weight of the samples. At the end of each drying stage, the sample was weighed and an oxygen permeability test was conducted using the falling head permeameter.

Samples to be vacuum dried were placed in a glass chamber which was evacuated to approximately 70 kPa below atmospheric pressure. The vacuum pump connected to the glass chamber was kept running for most of the duration of the drying period. Occasionally, for periods of up to two days, the pump was required for other projects or for maintenance. On these occasions, the glass chamber was isolated from the pump so that the vacuum pressure in the chamber was maintained.

A 330 x 220 x 60 mm deep plastic container, commonly used in domestic kitchens, was used for drying the samples over silica gel. A ±10 mm thick layer of self-indicating silica gel was placed in the bottom of the container and a 10 mm thick, plastic grating was placed on the silica gel. The samples were placed on this plastic grating so that they were not in direct contact with the silica gel. The container was then closed with its cover and, since this was not an air-tight cover, the joint between the cover and the container was sealed with plastic tape. The components and seal of this drying method are shown in Figure 4.16. The silica gel was regularly checked for colour change which indicated that it was not drawing any further

moisture from the samples. When this occurred, the silica gel was removed from the plastic container, dried in the 100 °C oven until the dry colour was achieved, cooled in a desiccator and returned to the plastic container. This process required approximately 8 hours to complete.



Figure 4.16 Various components and container sealing method used for the samples dried over silica gel.

Phosphorus pentoxide (P_2O_5) is a particularly strong drying agent and was used to further remove moisture from the samples after vacuum or silica gel drying. At the end of the silica gel drying phase, the silica gel was removed from the plastic containers and replaced with a ±3 mm thick layer of P_2O_5. The samples were then placed in the containers and dried in the same manner as for the silica gel drying. Unlike silica gel, P_2O_5 is not re-usable and has to be discarded when it has completely reacted with water. This makes it a more expensive method of sample drying.

Drying phases a) and b) (ie. vacuum, silica gel and P_2O_5) were considered to be "gentle" drying methods from the point of view of microstructural alteration through cracking. The intention was to use these drying methods as standards by which to compare the effects of drying by the more "severe" 50 °C and 100 °C methods.

At the end of the high temperature drying phases, the samples were allowed to cool to room temperature before being tested. The samples from the 100 °C oven were first placed in a desiccator until they were cool enough to handle and be weighed to determine the dry sample weight. These samples were then allowed to cool in air until the time of testing.

Results and discussion

Tables 4.12 (a) to (c) show the oxygen permeability of the samples tested, measured at the end of each drying phase. The % dryness shown on these tables indicates the proportion of total moisture removed from the sample at the end of the drying phase. This value is calculated as follows:

$$D(\%) = 100.\frac{M_{sat} - M_{test}}{M_{sat} - M_{dry}} \qquad 4.7$$

where: $D(\%)$ = % dryness;
M_{test} = mass of the sample at the time of testing;
M_{dry} = mass of sample after drying at 100 °C;
M_{sat} = water saturated mass of the sample.

Table 4.12(a) Measured oxygen permeability at the end of the various drying phases, for the OPC concretes

Mix and Sample I.D.	Drying Sequence	% Dryness	Measured Permeability k(x10^{-10} m/s)	% Relative Permeability (k/k_{100})
PC1.D1	Silica	88.4	125	85.6
	P_2O_5	90.3	135	92.5
	50 °C	89.0	136	93.1
	100 °C	99.2	146	100
PC1.D2	As Above	87.3	210	96.3
		89.6	215	98.6
		88.5	209	95.9
		99.0	218	100
PC2.D1	As Above	61.6	0.20	46.3
		87.7	0.26	61.5
		87.1	0.24	56.3
		99.2	0.42	100
PC1.V1	Vacuum	90.0	141	91.0
	P_2O_5	90.1	151	97.4
	50 °C	89.7	153	98.7
	100 °C	99.3	155	100
PC2.V1	As Above	87.0	0.24	48.9
		89.6	0.29	59.2
		88.9	0.26	53.1
		99.7	0.49	100
PC2.V2	As Above	84.7	0.58	56.2
		88.6	0.68	65.8
		87.9	0.72	69.5
		99.3	1.03	100

Table 4.12(b) Measured oxygen permeability at the end of the various drying phases, for the OPC/FA concretes

Mix and Sample I.D.	Drying Sequence	% Dryness	Measured Permeability $k(x10^{-10}$ m/s)	% Relative Permeability (k/k_{100})
FC1.D1	Silica	91.2	4.42	55.1
	P_2O_5	92.6	4.95	61.7
	50 °C	92.6	4.99	62.2
	100 °C	99.5	8.02	100
FC1.D2	As Above	91.0	0.41	47.1
		92.6	0.52	59.8
		92.0	0.47	54.0
		99.8	0.87	100
FC2.D1	As Above	84.4	0.61	48.4
		90.9	0.81	65.1
		90.3	0.88	70.1
		99.7	1.25	100
FC1.V1	Vaculum	90.6	0.60	53.8
	P_2O_5	93.3	0.63	56.3
	50 °C	92.8	0.67	59.6
	100 °C	99.6	1.12	100
FC2.V1	As Above	90.2	0.21	43.3
		91.4	0.27	55.9
		90.1	0.33	67.6
		99.7	0.49	100
FC2.V2	As Above	88.4	0.26	48.2
		90.3	0.24	43.9
		90.1	0.29	53.9
		99.9	0.54	100

Table 4.12(c) Measured oxygen permeability at the end of the various drying phases, for the OPC/GGBS concretes

Mix and Sample I.D.	Drying Sequence	% Dryness	Measured Permeability k($x10^{-10}$ m/s)	% Relative Permeability (k/k_{100})
SC1.D1	Silica	89.9	91.5	69.9
	P_2O_5	91.8	110	84.0
	50 °C	90.8	110	84.0
	100 °C	99.3	131	100
SC1.D2	As Above	89.8	231	78.0
		92.0	286	96.6
		90.8	244	82.4
		99.3	296	100
SC2.D1	As Above	88.8	8.15	52.2
		90.4	9.08	58.2
		89.7	9.51	60.9
		99.1	15.6	100
SC1.V1	Vacuum	90.2	52.3	75.3
	P_2O_5	92.9	57.2	82.3
	50 °C	91.1	58.4	84.0
	100 °C	99.1	69.5	100
SC2.V1	As Above	87.3	1.90	46.8
		91.2	1.98	48.8
		90.5	1.98	48.8
		99.4	4.06	100
SC2.V2	As Above	88.2	4.38	44.5
		91.8	5.41	55.0
		90.6	5.38	54.7
		99.3	9.84	100

The tables show that the % dryness is slightly less than 100% after 100 °C drying. This is because the samples absorbed some atmospheric moisture during the cooling period between removal from the desiccator and the start of the permeability test.

In order for the samples with different permeability values to be compared, the tables show the individual permeability values expressed in relative terms as a percentage of the permeability after drying at 100 °C. These relative values are shown as k/k_{100}.

The following observations are made from the data presented in these tables:

- There is very little difference in the extent of dryness achieved using silica gel or vacuum drying. With these methods, a range of dryness between 81.6% and 91.2%, with an average of 88.3% was achieved.
- The relatively short period during which the samples were exposed to P_2O_5 caused further drying of the samples with a generally greater effect being noted with the lower w/b ratio samples. In all cases, the increased dryness was accompanied by an increase in permeability.
- As evidenced by the decrease in % dryness, almost all the samples showed a slight increase in moisture content after being dried at 50 °C for 7 days. This is explained by the fact that the oven is air ventilated and is therefore subject to variations in the ambient relative humidity. Clearly, the combination of long term silica gel/vacuum drying followed by exposure to P_2O_5 removed slightly more moisture than could be removed by drying at 50 °C in the oven used. The

relative humidity in the oven must have been higher than in the P_2O_5 environment and some moisture was re-absorbed into the samples when placed in the oven.

- Contrary to expectations, the increase in the moisture content of the samples from the 50 °C oven did not always manifest itself in a decrease in permeability. This increase in permeability appears to occur randomly and only the fly ash samples reflected the increase in five of the six samples tested. Although there are only small differences in the permeabilities measured after P_2O_5 and 50 °C drying, it is felt that the increases in permeability with reduced dryness is evidence of microstructural damage caused by the higher drying temperature. This damage, in the form of micro-cracking, would have the effect of increasing the size and degree of interconnection between pores, thereby increasing the permeability of the material.

To indicate the effect of drying at 100 °C, the relative permeability values are plotted in Figures 4.17 (a) to (c). These figures are separated according to the binder type used in the concrete. In the legend below each figure, the permeability of each sample after drying at 100 °C (= 100%) is given in parentheses alongside the sample identification code.

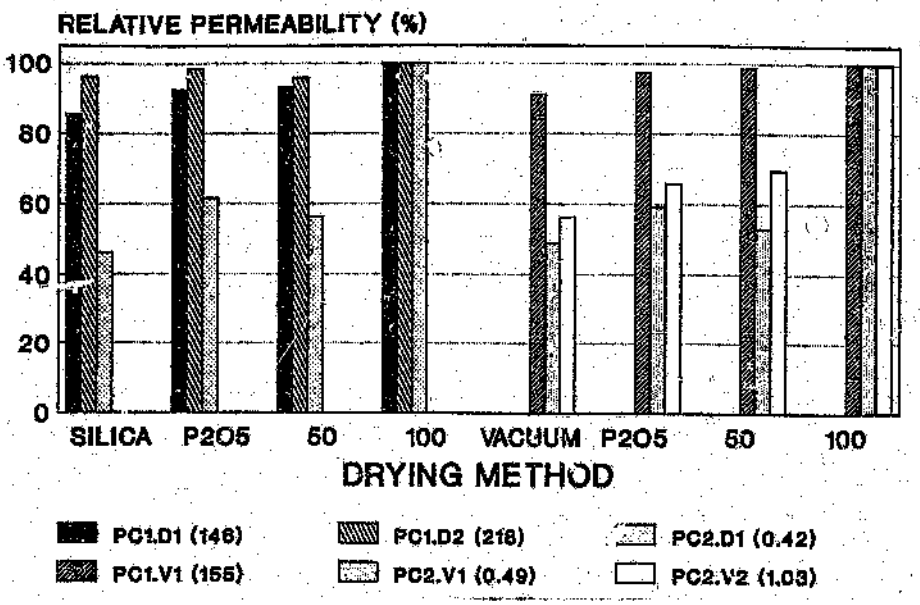

Figure 4.17(a) Permeability of samples after various drying methods relative to permeability after 100 °C drying of the OPC samples

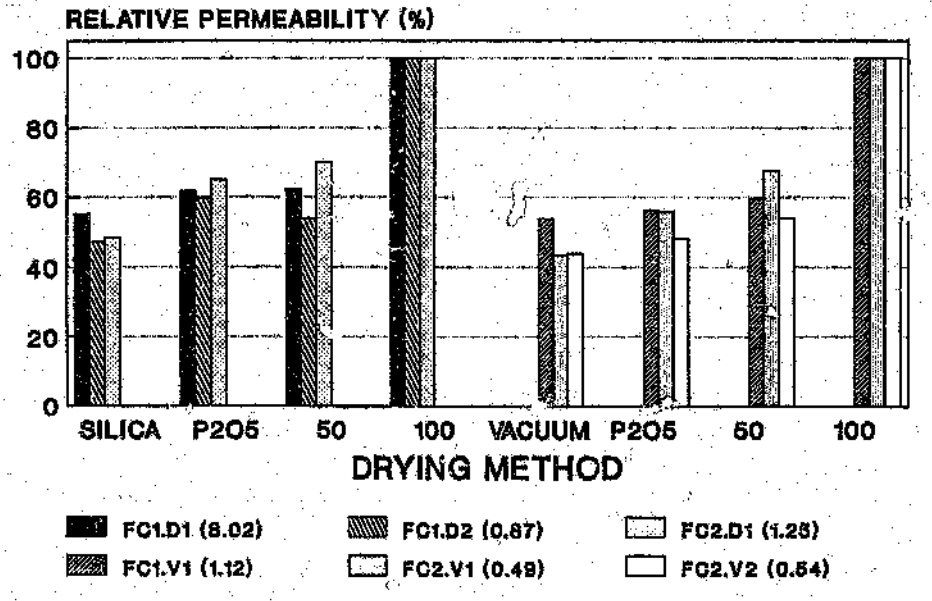

Figure 4.17(b) Permeability of samples after various drying methods relative to permeability after 100 °C drying of the OPC/FA samples

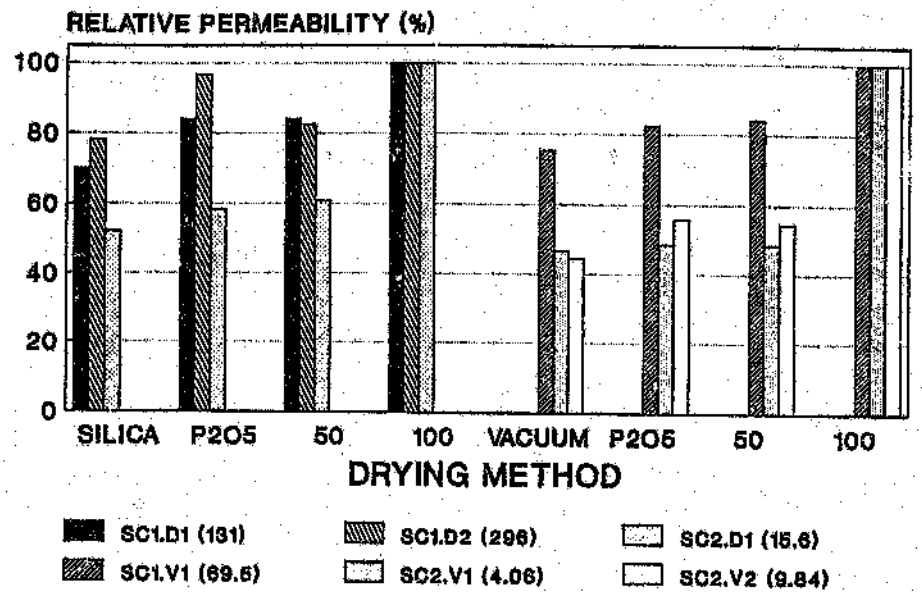

Figure 4.17(c) Permeability of samples after various drying methods relative to permeability after 100 °C drying of the OPC/GGBS samples

The following observations are made from the trends shown in Figure 4.17:

- Samples in the lower permeability range show small relative variations in permeability between silica gel or vacuum, P_2O_5 and 50 °C drying. However, this trend is followed by a large increases in permeability after being dried at 100 °C. Assuming a linear relationship between degree of dryness and air permeability[9], this increase cannot be explained by increased dryness alone. Drying at 100 °C has caused microstructural damage leading to increased permeability.
- On the other hand, samples in the high permeability range show a much smaller increase

in permeability after drying at 100 °C. These samples also show fairly uniform permeability values after the first three drying phases. The indication here is that the more permeable the concrete is, the less sensitive it is to the method of sample drying. This is possibly due to the fact that, for high permeability concretes, the permeability is dominated by large, interconnected capillary pores. Any micro-cracking caused by drying at 100 °C would make a relatively small contribution to "opening" the pore structure of such a concrete. This would translate to a marginal increase in permeability, a proportion of which is due to the increased dryness of the material when dried at 100 °C.

The results obtained in this part of the investigation show that drying the samples at 50 °C produces similar permeability results to that obtained when the samples are dried by "gentle" means, such as vacuum, silica gel or P_2O_5. While some evidence of microstructural alteration was observed with samples dried at 50 °C, the effect on measured permeability was very small.

On the other hand, microstructural alteration caused by drying at 100 °C has had a varying effect on the different concretes tested. Low permeability concretes were more severely affected than high permeability concretes. With reference to the argument presented in Section 4.2.3 (refer to Figure 4.6), drying at 100 °C has had the effect of translating Curve I into a relationship similar to Curve IV. As discussed, this may have the effect of increasing the sensitivity of gas permeability as an indicator of potential durability to a level where the results become unreliable.

4.3.5 The influence of drying method on water sorptivity measurements

As discussed in Section 4.2.3, there is only limited information in the literature on the effects of drying history on measured water absorption of concrete. In particular, there is no information on its influence on water sorptivity measurements. This series of tests was therefore aimed at addressing this lack of information in order to provide further guidance on the method of drying samples for the main test programme.

Samples from the same cubes as used in Section 4.3.3 above were used in this part of the investigation. The samples were also approximately 15 mm thick and were initially air or vacuum dried as discussed before. The water sorptivity test was conducted as described in Chapter 3 with the plastic tape being affixed to the samples at the end of the air or vacuum drying period. This drying phase was followed by oven drying at 50 °C for 7 days and 100 °C for 24 hours. A water sorptivity test was conducted at the end of each drying phase.

A problem was encountered in that, after removal from the 100 °C oven, the plastic tape had collapsed and was no longer usable. Fresh tape had to be affixed and the samples were stored in the 50 °C oven for a further 24 hours befor the water sorptivity test could be conducted. The change in the mass of each sample resulting from the fresh tape and resin, was accounted for by weighing the sample before and after the tape was affixed.

Results and discussion

The results of the water sorptivity tests after the different drying phases are presented in Table 4.13. The format of the data on this table is similar to that used for Tables 4.12 above. The relative sorptivity is expressed as a percentage of that obtained after drying at 100 °C. However, because of the need to place the samples in the 50 °C oven for 24 hours before the water sorptivity test could be conducted, the table shows a considerably lower degree of dryness after the 100 °C drying than the corresponding values in Tables 4.12.

A comparison of the relative sorptivities is shown in Figures 4.18(a) and 4.18(b). As previously, the sorptivity value representing 100% [illegible] is shown in parentheses in the legend, alongside the corresponding mix identification.

The results obtained indicate that water sorptivity is not as sensitive as oxygen permeability to the method of drying. After drying in the 50 °C oven, almost all the samples showed a decrease in the degree of dryness relative to the silica or vacuum drying conditions. Despite this decrease in dryness, many of the samples showed increases in sorptivity, indicating that the act of drying at this higher temperature has marginally increased the water absorption characteristics of the concrete.

In view of the relatively small increase, it is possible to ascribe the increase in sorptivity after 100 °C drying to the increased dryness of the sample. It may well be possible that a portion of this increase is due to the microstructural alteration caused by high temperature drying, but this again underlines the point

that water sorptivity measurements are relatively less sensitive to the drying history of the sample than oxygen permeability measurements.

4.3.6 Influence of the moisture content of the oxygen on measured permeability

In order to determine the influence of the moisture in the bottled oxygen on the measured permeability, a 100 mm high column of fresh silica gel was interposed in the gas line between the oxygen bottle and the permeameter. The same sample was used to determine permeability with the oxygen by-passing the silica gel as well as passing through the silica gel. No difference in permeability measurement was noted and it was decided to conduct all tests without attempting to remove moisture from the oxygen.

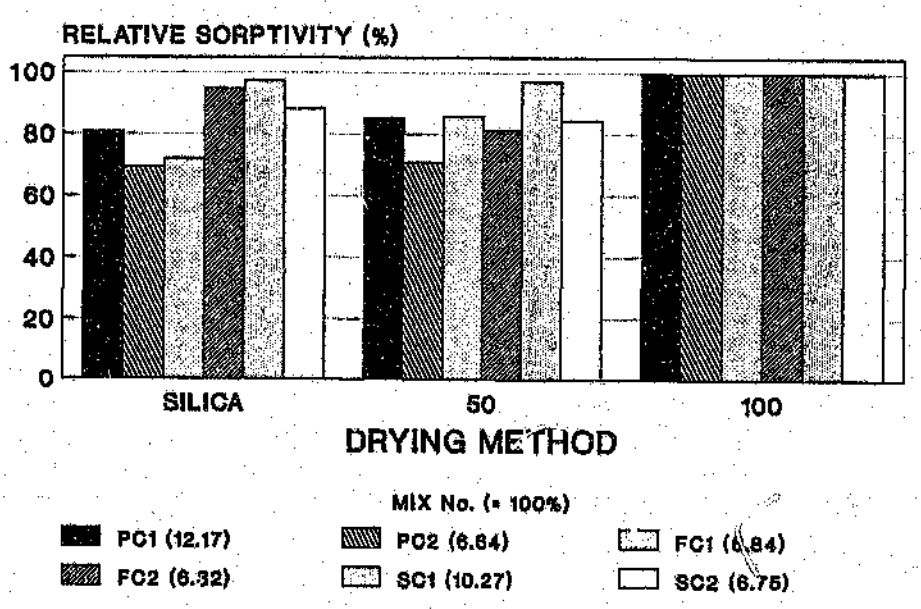

Figure 4.18(a) Relative sorptivities after various drying phases for samples initially dried over silica gel

Table 4.13 Results of water sorptivity tests conducted after various drying methods

Mix I.D.	Drying Sequence	% Dryness	Measured Sorptivity S ($mm/hr^{1/2}$)	% Relative Sorptivity (S/S_{100})
PC1	Silica	89.4	9.82	80.7
	50 °C	88.9	10.39	85.4
	100 °C	92.5	12.17	100
PC2	As Above	87.4	4.60	69.3
		87.1	4.70	70.8
		95.9	6.64	100
FC1	As Above	91.3	4.93	72.1
		91.3	5.88	85.7
		94.4	6.84	100
FC2	As Above	91.6	5.98	94.6
		89.5	5.14	81.3
		94.0	6.32	100
SC1	As Above	90.8	9.99	97.3
		89.6	9.97	97.0
		94.7	10.27	100
SC2	As Above	89.6	5.95	88.1
		88.5	5.69	84.3
		94.7	6.75	100
PC1	Vacuum	90.4	10.05	85.8
	50 °C	88.7	10.28	87.8
	100 °C	93.4	11.71	100
FC1	As Above	90.8	7.45	84.7
		91.7	7.55	85.7
		92.0	8.80	100
SC1	As Above	92.3	9.80	84.6
		90.3	9.83	84.9
		94.2	11.58	100

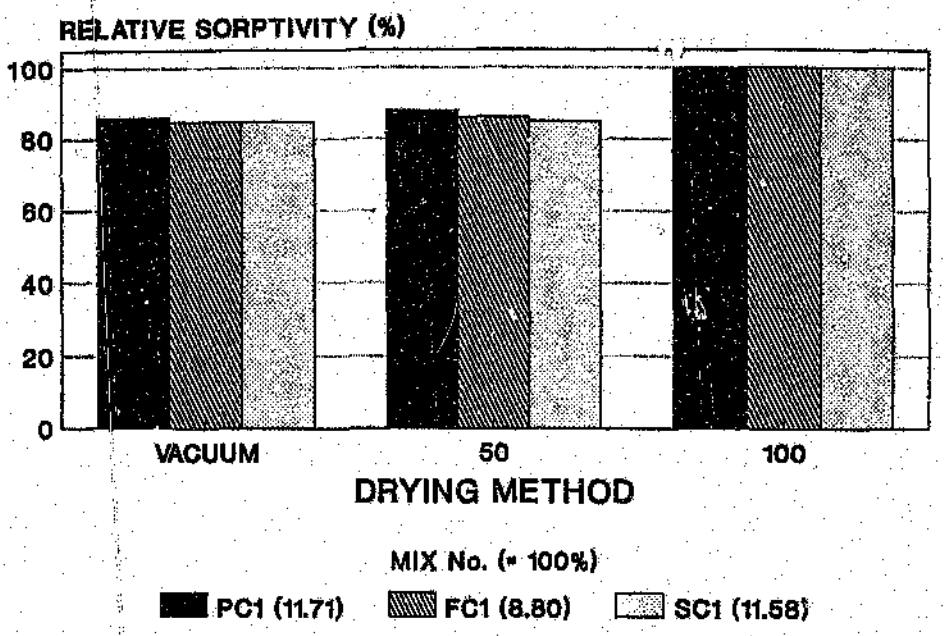

Figure 4.18(b) Relative sorptivities after various drying phases for samples initially vacuum dried

4.4 Conclusions

The literature review and the laboratory investigations presented in this chapter were intended to provide guidance on the test method to be used in the main research programme. The following conclusions are drawn in this regard:

a) it was considered acceptable that the concretes to be tested for this work contain a nominal 19 mm stone as coarse aggregate;

b) as a compromise between the requirements of the oxygen permeability test, the water absorption test and the need to obtain a measure of the gradation of properties in the cover zone, a sample thickness of approximately 15 mm was selected;

c) these samples were to be dried in an air ventilated oven at 50 °C for a minimum of 7 days before being tested;

d) care was to be taken to control the workability of the concretes tested in view of the sensitivity of permeability to the original water content of the mix;

List of References

1. Scrivener, K.L. and Pratt, P.L. The characterisation and quantification of cement and concrete microstructures, *Proceedings of the 1st International RILEM Congress: From Materials Science to Construction Materials Engineering. Volume 1.* Versailles, France. Sept. 1987.

2. Scrivener, K.L. and Pratt, P.L. A preliminary study of the microstructure of the cement/sand bond in mortars. Unpublished report. Imperial College, London. 1992.

3. Grube, H. The influence of concrete materials, mix design and construction techniques on permeability, *Symposium of The Concrete Society: Permeability of Concrete and its Control.* London. Dec. 1985. pp. 77-88.

4. Hooton, R.D. Problems inherent in permeability measurements, *Engineering Foundation Conference: Advances in Cement Manufacture and Use.* Potosi, Missouri. Aug. 1988. pp. 143-154.

5. Parrott, L. Water absorption in cover concrete. Awaiting publication. British Cement Association. 1990.

6. Ujike, I. and Nagataki, S. A study of the quantitative evaluation of air permeability of concrete, (English rearrangement). *Proceedings of the Japan Society of Civil Engineers*. vol. 13, June 1989, pp. 57-70.

7. Parrott, L. and Hong, C.Z. Some factors influencing air permeation measurements in cover concrete, *Materials and Structures*, vol. 24, 1991. pp. 403-408.

8. British Standards Institution, *Methods for testing concrete for other than strength*, London: British Standards Institution (1971)(BS 1881: Part 5).

9. Dhir, R.K. et al. Near surface characteristics of concrete: Assessment and development of in-situ test methods, *Magazine of Concrete Research*, vol. 39, No. 141, Dec. 1987. pp. 183-195.

10. Lampacher, B. Private communication, University of the Witwatersrand. May, 1992.

11. Schonlin, K. and Hilsdorf, H.K. Permeability as a measure of potential durability of concrete - Development of a suitable test apparatus, *ACI SP108: Permeability of Concrete*, American Concrete Institute, Detroit, 1988. pp. 99-115.

12. Kumar, A. and Roy, D.M. The effect of dessication on the porosity and pore structure of freeze dried hardened portland cement and slag-blended pastes, *Cement and Concrete Research*. vol. 16, 1986. pp. 74-78.

13. van Dijk, J. Private communication, June, 1990.

14. Parrott, L, Private communication Nov. 1990

15. Cabrera, J.G. and Lynsdale, C.J. A new gas permeameter for measuring the permeability of mortar and concrete, *Magazine of Concrete Research*, vol. 40, No. 144, Sept. 1988. pp. 177-182.

16. Dhir, R.K. et al. Near surface characteristics of concrete: intrinsic permeability, *Magazine of Concrete Research*, vol. 41, No. 147, June. 1989. pp. 87-97.

17. Lea, F.M. *The Chemistry of Cement and Concrete*, 3rd ed. London: Edward Arnold, 1970.

18. Kelham, S. A water absorption test for concrete, *Magazine of Concrete Research*, vol. 40, No. 143, June. 1988. pp. 106-110.

19. Nagataki, S. and Ujike, I. Effect of heating condition on air permeability of concrete, *Transactions of the Japan Concrete Institute*, vol. 10, 1988. pp. 147-154.

20. Young, H.D. *Statistical Treatment of Experimental Data*, McGraw-Hill, New York. 1962.

CHAPTER 5

LABORATORY INVESTIGATION AND RESULTS

5.1 Introduction

This chapter describes the laboratory test programme undertaken to measure the influence of curing on the surface properties of concrete. The objectives of the investigation were:

(a) to quantify the effect of curing using permeability and sorptivity measurements as described in Chapters 3 and 4;

(b) to quantify the response of concretes with varying mix parameters, to limited moist curing;

(c) to determine the adequacy of using parameters such as sorptivity and permeability, measured at early ages, to predict the long-term durability performance of concrete.

This chapter presents details of the test programme as well as the results obtained together with a general discussion of the results and the broad implications of curing on durability. A more detailed analysis of the results and a discussion of objective (c), with a view to developing prediction models is carried out in Chapter 6.

It has been found that the effect of carbonation on the surface permeability of concrete is different for different binder types. Kropp[1], discussing results obtained by Bier[2], shows that after carbonation, ordinary portland cement (OPC) concretes show a decrease in water permeability, while concrete with a 50% ground granulated blast furnace slag (GGBS) content

showed an approximately 600 times increase in permeability. This observation has not been reported widely and appears to hold negative implications for concretes made with GGBS.

Hence, a further objective of the test programme was to measure variations in permeability and sorptivity of the concretes tested after allowing carbonation to take place. This would allow an assessment of the extent of the problem observed by Bier.

5.2 Variables of the Test Programme

The variables used in the laboratory test programme related to intrinsic factors:

- binder type;
- nominal compressive strength;

and extrinsic factors:

- extent of early-age moist curing;
- depth into concrete from a surface exposed to drying; and
- age at testing.

these variables are discussed in more detail below.

5.2.1 Binder type

In the selection of the intrinsic variables, an important consideration was to ensure that the concretes tested reflected concretes commonly used in construction projects in South Africa.
Three binder types were used as follows:

- plain OPC
- a 50% OPC / 50% GGBS blend
- a 70% OPC / 30% fly ash (FA) blend.

5.2.2 Strength grade

It was decided to compare the performance of different concretes on the basis of equivalent strengths. The following nominal strengths were selected to cover the range of commonly used concretes in South Africa:

- 35 MPa
- 45 MPa
- 55 MPa.

The binder/water (b/w) ratios required to achieve these strengths with the different binder types were determined from Fulton[3] or from manufacturer's technical literature[4].

5.2.3 Early age moist curing

After casting, groups of samples were exposed to water curing for 1, 3, 7 and 28 days before being exposed to drying conditions. It was considered that water curing for up to 7 days represented the full range of site conditions while the 28 day water curing condition represented "ideal" curing, which would act as a control condition.

5.2.4 Depth from the concrete surface

Given the constraints discussed in Chapter 4 regarding the minimum test sample thickness, it was decided to test samples representing depths of 0 to 15 mm, 15 to 30 mm and 30 to 45 mm from the surface of the concrete. This also satisfied the requirement of obtaining a measure of the gradation of properties across the zone of cover concrete.

5.2.5 Age at testing

Two test ages were selected at which the permeability and sorptivity of the concretes would be determined:

- 28 days - to provide an early-age measure of these parameters on which the long-term durability

performance of the concretes could be based;
- 10 months - to provide a measure of the variation of these properties of the cover concrete with time.

5.3 Properties of the Materials Used

5.3.1 Cement

The cement used in the concretes was an OPC from the Dudfield plant of Anglo Alpha Limited. This was chosen because it reportedly does not contain the pozzolanic material typically added to South African OPCs at a dosage of approximately 5%. Three 50 kg pockets were selected from one day's production and, upon receipt at the laboratory, a sample (approximately 800 g) was obtained from each pocket and sent to Anglo Alpha's Technical Services Division for analysis. These analyses are presented in Table 5.1.

Each pocket of cement was stored in an air-tight drum in the laboratory. When batching cement for mixing, approximately equal proportions of the required amount of cement was taken from each pocket. Hence, the possible effects of the differences in the properties of the cement from different pockets was eliminated.

Table 5.1: Chemical and physical analyses of Dudfield OPC used in the concretes.

Pocket Number:	1	2	3
Chemical Tests (%):			
SiO_2	22.03	21.99	21.78
Al_2O_3	4.40	4.38	4.36
Fe_2O_3	2.68	2.64	2.62
CaO	65.00	64.79	64.43
MgO	1.89	1.86	1.85
K_2O	0.24	0.24	0.23
TiO_2	0.23	0.23	0.23
Na_2O	-	-	-
SO_3	1.69	1.53	1.99
Mn_2O_3	0.21	0.21	0.21
P_2O_5	0.07	0.06	0.07
Cr_2O_3	0.02	0.02	0.02
V_2O_5	-	-	-
L.O.I.	1.20	1.10	1.30
Physical tests:			
Fineness (m^2/kg)	305	305	305
Vibrated Mortar cube Compressive Strength:			
3 days (MPa)	35.0	35.5	35.5
7 days (MPa)	51.0	55.5	51.5
Setting times:			
Initial (min)	350	320	210
Final (min)	425	395	315

Table 5.1 shows that the three samples of OPC have uniform physical and chemical properties. The results obtained also show that this cement is typical of South African OPC[3].

5.3.2 Ground granulated blastfurnace slag

A 50 kg pocket of GGBS was obtained from the Vanderbijlpark plant of Slagment (Pty) Ltd. The results of chemical and physical analyses carried out on a sample from the pocket received, are presented in Table 5.2. Where appropriate, these tests were conducted in accordance with the requirements of SABS 1491:1989[5].

Table 5.2: Physical and chemical properties of the GGBS used in the concretes

Chemical compound (%):	
CaO	30.4
SiO_2	35.5
Al_2O_3	15.6
MgO	12.0
SO_3 (sulphate)	1.0
L.O.I.	0.5
Hydraulic Index*	1.63
Physical tests:	
Fineness (m^2/kg)	357
Glass content (%)	98
Soundness expansion (mm)	1.0

$$*H.I = \frac{[CaO] + [MgO] + [Al_2O_3]}{[SiO_2]} \geq 1$$

On the basis of the hydraulic index calculated in Table 5.2, this would be considered as an acceptable quality GGBS[5]. This is a typical South African GGBS and satisfies all the requirements of SABS 1491 Part 1[5].

5.3.3 Fly ash

A 50 kg pocket of the fly ash used in the concretes was

supplied by Ash Resources (Pty) Ltd. from the Lethabo power station. A typical analysis of this ash, conducted during the period when the 50 kg pocket was drawn, is shown in Table 5.3.

Table 5.3: Typical analysis of the fly ash used in the concretes

Chemical compound (%):	
SiO_2	53.40
Al_2O_3	31.90
Fe_2O_3	3.49
TiO_2	1.81
P_2O_5	0.54
CaO	4.68
MgO	1.40
Na_2O	0.40
K_2O	0.58
SO_3	0.17
L.O.I.	0.43

classification and extraction of fly ash for use in concrete has only recently started at the Lethabo power station. However, these results are typical for South African fly ashes[4] and satisfy the requirements of SABS 1491 Part 2[6]. In particular, the quality of this FA is enhanced by the low SO_3 and L.O.I values (maximum allowable is 2.5% and 5% respectively[6]).

5.3.4 Aggregates

In the development of the experimental component of the project, it was felt that optical and electron microscopy techniques could be used to characterise the development of the microstructure of concretes exposed to different curing regimes. In addition, there was the possibility that analytical techniques such as X-ray

diffraction (XRD) and energy dispersive analysis of X-rays (EDAX) would be used for quantitative assessments.

The use of these techniques in the analysis of concrete is often hampered by similarities in the chemical composition of the aggregate and binder components of the material. In order to avoid this problem, it was decided to use a crystalline silica as both sand and stone aggregate. This material was obtained from the Delmas Silica Mine of Samancor (Pty) Ltd.

Unfortunately, this mine produces crushed silica for the glass manufacturing industry and is not equipped to provide sand and stone with gradings suitable for concrete. It was therefore necessary to manually separate and reconstitute various size fractions in order to achieve suitable gradings. Details of the aggregate gradings and corrective measures undertaken are discussed below.

Sand: A sample of material classified by the mine as "-10 mm" was obtained and found to have a grading as shown in Table 5.4. The corresponding grading curve is shown in Figure 5.1. It can be seen from this analysis that the material as received was too coarse to be used as a concrete sand. The proportion of material retained on the 4750 μm and 2360 μm sieves is much higher than that required of a concrete sand. Also, the material retained on the 4750 μm sieve contained a large proportion of between 7 and 10 mm particles.At the other end of the size spectrum, the sand has a low proportion of the -300 μm fraction.

It was therefore decided to discard all the material retained on the 4750 μm sieve and half the material

retained on the 2360 μm sieve. These fractions were manually separated using 500 x 1200 mm sieves. The material retained on the 2360 μm sieve was passed through a sand separator and divided into two halves. One half was re-mixed with the sand while the other half was discarded. In this way, approximately 32% of the material received from the mine was discarded.

Table 5.5 shows a grading analysis of the reconstituted sand while the grading curve of this sand, after discarding the large size fractions as discussed, is shown in Figure 5.1.

Table 5.4: Grading analysis of the -10 mm material as received from the Delmas Silica Mine

Sieve Size (μm)	% Retained	Cumulative % Retained	% Passing
4750	16.6	16.6	83.4
2360	30.2	46.8	53.2
1180	10.8	57.7	42.3
600	5.3	62.9	37.1
300	18.3	81.2	18.8
150	13.8	95.1	4.9
75	2.7	97.7	2.3
Pan	2.3	100.0	
Fineness Modulus: 3.60			

Table 5.5: Grading analysis of the reconstituted silica sand used in the concretes.

Sieve Size (μm)	% Retained	Cumulative % Retained	% Passing
4750	0.0	0.0	100.0
2360	22.1	22.1	77.9
1180	15.9	38.0	62.0
600	7.7	45.7	54.3
300	26.8	72.5	27.5
150	20.3	92.8	7.2
75	3.9	96.7	3.3
Pan	3.3	100.0	
Fineness Modulus: 2.71			

Figure 5.1 also shows the preferred outer limits for the grading of concrete sands suggested by Fulton[3]. It can be seen that the grading curve of the modified silica sand generally lies between the suggested limits.

However, the gap-graded nature of the sand, caused by a deficiency in the -1180 +600 μm size fraction, is evident in the movement of the curve from the lower to the upper preferred limits. While this is not an ideal situation, the sand was accepted in view of the microscopy requirements discussed above.

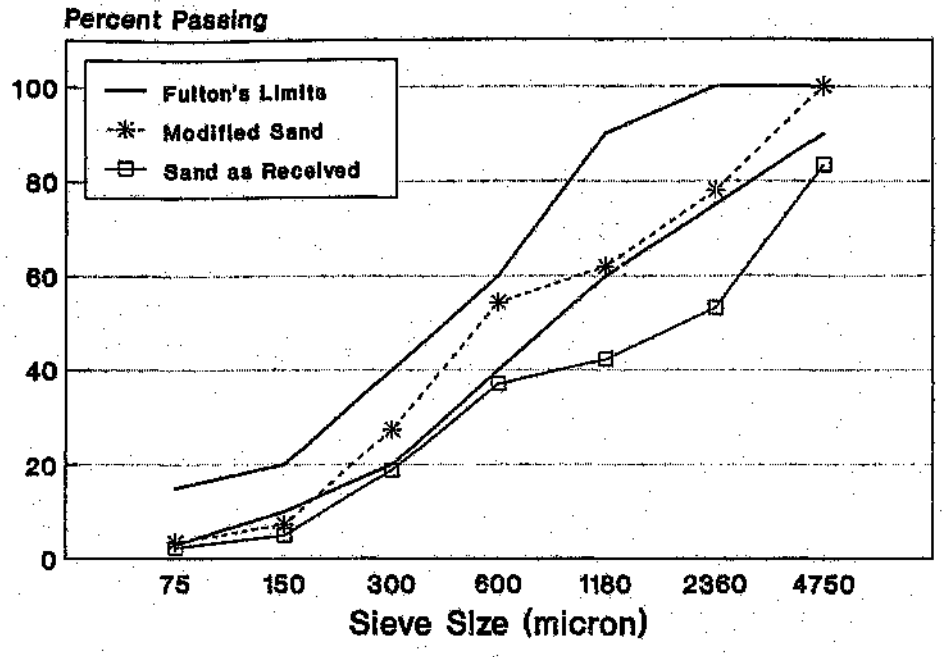

Figure 5.1: Grading curve of the modified silica sand in relation to Fulton's preferred grading limits.

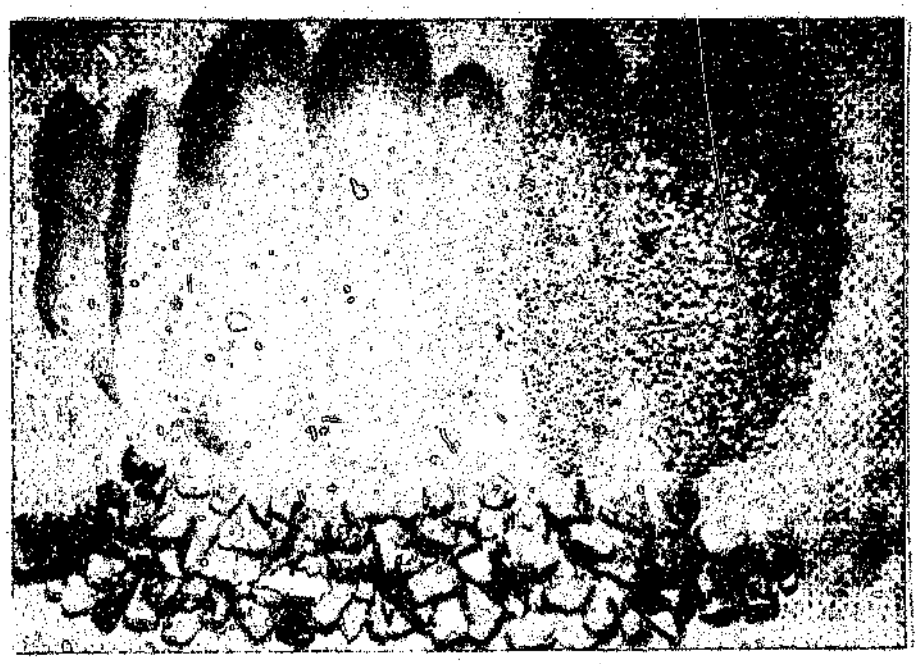

Figure 5.2: Photograph of sand and stone used, showing particle shape and grading

Stone: This fraction of material was obtained from the silica mine from a stockpile classified as "-25 mm". Particle sizes of this material ranged from 25 mm to dust fractions, with 87% of the material being retained on the 9.5 mm sieve. It was decided to discard all material passing the 9.5 mm sieve, leaving a well graded stone between 25 mm and 9.5 mm fractions. Figure 5.2 shows the sand and stone used in this project.

5.4 Laboratory procedure

5.4.1 Mixes

Concretes were prepared using the materials described above, with binder types and strength grades as discussed in Sections 5.2.1 and 5.2.2 respectively. All mixes were designed to have slumps ranging between 30 and 60 mm. Table 5.6 shows the mix proportions of each of the concretes used in the project. These proportions were determined on the basis of trial mixes. The coarse aggregate content of these mixes are lower than would normally be expected because of the coarseness of the sand used. Also, the low fines content of the sand meant that more sand was required to provide the mixes with suitable cohesiveness.

Table 5.6: Mix proportions (kg/m^3) of the various concretes used

Mix No.	Water	OPC	FA	GGBS	Coarse Agg.	Sand	w/b
P1	205	308	-	-	800	1033	0.67
P2	210	378	-	-	800	976	0.56
P3	210	441	-	-	800	923	0.47
F1	193	230	98	-	780	1053	0.59
F2	190	273	117	-	780	1003	0.49
F3	188	316	135	-	780	951	0.41
S1	205	164	-	164	780	1047	0.63
S2	202	197	-	197	790	989	0.51
S3	200	230	-	230	790	937	0.43

Note: w/b = water/binder ratio

5.4.2 Cube sample manufacture and storage

34 cubes measuring 101.6 x 101.6 x 101.6 mm (4 inches) were cast using each of the concretes listed in Table 5.5 above. Mixing was carried out in a 50 litre pan mixer and the following procedure was used:

- introduce dry materials into the mixer in the order of stone, binder and sand;
- activate the mixer and add the water over the first minute of mixing;
- mix for a further two minutes.

At the end of this mixing cycle, the mix was manually distributed in the pan using a hand-held scoop. This ensured a uniform distribution of the material as some

segregation was noted resulting from the operation of the mixer. A standard slump test was then conducted and the slump value was recorded to the nearest 5 mm. These values are given in Table 5.7 below.

Table 5.7: Measured slump values of the various mixes

Mix Number	Slump (mm)
P1	30
P2	40
P3	40
F1	50
F2	45
F3	45
S1	60
S2	50
S3	40

The cube moulds were filled in two layers, each layer compacted by holding the mould onto a high-speed vibrating table for approximately 30 seconds. The filled moulds were covered with plastic sheeting and placed in a room where the temperature and relative humidity was controlled at 23±1 °C and 65±5% respectively.

Samples were de-moulded after 22±2 hours and then subjected to the following curing conditions:

(a) in air at 23±1 °C and 62±5% RH for the entire period up to the time of testing;

(b) in a water curing tank at 22±1 °C for the next 2 days, then as for (a);

(c) in the water curing tank for the next 6 days, then

as for (a);

(d) in the water curing tank for the next 27 days, then as for (a).

Hence, nominal water curing periods of 1, 3, 7 and 28 days were used. These curing periods were chosen on the basis that they represent the following on-site conditions respectively:

- poor curing; formwork is removed approximately 18 hours after casting and the concrete is allowed to dry with no further active curing applied;
- average curing; this is considered to be the extent of curing achieved on most South African construction sites and is probably achieved with the correct use of curing compounds;
- good curing; this is the extent of curing called for by the specification[7] but is seldom achieved on site; it would normally be achieved by water ponding, water spraying or plastic wrapping of the concrete element;
- ideal curing; this duration of curing is rarely achieved intentionally and serves as a control or reference with which to compare the effects of the shorter curing durations; it would also be achieved using the methods as for good curing.

The 34 cube samples of each mix were divided for the purposes of curing and testing as shown in Table 5.8. This table shows that, for each curing regime, two samples were to be tested for oxygen permeability and water sorptivity at three ages after casting. Six cubes were cast for compressive strength testing at two ages and one cube of each mix was cast to monitor the progress of the depth of carbonation with time.

At the end of the stated moist curing period, the appropriate samples were removed from the water curing

tanks (or demoulded, in the case of the 1-day curing period) and transferred to the drying room. The temperature in this room was controlled at 23±1 °C using an air conditioning unit and relative humidity was controlled at 62±1 % using a room-temperature humidifying unit. The humidifying unit was only operational during the characteristically dry autumn and winter months in Johannesburg.

Table 5.8: Number of cube samples used for the various tests

Test	No. of Cubes for Curing Regime			
	(a)	(b)	(c)	(d)
Permeability and Sorptivity Tests at				
28 days	2	2	2	2
12 weeks	2	2	2	2
10 months	2	2	2	2
Compressive Strength at:				
28 days	-	-	-	3
10 months	-	-	-	3
Carbonation	1	1	1	1

These samples were surface dried and four contiguous surfaces of each cube were coated using a water-based epoxy (sold as "Wetseal" and supplied by RFK Industrials). The four coated surfaces included the top and bottom surfaces as cast (see Figure 5.4) and were arranged such that drying of the cubes took place through two opposite, formed faces. Two coats of the epoxy were applied, with the second coat being applied approximately 24 hours after the first.

When the second coat of epoxy had dried, the samples were placed on shelves so that one of the uncoated surfaces of each cube faced outwards. The cubes were arranged with a spacing of at least 50 mm between neighbouring cubes. A continuously operating fan, set on the opposite end of the room in relation to the position of the samples, ensured mixing and movement of the air. However, the effect of the fan was not large enough to cause wind effects at the surface of the samples, which would have accelerated the drying process. The arrangement of the samples on the shelves is shown in Figure 5.3.

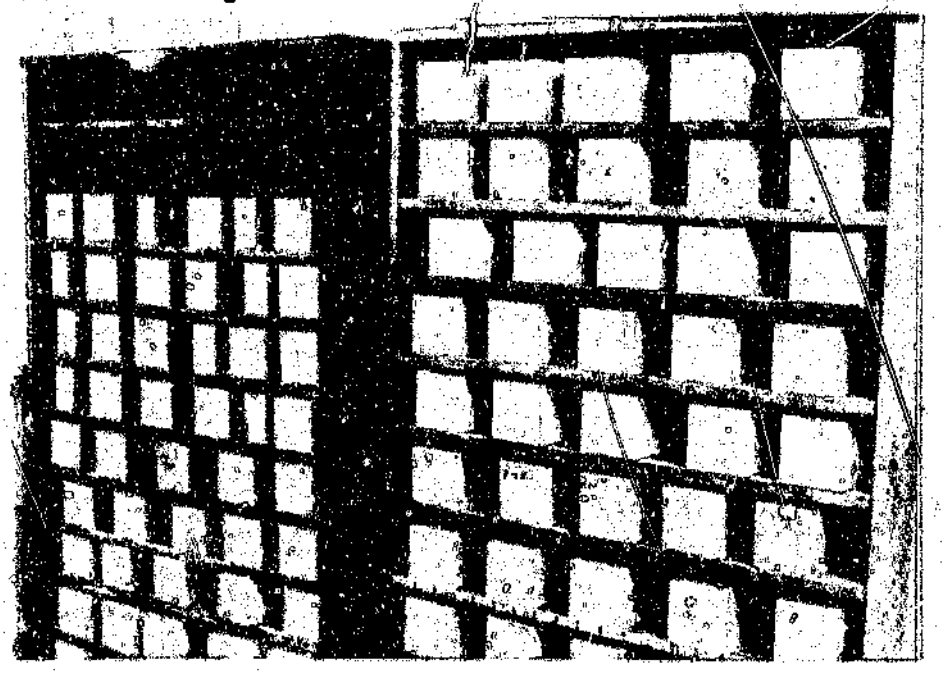

Figure 5.3: Arrangement of cube samples on shelves in the drying room.

5.5 Test Methods

5.5.1 Compressive strength tests

In order to characterise the mixes in compressive

strength terms, three cubes were prepared for testing in compression at 28 days under standard curing conditions. Cube compressive strength tests under standard wet curing conditions were also conducted at 10 months after casting so as to monitor the strength development of the different concretes and the influence that this may have on their durability performance. Tests were carried out in accordance with SABS method 863[8] using an Amsler compression testing machine with a capacity of 2000 kN. All samples were weighed in a saturated, surface dry condition to an accuracy of 5 g before being tested.

5.5.2 Durability index tests

Preparation of samples for durability index testing. At the appropriate time after casting as indicated in Table 5.7 above, sufficient samples were removed from the drying shelves and a central 68 mm diameter core was drilled into the drying face of each cube. With some of the earlier samples tested, a central 70 x 70 x 100 mm prism was cut from the cube so that the drying faces of the cube formed the small faces of the prism. The front end of the core or prism, with respect to its orientation on the shelf, was sliced to form disks or "tiles" representing depths of 0 to 15 mm, 15 to 30 mm and 30 to 45 mm into the concrete. A 2 mm thick, continuous diamond grit blade was used for cutting these slices and the actual thickness of the slices varied between 13 and 15 mm, depending on the straightness of the drilled core. Figure 5.4 shows the method of coring and cutting the cube samples. The prisms and "tiles" were orientated in the same direction as the core and disks respectively.

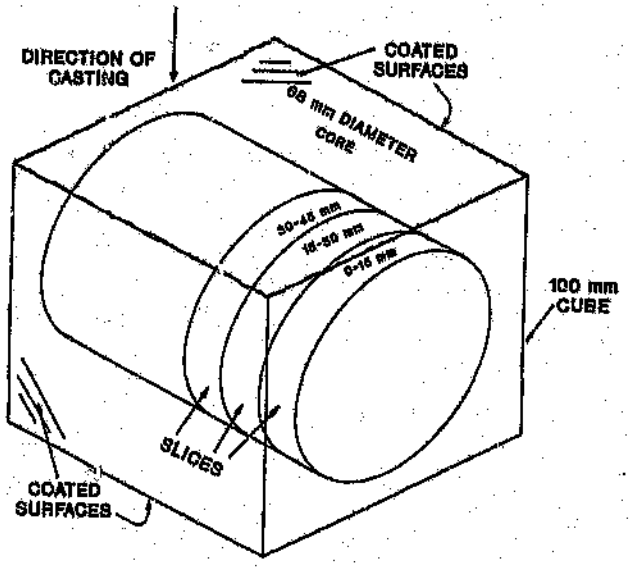

Figure 5.4: Method of cutting and coring cube samples

The slices were then transferred to a 48±2 °C ventilated oven (nominally at 50 °C) to be dried for 7 days before being tested. The back ends of the cores or prisms were also placed into the oven and retained in case repeat tests were required.

Oxygen permeability. At the end of the oven drying period, the slice samples were returned to the drying room and treated as follows:

- immediately weighed to an accuracy of 0.01 g to determine the 50 °C oven dry weight;
- left in the room for approximately one hour to allow them to cool to room temperature;
- re-weighed to determine the increase in mass due to absorption of atmospheric moisture.

The samples were then tested for oxygen permeability using the falling head permeameter as described in Chapter 3. Samples were orientated in the permeameters

such that the outer face of the sample (with respect to the direction of drying) was on the upstream side of the direction of oxygen flow.

Some of the early samples tested, for which 70 x 70 x 100 mm prisms were cut from the cubes, were tested for permeability using the PVC ring and epoxy sealing method. However, the majority of samples were tested in the form of 68 mm disks using the silicone rubber collar sealing method.

A bank of 12 permeameter cells was built for this part of the test programme. Because of the casting sequence, it was often necessary to test more than 12 samples on the same day. This meant that some samples had to be kept in the 50 °C oven for longer than 7 days. It was felt that this would not significantly affect the results of the test, since the samples reached uniform moisture condition at 7 days (refer to Figure 4.7 in Chapter 4). Also, because of the low relative humidity in the oven, it was considered that no further hydration would take place if the samples were left in the oven for a period longer than 7 days.

Water sorptivity. At the end of the oxygen permeability tests, a layer of epoxy was placed on the circumferential surface of the disk samples and a length of plastic tape was applied to this surface to form a reservoir for the water sorptivity test. This procedure is described in more detail in Chapter 3. The samples were kept in the test room for approximately 4 hours after the epoxy was applied and then transferred to the 50 °C oven for a further 12 hours.

In the case of the samples tested for permeability using the PVC ring and epoxy method, a reservoir for

the water sorptivity test is formed by the epoxy on the underside of the sample (as permeability tested) and no further preparation was required. These samples were therefore placed in the oven directly after permeability testing.

The water sorptivity test was then conducted as described in Section 3.6.2 of Chapter 3. The samples were weighed at 0, 1, 6 and 12 minutes to determine the rate of water absorption and were then vacuum saturated to determine their apparent porosity values and this was followed by drying at 105 °C for a determination of the dry weight of the samples.

5.5.3 Depth of carbonation

For all mixes, the depth of carbonation was measured at 10 months after casting on samples cured as shown in Table 5.7 above. The rate of carbonation was not accelerated and the samples tested were stored alongside those subjected to the durability characterisation tests. Samples of the GGBS and FA concretes were again tested for carbonation depth at 20 months after casting. Samples of the plain OPC and low strength FA concretes were inadvertently discarded after the 10-month measurement and the 20-month measurements are therefore not available.

A solution of 1% phenolphthalein in alcohol was sprayed onto a freshly broken surface of the concrete and the carbonated zone was indicated by the absence of colour change of the cement paste phase. Figure 5.5 shows the method of cutting and breaking the sample for the depth of carbonation test. Samples were broken by applying a line load in compression on two opposite faces of the

sample. This was achieved using a loading platen with a welded 10 mm mild steel bar, on the top and bottom of the sample as shown in Figure 5.6.

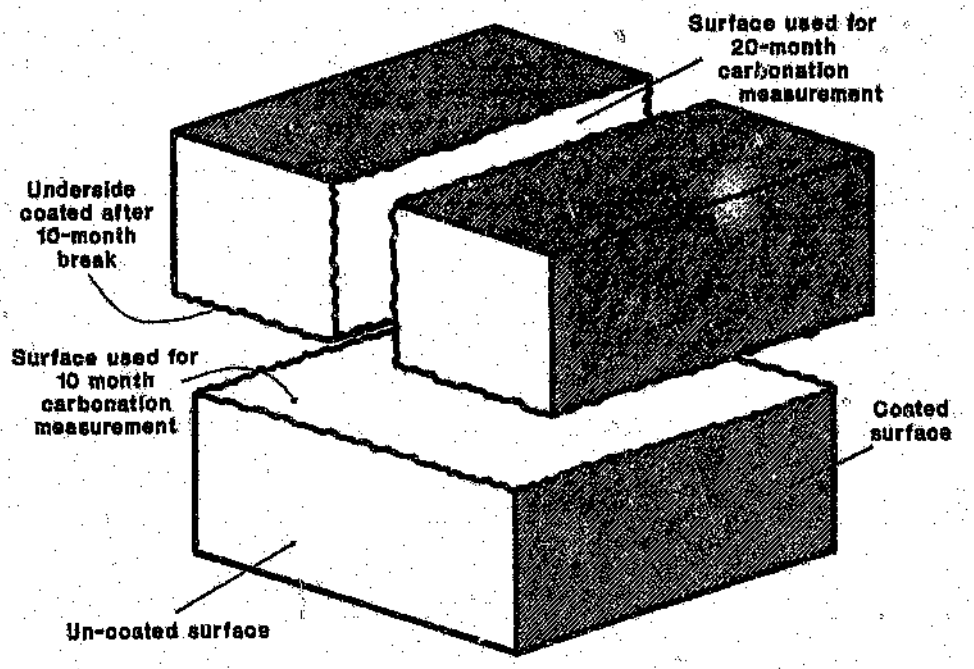

Figure 5.5: Concrete cube used for depth of carbonation determination at 10 and 20 months

The depth of carbonation was determined by taking the average of three measurements of the depth of the uncoloured zone of concrete. These measurements were taken from the surface of the sample which faced outwards when stored on the shelf. The depth of this zone was measured to an accuracy of 0.5 mm using a vernier calliper. Obvious distortions, such as the presence of aggregate particles or air voids near the surface, were avoided when the three measurements were taken.



Figure 5.6: Method of breaking cube segment for depth of carbonation determination

5.6 Results and Discussion

5.6.1 Compressive strength

Table 5.9 shows the average compressive strengths obtained for all the mixes at 28 days and 10 months after casting. Each value shown in this table represents the average of three individual cube compression tests. The individual results of sample mass and failure stress are presented in Tables A1 to A6 in the Appendix.

Table 5.9: Average compressive strengths of the various concretes at 28 days and 10 months

Mix No.	Average Compressive Strength (MPa) at:	
	28 days	10 months
P1	39.6	52.7
P2	47.7	67.3
P3	59.4	79.6
F1	30.3	
F2	45.3	73.3
F3	58.6	89.5
S1	37.1	52.1
S2	39.4	63.7
S3	53.2	80.0

The results shown in Table 5.8 are shown graphically in Figure 5.7. It should be noted that the mixes were intended to be designed for 28-day target strengths of 35, 45 and 55 MPa. Given these target strengths, mix P1 was over-designed for strength, while mix F1 was under-designed to approximately the same extent. On the other hand, mix S2, while also being under-designed, appears to be anomalous since decreasing the w/b ratio from 0.63 to 0.51 has only effected a strength increase from 37.1 MPa to 39.4 MPa.

Figure 5 8 shows the strength results plotted against the w/b ratio. In comparison with the other curves in this figure, the curve for the GGBS concrete strengths at 28-days shows that the anomaly is caused by the S1 concrete showing too high a 28 day strength value.

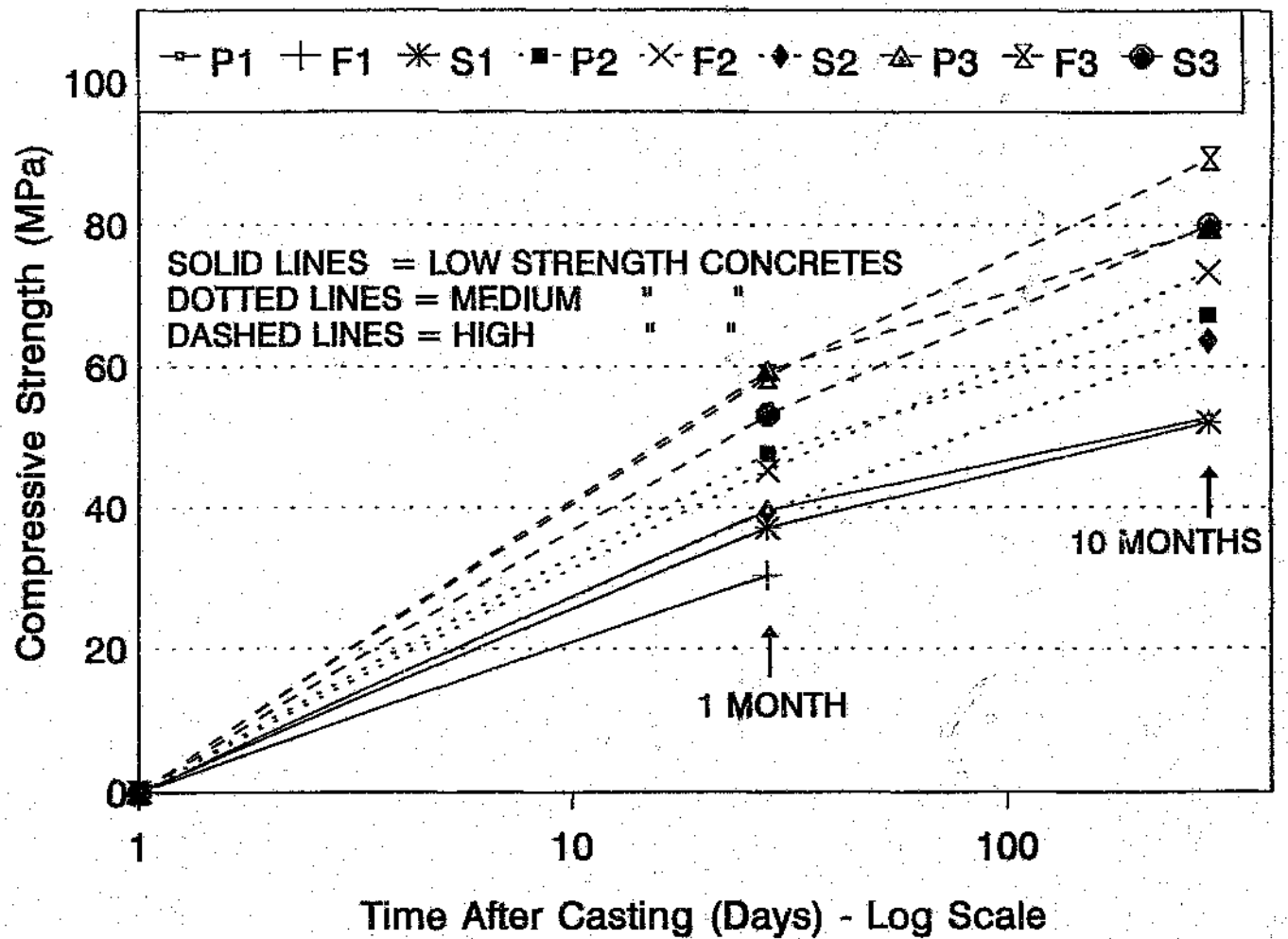

Figure 5.7: Compressive strength of the concretes at 1 and 10 months after casting

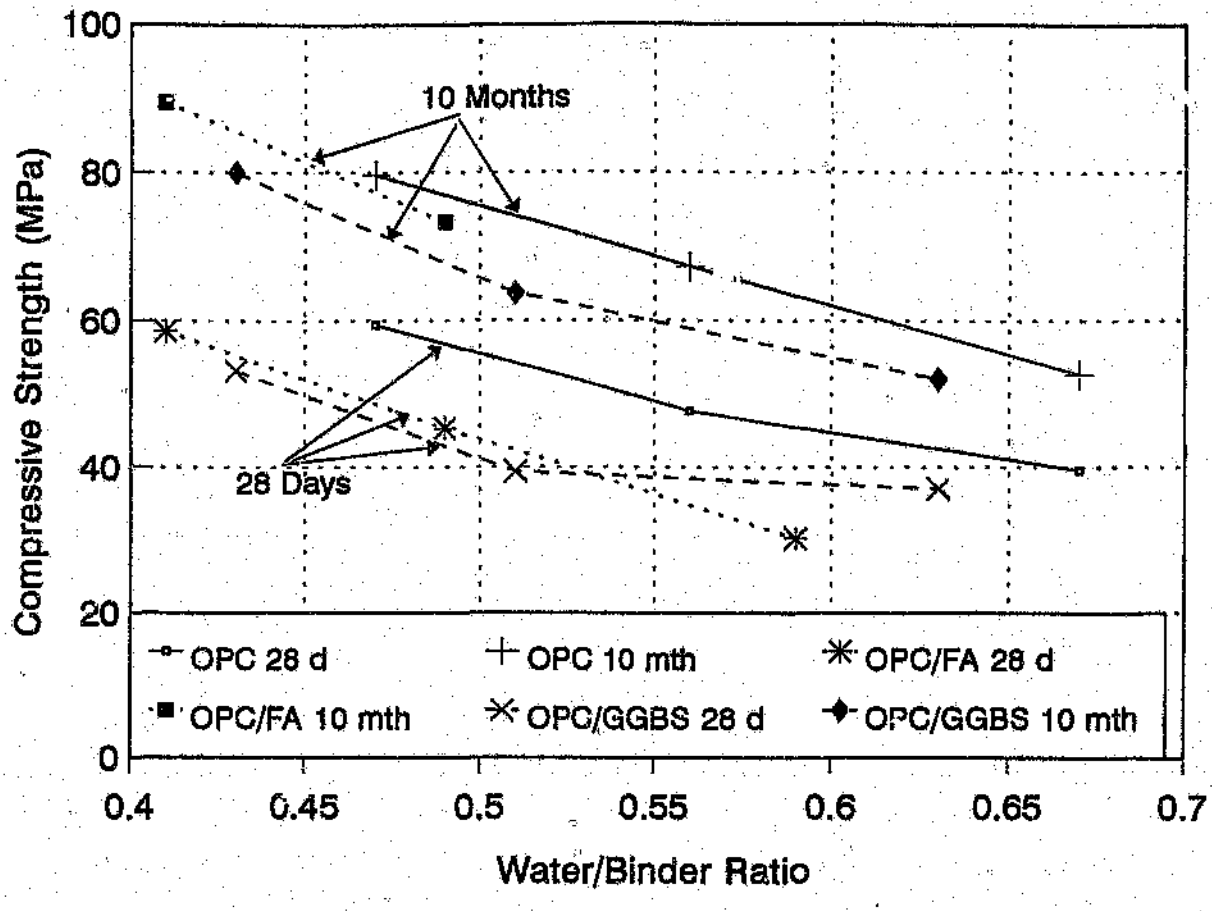

Figure 5.8: 28 day and 10 month strength vs. w/b ratio curves for the different binders tested

If it is assumed that the shape of the w/b ratio vs. strength curve for the GGBS concretes at 10 months is also obtained at 28 days, than the strength value for the S1 concrete reduces to 34.6 MPa. This implies that the strength of the S1 concrete is about 2.5 MPa above an expected value. In the absence of any evidence of an error in the mixing or testing of this concrete, the result can only be accepted as anomalous. The possible effect of this "error" in the assessment of the compressive strength of the S1 concrete, in relation to the measured durability parameters, will be discussed later.

5.6.2 Oxygen permeability at 28 days after casting

The average results of oxygen permeability obtained for the various concretes at 28 days after casting are presented in Tables 5.10 to 5.12 below. In these tables, the coefficient of permeability is quoted to 2 significant figures. Individual results are presented in Tables A7 to A9 in the Appendix.

At the time that the 28-day tests were undertaken, the problem of the variability of permeability measurements was not fully appreciated. As a result, only two samples per combination of mix type, curing regime and depth into concrete were tested initially, as shown in Table 5.8. The permeability values presented in Table 5.10 therefore generally represent the average of two measurements and, in some cases, the result of only one test. Some results had to be discarded because the test sample had a crack or flaw through the thickness, causing a "short circuit" for oxygen flow. These effects were easily identified as results showed unusually high permeability values. When this problem was recognised, it was decided to dispense with the 12-week tests in order to provide additional samples for the 28-day and 10-month tests. Tables A7 to A9 in the appendix indicate which of the results in Tables 5.10 to 5.12 represent the average of three individual test results.

Table 5.10: 28-day oxygen permeability (x 10^{-10} m/s) of the OPC concretes

Mix	Extent of Curing (Days)	Depth into Concrete (mm): 0 to 15	15 to 30	30 to 45
P1	1	32	27	23
	3	3.7	2.6	3.6
	7	4.4	2.1	2.9
	28	0.70	0.74	3.2
P2	1	13	7.7	11
	3	2.5	1.9	1.8
	7	0.82	0.88	1.1
	28	0.44	0.73	0.51
P3	1	3.7	2.7	3.3
	3	1.4	1.2	1.4
	7	0.96	0.53	0.62
	28	0.36	0.60	0.32

Table 5.11: 28-day oxygen permeability (x 10^{-10} m/s) of the OPC/FA concretes

Mix	Extent of Curing (Days)	Depth into Concrete (mm): 0 to 15	15 to 30	30 to 45
F1	1	23	19	24
	3	9.8	18	10
	7	3.3	3.9	4.5
	28	1.9	4.5	4.9
F2	1	7.9	7.7	6.4
	3	5.3	1.7	2.5
	7	0.76	0.72	0.55
	28	0.31	0.39	0.41
F3	1	3.8	3.3	3.0
	3	1.1	1.0	1.8
	7	0.84	0.49	0.45
	28	0.25	0.29	0.31

Table 5.12: 28-day oxygen permeability (x 10^{-10} m/s) of the OPC/GGBS Concretes

Mix	Extent of Curing (Days)	Depth into Concrete (mm):		
		0 to 15	15 to 30	30 to 45
S1	1	42	26	25.1
	3	16	12	11.5
	7	13	12	10.4
	28	3.7	3.9	3.6
S2	1	12	12	12
	3	4.6	4.2	5.3
	7	2.3	6.0	3.7
	28	0.85	0.59	1.2
S3	1	9.4	6.9	8.1
	3	2.4	2.4	1.9
	7	1.2	1.3	1.2
	28	2.0	2.2	1.5

Figure 5.9 shows the oxygen permeability results for the P1 concretes for the three depths from the surface and for the various extents of water curing considered. This figure shows a dramatic decrease in permeability when the extent of moist curing is increased from 1 day to 3 days. However, the linear scale used for the permeability axis, obscures the differences obtained for the different depth slices and Figure 5.10 shows the same data with the permeability axis in a log scale. The differences are now shown more clearly and, for the rest of this discussion, a log scale will be used when presenting permeability data in graphical form. All the graphs also show the 28-day, fully cured compressive strengths and w/b ratios of the respective concretes.

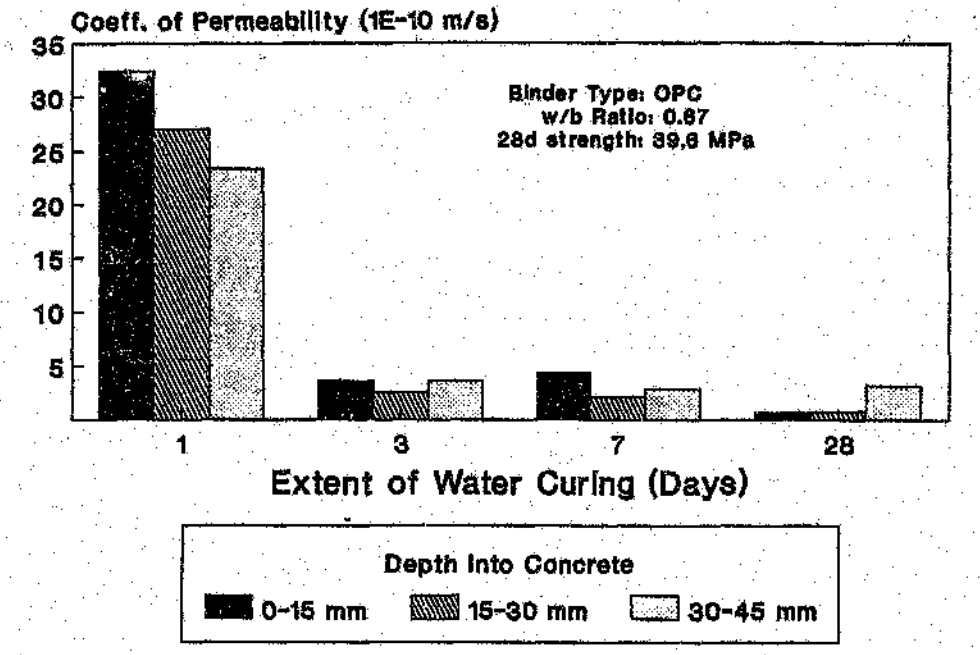

Figure 5.9 Permeability vs. extent of moist curing for the P1 concretes

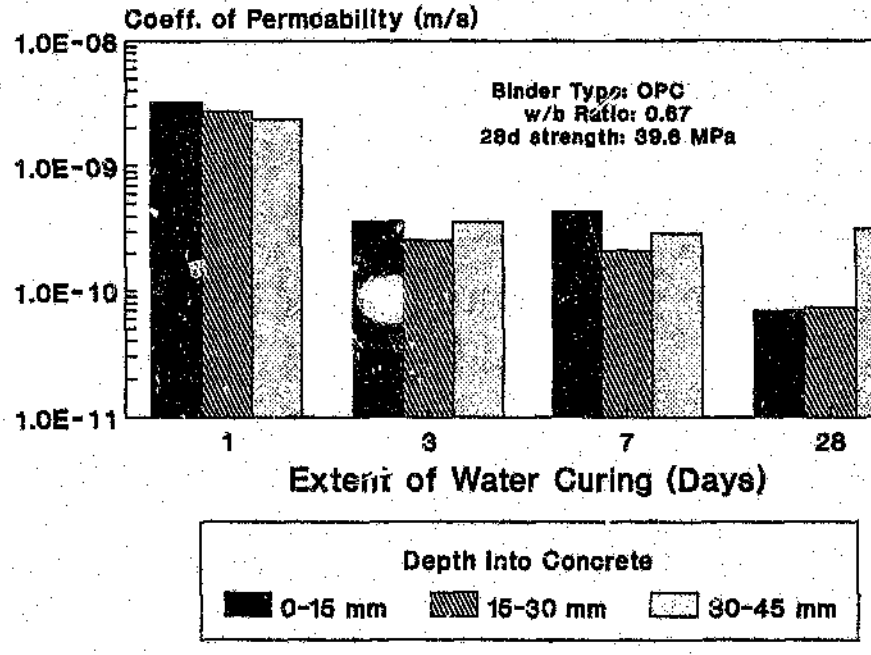

Figure 5.10 The data shown in Figure 5.10 with permeability plotted on a log scale

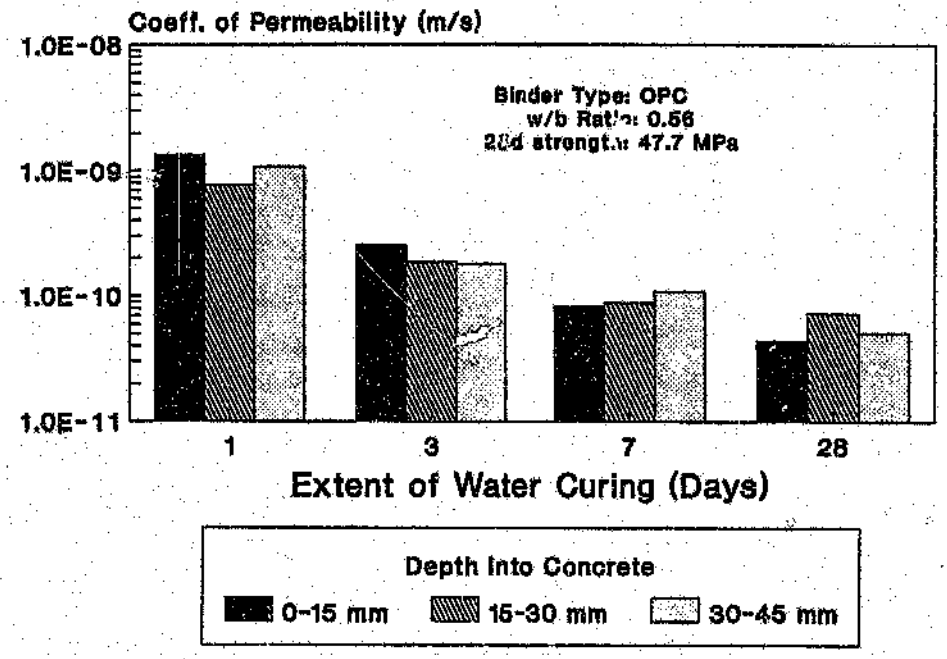

Figure 5.11 Permeability vs. extent of moist curing for the P2 concretes

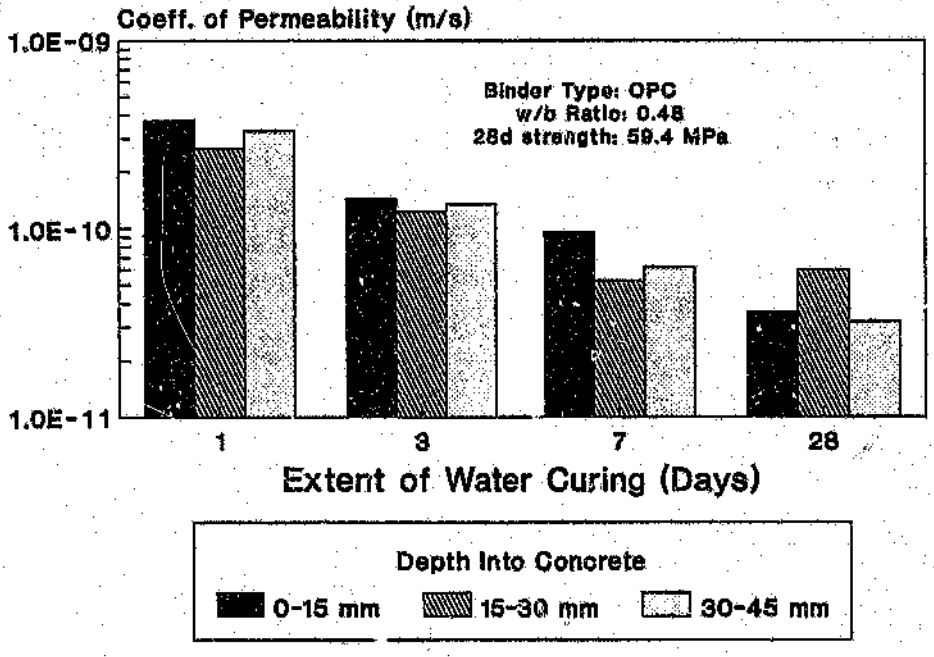

Figure 5.12 Permeability vs. extent of moist curing for the P3 concretes

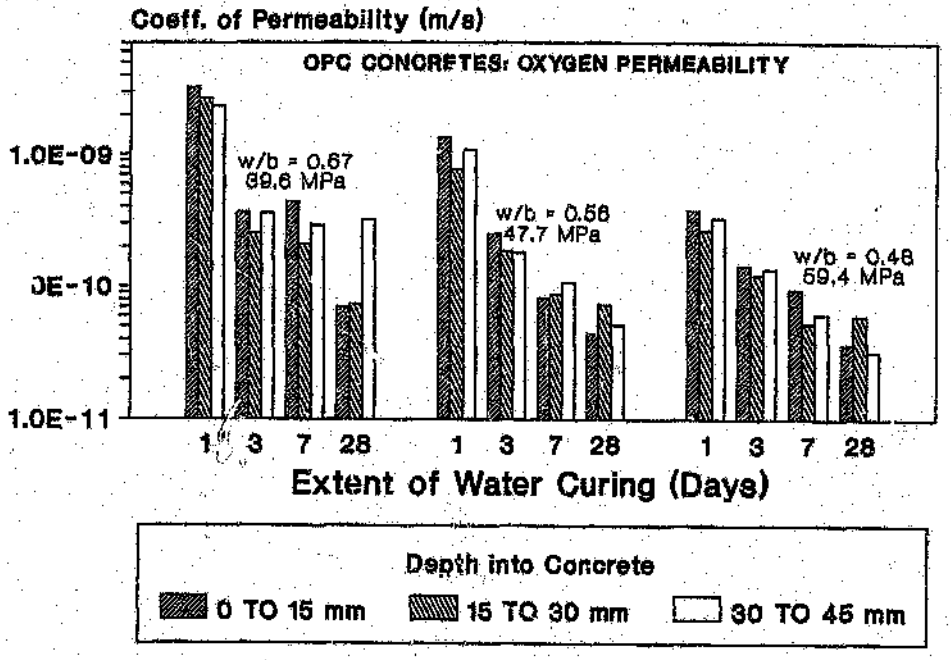

Figure 5.13 Combined results of 28-day oxygen permeability for the OPC concretes

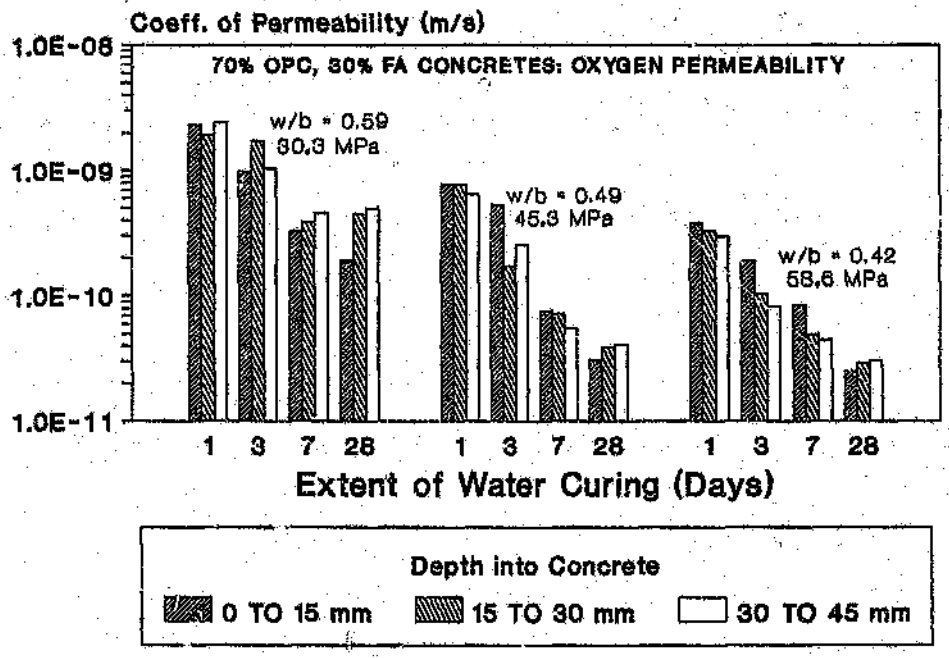

Figure 5.14 Combined results of 28-day oxygen permeability for the FA concretes

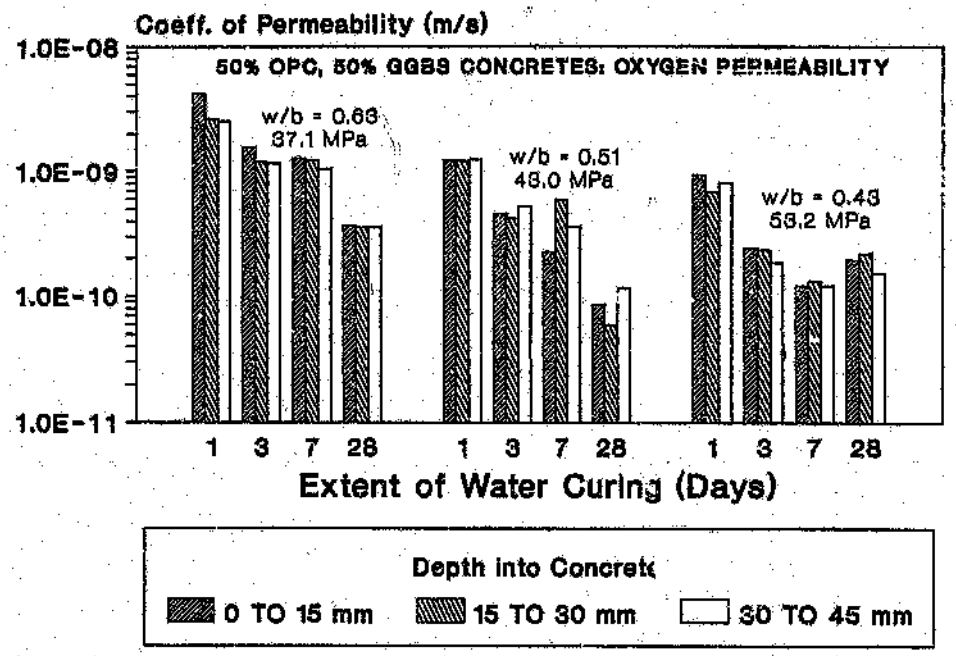

Figure 5.15 Combined results of 28-day oxygen permeability for the GGBS concretes

Figures 5.11 and 5.12 show the form of the results obtained for concretes P2 and P3 respectively plotted as in Figure 5.10. In order to allow comparison across the strength grades of the OPC concretes tested, Figure 5.13 shows a combination of the results in Figures 5.10 to 5.12. Figures 5.14 and 5.15 similarly show the combined results for the FA and GGBS concretes respectively.

From these figures it can be seen that:

- the extent of moist curing has a marked effect on the oxygen permeability of all the concretes. Curing for 28 days can cause an up to 50 times decrease in the permeability of surface concrete when compared with only one day curing;

- increasing the duration of curing from 1 to 3 days appears to effect a better proportional improvement in the low and medium strength OPC concretes than in the case of the corresponding OPC/GGBS and OPC/FA concretes. This is probably related to the slower rate of early hydration of the FA and GGBS components;
- within similar nominal strength grades, the OPC/FA blend generally showed the lowest oxygen permeability after 1 day of curing, while the OPC/GGBS concretes generally gave the highest permeability results for the same degree of curing; however, these differences appear to be significant only for the 28-day cured samples;
- although a number of samples show higher permeability of the surface slices compared with the internal slices, there appears to be no clear trend of decreasing permeability with depth. This indicates that the effect of drying on the permeability of covercrete is significant up to a depth of at least 45 mm.

Some of the permeability results shown are anomalous since the expected order of values is sometimes reversed. This is probably due to the high variability of the permeability measurements as discussed in Chapter 4.

5.6.3 Oxygen permeability at 10 months after casting

The average results of oxygen permeability measurements obtained for the various concretes at 10-months after casting are presented in Tables 5.13 to 5.15 below. Individual results are presented in Tables A10 to A12 in the Appendix.

Table 5.13: 10-month oxygen permeability (x 10^{-10} m/s) of the OPC concretes

Mix	Extent of Curing (Days)	Depth into Concrete (mm): 0 to 15	15 to 30	30 to 45
P1	1	24	18	17
	3	5.5	5.3	5.1
	7	3.4	3.1	3.0
	28	1.4	1.3	0.99
P2	1	9.6	7.9	9.7
	3	3.2	2.8	3.3
	7	1.3	1.7	2.9
	28	0.77	0.86	0.78
P3	1	8.3	8.7	11
	3	3.1	4.2	3.7
	7	1.7	1.5	1.6
	28	0.62	0.75	0.74

Table 5.14: 10-month oxygen permeability (x 10^{-10} m/s) of the OPC/FA concretes

Mix	Extent of Curing (Days)	Depth into Concrete (mm): 0 to 15	15 to 30	30 to 45
F1	1	21	20	19
	3	15	15	17
	7	7.7	6.8	6.2
	28	7.3	9.9	9.5
F2	1	11	12	11
	3	3.1	2.9	3.1
	7	3.0	1.5	1.7
	28	0.48	0.52	0.56
F3	1	4.7	4.5	4.9
	3	1.7	1.6	1.5
	7	0.82	0.61	0.68
	28	0.38	0.30	0.33

Table 5.15: 10-month oxygen permeability (x 10^{-10} m/s) of the OPC/GGBS Concretes

Mix	Extent of Curing (Days)	Depth into Concrete (mm): 0 to 15	15 to 30	30 to 45
S1	1	71	43	44
	3	23	15	25
	7	6.2	4.9	7.4
	28	6.3	4.7	4.5
S2	1	15	11	13
	3	4.7	4.6	5.7
	7	2.3	3.9	6.2
	28	2.9	2.4	3.2
S3	1	9.9	8.9	7.5
	3	2.3	2.5	2.2
	7	1.5	1.4	1.8
	28	1.8	1.4	0.98

These results are also presented graphically in Figures 5.16 to 5.18 below, in the form described in Section 5.6.2. The results show that, after 10 months of drying in the controlled atmosphere room, the relative effects of the different degrees of moist curing are largely unchanged. Given the conditions of exposure of these samples, the effects of inadequate initial curing on the cover concrete are therefore not reversed with time. However, it appears that at 10 months the permeability of the surface and internal slices tend towards the same value for a given concrete type and curing condition. Hence, the absence of a declining trend of permeability with depth from the drying face is more marked after 10 months of air drying than at 28 days after casting.

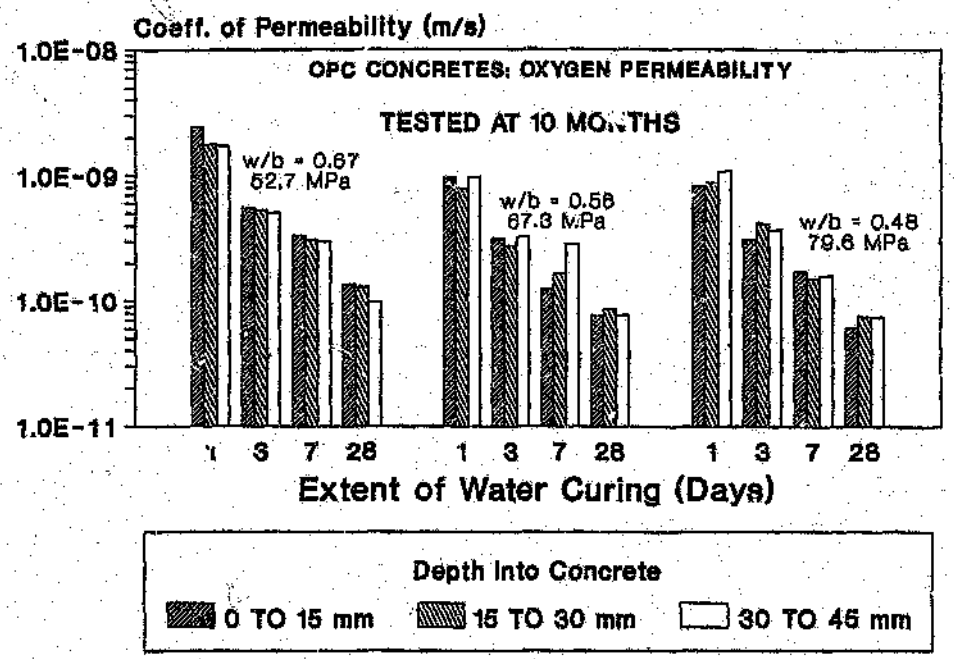

Figure 5.16 Combined results of the 10-month oxygen permeability for the OPC concretes

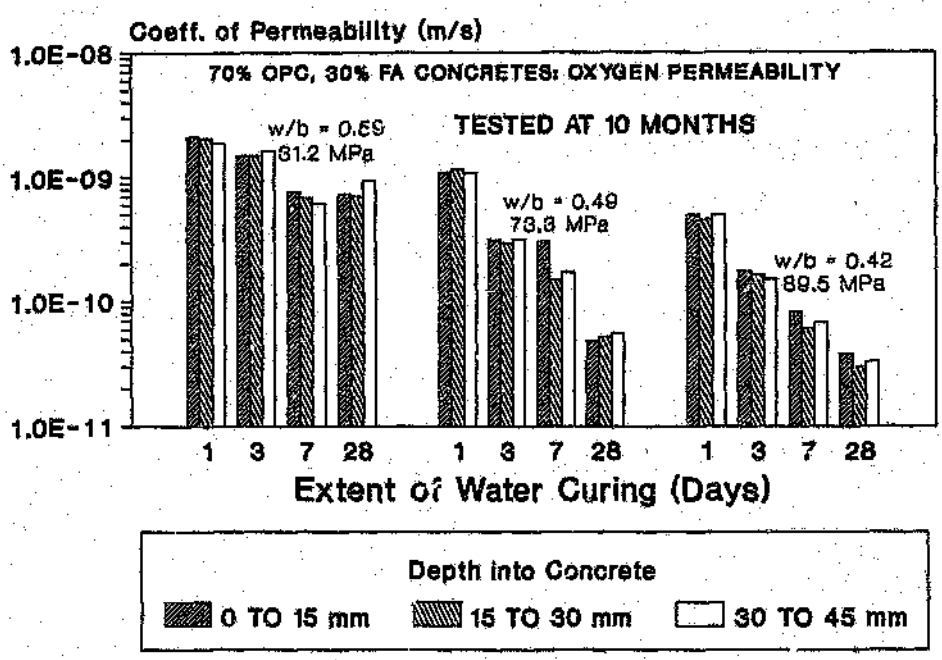

Figure 5.17 Combined results of the 10-month oxygen permeability for the FA concretes

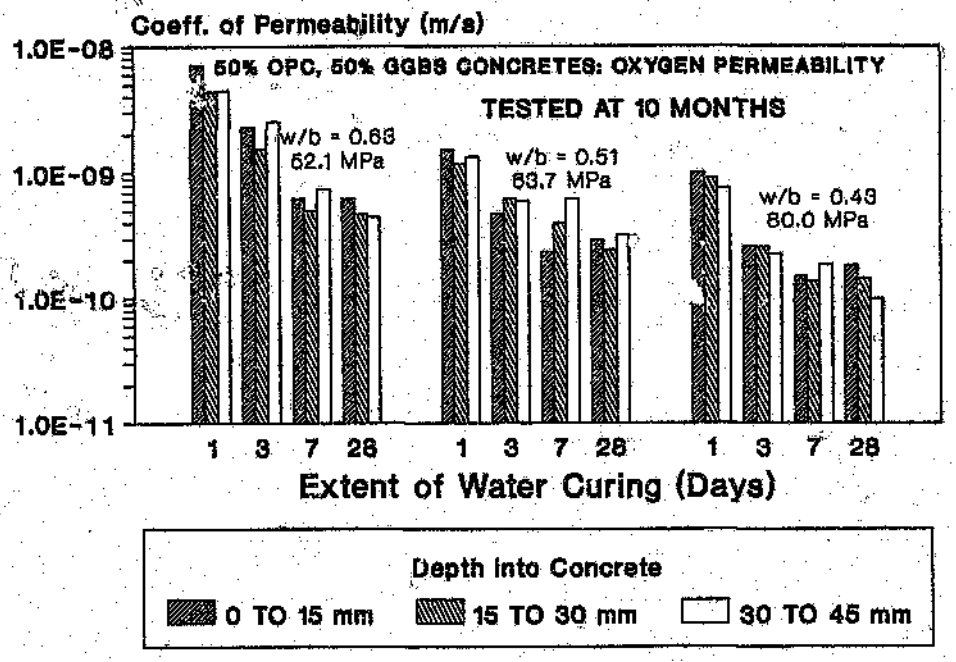

Figure 5.18 Combined results of 10-month oxygen permeability for the GGBS concretes

5.6.4 Water sorptivity at 28 days after casting

The average results of water sorptivity obtained for the various concretes at 28 days after casting are presented in Tables 5.16 to 5.18 below. In these tables, the water sorptivity values are quoted to one decimal place. Individual results are presented in Tables A13 to A15 in the Appendix.

Table 5.16: 28-day water sorptivity ($mm/hr^{1/2}$) of the OPC concretes

Mix	Extent of Curing (Days)	Depth into Concrete (mm):		
		0 to 15	15 to 30	30 to 45
P1	1	32.0	34.8	22.4
	3	22.4	13.0	14.4
	7	15.1	11.1	10.5
	28	10.6	10.1	10.2
P2	1	24.2	15.2	14.1
	3	16.5	10.4	9.4
	7	13.1	9.4	9.1
	28	10.0	9.3	9.1
P3	1	21.6	12.2	12.5
	3	15.5	9.3	9.5
	7	13.0	8.4	9.1
	28	9.6	8.5	9.6

Table 5.17: 28-day water sorptivity ($mm/hr^{\frac{1}{2}}$) of the FA concretes

Mix	Extent of Curing (Days)	Depth into Concrete (mm): 0 to 15	15 to 30	30 to 45
F1	1	26.4	19.9	18.0
	3	23.2	16.4	14.2
	7	18.9	11.6	13.5
	28	14.5	11.7	11.2
F2	1	25.9	18.5	17.3
	3	17.5	10.6	10.0
	7	12.7	8.95	7.9
	28	8.2	7.85	8.5
F3	1	20.6	14.7	13.6
	3	14.3	10.7	8.8
	7	12.0	9.4	8.9
	28	9.5	7.4	8.1

Table 5.18: 28-day water sorptivity (mm/hr$^{1/2}$) of the GGBS concretes

Mix	Extent of Curing (Days)	Depth into Concrete (mm): 0 to 15	15 to 30	30 to 45
S1	1	43.6	34.2	31.5
	3	22.4	16.7	16.0
	7	18.1	11.6	11.7
	28	14.7	7.7	8.2
S2	1	28.3	18.2	19.1
	3	19.3	9.8	9.4
	7	13.9	9.9	10.4
	28	12.6	5.5	6.1
S3	1	25.4	17.3	15.8
	3	12.9	8.7	7.2
	7	12.1	7.3	6.4
	28	14.2	6.7	6.3

These results are shown graphically in Figures 5.19 to 5.21 below. Here again, the results for the concretes with the same binder type are shown on the same figure.

The following points are noted from the water sorptivity results:

- The extent of moist curing has a considerable effect on the water sorptivity of cover concrete. However, in numerical terms, the response of sorptivity to changes in moist curing is less marked than in the case of oxygen permeability. For a given concrete, the largest difference in sorptivity values after 1 day and 28 day curing is a factor of approximately 3.

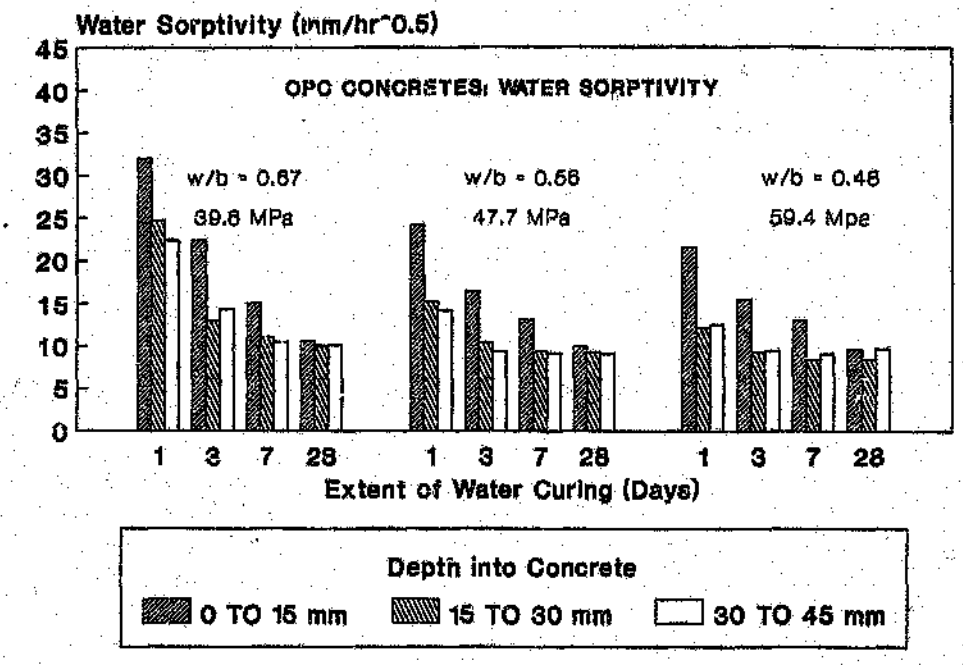

Figure 5.19 Combined results of 28-day water sorptivity for the OPC concretes

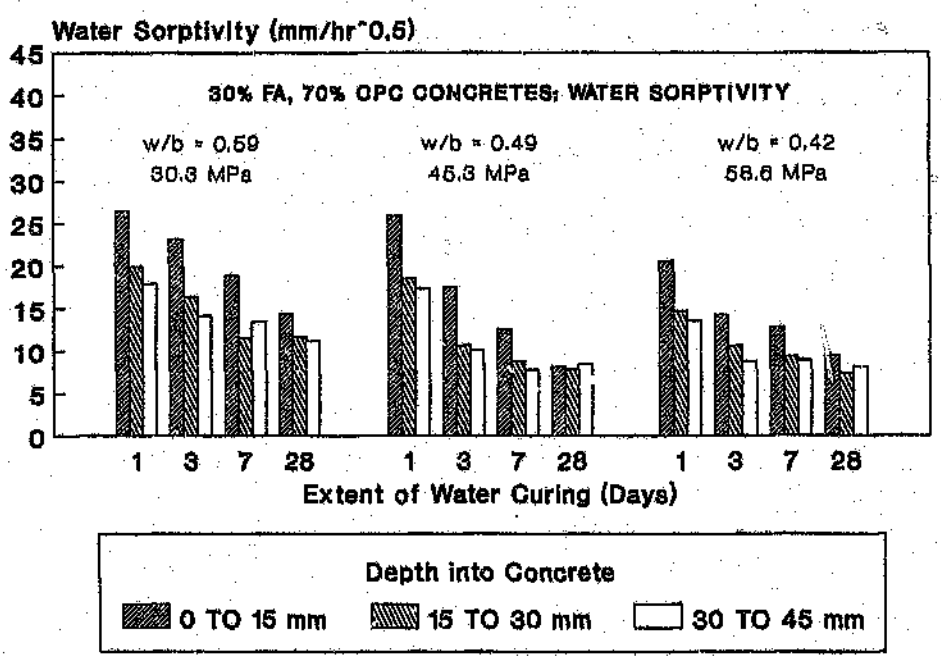

Figure 5.20 Combined results of 28-day water sorptivity for the FA concretes

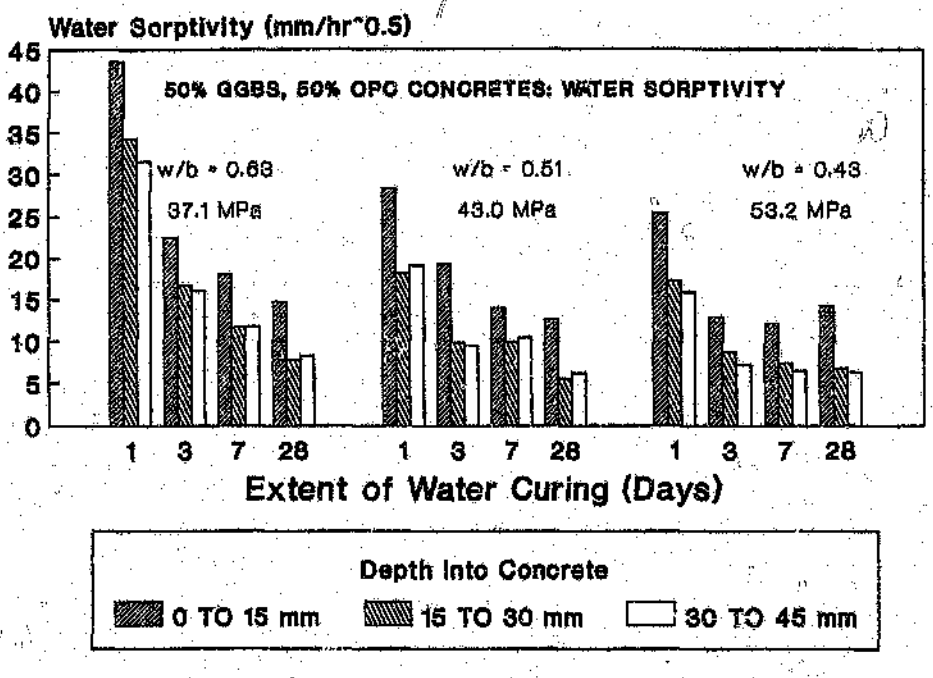

Figure 5.21 Combined results of 28-day water sorptivity for the GGBS concretes

At this stage, it is difficult to interpret this as an indication of lower sensitivity of the sorptivity test. Such an interpretation will depend on an assessment of the test in predicting actual durability performance of the concretes.

- For the depth 0 to 15 mm from the surface of the concrete, the OPC/GGBS concrete showed the highest water sorptivity with the OPC and OPC/FA concretes showing similar results;
- For the 15 to 30 mm and 30 to 45 mm depths, all three binder types showed similar results for curing periods longer than 3 days.
- The surface slices showed higher water sorptivity than the two internal slices, which gave similar values.
- An unexpected observation is that, with 28 days of

water curing, the GGBS concretes still show considerably greater sorptivities for the surface slices than for the internal slices. The reason for this is unclear and may require further testing to confirm the observation.

- For a given binder type and depth into concrete, with continuous curing up to 28 days, the water sorptivity tends towards the same value for all the strength grades tested. This is probably due to similar extents of capillary discontinuity being achieved for the 28-day water curing condition.

The results shown in Figures 5.19 to 5.21 are less erratic and the trends are clearer than the results of the oxygen permeability tests. This is probably due to the fact that bleed voids and other macro defects have a smaller effect on the rate of water absorption than on air permeability.

5.6.5 Water sorptivity at 10 months after casting

The average results of water sorptivity obtained for the various concretes at 10 months after casting are presented in Tables 5.19 to 5.21 below. Individual results are presented in Tables A16 to A18 in the Appendix.

Table 5.19: 10-month water sorptivity ($mm/hr^{1/2}$) of the OPC concretes

Mix	Extent of Curing (Days)	Depth into Concrete (mm):		
		0 to 15	15 to 30	30 to 45
P1	1	27.4	25.9	24.5
	3	20.7	17.7	18.0
	7	16.4	15.6	13.8
	28	13.1	12.0	11.3
P2	1	24.3	21.3	19.1
	3	17.0	14.5	14.4
	7	12.1	12.8	13.3
	28	10.7	11.3	10.9
P3	1	21.6	18.7	17.4
	3	14.8	13.6	13.1
	7	12.0	12.3	11.8
	28	10.3	9.34	9.9

Table 5.20: 10-month water sorptivity ($mm/hr^{1/2}$) of the FA concretes

Mix	Extent of Curing (Days)	Depth into Concrete (mm):		
		0 to 15	15 to 30	30 to 45
F1	1	29.7	25.2	24.6
	3	27.6	23.5	21.2
	7	20.9	15.9	16.1
	28	19.1	16.1	15.0
F2	1	25.9	25.6	23.9
	3	15.4	14.7	14.2
	7	13.4	12.3	11.9
	28	10.2	8.1	6.9
F3	1	20.5	16.6	15.9
	3	11.0	11.0	9.9
	7	9.7	9.5	8.4
	28	8.1	6.9	5.9

Table 5.21: 10-month water sorptivity (mm/hr$^{1/2}$) of the GGBS concretes

Mix	Extent of Curing (Days)	Depth into Concrete (mm):		
		0 to 15	15 to 30	30 to 4C
S1	1	31.9	26.3	27.9
	3	19.7	14.6	15.5
	7	15.0	9.1	8.3
	28	13.6	7.4	7.8
S2	1	25.3	16.1	14.8
	3	25.7	8.5	9.8
	7	12.2	8.5	8.8
	28	13.3	7.0	6.9
S3	1	21.8	16.6	14.9
	3	12.4	8.2	7.6
	7	9.3	6.3	6.3
	28	10.2	5.8	5.5

The combined results for each binder type are shown graphically in Figures 5.22 to 5.24 below.

In comparison with the 28-day sorptivity results, these results show that:

- the surface slices of the GGBS concretes have generally shown a decrease in water sorptivity after 10 months of drying;
- the surface slices of the OPC concretes showed similar water sorptivity values at 10 months as at 28 days after casting;
- the surface slices of the FA concretes showed increased water sorptivity values for the low strength concrete but similar to generally decreased values for the medium and high strength concretes;

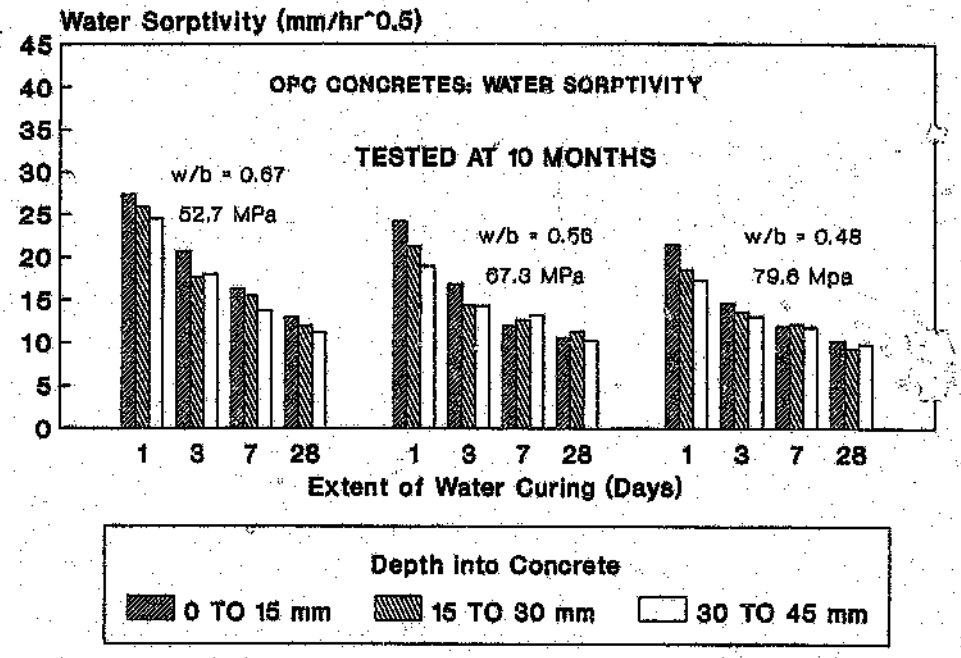

Figure 5.22 Combined results of 10-month water sorptivity for the OPC concretes

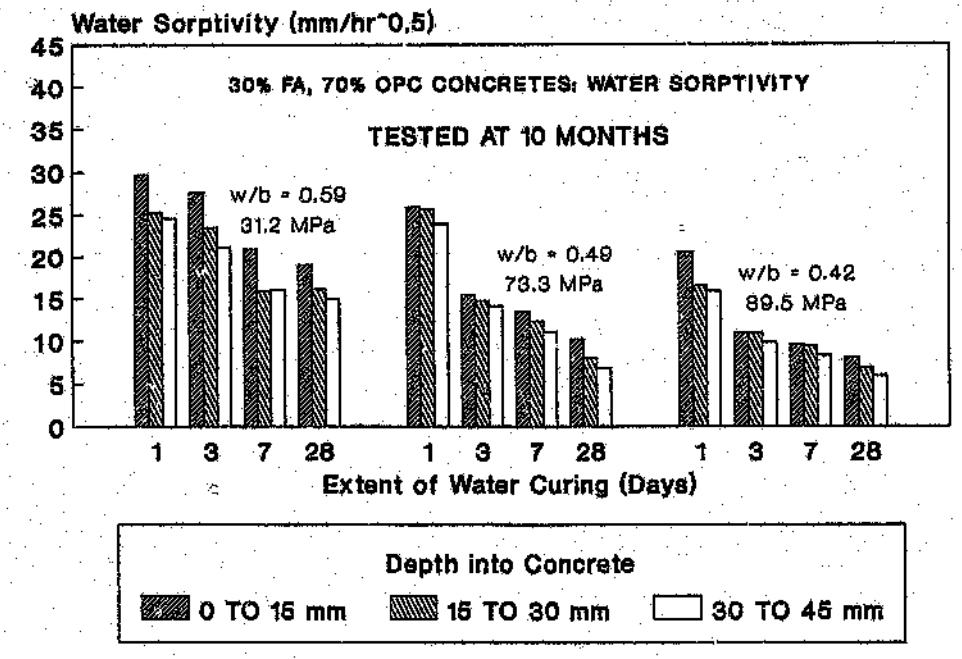

Figure 5.23 Combined results of 10-month water sorptivity for the FA concretes

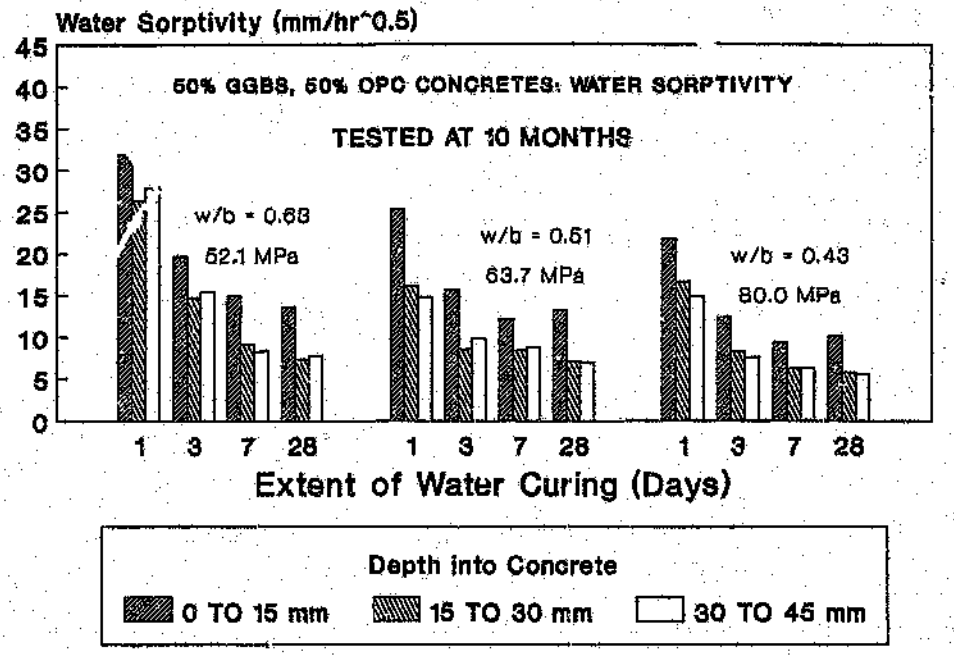

Figure 5.24 Combined results of 10-month water sorptivity for the GGBS concretes

- the differences between the water sorptivity of the surface and internal slices are not as marked at 10 months as at 28 days. This appears to result from increases in the water sorptivity of the internal slices more than decreases in the sorptivity of the surface slices. This effect is more pronounced with the OPC and FA concretes than with the GGBS concrete.

The reason for the internal slices showing an increase in sorptivity after 10 months is unclear at this stage and further testing will probably be necessary.

5.6.6 Depth of carbonation

Tables 5.22 to 5.24 show the measured depths of carbonation at 10 and 20 months after casting. Note

that carbonation depth measurements at 20 months were not measured for the OPC and the low strength FA concretes. These tables also show the calculated carbonation coefficient (D) based on the carbonation equation:

$$x = D.\sqrt{t}$$

where x is the depth of carbonation (mm) at time t (months) after casting. In the tables below, D_{10} and D_{20} are the carbonation coefficients calculated on the basis of the 10 and 20 month measurements respectively.

Table 5.22: 10-month carbonation depths (mm) and carbonation coefficient (mm/month$^{1/2}$) of the OPC concretes

Mix	Extent of Curing (Days)	Carbonation	
		Depth at 10 months (mm)	Coefficient D_{10} (mm/month$^{1/2}$)
P1	1	13.5	4.24
	3	10.5	3.32
	7	7.0	2.25
	28	5.0	1.61
P2	1	9.5	3.07
	3	7.0	2.18
	7	3.0	1.01
	28	2.0	0.63
P3	1	7.0	2.21
	3	5.5	1.68
	7	3.0	0.92
	28	1.5	0.41

Table 5.23: 10 and 20-month carbonation depths (mm) and carbonation coefficient (mm/month^{½}) of the FA concretes

Mix	Extent of curing (Days)	Carbonation depth (mm) at:		Carbonation coefficient (mm/month^{½})	
		10 mths	20 mths	D_{10}	D_{20}
F1	1	13.5	-	4.27	-
	3	11.5	-	3.64	-
	7	10.5	-	3.32	-
	28	6.50	-	2.06	-
F2	1	11.5	20.5	3.64	4.63
	3	7.0	14.0	2.21	3.13
	7	5.0	12.5	1.58	2.84
	28	4.0	10.0	1.20	2.24
F3	1	10.5	19.0	3.29	4.24
	3	7.0	13.0	2.18	2.91
	7	5.5	9.5	1.68	2.17
	28	2.5	6.0	0.79	1.34

Table 5.24: 10 and 20-month carbonation depths (mm) and carbonation coefficient (mm/month^{½}) of the GGBS concretes

Mix	Extent of curing (Days)	Carbonation depth at:		Carbonation coefficient	
		10 mths	20 mths	D_{10}	D_{20}
S1	1	18.5	28.0	5.79	6.26
	3	14.0	23.5	4.36	5.30
	7	10.5	19.0	3.32	4.25
	28	6.0	10.0	1.96	2.24
S2	1	13.5	26.5	4.30	5.97
	3	9.5	17.0	3.04	3.80
	7	7.5	14.0	2.31	3.11
	28	4.5	7.0	1.49	1.56
S3	1	12.0	21.5	3.79	4.76
	3	8.0	11.5	2.53	2.52
	7	4.0	7.5	1.26	1.72
	28	1.5	6.5	0.47	1.50

These results are shown graphically in Figures 5.25 to 5.28 below.

As an example, Figure 5.28 shows the broken surfaces of the P2 group of samples after being sprayed with phenolphthalein at 10 months after casting. The letters A to D refer to the extent of initial water curing as described in Section 5.4.2 above. This figure clearly shows the increasing depth of carbonation with reduced durations of initial moist curing. The effectiveness of the epoxy coating in preventing CO_2 ingress is evident from the absence of a carbonation front at the side surfaces of the samples.

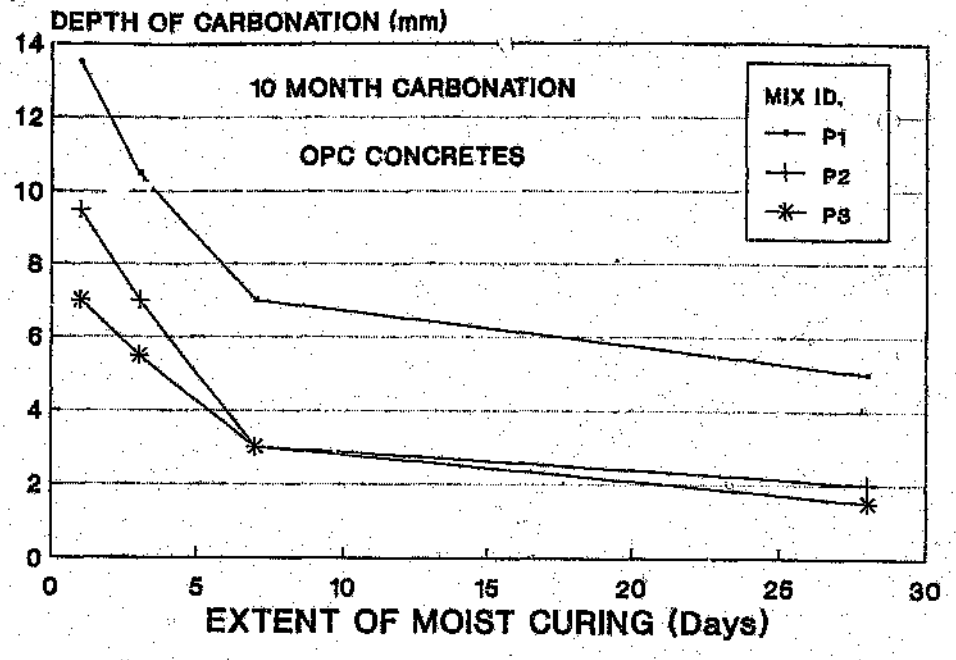

Figure 5.25: Carbonation depths of the OPC concretes at different degrees of moist curing

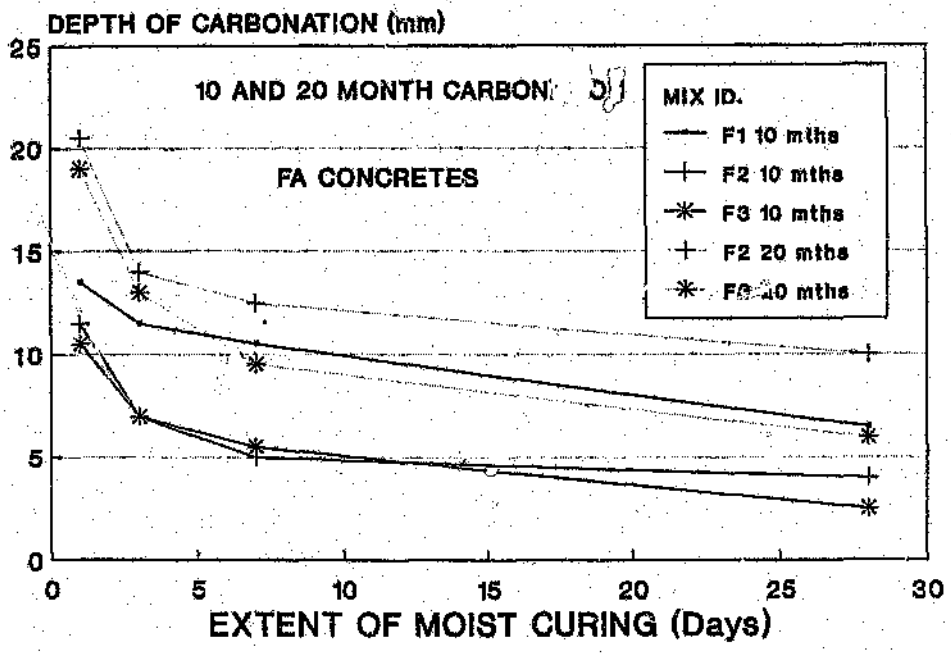

Figure 5.26: Carbonation depths of the FA concretes at different degrees of moist curing

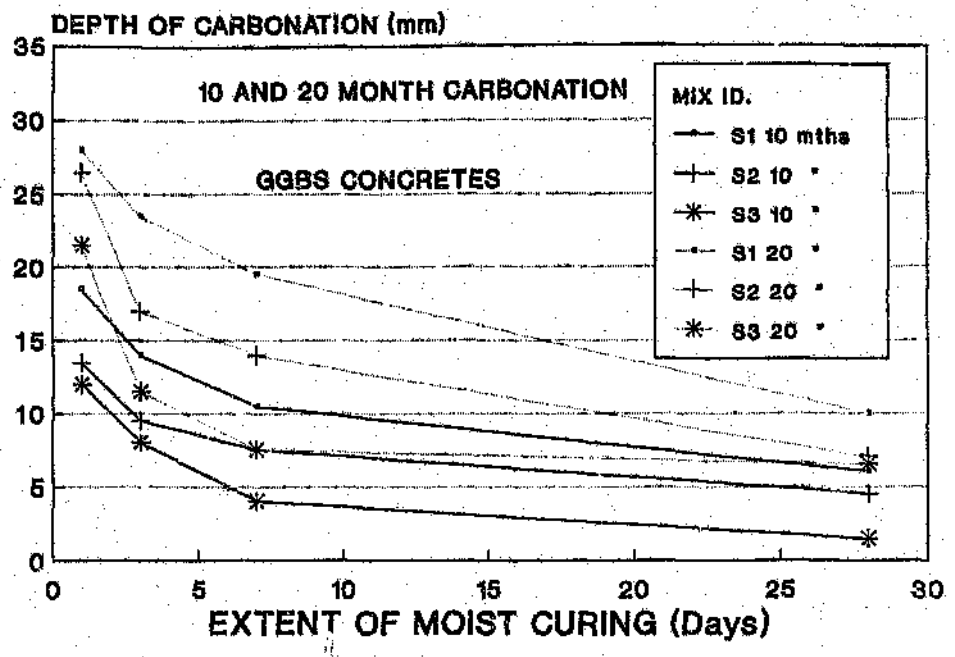

Figure 5.27: Carbonation depths of the GGBS concretes at different degrees of moist curing

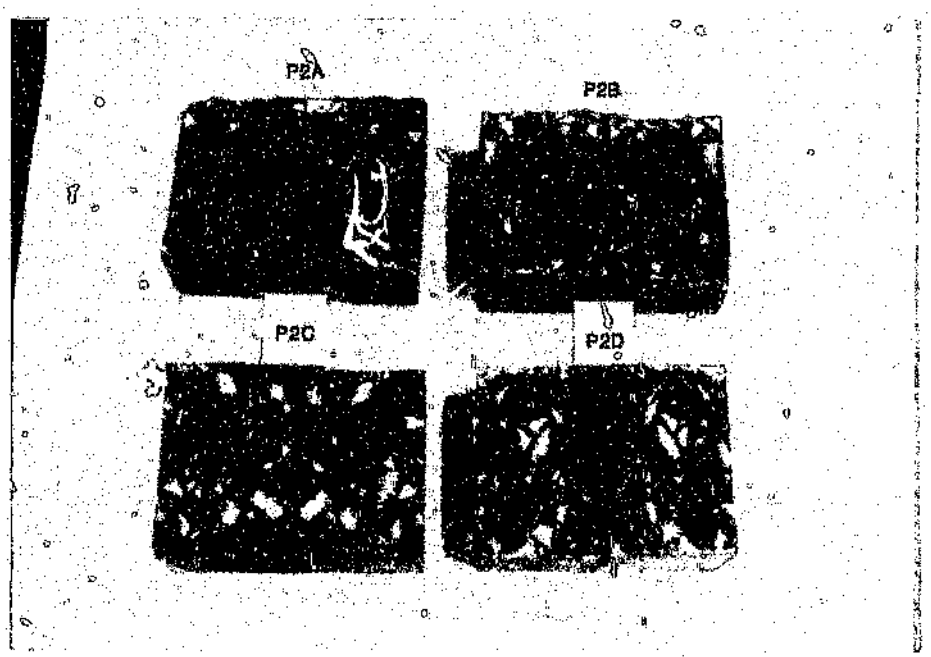

Figure 5.28: Samples of the P2 concrete sprayed with phenolphthalein to determine the depth of carbonation.

Another interesting aspect shown by this figure is the effect of initial curing on the strength of the concrete. The number of broken aggregate particles can be taken as an indication of the strength of the cement paste matrix, since, the stronger the cement paste, the greater would be the tendency for cracks to pass through, rather than around the aggregate particles. On this basis, Figure 5.28 shows a marked increase in strength as the extent of curing increases from 1 to 7 days. There appears to be no noticeable increase in the number of fractured aggregate particles as the extent of initial curing is increased from 7 to 28 days.

The following points are noted from the carbonation results presented above:

- increasing the extent of initial moist curing has a significant effect in reducing the rate of carbonation of all the concretes tested;
- when comparing the carbonation rates of the 1-day and 28-day cured concretes, the OPC and GGBS concretes appear to be more sensitive to the duration of initial curing than the FA concretes;
- within similar nominal strength grades, the GGBS concretes generally showed the largest depths of carbonation while the OPC concretes showed the lowest depths of carbonation;
- all the concretes tested for carbonation depth at 20 months gave D_{20} which were greater than the corresponding D_{10} values. These are anomalous results since they indicate that the rate of carbonation increases with time. The opposite effect would be expected since, for the samples with limited initial curing, the accessibility of CO_2 into the concrete reduces with depth, as indicated by the reductions in permeability and sorptivity with depth. Figure 5.29 graphically

shows the relationship between D_{10} and D_{20}.

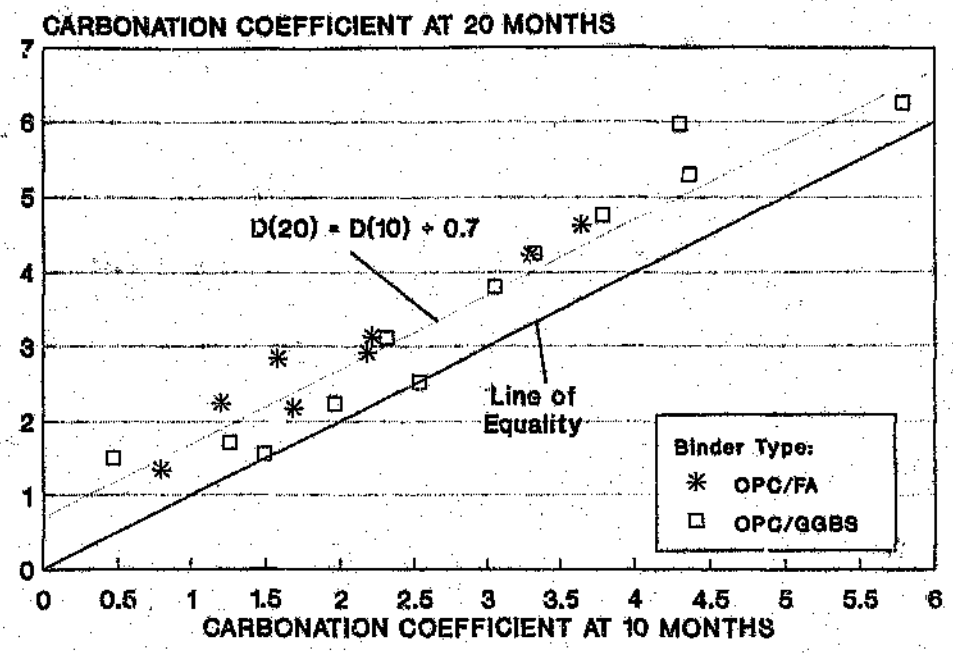

Figure 5.29: Relationship between D_{10} and D_{20} for the FA and GGBS concretes

Figure 5.29 shows that there is an approximately 0.7 mm/month^{½} upward shift in the relationship between D_{10} and D_{20}. The reason for this is possibly a combination of the following factors:

- The differences are magnified because of the relatively early ages at which the measurements are being taken. It may be that the coefficient stabilises at the D_{20} value at later ages.
- The low rate of carbonation after 10 months could be caused by the higher cement content of the surface layer of the samples. The amount of carbonatable material would be greater in this area and the rate of advance of the carbonation front would therefore be slower.
- The square-root relationship for the time rate of

carbonation may not be entirely valid. This relationship has been questioned by Bentur and Jaegermann[9] who have proposed an alternative relationship of the form:

$$x = D.t^{(0.4)}$$

However, applying this form of the equation does not improve the D_{10}/D_{20} relationship indicating that the form of the equation may be in question.

5.7 General Discussion of the Results

The effects of curing duration and c t content: The results of both oxygen permeability and water sorptivity clearly show that larger improvements in permeability and absorption can be effected by increased moist curing than by increased c/w ratios. For example, assume the conditions of a particular project requires a 28-day durability "index" of say, 3 x 10^{-10} m/s (in oxygen permeability terms). Reference to Figure 5.13 shows that this can be achieved using an OPC concrete with a w/b ratio of 0.67 and water cured for 3 days. However, if the concrete is to be moist cured for only one day, the w/b ratio has to be decreased to 0.47 to satisfy the durability requirement. Assuming a constant water content of 200 ℓ/m^3, this represents a cement content increase of 125 kg/m^3 or a cost increase of approximately R25-00/m^3 of concrete (cement currently costs approximately R0.20/kg).

While it may be more efficient to improve the durability of a particular concrete by increasing the duration of early-age curing, this may not be the most

cost-effective option. On a particular project, the engineers may find it more cost effective to increase the cement content rather than increase the duration of early-age curing. Hence, the cost of additional moist curing must be weighed against the cost of additional binder required to give the same permeability and absorption characteristics.

It should also be noted that, for a cost assessment, the results of permeability, sorptivity and carbonation depth show the "diminishing returns" effect. The duration of moist curing required to effect a unit improvement in the quality of the surface concrete, increases with increasing duration of curing.

Effect of curing on depth from a drying surface: It was found that the 15 to 30 mm and 30 to 45 mm slices gave similar permeability and sorptivity results, generally lower than those of the surface slices. Hence, drying has a similar effect on the zone of concrete 15 to 45 mm from the surface. Also, increased duration of moist curing has a significant effect on this 15 to 45 mm zone of the cover concrete, as shown by the reduction in permeability and sorptivity with increasing curing duration.

Effect of Binder type: For the range of concretes tested, the FA concretes have generally performed better than the OPC and GGBS concretes from the point of view of oxygen permeability and water sorptivity. This is probably due to the pore refining effect which FA has on OPC concretes because of its small particle size and pozzolanic effect.

The GGBS concretes generally showed the highest permeability and sorptivity results for the range of

concretes tested. However, this could, at least in part, be explained by the lower 28-day compressive strengths obtained for the medium and high strength concretes. These results indicate that, for the GGBS mixes, lower w/b ratios should have been used than those suggested by Fulton[3].

Comparing the permeability and sorptivity tests: The results appear to indicate that water sorptivity is a more sensitive measure of changes in the development of cement phase microstructure than is oxygen permeability. This is noted from the differences in results obtained for the 0 to 15 mm slices compared to the 'internal' slices. The differences are much clearer with the water sorptivity results than with the oxygen permeability results. However, in considering the merits of these tests as durability indicators, it must be noted that gas permeability and water absorption represent distinctly different transport mechanisms of fluids in concrete. The test results may therefore have to be considered in relation to the expected dominant mode of deterioration if water sorptivity or permeability are to be used as durability index parameters.

5.8 Conclusions

The following conclusions are drawn on the basis of the results and discussions presented in this Chapter:

- The measured compressive strength of the low-strength GGBS concrete is anomalous when viewed with respect to a w/b to strength relationship. However, this does not appear to have unduly influenced the permeability and water sorptivity

results of this concrete.

- The problem of the variability of gas permeability results of concrete must be investigated further. It appears that, for the test conditions used in this project, the minimum number of test samples should be increased to greater than three.
- Increasing the duration of curing has a significant effect in reducing the permeability and sorptivity of the surface zone of concrete made with each of the three binder types used.
- The decrease in permeability and sorptivity is most significant for curing periods from 1 to 7 days. Thereafter, only small decreases in these parameters are observed with increasing durations of curing.
- Within similar strength grades, the OPC/FA concretes showed the lowest permeability results while the GGBS concretes gave the highest permeability results for the same degree of curing.
- The effect of drying in limiting the development of low permeability and sorptivity, was noted at depths of up to 45 mm.
- No clear trend of the permeability with depth into concrete could be identified.
- The water sorptivity results are considerably less erratic than the permeability results. Also, a clear trend of decreasing sorptivity with depth into concrete was noted with these results.
- For the surface (0-15 mm) slices, the OPC/GGBS concretes showed the highest sorptivity results, with the OPC and OPC/FA concretes showing similar results. For the two internal slices, all the concretes showed similar sorptivity results for curing periods longer than 3 days.
- For a given binder type and depth into concrete

and under continuous curing conditions, water sorptivity tends towards the same value for all the strength grades tested.

- Considering the permeability results obtained at 10 months and the sample storage conditions used in this project, the effects of initial inadequate curing are not reversed with time.
- The surface slices of the OPC and OPC/GGBS concretes showed a decrease in sorptivity after 10 months of drying, while the sorptivity of the OPC/FA concrete appears to have been unaffected in this period.
- Continued early age moist curing significantly reduces the rate of carbonation of all the concretes tested.
- Comparing the relative carbonation rates for 1-day and 28-day cured samples, the OPC and OPC/GGBS concretes appear to be more sensitive to the duration of initial curing than the OPC/FA concrete.
- For similar strength grade concretes, the OPC/GGBS concrete generally showed the highest rate of carbonation.
- On the basis of the commonly used square root relationship, the concretes tested showed higher carbonation coefficient values after 20 months than after 10 months. Further research is required to establish a reason for this apparently anomalous result.
- In general, the results show that increasing the duration of moist curing of a nominal 35 MPa concrete from 1 to 3 days, has a similar effect on surface permeability and sorptivity as increasing the strength grade to 55 MPa, with only 1 day of moist curing. However, in choosing one of these options to improve the surface quality of the

concrete, economic parameters related to particular projects must be considered.

List of References

1. Kropp, J. Relations between different types of permeability and selected durability characteristics of concrete. RILEM Technical Committee PCD-116: *Permeability of Concrete as a Criterion of its Durability*. Pre-draft report, October 1990.

2. Bier, T. *Karbonatisierung und realkalisierung von zenmentstein und beton*. Report by the Institutes fur Massivbau und Baustofftechnologie, University Karlsruhe. 1988.

3. Addis, B.J. (Ed.) *Fulton's concrete technology*. Portland Cement Institute, Midrand. South Africa. Sixth Edition, 1986.

4 Ash Resources (Pty) Ltd. *The design of Pfa concrete mixes*. Techincal Information Bulletin, Issue No. 5. Nov. 1986.

5. SABS 1491-1 *Portland cement extenders - Part I: Ground granulated blastfurnace slag*. South African Bureau of Standards, Pretoria. 1989.

6. SABS 1491-2. *Portland cement extenders - Part II: Fly Ash*. South African Bureau of Standards, Pretoria. 1989.

7. SABS Code of Practice 0100-1992, *The structural use of concrete. Part 2: Materials and execution of work*. South African Bureau of Standards,

Pretoria. 1992.

8. SABS method 863 *Compressive strength of concrete (including making and curing of the test cubes)*. South African Bureau of Standards, Pretoria. 1976.

9. Bentur, A and Jaegermann, C. Effect of curing on the properties of the outer skin of concrete. *ASCE Jnl. of Materials in Civil Engineering*. Vol. 3, No. 4. Nov. 1991. pp. 252-262.

CHAPTER 6

DEVELOPMENT OF A GENERALISED APPROACH TO THE EFFECT OF CURING ON DURABILITY

6.1 Introduction

This chapter presents more detailed analyses of the results presented in Chapter 5, with the intention of developing a generalised approach to the effect of curing on concrete durability. Consideration is given to the relationship between the measured durability index values (permeability and sorptivity) and the following parameters:

(a) binder/water (b/w) ratio;
(b) compressive strength;
(c) duration of initial curing;
(d) depth into concrete;
(e) rate of carbonation.

Note that in this chapter, it was decided to use b/w ratio rather than the more conventional w/b ratio. The reason for this is that, in the numerical models developed later, it was found that the b/w raio form simplifies the relationships considerably.

For the relationships (a) and (b) above, the nature and implication of the observed trends are discussed, while in the case of (c), (d) and (e), mathematical models are developed to represent the relationships. The models are empirical and are derived from regression analyses of the data using standard forms of regression equations.

An important objective of this study was to consider the usefulness of early-age index testing as a means

of:

- monitoring the quality of cover concrete, and
- predicting the long-term durability performance of the material.

All the analyses and comparisons in this chapter refer to the 28-day permeability and sorptivity results and are intended as contributions to answering the following questions:

- Within the scope of the variables used in the study, how should mix parameters and curing conditions be selected to achieve a particular level of durability index at 28 days after casting?
- Having achieved a particular durability index at 28 days, what long-term durability performance is to be expected from the concrete?

While it is not the intention of this study, a probabilistic approach to addressing these issues will have to be considered. It will be necessary to focus further research in the field of concrete durability in this direction.

6.2 Effect of Binder/Water Ratio on Durability Index Values

6.2.1 Permeability

Figures 6.1 to 6.3 show the relationships between the coefficient of oxygen permeability and b/w ratio for the three binder types tested. The figures show the permeability measurements of the 0-15, 15-30 and 30-45 mm depths respectively, for the four curing regimes.

These curves show that, for a given b/w ratio and curing condition, plain OPC concrete generally gives the lowest permeability value. FA concretes give similar results to those of the OPC concretes only for b/w ratios greater than approximately 2.0 combined with water curing periods greater than 7 days. The GGBS concretes showed similar performance to the FA concretes for water curing periods of 1 and 3 days. The effectiveness of longer curing periods is less pronounced for the GGBS concretes and these show higher permeability values after 7 and 28 days of water curing.

It is also interesting to note that, with increasing durations of initial moist curing, the permeability of the OPC concretes become relatively less sensitive to changes in b/w ratio than the FA and GGBS concretes. As mentioned in Chapter 5, this is possibly an indication of the greater extent of capillary discontinuity being achieved with continued hydration of the OPC concretes. This effect is more significant in the lower range of b/w ratios.

While the curves generally show trends of decreasing permeability with increasing b/w ratio, these trends are not uniform and, hence, no attempt was made to describe these curves mathematically. The influence of b/w ratio is accounted for in a mathematical model developed later.

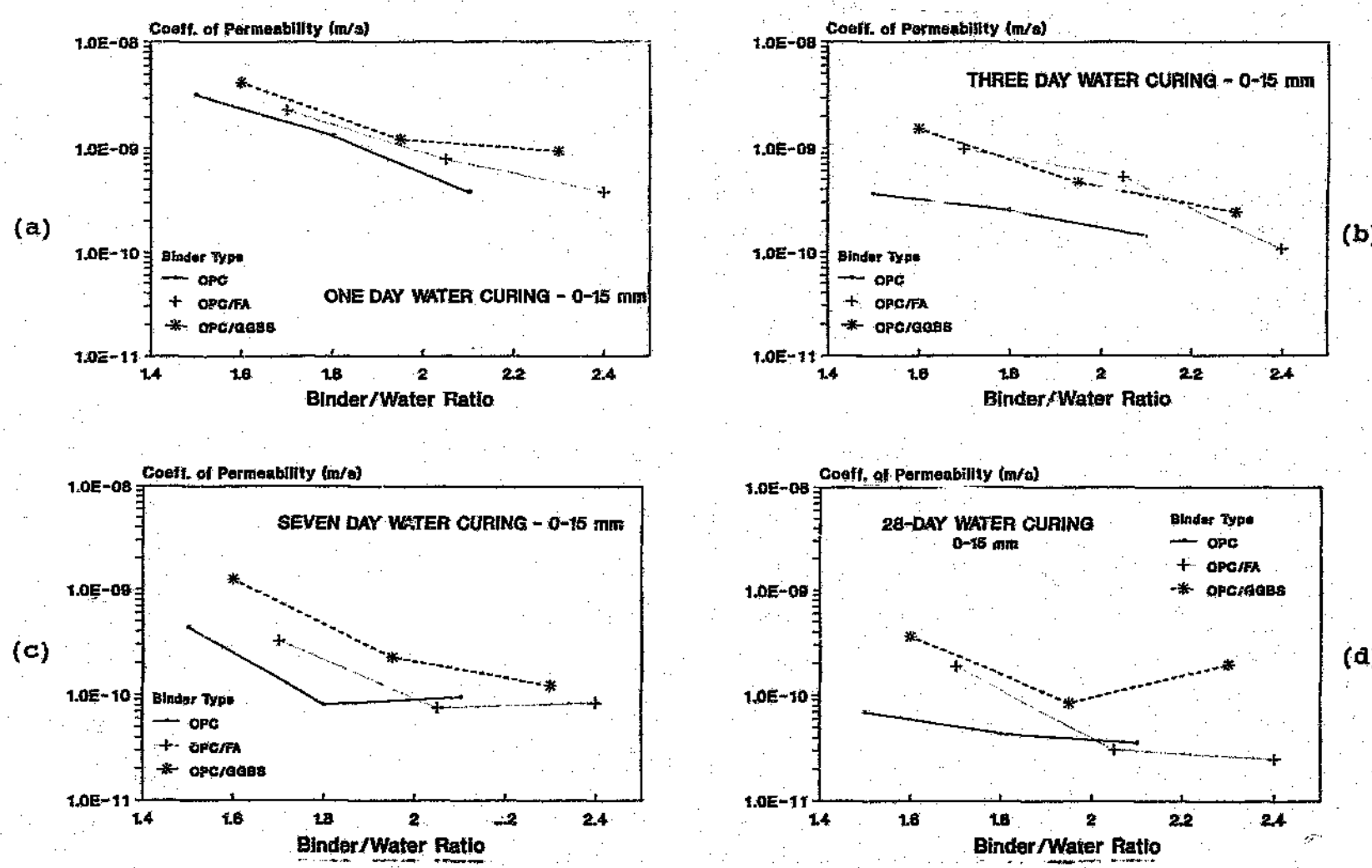

Figure 6.1 28-day oxygen permeability vs. b/w ratio for the 0-15 mm slices of the three binder type concretes.

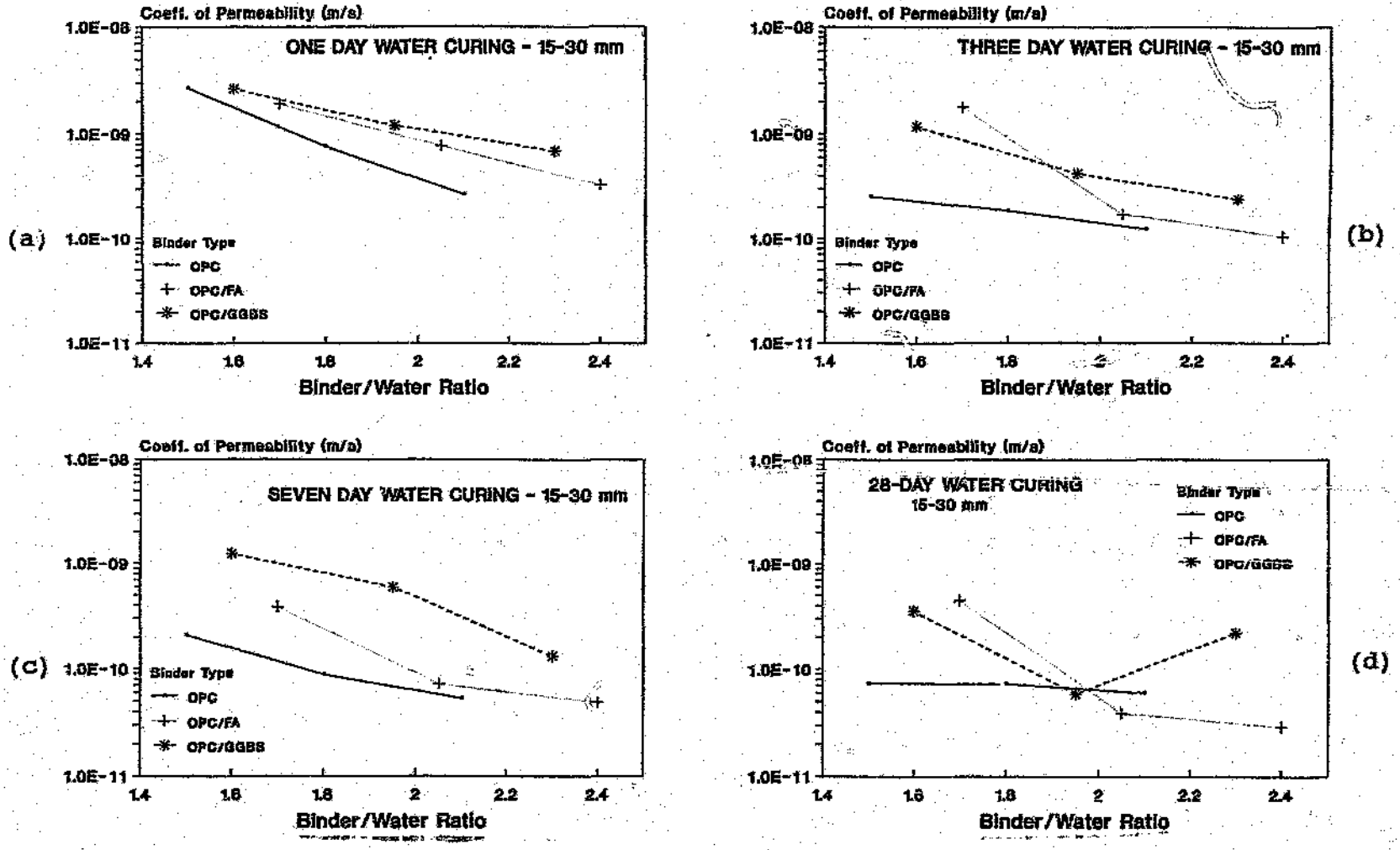

Figure 6.2 28-day oxygen permeability vs. b/w ratio for the 15-30 mm slices of the three binder type concretes.